Politechnika Wrocławska
Wydział Inżynierii Środowiska

**ROZPRAWA DOKTORSKA**

mgr inż. **Tomasz Mach**

# Skład pierwiastkowy PM badany z wysoką rozdzielczością czasową (0,5-1h) jako narzędzie w ocenie pochodzenia zanieczyszczeń pyłowych powietrza wybranych regionów Polski

Promotor:
dr hab. Justyna Rybak, prof. uczelni
Opiekun pomocniczy:
mgr inż. Krzysztof Grabowski

Katowice, 2023

Spis treści

# I. Streszczenie

Jednym z najważniejszych czynników znacząco wpływających na jakość życia człowieka jest zanieczyszczenie powietrza atmosferycznego. Poziom życia człowieka, jest powiązany z jego zdrowiem, a na to ma zasadniczy wpływ stan środowiska w którym żyjemy. Dlatego też, ciągła kontrola coraz bardziej nowocześniejszymi metodykami/narzędziami pomiarowymi zanieczyszczenia powietrza atmosferycznego, jest konieczna do zminimalizowania wpływu tegoż zanieczyszczenia na zdrowie człowieka. Głównym czynnikiem wpływającym na jakość powietrza atmosferycznego, zwłaszcza w obszarach zurbanizowanych, jest pył zawieszony (PM) (cyt) [1-4].

W niniejszej rozprawie doktorskiej prezentuję szereg moich publikacji dotyczących badań związanych z identyfikacją źródeł/pochodzenia pyłu zawieszonego ($PM_{10}$ oraz $PM_{2.5}$) na podstawie analizy elementarnej badanych próbek pyłu. Do wykonania niniejszych badań wykorzystano analizator Horiba PX-375, umożliwiający pomiar składu pierwiastkowego pyłu z wysoka rozdzielczością czasową (0,5-1h). W tym miejscu chciałbym zaznaczyć, że nie byłoby to możliwe bez wsparcia firmy Horiba GmbH z siedzibą w Austrii, która udostępniła mi do celów badawczych, związanych z niniejszym doktoratem, analizator Horiba PX-375. Badania prowadzone były w trakcie kilku kampanii pomiarowych w latach 2019 – 2021. W tym okresie zaplanowano cykl pomiarowy składający się z kilku sesji pomiarowych. Pierwszy cykl tych serii stanowiły trzy kampanie: zimowa 2019, letnia 2020 oraz zimowa 2020. Pomiary wykonano w miejscowości Kotórz Mały (województwo opolskie) w specjalnie zbudowanej na ten cele stacji pomiarowej. Wykonanie trzech serii pomiarów pozwoliło na zebranie bardzo dużego zestawu reprezentatywnych danych pomiarowych. W ramach tych kampanii określono skład pierwiastkowy $PM_{10}$ w próbkach jednogodzinowych. Kolejna sesja pomiarowa miała miejsce w lutym 2020. Były to dwudniowe badania przeprowadzone w laboratorium Szkoły Głównej Służby Pożarniczej. Celem tych badań było wyznaczenie i matematyczny opis rozkładu masy i liczby ziaren pyłu względem średnicy aerodynamicznej podczas spalania różnego rodzaju materiałów w pożarach. Następne siedmiodniowe badania zostały przeprowadzone w sierpniu 2021 r. Celem głównym było tu przeprowadzenie wstępnych badań dobowej i godzinowej zmienności stężeń pięciu wybranych pierwiastków (Pb, Ni, Zn, Mn i V) związanych z drobnym pyłem zawieszonym $PM_{2.5}$ w typowym ośrodku miejskim pod Warszawą. Dodatkowo w roku 2021 przeprowadzono badania porównawcze pomiędzy wykorzystywaną metodyka pomiarową a metodyką referencyjną (metoda grawimetryczna + atomowa spektrometria absorpcyjna GM+AAS), a także szereg badań w wybranych receptorach w Warszawie zlokalizowanych przy dużych trasach komunikacyjnych oraz remizach strażackich wyposażonych w ciężki sprzęt strażacki.

Ponadto, uzyskane wyniki zestawiono i porównano z metodami bioindykacyjnymi (wykorzystujące bioindykatory do oceny jakości powietrza), co stanowiło uzupełnienie klasycznych badań.

Badania były prowadzone we współpracy z kilkoma ośrodkami naukowymi w Polsce, m. in.: Szkołą Główną Służby Pożarniczej w Warszawie, Politechniką Opolską, Szkołą Główną Gospodarstwa Wiejskiego Uniwersytetem Wrocławskim oraz Instytutem Podstaw Inżynierii Środowiska PAN w Zabrzu.

Przeprowadzone badania wykazały znakomitą użyteczność stosowanej metodyki do celów identyfikacji pochodzenia pyłu zawieszonego, a w dalszej konsekwencji możliwość zaproponowania i zastosowania ww. metodyki jako jednego z kluczowych elementów działań prowadzących do obniżenia stężenia pyłu zawieszonego w powietrzu atmosferycznym.

**Summary**

One of the most significant factors having a great impact on human living standards is air pollution. Man's standard of living, is linked to his health, and this is fundamentally influenced by the state of the environment where we live. Therefore, constant control of the level of air pollution with modern measurement methodologies is necessary to minimize its impact on human health. The main factor which contributes the level of air pollution, is particulate matter (citation) [1-4].

In this dissertation, I present a series of papers related to the identification of sources of particulate matter ($PM_{10}$ and $PM_{2.5}$) on the basis of elemental analysis of particle samples studied. The Horiba PX-375 analyser, which enables the measurement of the elemental composition of particle with high temporal resolution (0.5-1h), was used to perform the present study. At the same time, I would like to thank Horiba GmbH, based in Austria, for making the Horiba PX-375 analyser available to me for research purposes related to Ph.D. The studies were conducted during several measurement campaigns in the years 2019 - 2021. In 2019-2020, a measurement cycle consisting of three sessions was performed in winter 2019, summer 2020 and winter 2020. The study was performed in the village of Kotórz Mały (Opolskie Voivodeship) in a measurement station specially built for this purpose. The results obtained from three sessions allowed a very large set of representative measurement data to be collected. As part of these campaigns, the elemental composition of $PM_{10}$ was measured in one-hour sampling campaign. The next measurement session took place in February 2020, it was a two-day study in the laboratory of the School of Fire Service. The aim of this studywas to determine and mathematically interpret the mass distribution and number of dust grains relative to aerodynamic diameter during the combustion of different types of materials in fires. A further seven-day study was conducted in August 2021. The main objective of the study was to assess the diurnal and hourly variability of concentrations of five selected elements (Pb, Ni, Zn, Mn and V) associated with $PM_{2.5}$ fine particulate matter in a typical urban center near Warsaw.

In addition, a comparative study between the measurement methodology used and the reference methodology (gravimetric method + atomic absorption spectrometry GM+AAS) was carried out in 2021, as well as a number of studies were carried out at selected receptors in Warsaw located along major traffic routes and fire stations equipped with heavy firefighting equipment.

In addition, the obtained results were compared with bioindication methods (using bioindicators to assess air quality), which was a supplement to classical studies.

My studies were conducted in cooperation with numerous scientific centers in Poland, including: The Higher School of Fire Service in Warsaw, the Opole University of Technology, the Warsaw University of Life Sciences, University of Wroclaw and the

Institute of Fundamentals of Environmental Engineering of the Polish Academy of Sciences in Zabrze.

The studies have demonstrated the excellent the excellent usability of the applied methodology for the purpose of identifying the origin of particle matter, and as a consequence, the possibility of proposing and using the above-mentioned methods. methodology as one of the key elements leading to the reduction of the concentration of PM - bound pollutants in air..

## II. Posiadane dyplomy, stopnie naukowe/ artystyczne – z podaniem nazwy, miejsca i roku ich uzyskania oraz tytuł rozprawy doktorskiej

1. Imię i nazwisko

   Tomasz Mach

Identyfikatory baz danych:

- ORCID ID 0000-0001-7371-3499
- Web of Science Researcher ID HJH-5877-2023
- Scopus Author ID 57209293156

2. Posiadane dyplomy, stopnie naukowe lub artystyczne – z podaniem podmiotu nadającego stopień, roku ich uzyskania oraz tytułu rozprawy magisterskiej

2.1. 2002 r. dyplom magister inżynier, specjalizacja: optoelektronika; kierunek: fizyka techniczna; wydział: matematyczno-fizyczny, Politechnika Śląska w Gliwicach.
Tytuł pracy: Nanostruktury krzemian-surfakant do oznaczenia $SO_2$ w powietrzu z wykorzystaniem AFP.

2.2. 2007 – 2010 r. dyplom studium podyplomowego organizowanego przez Akademię Ekonomiczną im. Karola Adamieckiego w Katowicach; specjalizacja: zarządzanie firmą.
Tytuł pracy: Projekt kluczowych procesów firmy X.

3. Wskazanie osiągnięcia wynikającego z art. 16 ust. 2 ustawy z dnia 14 marca 2003 o stopniach naukowych i tytule naukowym oraz o stopniach i tytule w zakresie sztuki (Dz. U. nr 65, poz. 595 ze zm.)

3.1. Osiągnięcia naukowe stanowi cykl publikacji składający się z 12 prac oryginalnych o łącznej punktacji IF: 20.18 oraz MNiSW/KBN= 925 pkt

- (Publ.1) Tomasz Mach, Jan Bihałowicz
  How to effectively analyze the impact of air quality on society - review of modern measurement techniques and apparatus

Zeszyty naukowe SGSP, ZN SGSP 2022, nr 84. Punktacja MEiN z: 2019-2021: 70;
Badania zostały wykonane jako część Doktoratu wdrożeniowego II edycja II, W-7 (03DW/0001/18) finansowanego przez Narodowe Centrum Badań i Rozwoju, Polska.
Mój udział polegał na: opracowaniu koncepcji artykułu, wykonaniu przeglądu literatury krajowej jak i zagranicznej, wykonaniu przeglądu metodyk pomiarowych pyłu, zestawieniu tekstu, porównaniu metodyk i określeniu stopnia zastosowania aparatury dobranego do rodzaju pożądanego zakresu pomiarowego, oraz redagowaniu tekstu manuskryptu.

- (Publ.2) Radosław Rutkowski, Justyna Rybak, Tomasz Mach, Wioletta Rogula-Kozłowska
  Spider webs in monitoring of air pollution
  The 10th Jubilee Scientific Conference : InfoGlob 2018: Gdańsk - Nynäshamn, Poland, September 18-20, 2018. O. Dębicka, W. Rogula-Kozłowska and P. Rogula-Kopiec. [Les Ulis] : EDP Sciences, 2018. art. 02011, s. 1-8.(SHS Web of Conferences, ISSN 2261-2424; vol. 57). Punktacja MNiSW/KBN: 15.
  Mój udział polegał na: wykonaniu przeglądu literatury krajowej jak i zagranicznej.

- (Publ.3) Agnieszka Stojanowska, Tomasz Mach, Tomasz Olszowski, Jan Bihałowicz, Maciej Górka, Justyna Rybak, Małgorzata Rajfur, Paweł Świsłowski
  Air pollution research based on spider web and parallel continuous particulate monitoring - a comparison study coupled with identification of sources.
  Minerals. 2021, vol. 11, nr 8, art. 812, s. 1-20. Punktacja MEiN z: 2019-2021: 100;Lista Filadelfijska Impact Factor: 02.818 (2021)
  Badania zostały wykonane jako część Doktoratu wdrożeniowego II edycja II, W-7 (03DW/0001/18) finansowanego przez Narodowe Centrum Badań i Rozwoju, Polska.
  Mój udział polegał na: opracowaniu koncepcji artykułu, przeglądzie literatury, przeprowadzeniu części doświadczenia oraz pomiarów.

- (Publ.4) Tomasz Mach, Wioletta Rogula-Kozłowska, Justyna Rybak, Patrycja Rogula-Kopiec, Grzegorz Majewski
  Analysis of the hourly variability in the PM10 elemental composition and its sources: The case study of a rural area in the southern part of Poland.
  Analiza godzinowej zmienności składu pierwiastkowego i źródeł PM10 : stadium przypadku obszaru wiejskiego w południowej części Polski.
  XI Konferencja Naukowa Ochrona Powietrza w Teorii i Praktyce: Zakopane, 22-25 październik 2019 r. Zabrze : Institute of Environmental Engineering of the Polish Academy of Sciences, 2019. s. 92-93.
  Mój udział polegał na: opracowaniu koncepcji artykułu, przeglądzie literatury, przeprowadzeniu doświadczenia oraz pomiarów, opracowaniu zestawień i zilustrowaniu wyników oraz przygotowaniu części tekstu manuskryptu, redagowaniu tekstu manuskryptu.

- (Publ.5) Tomasz Mach, Wioletta Rogula-Kozłowska, Karolina Bralewska, Grzegorz Majewski Patrycja Rogula-Kopiec, Justyna Rybak
  Impact of municipal, road traffic, and natural sources on PM10: the hourly variability at a rural site in Poland.
  Energies. 2021, vol. 14, nr 9, art. 2654, s. 1-23, Punktacja MEiN z: 2019-2021: 140; Lista Filadelfijska Impact Factor: 03.252 (2021)
  Badania zostały wykonane jako część Doktoratu wdrożeniowego II edycja II, W-7 (03DW/0001/18) finansowanego przez Narodowe Centrum Badań i Rozwoju, Polska.
  opracowaniu koncepcji artykułu, przeglądzie literatury, przeprowadzeniu doświadczenia oraz pomiarów, opracowaniu zestawień i zilustrowaniu wyników oraz przygotowaniu części tekstu manuskryptu, redagowaniu tekstu manuskryptu.

- (Publ.6) Tomasz Mach, Tomasz Olszowski, Wioletta Rogula-Kozłowska, Justyna Rybak, Karolina Bralewska, Patrycja Rogula-Kopiec, Marta Bożym, Grzegorz Majewski, Zbigniew Ziembik, Anna Kuczuk
  Comparative study of PM10 concentrations and their elemental composition using two different techniques during winter–spring field observation in Polish village.
  Energies. 2022, vol. 15, nr 13, art. 4769, 1-21, Punktacja MEiN z: 2019-2021: 140; Lista Filadelfijska Impact Factor: 03.252 (2021)
  opracowaniu koncepcji artykułu, przeglądzie literatury, przeprowadzeniu doświadczenia oraz pomiarów, opracowaniu zestawień i zilustrowaniu wyników oraz przygotowaniu części tekstu manuskryptu, redagowaniu tekstu manuskryptu.

- (Publ.7) Jan Bihałowicz, Wioletta Rogula-Kozłowska, Adam Krasuski, Małgorzata Majder-Łopatka, Agata Walczak, Mateusz Fliszkiewicz, Patrycja Rogula-Kopiec, Tomasz Mach
  Characteristics of particles emitted from waste fires - a construction materials case study.
  Materials. 2022, vol. 15, nr 1, art. 152, s. 1-15, Punktacja MEiN z: 2019-2021: 140; Lista Filadelfijska Impact Factor: 03.748 (2021)
  Badania te były wspierane w ramach programu finansowania PRELUDIUM 19: Wpływ pożarów składowisk odpadów na jakość powietrza atmosferycznego - metodyka i szacowanie emisji (Narodowe Centrum Nauki, Polska, 2020/37/N/ST10/02997). Badania te były również częścią Doktoratu wdrożeniowego II edycja II, W-7 (03DW/0001/18) finansowanego przez Narodowe Centrum Badań i Rozwoju, Polska. Metodologia badań była wynikiem finansowania w ramach programu OPUS 12 schemat: Przejścia niektórych pierwiastków chemicznych (metali i metaloidów) podczas migracji na drodze emitor-atmosfera-gleba (Narodowe Centrum Nauki, Polska, 2016/23/B/ST10/02789). Publikacja artykułu została wsparta dotacją

Ministerstwa Spraw Wewnętrznych i Administracji, Polska, do Szkoły Głównej Służby Pożarniczej, Warszawa, Polska.
Mój udział polegał na: przygotowaniu aparatury, przeprowadzaniu pomiarów.

- (Publ.8) Wioletta Rogula-Kozłowska, Jan Stefan Bihałowicz, Adam Krasuski, Małgorzata Majder-Łopatka, Agata Walczak, Tomasz Mach
  High time-resolution measurements of particulate size distribution in controlled fires of construction materials
  Abstract Book, 11th International Aerosol Conference, Ateny, Grecja, 04-09.09.2022
  Badania te były wspierane w ramach programu finansowania PRELUDIUM 19: Wpływ pożarów składowisk odpadów na jakość powietrza atmosferycznego - metodyka i szacowanie emisji (Narodowe Centrum Nauki, Polska, 2020/37/N/ST10/02997).
  Mój udział polegał na: przeprowadzaniu pomiarów, opracowaniu wyników, przygotowaniu tekstu manuskryptu.

- (Publ.9) Tomasz Mach, Jan Bihałowicz, Joanna Bihałowicz
  Dobowa i godzinowa zmienność stężeń Pb, Ni, Zn, Mn, i V w powietrzu atmosferycznym: badania pilotażowe w wybranym receptorze centralnej Polski
  Energetyka i Ochrona Środowiska - współczesne rozwiązania i perspektywy na przyszłość red. Alicja Danielewska, Kinga Kalbarczyk. Lublin : Wydawnictwo Naukowe TYGIEL sp. z o.o., cop. 2021. s. 145-163, Poziom wydawcy z wykazu MEiN: 1.Punktacja: 20 pkt
  Badania zostały wykonane jako część Doktoratu wdrożeniowego II edycja II, W-7 (03DW/0001/18) finansowanego przez Narodowe Centrum Badań i Rozwoju, Polska.
  Mój udział polegał na: opracowaniu koncepcji artykułu, przeglądzie literatury, przeprowadzeniu doświadczenia oraz pomiarów, opracowaniu wyników, wykonaniu zestawień graficznych oraz przeprowadzeniu analizy wyników, udział w przygotowaniu części tekstu manuskryptu, redagowaniu tekstu manuskryptu.

- (Publ.10) Tomasz Mach, Justyna Rybak, Jan Bihałowicz, Wioletta Rogula-Kozłowska
  Quasi real-time XRF spectrometer in source apportionment of PM10 in a typical suburban area
  Journal of Ecological Engineering (JEE); 23(10):89–97; Punktacja MEiN z: 2019-2021- 70 pkt Badania były częścią Doktoratu wdrożeniowego II edycja II, W-7 (03DW/0001/18) finansowanego przez Narodowe Centrum Badań i Rozwoju, Polska. Metodologia badań była wynikiem finansowania w ramach programu OPUS 12 schemat: Przejścia niektórych pierwiastków chemicznych (metali i metaloidów) podczas migracji na drodze emitor-atmosfera-gleba (Narodowe Centrum Nauki, Polska, 2016/23/B/ST10/02789).
  opracowaniu koncepcji artykułu, przeglądzie literatury, przeprowadzeniu doświadczenia oraz pomiarów, opracowaniu wyników, wykonaniu zestawień

graficznych oraz przeprowadzeniu analizy wyników, przygotowaniu tekstu manuskryptu, redagowaniu tekstu publikacji.

- (Publ.11) Wioletta Rogula-Kozłowska, Tomasz Mach, Patrycja Rogula-Kopiec, Justyna Rybak, Katarzyna Nocoń
  Concentration and elemental composition of quasi-ultrafine particles in Upper Silesia.
  Environment Protection Engineering. 2019, vol. 45, nr 1, s. 171-184, Punktacja MEiN z 2019-2021: 70; Lista Filadelfijska Impact Factor: 00.812 (2019)
  Mój udział polegał na: przeglądzie literatury, opracowaniu wyników, interpretacji wyników, przygotowaniu tekstu manuskryptu.

- (Publ.12) Tomasz Mach, Wioletta Rogula-Kozłowska, Jan Bihałowicz, Justyna Rybak
  Elemental composition and origin of PM10 in selected Polish fire station: real time results from XRF analysis
  Environment Protection Engineering, Vol. 49, 2023, No. 1, s. 57-72, MEiN z 2019-2021: 70 pkt, Impact Factor: 0,887 (2021)
  Mój udział polegał na: opracowaniu koncepcji artykułu, przeglądzie literatury, przeprowadzeniu doświadczenia oraz pomiarów, opracowaniu wyników, oraz interpretacji wyników, wykonaniu zestawień graficznych, przygotowaniu redagowaniu tekstu manuskryptu,.

3.2. Inne formy prezentacji upowszechniania wyników pracy

- XI Konferencja Naukowa: Ochrona Powietrza w Teorii i Praktyce Zakopane, 22-25 października 2019r. „Analiza godzinowej zmienności składu pierwiastkowego i źródeł PM10: studium przypadku obszaru wiejskiego w południowej części Polski”
- III Ogólnopolska Konferencja Naukowa „Ochrona środowiska – rozwiązania i perspektywy” Lublin, 21.05.2021 „Dobowa i godzinowa zmienność stężeń Pb, Ni, Zn, Mn i V badania pilotażowe w dużym ośrodku miejskim”
- EKO DOK Konferencja Naukowa Interdyscyplinarne Zagadnienia w Inżynierii i Ochronie Środowiska, 06-08.06.2022
  - „Nowoczesne techniki i aparatura w badaniach jakości powietrza”
  - „Spektrometr XRF pracujący w czasie quazi-rzeczywistym w podziel źródeł emisji PM10 w typowym obszarze podmiejskim”
- 13th Annual Sales and Service Training by Horiba Ltd., 8-09.2022 r. Wystąpienie: Kotórz Mały: identification of the origin air pollution with PX-375. Preliminary analysis.
- 11th International Aerosol Conference, Ateny, Grecja, 04-09.09.2022 Wioletta Rogula-Kozłowska, Jan Stefan Bihałowicz, A. Krasuski, M. Majder-Łopatka, A. Walczak and Tomasz Mach “High time-resolution measurements of particulate size distribution in controlled fires of construction materials”

# III. Omówienie celu naukowego ww. pracy i osiągniętych wyników

## 1. Tło problemu

Zanieczyszczenie powietrza atmosferycznego ma istotny wpływ na zdrowie człowieka oraz jego długość życia. Szacowane jest, że każdego roku ponad 400 tysięcy zgonów w krajach Unii Europejskiej spowodowanych jest takimi chorobami jak choroby układu oddechowego, czy też rak płuc. Badania WHO wykazały, że trzy do pięciu procent z tych zgonów jest spowodowane narażeniem organizmów na długotrwały wpływ pyłu zawszonego (PM) [1,5]. W ostatnich latach pył drobny $PM_{2.5}$, jest klasyfikowany w gronie dziesięciu najbardziej istotnych czynników ryzyka mających wpływ na zdrowie człowieka. Zgodnie z tymi badaniami [6] pył zawieszony $PM_{2.5}$ odpowiada globalnie nawet za 3,1% straconych lat życia. Należy zwrócić uwagę na fakt, że nie tylko wartość ilościowa pyłu w powietrzu atmosferycznym ma wpływ na zdrowie człowieka. Niemniej ważna jest również jego wartość jakościowa, czyli jakie związki elementarne wchodzą w skład pyłu oraz jego budowa chemiczna. Udowodniona została, korelacja pomiędzy występowaniem większej ilości metali ciężkich czy też wielopierścieniowych węglowodorów aromatycznych a wzrostem zachorowalności przez człowieka na nowotwory płuc [7-12]. Dlatego od wielu lat, również w Polsce, prowadzony jest szereg działań w celu ograniczenia zanieczyszczenia powietrza atmosferycznego [13-15]. Pomimo tego, jest ono wciąż istotnym czynnikiem wpływającym na zdrowie człowieka oraz na jakość jego życia. Dodatkowo zanieczyszczenie środowiska jak i walka z jego efektami generuje olbrzymie koszty dla gospodarki światowej [16]. Choroby spowodowane zanieczyszczeniem środowiska i ich leczenie powodują spadek produktywności populacji ludzkiej, a co za tym idzie gigantyczne koszty jakie ponosi społeczeństwo.

Zanieczyszczenie powietrza atmosferycznego ma nie tylko wpływ na zdrowie człowieka. Efektem ubocznym wzrostu zanieczyszczenia powietrza (również zanieczyszczeniem pyłem zawieszonym) są zmiany klimatyczne oraz korozja materiałów mających kontakt z pyłem (przede wszystkim materiały budowlane). Ma ono również istotny wpływ na otaczający nas ekosystem. Aerosol wpływa na klimat poprzez jego oddziaływanie na transfer promieniowania w atmosferze oraz na właściwości fizyczne chmur [1].

Wszystkie powyższe aspekty wzrostu zanieczyszczenia środowiska, a w szczególności powietrza atmosferycznego pyłem zawieszonym obciążają olbrzymim kosztem społeczeństwa. Szacuje się, że globalne roczne straty społeczne wynikające z zanieczyszczenia środowiska są na poziomie 4-5 biliona USD i stale rosną [17].

Pył zawieszony PM jest głównym czynnikiem wpływającym na poziom zanieczyszczenia powietrza atmosferycznego. Jest on zanieczyszczeniem mogącym pochodzić ze źródeł naturalnych jak i z działalności człowieka (źródła antropogeniczne). Dodatkowo należy rozróżnić pyły pierwotne związane bezpośrednio z emisją zanieczyszczeń do atmosfery oraz pyły wtórne powstające w wyniku reakcji i

przemian chemicznych z pyłów pierwotnych [18-21]. Pył pochodzący ze źródeł naturalnych to ten będący na przykład:

- efektem działalności wulkanów [22, 23],
- wszelkiego rodzaju naturalnych pożarów (pożary lasów, łąk i innej biomasy) [24]
- wznoszenia przez wiatr cząsteczek drobnego piasku na terenach poddanych erozji gleby (np.: rejon subsaharyjski) [25-28],
- aerozol biologiczny taki jak pyłki roślinne, zarodniki grzybów, ich fragmenty, bakterie, czy też wirusy [29-32],
- wzbudzone przez wiatr drobinki kropel słonej wody na obszarach morskich [33-36],
- wyładowania elektryczne (takiej jak błyskawice) [37, 38],

Pył pochodzenia antropogenicznego to ta część pyłu, której źródłem pochodzenia jest działalność człowieka. Głównymi źródłami pyłu pierwotnego jest wszelkiego rodzaju działalność człowieka związana z procesami spalania paliw, a w szczególności spalania paliw stałych przede wszystkim w trakcie procesów produkcyjnych [39, 40]. Jednymi z najbardziej istotnych źródeł emisji pyłu do atmosfery, są takie źródła jak: zakłady energetyczne (zarówno zawodowe jak i przemysłowe) [41], zakłady przemysłowe (przemysłowe technologie procesowe) [42], lokalne kotłownie, paleniska domowe, mikro-przemysł (małe zakłady rzemieślnicze), rolnictwo oraz źródła mobilne takie jak transport publiczny i prywatny (morski, lądowy i powietrzny) [43-46].

Głównym czynnikiem od którego uzależniona jest emisja zanieczyszczeń pyłowych pochodzących ze źródeł energetycznych oraz przemysłowych jest rodzaj przemysłu i stosowana w nich technologia. Zarówno wielkość emisji pyłu jak i jego struktura chemiczna zależy od wielu indywidualnych czynników danego źródła (kotła, silnika itp.). Są to takie parametry jak:

- rodzaj paliwa i wielkości jego zużycia,
- wartość opałowa paliwa,
- zawartość w nim popiołu,
- poziom zawilgocenia paliwa,
- sposób podawania paliwa,
- temperatura prowadzenia procesu,
- ilość tlenu w trakcie procesu spalania,
- rodzaj emitora,
- sposób prowadzenia procesu,
- czy też zabudowanego w układzie systemu redukcji emisji pyłów.

Wszystkie te elementy (i wiele innych) składają się na niepowtarzalną, z punku widzenia ilościowego jak i jakościowego, emisję zanieczyszczeń powietrza (w tym zanieczyszczeń pyłem) z danego emitora.

W Polsce istotnym źródłem emisji zanieczyszczeń pyłów jest energetyka, zaopatrująca przemysł, instytucje państwowe i gospodarstwa domowe w energię oraz ciepło. Głównym paliwem jest węgiel kamienny i brunatny [47], następnie gaz ziemny i ropa naftowa, a także biomasa [48-50] (przy czym paliwa stałe stanowią wciąż większość). Efektem ubocznym działalności zakładów energetycznych jest emisja do powietrza

atmosferycznego pyłu zawierającego duże ilości węgla i siarki, ale także rtęć, czy też fluorowodory [51-59].

Istotnymi źródłami przemysłowymi emisji pyłu są takie branże jak:

- branża metalurgiczna, która jest źródłem emisji pyłów zawierających takie metale jak żelazo, nikiel, cynk, chrom, kadm, ołów i inne,
- branża budowlana (zwłaszcza przemysł cementowy, wapienniczy, gipsowy), gdzie na każdym etapie, poczynając od wydobycia poprzez transport i kończąc na procesie produkcyjnym dochodzi o znaczących emisji pyłu składających się z takich pierwiastków jak potas, węgiel, glin, krzem, siarka, wapń, żelazo, oraz alkalia,
- branża koksownicza z emisją bardzo rakotwórczych wielopierścieniowych węglowodorów aromatycznych, czy też benzo(a)pirenu [60-62]

Kolejnym istotnym źródłem emisji pyłu jest branża transportowa, bez względu na to, czy jest to transport drogowy, lotniczy czy morski. Emisja ta pochodzi zarówno ze spalania paliwa w silnikach np.: Diesla, ale również ze ścierania się opon, nawierzchni dróg, klocków hamulcowych. Dodatkowym aspektem jest ponowne podrywanie pyłu osadzonego na drodze przez przejeżdżające samochody. Mamy tu do czynienia z pyłem o składzie chemicznym zdominowanym przez węgiel, azot, węglowodory i metale ciężkie [52, 63-64].

Następnym znaczącym źródłem emisji pyłu jest sektor komunalny, czyli efekt uboczny spalania paliw stałych w procesie ogrzewania budynków. Tutaj skład pierwiastkowy emitowanego pyłu jest zbliżony do tego pochodzącego z branży energetycznej, jednak zawiera on dużo większą ilość tych najbardziej szkodliwych związków, ze względu na mniejsza sprawność stosowanych pieców oraz praktyczny brak stosowania filtrów eliminujących emisje zanieczyszczeń [65-67].

Wreszcie rolnictwo również jest źródłem emisji pyłów i to zarówno w przypadku upraw roślinnych jak i hodowli zwierząt. W tym wypadku dominującymi w pyle cząstkami elementarnymi są węgiel, azot, krzem, potas, wapń [24, 68].

Jak zasygnalizowano wcześniej, każde źródło pyłu zawieszonego, zarówno to rozumiane jako proces fizykochemiczny (spalanie, erozja, resuspensja) jak i fizyczne/technologiczne (rura wydechowa samochodu, komin elektrowni, bateria koksownicza) ma swój profil emisji, to znaczy PM z tego źródła ma mniej lub bardziej ustalony skład chemiczny w tym zwłaszcza skład pierwiastkowy [69-75]. Relacje pomiędzy składem chemicznym emitowanych cząstek i cząstek w próbce powietrza atmosferycznego dają się względnie łatwo wyznaczyć, bo związki chemiczne/pierwiastki najczęściej występujące u źródła są na ogół najobfitsze w punkcie pomiarowym. Daje to możliwość powiązania pyłu w punkcie pomiarowym z lokalnymi źródłami, albo szerzej, przy powiązaniu pomiarów stężeń PM z warunkami meteorologicznymi czy klimatologicznymi, przypisać mu odpowiednie pochodzenie (transport). Na całym świecie, przy wykorzystaniu różnych metod, informacje o składzie chemicznym PM (najczęściej o składzie pierwiastkowym) od dawna wykorzystywane są do identyfikacji źródeł PM. Z powodzeniem stosowane są zarówno metody najprostsze, oparte na wyznaczaniu korelacji między danymi z monitoringu i

warunkami meteorologicznymi (prędkość i kierunek wiatru, opad atmosferyczny, temperatura), czy porównywaniu stężeń zmierzonych w tzw. tle np. regionalnym ze stężeniami w wybranych punktach obszarów miejskich (tło miejskie, kanion uliczny, itp.), ale też zaawansowane modele statystyczne (analiza składowych głównych PCA i jej modyfikacje i modele receptorowe [np. 76-94].

Modele statystyczne i receptorowe wymagają dużej liczby danych wejściowych (z pomiarów lub analiz). Dodatkowo, np. w przypadku oddziaływania na punkt pomiarowy kilku źródeł PM o zbliżonym profilu chemicznym, (np. emisja komunikacyjna i emisja z niektórych procesów przemysłowych, albo emisja ze spalania węgla i emisja niezorganizowana z procesu koksowania węgla [70, 75, 79-80], trzeba znaleźć i zastosować specyficzne dla zidentyfikowanych źródeł markery emisji lub/i znaleźć odpowiednie zależności pomiędzy emitowanymi z tych źródeł składnikami PM (najlepiej dla wszystkich istotnych w danym obszarze źródeł) [95]. W praktyce jest to zazwyczaj niemożliwe; profile emisji źródeł najczęściej bierze się z literatury lub/i pomiarów emisji prowadzonych często w zupełnie odmiennych warunkach aniżeli te, w których pracują rzeczywiste źródła stanowiące obiekt zainteresowania.

Analiza składowych głównych (PCA) jest jedną z technik redukcji wymiarowości problemu. W sytuacji kiedy mamy mierzone stężenia j związków chemicznych w jednej próbce zasadna jest próba, zwłaszcza w przypadku n>10, zmniejszenia wymiarowości problemu poprzez analizę PCA. W wyniku tej analizy konstruowane są nowe zmienne będące kombinacjami liniowymi zmierzonych stężeń a następnie mogą zostać one uporządkowane w taki sposób, aby wariancja (odchylenie standardowe) nowej zmiennej było jak najmniejsze. W wyniku tej procedury dane opisane są za pomocą j nowych zmiennych (opisują one 100% zmienności w próbce). Redukcja wymiarowości problemu polega na wybraniu ile pierwszych (mających kolejno najmniejsze wariancje) zmiennych będzie używanych w dalszej analizie, na podstawie tego, ile procent zmienności mają one opisywać. W praktyce pomiarów środowiskowych można zredukować liczbę wymiarów nawet czterokrotnie zachowując opis 90% zmienności w próbce [96-98]. Wyznaczone wektory PCA mają składowe zarówno o wartościach dodatnich jak i ujemnych. Procedura ta eliminuje przede wszystkim skorelowane wzajemnie zmienne, ponieważ w przypadku wysokiej korelacji między, np. trzema źródłami rozwiązywane zagadnienie może zostać uproszczone do analizy j-3 zmiennych bez utraty precyzji. Jednym z rodzajów modeli receptorowych są modele oparte na równaniu równowagi chemicznej (CMB). Podstawową różnicą względem PCA jest to iż zakładają one a priori istnienie niepewności między opisem a punktami pomiarowymi. W tych modelach określane są profile emisji którymi można opisać zaobserwowane stężenia substancji a następnie określane są ich udziały w tej próbce. Jest wiele modeli opartych na równaniu CMB jednakże różnią się one funkcjami celu, do najpopularniejszych należą, m.in., EPA CMB oraz EPA PMF.
EPA CMB jest modelem który minimalizuje sumę kwadratów różnic między zaobserwowanymi a modelowanymi stężeniami. Pozwala on na dopasowywanie typów źródeł, a nie poszczególnych emiterów, o uprzednio zdefiniowanych profilach, do danych pomiarowych. Źródła o podobnych profilach emisji nie mogą być rozróżnione za pomocą tego modelu [99].
EPA PMF jest modelem który w dopasowywaniu źródeł uwzględnia również niepewności wyznaczenia stężeń. Minimalizowana funkcja jest, podobnie jak w przypadku EPA CMB, kwadratem różnicy obserwacji i modelu, jednakże te różnice są ważone poprzez kwadrat niepewności względnej pomiaru stężenia [100]. Dodatkowo,

w dopasowaniu są uwzględniane dolne granice detekcji jak i zaimplementowana jest obsługa brakujących stężeń co ma istotne znaczenie w przypadku analizy stężeń, których wartości mogą być w okolicy granicy wykrywalności.

Aktualnie znane są różnego rodzaju urządzenia i techniki do pomiaru stężenia i składu pierwiastkowego PM. Najpopularniejszą metodą manualną, jest pobór pyłu na filtr a następnie ważenie uzyskanej próbki za pomocą mikrowagi. Pobór ten jest realizowany za pomocą tzw. niskoprzepływowych poborników pyłu LVS (czy też sekwencyjnych niskoprzepływowych poborników pyłu) wyposażonych w znormalizowany wlot tj. głowicę pomiarową. której konstrukcja jest opisana tej normie PN-EN 12341:2014 [101]. Pobornik pyłu pracuje przy nominalnym natężeniu przepływu 2,3 $m^3$/h. Nominalny okres pobierania próbek wynosi 24 godziny (średnie 24-rogodzinne). Wyniki pomiarów wyrażane są w µg/$m^3$, gdzie objętość pobranego do badania powietrza odpowiada objętości powietrza w warunkach otoczenia w pobliżu wlotu w momencie pobierania prób. Automatycznych metod wykorzystywanych do pomiaru masy pyłu jest dostępnych kilka. Najbardziej popularne to:

- Mikrowaga oscylacyjna TEOM. Metodyka niezwykle popularna w latach 90tych poprzedniego stulecia. Zmierzch jej powoli następuje od II dziesięciolecia XXI wieku. Jedna z pierwszych metodyk niewykorzystujących źródeł promieniotwórczych. Metodyka bardzo dokładna, jednak ze względu na wysoką cenę, duży rozmiar analizatorów, coraz mniej popularna.
- Tłumienia promieniowania β. Jedna z najstarszych automatycznych metodyk i wciąż popularna. Od początku jej problemem było wykorzystywanie źródeł radioaktywnych. Na szczęście w dzisiejszych analizatorach wykorzystujące metodę tłumienia beta, pozom radioaktywności jest minimalny. Wadą metodyki jest pomiar tylko jednej frakcji pyłu zawieszonego.
- Metody optyczne (nefelometryczna, spektroskopia i inne). W ostatnich latach coraz większą popularność zdobywają metody optyczne. Są one tańszym rozwiązaniem, a część z nich jakością nie odbiega od innych metodyk. Zasadniczą zaletą metod optycznych (spektroskopia) jest możliwość pomiaru kilku frakcji pyłu zawieszonego jednocześnie.
- Ciekawą metodą pomiaru ilości i stężenia pyłu zawieszonego jest pomiar przy pomocy elektrycznego impaktora kaskadowego. Wbudowany impaktor kaskadowy rozdziela próbkę pyłu na kolejne frakcje, które to są osadzane na filtrach umieszczonych na poszczególnych stopniach impaktora (dzięki temu nadaje się on do dalszej analizy laboratoryjnej). Jednocześnie na wlocie do analizatora próbka PM zostaje naładowana ładunkiem elektrycznym, a elektrometry umieszczone bezpośrednio nad każdym ze stopni impaktora mierzą ładunek osadzonego pyłu. Wartość tego ładunku jest wprost proporcjonalna do masy zebranego pyłu na każdym z filtrów.

Wszystkie powyżej opisane metodyki pomiarowe, obowiązująca norma PN-EN16450:2017, normalizująca automatyczny pomiar stężenia masy pyłu [102], dopuszcza do stosowania w pomiarach pyłu zawieszonego. Widać wyraźnie, że te

urządzenia i techniki pomiarowe, które dają dużą ilość wyników i jednocześnie polegają na automatycznych pomiarach pewnych, wybranych, specyficznych własności fizycznych pyłu zawieszonego, zwykle nie pozwalają na zbieranie próbki do badań i określanie, m.in. składu chemicznego. Pozostałe zaś metodyki, pozwalają na zbieranie próbek pyłu zawieszonego, niemniej czas jaki potrzebny jest na zgromadzenie np. na filtrach wystarczającej masy pyłu zawieszonego, która w sposób poprawny może być zważona przy obecnie dostępnej technologii, to średnio jedna doba. Ograniczeniem tutaj są nie tylko warunki ważenia i jakość dostępnych wag ale również czułość i selektywność metod stosowanych w badaniach składu chemicznego cząstek pyłu. Do najczęściej stosowanych metod w zakresie oznaczania składu pierwiastkowego należą AAS (Atomic Absorption Spectroscopy), CE (Capillary Electrophoresis), ICP-MS (Inductively Coupled Plasma Mass Spectrometry), ICP-OES (Inductively Coupled Plasma Optical Emission Spectrometry), EDXRF (Energy Dispersive X-ray Fluorescence)I WDXRF (Wavelength Dispersive X-ray Fluorescence). Szczególnie pierwsze cztery wymienione wymagają odpowiedniej wielkości (masy) badanej próbki ze względu na konieczność wcześniejszego jej przygotowania (mineralizacja/ekstrakcja itp.). Istotne są również artefakty, które mogą mieć wpływ ze względu na obecność różnego rodzaju metali i innych zanieczyszczeń w samym materiale z którego zbudowane są filtry pomiarowe jak również wpływ transportu i przechowywania próbek na końcowe wyniki [103-105]. Oczywiście pewnym rozwiązaniem wskazanych problemów może być zastosowanie wysokoprzepływowych poborników pyłu jak np. Digitel High Volume Aerosol Sampler DHA-80, [106-107] i wykonywanie poborów i oznaczeń składu chemicznego z dużą rozdzielczością czasową. Niemniej takie rozwiązania są bardzo kosztowne i najczęściej poza zasięgiem zarówno w przypadku operatorów w podstawowym monitoringu jakości powietrza jak i naukowców realizujących wybrane projekty badawcze. Jest to problematyczne tym bardziej w większości obszarów w Polsce, gdzie aby seria pomiarów była reprezentatywna dla danego obszaru powinna obejmować kilka różnych okresów w roku tak aby uchwycić wpływ możliwie dużej liczby znaczących źródeł oddziałujących na stężenia i skład chemiczny PM w tym obszarze. Dlatego też niekiedy alternatywnie stosowane są różnego rodzaju metody wskaźnikowe dla uchwycenia wpływu różnych źródeł na PM. Do takich celów stosowane są bioindykatory, czyli organizmy żywe i ich produkty. Najczęściej stosuje się porosty, mchy i rośliny wyższe [108-110]. Zwierzęta są rzadko wykorzystywane ze względu na inwazyjność takich badań. W nielicznych badaniach stosowano produkty pochodzenia zwierzęcego, takie jak ptasie pióra i jaja, sierść zwierzęca [111-112] czy włosy. Wszystkie wymienione powyżej metody mają swoje zalety i wady. Stosowanie bioindykatorów, takich jak rośliny wyższe, mchy i porosty, ogranicza się do czasu trwania sezonu wegetacyjnego. Pewne problemy stwarza również wykorzystywanie zwierząt i produktów ludzkich (jaja, pióra, sierść). Na przykład ptasie jaja jako produkt samic reprezentują tylko żeńską część populacji. Z drugiej strony schemat dystrybucji zanieczyszczeń w ptasich piórach jest różny w zależności od etapu życia ptaków i rodzaju zanieczyszczeń. Ponadto zawartość zanieczyszczeń we włosach ludzkich lub zwierzęcych zależy od wielu czynników takich jak m.in. wiek, historia medyczna itp. Innym stosowanym bioindykatorem, który wydaje się mieć mniej wad, jest sieć pajęcza która ostatnio jest powszechnie badana jako pasywny próbnik do monitorowania zanieczyszczeń powietrza [113-116]. Wykazuje ona bardzo dobre właściwości w

zbieraniu pyłu zawieszonego (PM). Ten bioindykator ma wiele zalet, m.in. jest tani, łatwo dostępny i prosty w użyciu. Pajęczyny są wszechobecne. Występują powszechnie w środowisku naturalnym, jak również w uprzemysłowionych obszarach miejskich. Sieci pajęcze kumulują zanieczyszczenia, na które jesteśmy narażeni, dlatego są doskonałym źródłem informacji o środowisku. Ponieważ naturalnie adsorbują zanieczyszczenia powietrza, mogą być użytecznymi wskaźnikami jakości środowiska.

Główne zalety stosowania pajęczyn to:

- powszechna dostępność materiału badawczego,
- dogodne umiejscowienie (zwykle tkane są w odosobnionych miejscach) zapobiegających ich zniszczeniu wskutek warunków atmosferycznych (deszcz, wiatr itp.),
- niski koszt i łatwość pobierania próbek oraz nieinwazyjność badań,
- narzędzie niespecyficzne i uniwersalne, gdyż pobór sieci nie wymaga żadnego przygotowania,
- są organiczne, naturalne i przyjazne dla środowiska (brak produkcji odpadów np. jak w przypadku zużytych sorbentów),
- pająki można hodować w warunkach laboratoryjnych, a otrzymane sieci wykorzystać następnie w dowolnym miejscu do badań,

Z powyższych powodów, aby uzyskać z jednej strony wiarygodne dane do identyfikacji źródeł emisji pyłu a z drugiej strony oprzeć je na realnych pomiarach wymagających realnych nakładów czasowych, ekonomicznych i pracy ludzkiej uważam, że istnieje konieczność jednoczesnego pomiaru pyłu zawieszonego PM i analizy jego właściwości chemicznych w wysokiej rozdzielczości czasowej (≤1h) z użyciem aparatury quazi-bezobsługowej, która daje wyniki niemal w czasie rzeczywistym [117]. Niezwykle istotne jest ponadto wypracowanie odpowiedniej metodyki postępowania z danymi z takich pomiarów aby w dalszej kolejności można było ją wdrożyć do rutynowego monitoringu jakości powietrza w Polsce.

Wysoka rozdzielczość pomiarowa pozwala na zaobserwowanie i identyfikację wpływu na PM szybko zmieniających się emisji/źródeł. Jest to szczególnie przydatne na obszarach gdzie emisje PM z różnych źródeł nakładają się na siebie (co w znaczący sposób utrudnia ich identyfikację tradycyjnymi metodami), albo mamy do czynienia z dominującym jednym źródłem i problemem jest prawidłowe określenie pochodzenia PM. Dlatego też w badaniach zastosowałem nowoczesne urządzenie pomiarowe analizator PX-375 firmy Horiba, które umożliwia pomiar zarówno wielkości zanieczyszczania pyłu (o frakcji $PM_{2.5}$ lub $PM_{10}$) jak i jego składu pierwiastkowego. Uzyskane dane pochodzą z uśredniania pomiarów w krótszych niż doba odcinkach czasu (0,5-24h). Zastosowanie konwencjonalnych technik analizy wyklucza uchwycenie krótkoterminowych podwyższonych stężeń pierwiastków w atmosferze. Długoterminowy pomiar pozwala zarówno na zdefiniowanie krótkotrwałych zmian jak i na charakterystykę zanieczyszczeń na poziomie regionalnym, a także na wykorzystanie zarejestrowanych stężeń pierwiastków nieorganicznych jako wskaźników w identyfikacji źródeł zanieczyszczeń.

Analizator Horiba PX-375 pobiera próbkę pyłu na dwuwarstwową taśmę z włókniny PTFE o bardzo dużej czystości pierwiastkowej (pozbawionej śladów metali). Przepływ zasysanego, przez pompę zewnętrzną sterowaną automatyczne przez analizator, powietrza jest stabilizowany regulatorem masowym i wynosi 16,7 L/min (1 m3/h), średnica zebranych próbek na taśmie wynosi ok. 11 mm każda. Następnie przy pomocy czujnika wykorzystującego metodę tłumienia promieniowania β, przyrząd wyznacza całkowitą masę pyłu $PM_{10}$ lub $PM_{2.5}$. Na kolejnym etapie przy zastosowaniu, nieniszczącej techniki analizy spektroskopowej EDXRF (energy-dispersive X-ray fluorescence) wyznaczone jest stężenie wybranych pierwiastków (w zależności od skalibrowania). Moduł EDXRF wyposażony jest dodatkowo w kamerę CMOS do obrazowania mierzonych próbek. Po pobraniu próbek przyrząd w odpowiednio przyjętej rozdzielczości czasowej przeprowadza analizę EDXRF przez 500 s (15 kV lub 50 kV w zależności od ilości osadzonego na filtrze pierwiastka w próbce godzinowej).

## 2. Cel pracy badawczej

Głównym celem pracy badawczej było ustalenie aktualnej hierarchii źródeł pyłu zawieszonego w powietrzu atmosferycznym (PM) mające na celu systematyczne obniżanie jego stężeń w dłuższej perspektywie czasowej. Tym samym, celem pośrednim tej pracy było wykazanie możliwości wykorzystania wyników o wysokiej rozdzielczości czasowej (0,5-1h), zmienności stężenia pyłu i związanych z nim pierwiastków do bardzo prostej i szybkiej oceny jakościowej wpływu konkretnego źródła emisji na ich stężenie w powietrzu. Taka identyfikacja źródeł emisji pozwala na dokładniejsze opracowanie w przyszłości programów i scenariuszy redukcji emisji pyłów zarówno dla poszczególnych regionów Polski jak i dla całego kraju. Pozwala także kompleksowo podejść do zagadnienia składu pierwiastkowego pyłu z różnych źródeł co z kolei umożliwia zoptymalizowanie modelu badawczego – do oceny pochodzenia pyłu w różnych obszarach.

Do najistotniejszych problemów badawczych należał:

- dobór odpowiedniego sprzętu pomiarowego, umożliwiającego w trybie automatycznym, z wysoką rozdzielczością czasową, prowadzić nie tylko pomiary koncentracji pobranego pyłu, ale również jego składu pierwiastkowego,
- dobór sprzętu pomocniczego (np. czujniki meteo, automatyczne analizatory gazowe, referencyjny analizator pyłu, kontener pomiarowy itp.) wspomagającego badania parametrów środowiska i warunków/charakterystyki otoczenia receptora,
- wybór kilku reprezentatywnych z punktu widzenia różnorodności źródeł pochodzenia pyłu zawieszonego receptorów pomiarowych (obecność emisji ze źródeł: przemysłowych, energetyki, transportu, rolnictwa, komunalnego) oraz receptorów charakterystycznych,
- zapewnienie wiarygodności danych (dobór referencyjnych metodyk pomiarowych, oraz badania porównawcze z innymi metodykami takimi jak metody bioindykacyjne oparte na wykorzystaniu organizmów żywych i ich produktów),

- dobór odpowiednich narzędzi analizy statystycznej.
- weryfikacja badań i walidacja wyników uzyskanych innymi metodami (bioindykacja z wykorzystaniem sieci pajęczych) z danymi uzyskanymi z EDXRF.

Zasadniczym zagadnieniem do rozstrzygnięcia był dobór automatycznego analizatora do pomiaru koncentracji pobranego pyłu, oraz jego składu chemicznego. Tego typu analizatory są rozwiązaniami nowatorskimi. W momencie rozpoczynania prac badawczych komercyjnymi produktami dostępnymi na rynku umożliwiającymi prowadzenie badań w terenie, były analizatory Horiba PX-375 firmy Horiba oraz Xact625i firmy Cooper Environmental Services (w trakcie opracowywania było kilka produktów chińskich producentów m.in. Focused Photonics Inc., Skyray Instrument, NCS Testing Technology, Beijing SDL Technology, ale nie były one jeszcze dostępne na rynku). Dużą zaletą analizatora PX-375 była możliwość automatycznego jednoczesnego pomiaru zarówno stężenia masowego pyłu $PM_{10}$ lub $PM_{2.5}$ (w zależności od stosowanej głowicy pomiarowej) oraz równocześnie jego składu elementarnego. Pozostałe produkty umożliwiały tylko automatyczny pomiar składu elementarnego pyłu $PM_{10}$ lub $PM_{2.5}$ (w zależności od stosowanej głowicy pomiarowej). W związku z tym decydując się na inne rozwiązanie niż Horiba PX-375, konieczne byłoby stosowanie równolegle dodatkowego analizatora pyłu do określania jego stężenia masowego. Analizator PX-375 posiadał kilka innych zalet w porównaniu z przyrządami konkurencyjnymi (mniejszy rozmiar i waga, szerszy zakres temperatur w których może pracować, lepsza dokładność oznaczeń dla większości analizowanych pierwiastków przy pomiarach w wysokiej rozdzielczości czasowej [4]). Analizator PX-375 wykorzystuje unikalne połączenie dwóch metodyk pomiarowych. Najpierw przy pomocy metody tłumienia promieniowania β automatycznie analizuje pobraną próbkę pyłu $PM_{10}$ lub $PM_{2.5}$ celem wyznaczenia jej masy, a następnie przy pomocy spektrometrii XRF, analizuje tą samą próbkę pod kątem składu pierwiastkowego. Do określenia składu pierwiastkowego widm rentgenowskich i kontroli jakości wyników stosuje się odpowiedni, certyfikowany materiał wzorcowy (m.in. SRM 2783 z NIST) w postaci pyłu osadzonego na podłożu filtracyjnym. Czułość spektrometru, czyli dolna granica detekcji, jest niezależna dla każdego pierwiastka, a dla konkretnie określonego przypadku zastosowanego w opisywanych badaniach urządzenia wynosi:: Al (56.7 $ng/m^3$), As (3.7 $ng/m^3$), Ca (1.1 $ng/m^3$), Cr (2.05 $ng/m^3$), Cu (1.85 $ng/m^3$), Fe (7.00 $ng/m^3$), K (4.8 $ng/m^3$), Mn (1.45 $ng/m^3$), Ni (0.9 $ng/m^3$), Pb (1.05 $ng/m^3$), S (1.55 $ng/m^3$), Si (8.85 $ng/m^3$), Ti (0.25 $ng/m^3$), V (1.7 $ng/m^3$), oraz dla Zn (1.25 $ng/m^3$).

Przyrząd umożliwia prowadzenie badań w rozdzielczości czasowej od 0,5h nawet do 24h. Dzięki temu umożliwia szybkie badania zmienności stężeń w danym rejonie zarówno w przypadku tzw. hot-spotów, ale również w miejscach o minimalnych stężeniach pyłu. Dzięki nawiązaniu współpracy z austriackim oddziałem firmy Horiba Ltd., możliwe było wypożyczenie analizatora PX-375 na cały okres planowanych badań. Dodatkowo, w części badań równolegle wykorzystywano do pomiaru pyłu Teom 1400 firmy Rupprecht & Pataschnick wykorzystujący metodę mikrowagi oscylacyjnej. Przyrząd był zainstalowany z głowicą $PM_{2.5}$, analizator PX-375 pracował z głowicą $PM_{10}$. Równolegle prowadzono pomiary analizatorami MLU100: $SO_2$

(fluorescencja UV), MLU300: CO (niedyspersyjna spektroskopia IR), MLU400: $O_3$ (fotometria UV) oraz MLU200: NO-$NO_2$-NO (chemiluminescencja) (rysunek 1). W każdym z tych przyrządów zastosowano metodykę referencyjną.


*Rysunek 1. Zdjęcie przestawiające zbudowane stanowisko pomiarowe (zdjęcie: zasoby własne)*

W trakcie badań nawiązałem współpracę z Wyższą Szkołą Służby Pożarniczej oraz fińską firmą Dekati, która jest producentem automatycznego niskociśnieniowego impaktora kaskadowego ELPI+. Dzięki tej współpracy wykonaliśmy wspólnie badania polegające na spalaniu różnych materiałów i analizie rozkładu masy, objętości a także liczby ziaren pyłu powstałych w trakcie spalania. Uzyskane charakterystyki pomogą w ocenie pochodzenia zanieczyszczeń pyłowych, a zwłaszcza tych szybkozmiennych. Do przeprowadzenia powyższych badań wykorzystano analizator ELPI+ firmy Dekati. ELPI+ jest automatycznym niskociśnieniowym impaktorem kaskadowym. Przyrząd rozdziela (w sposób grawimetryczny) próbkę pyłu na 14 różnych frakcji w przedziale 0.006 - 10 μm, a zebrany pył na filtrach 25mm umieszczonych w poszczególnych stopniach impaktora, można poddać analizie laboratoryjnej. ELPI+ jednocześnie w sposób automatyczny zlicza cząsteczki zebrane na poszczególnych stopniach impaktora kaskadowego, a następnie wylicza ich masę aerodynamiczną. Do pomiaru automatycznego, wykorzystuje elektryczny układ ładowania cząsteczek (za pomocą ładowarki umieszczonej na wlocie do analizatora), a następnie dokonuje pomiaru ich ładunku elektrycznego na każdym ze stopni impaktora kaskadowego (przy pomocy elektrometrów zlokalizowanych bezpośrednio nad każdym ze stopni impaktora).

## 3. Omówienia prac wchodzących w skład jednolitego cyklu publikacji i zagadnień podnoszonych w publikacjach

(Publ. 1) W artykule przeglądowym *„How to effectively analyse the impact of air quality on society – review of modern measurement techniques and apparaturus: particulates”* [118] omówione zostały dostępne na rynku nowoczesne techniki pomiarowe i aparatura służąca do badań jakości powietrza. Opisana została

budowa automatycznych systemów pomiarowych wykorzystujących takie metody jak:

- metoda mikrowagi oscylacyjnej,
- metody wykorzystujące oddziaływania promieniowania jonizującego z materią - tłumienie promieniowania beta oraz spektrometria promieniowania gamma,
- metody optyczne, oparte o rozpraszanie światła na cząstkach pyłu,
- a także rozwiązania łączące w sobie więcej niż jedną metodę pomiarową.

Dodatkowo porównałem ze sobą stosowane metodyki z uwzględnieniem ich zalet jak i wad, a także pokusiłem się o uszeregowanie prezentowanych rozwiązań z punktu widzenia ich zastosowań dla konkretnych aplikacji. Założeniem publikacji było podsumowanie wiedzy na temat istniejących rozwiązań, a także wskazanie możliwości doboru odpowiedniej aparatury w potencjalnych pomiarach zanieczyszczenia powietrza, w szczególności zanieczyszczeń pyłem zawieszonym. Druga część publikacji dotycząca aparatury służącej do pomiarów zanieczyszczeń powietrza związkami gazowymi (takimi jak $O_3$, $SO_2$, $NO/NO_2/NO_x$, CO, $NH_3$, CO, $H_2S$, $C_6H_6$, czy też formaldehyd) jest ukończona i zostanie niebawem opublikowana.

Badania terenowe w ramach pracy doktorskiej prowadziłem w trakcie kilku niezależnych kampanii pomiarowych w latach 2018-2021. W poniżej opisanych publikacjach korzystałem z danych pomiarowych uzyskanych w trakcie tych kampanii.

W pierwszym etapie badań związanych z realizacją pracy doktorskiej, przeprowadziłem dwie sesje pomiarowe: letnią 2018 i zimową 2019. Po wstępnej analizie wyników pomiarów prowadzonych w sesji zimowej wykonanej w roku 2019 oceniono, że dni w których temperatura powietrza była mniejsza niż 0$^o$C, było dosłownie kilka. A właśnie w dniach kiedy temperatura powietrza jest niska obserwuje się w Polsce znaczny wpływ ogrzewania z palenisk domowych na jakość powietrza atmosferycznego, w tym szczególnie zaznacza się wpływ emisji komunalnej na stężenie pyłu zawieszonego. Aby zaobserwować wpływ niskich temperatur powietrza na zmianę składu pierwiastkowego pyłu zawieszonego, wynikającej ze zwiększonego udziału pyłu pochodzenia lokalnego, postanowiłem przeprowadzić trzecią sesję, w tym samum punkcie pomiarowym, ponownie zimą w roku 2020. Pomiary te zostały wykonane w okresie styczeń – marzec 2020. Tym razem oczekiwanych dni o średniej temperaturze powietrza poniżej 0$^o$C było ok. 20. Wszystkie trzy sesje zrealizowane zostały na stworzonym specjalnie do tych badań, stanowisku pomiarowym. Skupiono się w tych badaniach na pomiarach masy i składu pierwiastkowego $PM_{10}$. Dane z analizatora PX-375 zapisywano z rozdzielczością 1 godzina. Dane z analizatorów TEOM, MLU100, 200, 300, 400 zapisywano z rozdzielczością 1 min. Jako punkt pomiarowy - receptor wybrano rejon w miejscowości Kotórz Mały, w pobliżu umiarkowanie zamieszkałego obszaru wiejskiego (województwo opolskie) – rysunek 2. Wybrano punkt pomiarowy w północnej części wsi zlokalizowany pomiędzy w polami uprawnymi, łąkami i niskimi krzewami. Z okoliczną zabudową domów jednorodzinnych ogrzewanych przy pomocy pieców na paliwa stałe lub płynne, oraz kilkoma warsztatami rodzinnymi (trzy warsztaty serwisów samochodowych, dwa zakłady lakierowania powierzchni metalowych oraz dwie stolarnie, obie wyposażone są w

wysokosprawne systemy odpylania). Poza nimi w wiosce nie występują inne lokalne źródła zanieczyszczeń powietrza. Kotórz Mały jest typowym przykładem dla rejonu Polski, gdzie głównym źródłem zanieczyszczenia powietrza w ciepłych porach roku jest emisja naturalna, natomiast w chłodnych porach roku są to domowe systemy grzewcze, tzw. emisja komunalna. Ponadto, w odległości kilku kilometrów znajdują się dwie drogi krajowe (droga krajowa 45 na północnym zachodzie oraz 46 na południowym wschodzie). Ze względu na położenie makro obszaru badań założono również możliwość zaobserwowania emisji zanieczyszczeń pochodzących z sąsiadujących dużych ośrodków przemysłowych tj:

- od zachodu region Dolnego Śląsak z konglomeratem metalurgicznym KGHM,
- od wschodu Górny Śląsk z przemysłem górniczo-hutniczym,
- oraz usytuowane w okolicach Opola: duża cementowania i nowo powstała elektrownia. (rysunek 2).


*Rysunek 2. Zdjęcia miejsca usytuowania stanowiska pomiarowego (zdjęcie: zasoby własne)*

Wykonanie trzech sesji pozwoliło na zebranie bardzo dużego zestawu danych. Wstępnie wytypowałem też źródła i profile pierwiastkowe $PM_{10}$.

(Publ. 2) Biomonitoring jest ważnym narzędziem ochrony środowiska. Na świecie stosuje się różnorodne bioindykatory, w szczególności mchy, porosty i liście drzew. Jednak mają one pewne wady, np. ich wykorzystanie jest często ograniczone do sezonu wegetacyjnego, mają duże zapotrzebowanie wodne, są też narażone na trudne warunki atmosferyczne, co może skutkować ich zniszczeniem lub

zafałszowaniem wyników . Ograniczeniem jest też sam czas trwania monitoringu. Z tego powodu w pracy dokonano przeglądu aktualnej wiedzy na temat zastosowania sieci pajęczych w monitoringu zanieczyszczeń powietrza, które odznaczają się wieloma cechami bardzo przydatnymi w bioindykacji [115,119-123]. W pracy podsumowano zalety sieci pajęczych, opisano dlaczego jedwab pajęczy jest bardzo wydajnym, nieselektywnym akumulatorem zanieczyszczeń, co pozwala na długoterminowy monitoring. Dzięki swoim unikatowym właściwościom akumulacyjnym pajęczyny okazały się niezwykle użytecznymi bioindykatorami zanieczyszczeń powietrza. W pracy przeanalizowano ich skuteczność w monitorowaniu metali ciężkich, wielopierścieniowych węglowodorów aromatycznych (WWA), dioksyn, czyli ich skuteczność w ocenie działania mutagennego, antropopresji oraz możliwości wskazania dominującego źródła zanieczyszczeń. Większość badań dotyczy zastosowania pajęczyn jako bioindykatorów przeprowadzonych we Wrocławiu. W pracy zestawiono też ich skuteczność w porównaniu do klasycznych metod pomiarowych. Przede wszystkim sieci dają możliwość oceny poziomu zanieczyszczenia powietrza w długim okresie, w przeciwieństwie do klasycznych pomiarów. Poborniki są również drogie i wymagają ciągłego nadzoru. Jedwab pajęczy jest nieselektywnym i wysoce wydajnym naturalnym pasywnym próbnikiem, więc może służyć do monitorowania szerokiego zakresu zanieczyszczeń powietrza, takich jak metale ciężkie, WWA, dioksyny za jednym razem. Praca o charakterze przeglądowym porządkuje wiedzę na temat innych alternatywnych metod stosowanych w ocenie źródeł i pochodzenia i identyfikacji zanieczyszczeń i stanowi solidne wprowadzenie w tematykę badawczą mojej pracy doktorskiej.

(Publ. 3) Prowadząc badania pomiarowe w Kotorzu Małym nawiązałem współpracę z doktorantką Agnieszką Stojanowską, która badała w ramach swojej pracy doktorskiej użyteczność sieci pajęczych w biomonitoringu zanieczyszczeń powietrza (czyli testował użyteczność wykorzystania do pomiarów zanieczyszczeń powietrza, takich materiałów jak sieci pajęcze). Efektem naszej współpracy jest publikacja *„Air Pollution Research Based on Spider Web and Parallel Continuous Particulate Monitoring—A Comparison Study Coupled with Identification of Sources”.* W niniejszej publikacji porównano stężenie metali uzyskane z monitoringu pajęczyn przy użyciu atomowej absorpcyjnej spektrometrii płomieniowej (F-AAS) z wynikami pomiarów składu pierwiastkowego pyłu zawieszonego $PM_{10}$ wykonywanych metodą fluorescencji rentgenowskiej (XRF). z dyspersją energii (EDXRF) gdzie wykorzystano analizator Horiba PX-375.

Sprawdzono również zależności między wynikami uzyskanymi z obu metod. Głównym celem badań naszych wspólnych była weryfikacja i walidacja wyników metody bioindykacyjnej z danymi EDXRF.. Dodatkowym celem mojej współpracy, było nabranie doświadczenia i wiedzy na temat stosowanych przez innych naukowców metod analitycznych oraz sposobów opracowywania modeli. Umiejętności te były przydatne do opracowywania dużych ilości danych pomiarowych uzyskanych z kolejnych kampanii pomiarowych.

W bioindykacji ocena zanieczyszczenia środowiska może być realizowana z wykorzystaniem organizmów żywych (jak porosty, mchy, liście drzew) lub ich wytworów, np. pajęczyny. Stosownie pajęczyn w badaniach jest dość nowatorskim

pomysłem, ale zostało już udowodnione, że narzędzie to może zapewnić wiarygodne wyniki, zwłaszcza w przypadku akumulacji potencjalnie toksycznych pierwiastków (potentially toxic elements PTE). W trakcie prowadzonych sesji pomiarowych w roku 2019, równolegle do automatycznych pomiarów realizowanych przeze mnie analizatorem EDXRF, rozłożono wokół stacji pomiarowej czyste sieci pajęcze (wyhodowane w laboratorium) kumulujące pył zawieszony PM. Podsumowując eksperyment, monitoring z wykorzystaniem pajęczyn i przyrządów automatycznych może dawać zadowalające rezultaty, ale ich porównanie nie zawsze jest jednoznaczne. Jest to spowodowane różnymi mechanizmami akumulacji cząstek. Wykazano, że stężenia większości pierwiastków, z wyjątkiem cynku Zn, były wyższe w przypadku pajęczyn, co wskazuje na to, że część cząstek może występować w rozmiarach większych niż $PM_{10}$ (których to frakcji pyłu, analizator PX-375 z zainstalowaną w trakcie badań głowicą odcięcia $PM_{10}$ nie analizował). Prowadziło do różnic uzyskanych wyników pomiędzy obiema metodami. Jednakże, stwierdzono,że udział procentowy wybranych pierwiastków jest bardzo podobny w obu metodach, a różnice w wynikach można wyjaśnić, faktem pochodzenia cząstek i występowania danych pierwiastków w różnych frakcjach. Dodatkowo zaobserwowano, że kolejność występowania pierwiastków była podobna. Warto, jednak w przyszłości wykonać, bardziej szczegółowe badania zwłaszcza korelacji pomiędzy PTE w innych frakcjach ($PM_{2.5}$, pyłu całkowitego TSP). Przeprowadzenie w trakcie wyżej opisanych badań, analizy związanej z tworzeniem modelu częstotliwości trajektorii wstecznych (HYSPLIT), pozwoliły na pozyskanie umiejętności, które zostały wykorzystane w kolejnych moich pracach. Przygotowanie danych wejściowych i założeń do zamodelowania trajektorii wstecznych (HYSPLIT) jest konieczne do oceny pochodzenia pyłu. Na podstawie składu pierwiastkowego pyłu możliwe jest wyznaczenie wstecz do 48h pochodzenia mas powietrza w danym punkcie pomiarowym (kierunków z których powietrze napływało).

(Publ. 4) W publikacji pod tytułem *"Analiza godzinowej zmienności składu pierwiastkowego i źródeł PM10 : studium przypadku obszaru wiejskiego w południowej części Polski"*, zaprezentowane zostały wyniki pomiarowe uzyskane w trakcie pierwszej sesji pomiarowej wraz z analizą statystyczną. Średnio w okresie kampanii pomiarowej tj. 3-31 stycznia, badane w trakcie pomiarów pierwiastki związane z pyłem $PM_{10}$ można było uszeregować następująco pod względem stężenia w powietrzu: As<V<Ni<Pb<Cr<Mn<Cu<Ti<Zn<K<Fe<Ca<Al<Si<S (Tabela 1).

| Mierzony parametr | Statystyki opisowe | | | | |
|---|---|---|---|---|---|
| | N ważnych | Średnia | Minimum | Maksimum | Odch. std |
| PM10, µg/m$^3$ | 29 | 20,8 | 7,1 | 48,4 | 7,5 |
| Al, ng/m$^3$ | 29 | 357,2 | 76,4 | 675,0 | 154,9 |
| As, ng/m$^3$ | 29 | 0,5 | 0,0 | 4,5 | 1,0 |
| Ca, ng/m$^3$ | 29 | 256,2 | 64,6 | 517,5 | 134,1 |
| Cr, ng/m$^3$ | 29 | 6,1 | 5,2 | 7,3 | 0,5 |
| Cu, ng/m$^3$ | 29 | 11,2 | 7,1 | 22,8 | 3,1 |

| | | | | | |
|---|---|---|---|---|---|
| Fe, ng/m$^3$ | 29 | 195,2 | 63,9 | 355,4 | 77,1 |
| K, ng/m$^3$ | 29 | 76,7 | 5,4 | 132,5 | 34,3 |
| Mn, ng/m$^3$ | 29 | 6,9 | 3,0 | 12,7 | 2,5 |
| Ni, ng/m$^3$ | 29 | 5,4 | 4,5 | 8,5 | 0,9 |
| NO, µg/m$^3$ | 29 | 1,0 | 0,5 | 2,8 | 0,5 |
| NO2, µg/m$^3$ | 29 | 6,2 | 3,1 | 8,2 | 1,3 |
| O3, µg/m$^3$ | 16 | 25,1 | 19,3 | 33,1 | 3,8 |
| Pb, ng/m$^3$ | 29 | 6,1 | 1,4 | 14,9 | 3,9 |
| S, ng/m$^3$ | 29 | 1485,5 | 556,7 | 2352,4 | 487,4 |
| Si, ng/m$^3$ | 29 | 770,3 | 98,5 | 1722,8 | 455,8 |
| SO2, µg/m$^3$ | 29 | 3,4 | 1,8 | 4,9 | 0,9 |
| Ti, ng/m$^3$ | 29 | 12,8 | 0,3 | 54,8 | 11,7 |
| V, ng/m$^3$ | 29 | 2,1 | 1,8 | 2,5 | 0,2 |
| Zn, ng/m$^3$ | 29 | 14,5 | 4,4 | 37,6 | 7,7 |
| CO, µg/m$^3$ | 16 | 0,4 | 0,2 | 0,5 | 0,1 |
| Temperatura max., st. C | 29 | 27,8 | 19,0 | 32,6 | 3,4 |
| Temperatura min., st. C | 29 | 14,8 | 10,5 | 18,6 | 2,2 |
| Temperatura śr., st. C | 29 | 21,1 | 16,8 | 25,6 | 2,3 |
| Wilg. powietrza, % | 29 | 67,6 | 47,7 | 97,7 | 13,8 |
| Prędkość wiatru, m/s | 29 | 7,1 | 4,2 | 11,7 | 1,9 |
| Ciśnienie atmosferyczne, hPa | 29 | 1013,7 | 1008,2 | 1017,4 | 2,4 |
| Opad atmosferyczny, mm | 29 | 1,7 | 0,0 | 12,0 | 3,6 |

*Tabela 1. Przykładowe statystyki opisowe stężeń dobowych badanych parametrów*

Potwierdziło się, że pierwiastki śladowe, w tym toksyczne, takie jak As, V, Ni, Pb, Cr, Mn występowały w bardzo niskich stężeniach, nieprzekraczających 10 ng/m$^3$ (jest to średniodobowa wartość). Pierwiastki te miały dość wyrównane stężenia zarówno średniodobowe oraz średniogodzinowe. Niewielki wzrost stężeń większości z powyższych pierwiastków śladowych, jak i stężeń $PM_{10}$ zaobserwowano w godzinach 12.00-14.00. Potwierdziło się także, że stężenia pierwiastków głównych w pyle $PM_{10}$ w badanym receptorze podlegały silnym zmianom godzinowym związanym ze zmiennością źródeł i ze zmianami prędkości i kierunku wiatru, co wykazano stosując analizę PCA wskazującą pochodzenie badanych zanieczyszczeń zanieczyszczenia. Liczba wariancji wyjaśniona przez główne składniki zmieniała się z godziny na godzinę, co sugeruje zmienność wpływu różnych źródeł emisji w ciągu dnia. Stwierdzono też, że składowe główne charakteryzują się źródłami PM10, których wydajność zmieniała się nie tylko zgodnie z kierunkiem wiatru, ale także z jego prędkością, która decyduje o odległości, na jakie przenoszone są zanieczyszczenia.

Dodatkowo należy również zauważyć, że wyniki uzyskane przy pomocy analizy składowych głównych (PCA), wskazują, że w godzinach popołudniowych w badanym okresie może oddziaływać intensywnie emisja komunikacyjna w punkcie pomiarowym (rysunek 3).

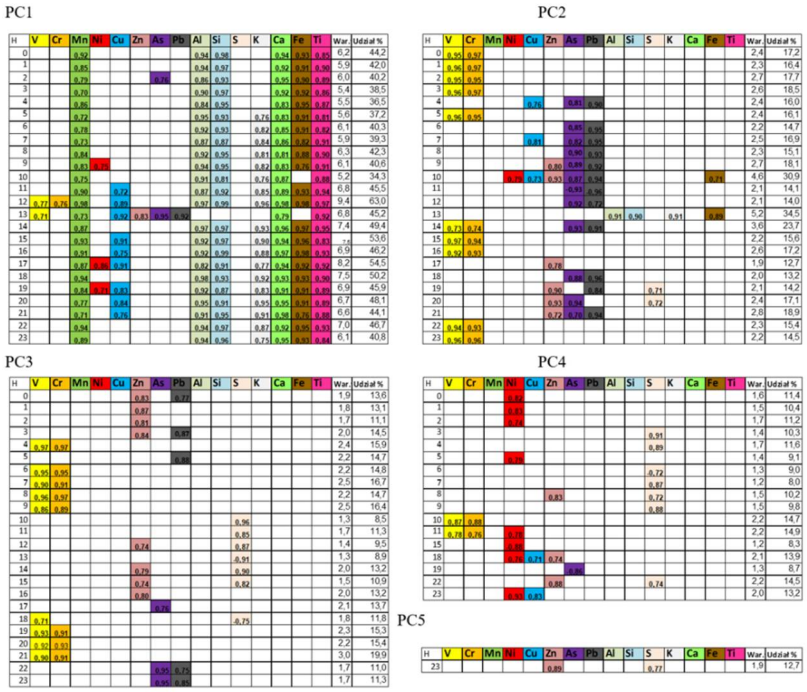


*Rysunek 3.* Zbiorcze zestawienie wyników analizy składowych głównych (PCA) wykonanej dla danych godzinowych o składzie pierwiastkowym PM10. Dla każdej godziny wykorzystano 29 danych, a w tabelach zestawiono tylko te pierwiastki, które każdorazowo skorelowane były z nowymi zmiennymi PC1-PC5 (współczynnik korelacji r > 0.7).

Wykazano zatem, że w typowym obszarze wiejskim w południowej części Polski na skład pierwiastkowy $PM_{10}$ zauważalnie wpływa emisja ze spalania węgla bez względu na porę dnia. Zaobserwowano (szczególnie nocą i we wczesnych godzinach porannych) znaczący wpływ emisji komunalnych pochodzących z okolicznych budynków na skład pierwiastkowy $PM_{10}$. Wykazano, że emisje transportowe mierzone w wybranym receptorze mogą mieć intensywny wpływ na $PM_{10}$ w godzinach popołudniowych. Prezentowana praca była pierwszą w jakiej udowodniono, że pomiary składu pierwiastkowego prowadzone w krótkim okresie czas tj. 28 dni (3-31 stycznia) pozwalają na dość precyzyjne określenie pochodzenia PM pod warunkiem zastosowania rozdzielczości czasowej tych pomiarów co najmniej 1 godzina. Pozwala to na uchwycenie zmienności oddziaływania poszczególnych źródeł równolegle z obserwacjami zmieniającej się intensywności ich oddziaływania w ciągu dnia.

(Publ. 5) W publikacji *“Impact of municipal, road traffic, and natural sources on PM10: the hourly variability at a rural site in Poland”*, przeanalizowano i zaprezentowano dane z miesięcznej kampanii pomiarowej (od 3 do 31 lipca 2018 roku). Stężenie masowe pyłu $PM_{10}$ i stężenia występujących w nim pierwiastków Al, As, Ca, Cr, Cu, Fe, K, Mn, Ni, Pb, S, Si, Ti, V i Zn były mierzone z godzinową częstotliwością przy wykorzystaniu automatycznego analizatora do pomiarów ciągłych Horiba PX-375. Poza stężeniem

pyłu $PM_{10}$ i jego składu pierwiastkowego badano również zmienność godzinową stężeń zanieczyszczeń powietrza dla następujących związków gazowych:

- Pomiar $SO_2$ (za pomocą automatycznego analizatora API-MLU100, który jest oparty na zasadzie fluorescencji UV).
- Pomiar $NO/NO_2/NO_x$ (za pomocą automatycznego analizatora MLU200A, analizator ten oparty jest na zasadzie detekcji chemiluminescencji).
- Pomiar $O_3$ (za pomocą automatycznego analizatora MLU400A, jako metodę pomiaru wykorzystuje on fotometrię UV).
- Pomiar CO (za pomocą automatycznego analizatora MLU400A, który jest oparty na zasadzie niedyspersyjnej spektroskopii w podczerwieni).

Równolegle, prowadzono również pomiar parametrów meteorologicznych w tym: temperatury powietrza, wilgotności względnej, prędkości wiatru, kierunku wiatru - za pomocą urządzeń Gill Windsonic 2D oraz LSI DMA572.

W tej pracy wykazano, że niezależnie od faktu, że w badaniach wykorzystano dane z okresu letniego, w receptorze zlokalizowanym w typowym obszarze wiejskim w południowej części Polski, wpływ emisji ze spalania węgla na skład pierwiastkowy pyłu zawieszonego $PM_{10}$ jest zauważalny niemal w każdej godzinie doby. W okresie pomiarowym, szczególnie w nocy i we wczesnych godzinach porannych, zaobserwowano wyraźny wpływ emisji komunalnej na skład pierwiastkowy pyłu $PM_{10}$. Jest to prawdopodobnie skutek tego, że produkcja energii elektrycznej i cieplnej w Polsce oparta jest na spalaniu węgla (elektrownie i elektrociepłownie). Dlatego też nawet w sezonie letnim wpływ ten jest zauważalny i widać wyraźnie, że produkcja energii o jedno z głównych źródeł PM, nawet w rejonie gdzie nie ma aktywnych w sezonie letnim lokalnych źródeł tego typu. Jednak emisja naturalna (gleba, piasek) oraz spaliny pochodzące z ruchu pojazdów miały silniejszy i bardziej dominujący wpływ na skład pierwiastkowy pyłu zawieszonego $PM_{10}$ w okresie badawczym. Jest wysoce prawdopodobne, że gdyby analizę pochodzenia pyłu $PM_{10}$ w tym okresie pomiarowym przeprowadzono na podstawie danych dobowych o składzie pierwiastkowym pyłu $PM_{10}$, jak to zwykle bywa w tego typu badaniach (zbierane są i analizowane próbki dobowe), to wpływ innych źródeł nie zostałby zauważony. Wykazano zatem, że wykorzystując godzinowe stężeń wybranych pierwiastków, możliwa jest ocena pochodzenia pyłu $PM_{10}$ oraz i zmienności udziału wybranych źródeł w kształtowaniu stężeń pyłu w ciągu doby, nawet przy wykorzystaniu danych ze stosunkowo krótkiego okresu pomiarowego.

Jak wynika z przeprowadzonej analizy PCA, wielkość wariancji układu opisanej przez poszczególne składowe główne zmienia się w zależności od godziny, co sugeruje zmienność wpływu różnych źródeł emisji w ciągu doby. Ponadto, przeprowadzone badania i obserwacje pozwalają stwierdzić, że udział kolejnych składowych charakteryzujących konkretne źródła $PM_{10}$ zmieniał się nie tylko wraz z kierunkiem wiatru, ale również wraz z jego prędkością, co bezpośrednio pokazuje wpływ transportu zanieczyszczeń w atmosferze na lokalne stężenia PM i związanych z nim pierwiastków.

(Publ. 6) W kolejnej publikacji "*Impact of municipal, road traffic, and natural sources on PM10: the hourly variability at a rural site in Poland"* porównana została zgodność

wyników, uzyskanych różnymi technikami pomiarowymi (w okresach zimowym i wiosennym). Do badania stężeń $PM_{10}$ oraz ich składu chemicznego wykorzystałem dwie kombinacje różnych metodyk pomiarowych:

- metodę grawimetryczną z atomową spektrometrią absorpcyjną (GM+AAS);
- ciągły pomiar PM metodą tłumienia promieniowania β wraz z fluorescencją rentgenowską z dyspersją energii (CPM+EDXRF).

Na podstawie wykonanych badań wywnioskowano, że zimą średnie w całym okresie pomiarowym stężenia $PM_{10}$ mierzone przy pomocy metody grawimetrycznej oraz tłumienia promieniowania β były do siebie bardziej zbliżone (GM 44,3 $\mu g/m^3$; CPM 34,0 $\mu g/m^3$),niż wiosną (GM 49,5 $\mu g/m^3$; CPM 29,8 $\mu g/m^3$). W przypadku obu metod pomiarowych składu pierwiastkowego pyłu - AAS i EDXRF - stwierdziłem, że w obu sezonach największy udział w masie $PM_{10}$ miały Ca, K i Fe. Jeśli chodzi o stężenia masowe pierwiastków śladowych, czyli tych o najniższym udziale w masie $PM_{10}$, to wskazania obu metod dla całego okresu pomiarowego różniły się wyraźnie. Niemniej według danych uzyskanych przy pomocy AAS i EDXRF najniższe stężenia w obu okresach pomiarowych (zima i wiosna) obserwowano dla Ni i Cr. Najwyższe stężenia zaobserwowano dla Ca, Fe oraz K. Do wyznaczenia rodzajów źródeł mających wpływ na jakość powietrza w obrębie badanego receptora zastosowałem analizę czynnikową (Factor Analysis). Aby uniknąć problemu ze zbyt małą liczbą zmiennych w stosunku do przypadków, w analizie wybrałem tylko dane o stężeniach tych pierwiastków, które wykazały wysoką korelację dla obu zastosowanych technik pomiarowych, czyli Ca, Cu, Fe, Mn i Zn. W tej grupie były pierwiastki zwyczajowo uważane za pochodzące zarówno z emisji naturalnych, ale również z emisji wywołanych przez człowieka (antropogenicznych). Analiza czynnikowa wykazała, że jakość powietrza w receptorze była determinowana przez erozję gleby, spalanie węgla i biomasy w okolicznych budynkach oraz spalanie paliw w silnikach spalinowych. Wiosną na jakość powietrza wpływała również działalność rolnicza. Dodatkowo, stwierdziłem istotny wpływ temperatury i opadów atmosferycznych na stężenia pyłu $PM_{10}$. Zastosowanie kilku metod analitycznych pozwoliło mi, na precyzyjne określenie czynników wpływających na stężenia badanych zanieczyszczeń. Podsumowując, na podstawie wykonanych badań, stwierdziłem, że badania porównawcze: metoda grawimetryczna + atomowa spektrometria absorpcyjna vs. ciągły pomiar PM metodą tłumienia promieniowania β + fluorescencja rentgenowska z dyspersją energii wykazały, że nawet niewielka odległość (w przypadku realizowanych badań było to 18 m) może wpływać na zmienność wyników i pewne różnice w stężeniach pyłu zawieszonego $PM_{10}$ oraz jego składu pierwiastkowego.

(Publ. 7 i 8) Efektem wspólnych badań z Wyższą Szkołą Służby Pożarniczej są publikacje:

- *“Characteristics of particles emitted from waste fires - a construction materials case study”,*
- *“High time-resolution measurements of particulate size distribution in controlled fires of construction materials”.*

Zaprezentowana została w nich analiza wyników wspólnych badań z eksperymentu, polegającego na spalaniu w zamkniętym pomieszczeniu popularnych materiałów użytkowych i analizie emisji pyłu zawieszonego pod kątem rozkładu frakcyjnego.
Utylizacja odpadów stanowi duży problem cywilizacyjny człowieka. Zarówno kraje rozwinięte jak i i rozwijające się mierzą się z problemem sposobu utylizacji coraz to nowszych produktów lub ich opakowań. Pomimo prób ograniczania produkcji odpadów, poddawania recyklingowi coraz to większej ich ilości, w najbliższej przyszłości nie ma szans na przejście człowieka na gospodarkę bezodpadową. Dlatego stosowane są różne metody neutralizacji odpadów [124]. Poza najpopularniejszą metodą utylizacji jaką jest składowanie, coraz częściej stosuje się również ich spalanie w zawodowych spalarniach odpadów. Dodatkowo w Polsce, często mamy do czynienia z nielegalnym spalaniem odpadów zarówno w celach komunalnych (dogrzewaniem nimi budynków mieszkalnych), jak i ze spalaniem odpadów na nielegalnych czy legalnych wysypiskach śmieci, spalaniem odpadów rolnych, wypalaniem łąk, czy też spalaniem odpadów powstających w pozamiejskich gospodarstwach domowych [125-126]. Dlatego niezwykle ważne jest ograniczenie tego typu nielegalnego spalania odpadów, i aby móc je ograniczyć, konieczna jest szybka identyfikacja miejsca i czasu takiego zdarzenia. Z powyższych względów, istotne dla mnie było zidentyfikowanie i charakterystyka cząstek stałych z takich procesów. W tym celu kolejną sesję pomiarową przeprowadziłem w lutym 2020 przy współpracy ze Szkołą Główną Służby Pożarniczej (SGSP). Wykonałem dwudniowe badania, których celem było wyznaczenie i matematyczny opis rozkładu masy, objętości i liczby ziaren pyłu względem średnicy aerodynamicznej powstałych podczas spalania różnego rodzaju materiałów (Rysunek 4).

*Rysunek 4. zdjęcia miejsce usytuowania stanowiska pomiarowego (zdjęcie: zasoby własne)*

Znajomość parametrów rozkładu (średnicy medialnej i odchylenia geometrycznego) pozwala identyfikować pochodzenie pyłu w danym obszarze i umożliwia powiązanie epizodów pochodzących zarówno z pożarów jak i spalania odpadów przez człowieka ze zmianami tych parametrów, które są charakterystyczne dla dowolnego miejsca i czasu. Obiektem badań były popularne materiały stosowane w budownictwie i meblarstwie:

- drewno sosnowe, jako jedno z najpopularniejszych materiałów budowlanych stosowanym do budowy domów jednorodzinnych i innych mniejszych zabudowań, również popularne w przemyśle meblarskim,
- płyta wiórowa laminowana, jako najpopularniejszy aktualnie materiał wykorzystywany w branży meblarskiej,
- poliuretan, wykorzystywany praktycznie w każdej nowoczesnej branży przemysłowej, m.in. do wyrobu żywic lanych, miękkich i twardych pianek, lakierów, klejów, włókien poliuretanowych, kauczuków itp.
- poli(metakrylan metylu), podobnie jak poliuretan mający wiele zastosowań, m.in. dekoracje stoisk oraz elementy wyposażenia sklepów, przeszklenia i ścianki działowe, tablice podświetlane, panele reklamowe, ekspozycje sklepowe, reflektory i owiewki samochodowe, przeszklenia szklarni i ogrodów zimowych, bariery dźwiękochłonne, wypełnienia drzwi i wiele innych.

W trakcie badań wykorzystaliśmy cztery wyżej opisane materiały oraz ich mieszankę. Badania były wykonywane w pomieszczeniu o kubaturze 75m$^3$. Miejsce spalana było usytuowane bezpośrednio obok zestawu pomiarowego. Zastosowaliśmy dwie metodyki pomiarowe: niskociśnieniowy elektryczny impaktor kaskadowy do pomiaru liczby cząsteczek i ich objętości, oraz ważenie filtrów (pochodzących z ww. impaktora) do określenia masy zebranych cząsteczek. Do badań wykorzystaliśmy elektryczny niskociśnieniowy impaktor kaskadowy ELPI+® fińskiego producenta Dekati, za pomocą którego to wyznaczone zostały rozkład liczby oraz objętości cząstek pyły, jednocześnie na każdym ze stopni impaktora zainstalowaliśmy aluminiowe folie 25mm w celu zebrania próbki pyłu i wyznaczenia masy (metodą grawimetryczną) poszczególnych frakcji rozmiarowych. Wyniki badań pozwoliły dokonać pełnej charakterystyki populacji cząstek emitowanych w trakcie spalania wybranych materiałów. Zatem pozwoliły na poszerzenie stanu wiedzy w tym zakresie jako, że do tej pory badań takich nie wykonywano. Co więcej, uzyskane dane będzie można w przyszłości wykorzystać do lepszej identyfikacji źródeł pochodzenia cząsteczek i lepszego ilościowego przypisania emisji do zidentyfikowanych źródeł. Ma to znaczenie zwłaszcza w obszarach gdzie zanieczyszczenia powietrza pochodzą z wielu źródeł jednocześnie i wpływ tych źródeł trudno jest jednoznacznie skwantyfikować.

(Publ. 9, 10) Kolejne publikacje prezentują wyniki pomiarowe pozyskane podczas kampanii pomiarowej przeprowadzanej w sierpniu 2020 roku. Przeanalizowano dobową i godzinową zmienność krytycznych pierwiastków wchodzących w skład mierzonego pyłu, zarówno $PM_{10}$ jak i $PM_{2.5}$ oraz przeprowadzono identyfikację źródeł pochodzenia ich emisji:

- *„Dobowa i godzinowa zmienność stężeń Pb, Ni, Zn, Mn, i V w powietrzu atmosferycznym: badania pilotażowe w wybranym receptorze centralnej Polski”,*
- *„Quasi real-time XRF spectrometer in source apportionment of PM10 in a typical suburban area”.*

W otaczającym nas powietrzu atmosferycznym, a dokładnie rzecz biorąc w pyle zawieszonym występuje ponad 40 pierwiastków śladowych. Takie pierwiastki jak: Arsen (As), Kadm (Cd), Chrom (Cr), Rtęć (Hg), Mangan (Mn), Nikiel (Ni), Ołów (Pb) i

Vanad (V) –zostały wpisane na listę 35 substancji niezwykle niebezpiecznych dla zdrowia i życia człowieka przez Światową Organizację Zdrowia (WHO) [127]. Równolegle według klasyfikacji Międzynarodowej Agencji Badań nad Nowotworami (IARC) pierwiastki takie jak As, Cd, Cr (VI) i Ni klasyfikuje się jako te które w istotny sposób przyczyniają się do nowotworowych. Pierwiastki śladowe w pyle mogą pochodzić ze źródeł naturalnych, np. parowania mórz i oceanów, erozji gleb czy też wybuchów wulkanów oraz z działalności człowieka (pochodzenie antropogeniczne), czyli ze spalania paliw, odpadów, a także wszelkiego rodzaju działalności przemysłowej, m.in. takiej jak wytapiania i produkcji metali, stopów metali, itp. [1]. W zurbanizowanych obszarach Polski najpoważniejszym źródłem pierwiastków śladowych, w tym zwłaszcza tych toksycznych i kancerogennych, jest spalanie paliw stałych i płynnych [2]. Emisja zanieczyszczeń pochodzenia komunikacyjnego (wszelkiego rodzaju transport zbudowany gównie na silnikach spalinowych) stanowi w wielu polskich miastach zasadniczy problem zanieczyszczenia powietrza większością metali. Powoduje to tym samym największy masowy udział wielu metali, w tym metali toksycznych, w pyle drobnym $PM_{2.5}$. [128-129]. Spowodowane jest to głównie ze względu na sposób procesów rządzących tego typu emisją: kondensacja i zestalanie par metali. Natomiast we frakcjach grubego pyłu udział różnych pierwiastków kształtowany jest zazwyczaj przez źródła naturalne oraz szereg różnego rodzaju procesów mechanicznych [130]. Tematykę tą starałem się zagłębić w publikacjach:

Następną sesję pomiarową poświęciłem zatem charakterystyce składu pierwiastkowego i pochodzenia pyłu w obszarze, gdzie parametry te jak dotąd pozostają słabo rozpoznane. Wybrałem okres pomiarowy w sierpniu 2020 r. (celowo poza okresem grzewczym). Była to dwutygodniowa kampania poświęcona strefie podmiejskiej w województwie mazowieckim. W pierwszym tygodniu badań analizowany był pył zawieszony $PM_{2.5}$ i jego skład pierwiastkowy, a w drugim tygodniu pył zawieszony $PM_{10}$ wraz z analizą jego składu elementarnego. W tym przypadku punkt pomiarowy został zlokalizowany na skrzyżowaniu tras komunikacyjnych w odległości ok. 9m od osi drogi oraz w sąsiedztwie typowego osiedla mieszkaniowego (Rysunek 5). Skrzyżowanie to jest stosunkowo ruchliwe i często (zwłaszcza w godzinach porannych i popołudniowych) dochodzi na nim do zatrzymań ruchu związanych z dużym natężeniem skrętów pojazdów w lewo na skrzyżowaniu. Skrzyżowanie to nie posiada sygnalizacji świetlnej. W godzinach szczytu komunikacyjnego korki do tego skrzyżowania osiągają nawet do 1 km długości. W okolicach skrzyżowania znajduje się dodatkowo sklep spożywczy z parkingiem (jeden z większych w okolicy). W niedalekiej odległości od punktu pomiarowego przebiega zelektryfikowana linia kolejowej Warszawa-Białystok oraz zlokalizowana jest nieduża elektrociepłownia.

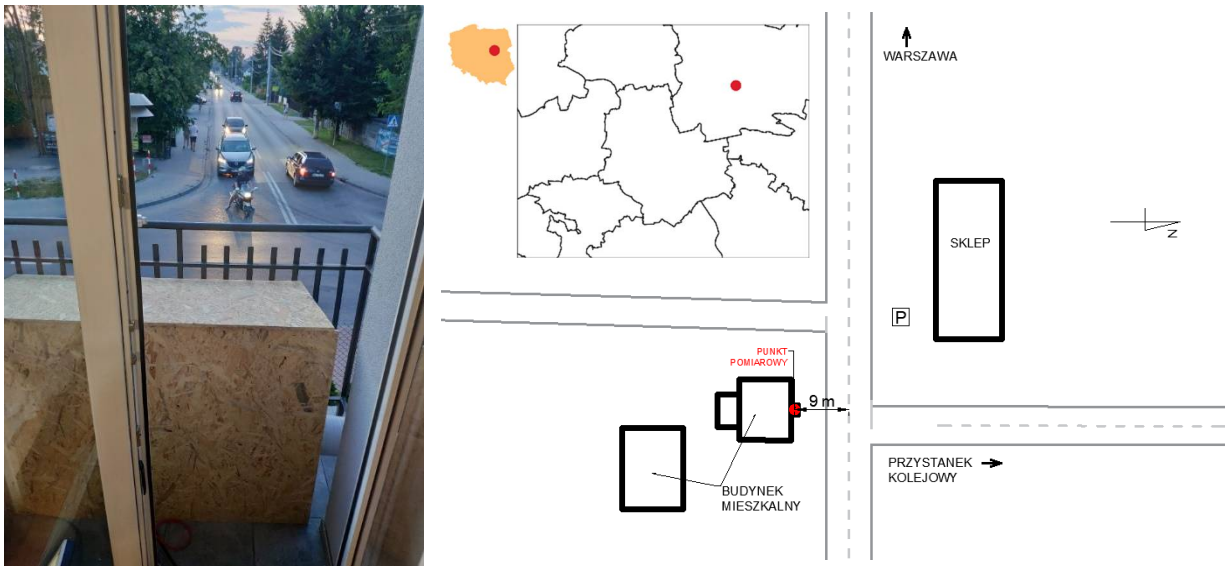


*Rysunek 5. zdjęcie i schemat lokalizacji punktu pomiarowego, który przedstawia miejsce przeprowadzonych badań względem granic Warszawy jak i usytuowanie aparatury pomiarowej przy skrzyżowaniu [opracowanie własne]*

Do badań został wykorzystany analizator Horiba PX-370. Za pomocą tego urządzenia w badanym receptorze z częstotliwością godzinową została zmierzona masa pyłu $PM_{2.5}$ lub $PM_{10}$ oraz stężenia V, Mn, Ni, Zn i Pb.

Zasadniczym celem przeprowadzonych prac było określenie godzinowej oraz dobowej zmienności stężeń wybranych pierwiastków (Pb, Ni, Zn, Mn i V) związanych z drobnym pyłem zawieszonym $PM_{2.5}$ w typowym ośrodku miejskim pod Warszawą. Pierwiastki które zostały wytypowane do badań są zazwyczaj wskazywane jako tzw. markery oddziaływania emisji komunikacyjnej, a punkt pomiarowy jest miejscem o znacznym narażeniu na oddziaływanie takiej emisji [131]. Kolejnym istotnym celem przeprowadzonych badań była próba udowodnienia, że wyniki godzinowej zmienności stężenia pyłu oraz jego składu elementarnego mogą być stosowane do prostej i szybkiej identyfikacji poszczególnych źródeł emisji oraz oceny jakościowej wpływu konkretnego źródła emisji na ich stężenie w powietrzu atmosferycznym. Analizując przebieg średnich stężeń dobowych, nie zaobserwowaliśmy znaczących różnic w ich odczytach w trakcie kolejnych siedmiu dni pomiarowych. Zmienność (stężeń $PM_{2.5}$ oraz badanych pierwiastków V, Mn, Ni, Zn i Pb) zarówno godzinowa jak i dobowa nie była duża. Może to być związane z faktem, że w trakcie realizacji prac, jakość powietrza badanym receptorze była bardzo dobra. Średnio stężenie dobowe $PM_{2.5}$ nie przekraczało 14μg/m$^3$. Czynnikiem warunkującym stężenia badanych substancji i ich zmienność w sezonie letnim była intensywność emisji związanej z ruchem drogowym. W pracy wykazano, że nawet przy bardzo krótkim okresie pomiarowym zastosowanie analizatora umożliwiającego pomiar stężenia pyłu oraz jego składu pierwiastkowego z dużą rozdzielczością czasową, pozwala na jakościowe powiązanie niektórych pierwiastków śladowych w powietrzu ze źródłami emisji. Najlepsze rezultaty w tym zakresie daje analiza zmienności godzinowej stężeń tych pierwiastków w ciągu doby. Oczywistym jest, że zastosowanie urządzeń typu Horiba PX-375 w systemie monitoringu jakości powietrza w Polsce pozwala prowadzić ten monitoring znacznie wydajniej. Przyrządy takie zamiast wieloletnich pomiarów umożliwiłyby pomiary w

krótkich okresach czasowych (np. miesiąc w okresie letnim oraz kolejny miesiąc w okresie zimowym) z wysoką dokładnością a dalej na podstawie uzyskanych wyników ocenić pochodzenie występującego w danym receptorze pyłu i związanych z nim priorytetowych metali. Takie podejście w dalszej kolejności pozwala wyznaczyć dużo dokładniej niż ma to miejsce obecnie, przestrzenne zmiany stężenia w Polsce, a na tej podstawie narażenie mieszkańców w wielu rejonach kraju, co obecnie jest niemożliwe.

W drugim tygodniu badań do realizacji zastosowano ten sam zestaw pomiarowy i taką samą metodykę pomiarową. Jedną różnicą było zdemontowanie cyklonu $PM_{2.5}$ odcinającego frakcje pyłu o rozmiarach powyżej $PM_{2.5}$. W związku z tym, w drugim tygodniu sesji pomiarowej, analizowaliśmy pył zawieszony $PM_{10}$ wraz z jego składem pierwiastkowym. Tym razem oznaczono stężenia Ti, V, Cr, Mn, Fe, Ni, Cu, Zn, Pb, Al, Si, S, K oraz Ca. Dane zbierano przez 7 pełnych dni uzyskując 168 danych pomiarowych. Aby określić wpływ źródeł antropogenicznych na skład pierwiastkowy mierzonego pyłu obliczono współczynniki wzbogacenia $EF$ [132], (wzór 1). Wyraża on stosunek współczynnika wpływu czynnika pochodzenia antropogenicznego $CF_n$ dla badanego pierwiastka $n$ podzielony przez tenże współczynnik dla pierwiastka referencyjnego $CF_{ref}$. Współczynnik $CF$ jest stosunkiem stężenia badanego pierwiastka w $PM_{10}$ $C_n$ podzielony przez stężenie w otoczeniu $C_{n,b}$.

$$EF_n = \frac{CF_n}{CF_{ref}} = \frac{\frac{C_n}{C_{n,b}}}{\frac{C_{ref}}{C_{ref,b}}} \qquad (1)$$

Stężenia pierwiastków występujące w górnej skorupie ziemskiej, zostały uznane za wartości tła [128]. Glin często występuje w literaturze jako pierwiastek odniesienia [116, 129-130]. Wyznaczone wartości współczynników EF mieszczą się w pięciu klasach, dla których wzbogacenie $PM_{10}$ w konkretny pierwiastek jest:

- dla współczynnika EF≤2 wzbogacenie $PM_{10}$ w $n$ pierwiastek jest minimalne,
- dla współczynnika 2<EF≤5 wzbogacenie $PM_{10}$ w $n$ pierwiastek jest umiarkowane,
- dla współczynnika 5<EF≤20 wzbogacenie $PM_{10}$ w $n$ pierwiastek jest istotne,
- dla współczynnika 20<EF≤40 wzbogacenie $PM_{10}$ w $n$ pierwiastek jest bardzo wysokie,
- dla współczynnika EF>40 wzbogacenie $PM_{10}$ w $n$ pierwiastek jest ekstremalnie wysokie [136].

Analiza współczynników EF została przeprowadzona niezależnie dla każdego przedziału czasowego, dzięki czemu uzyskano informację na temat czasowej zmienności wzbogacenia $PM_{10}$ dla każdego z badanych pierwiastków.

Ponadto, przeprowadzono analizę składowych głównych PCA [134, 137-142]. W trakcie prowadzonych analiz wyodrębniono 4 główne składowe PC niezależnie dla wszystkich przyjętych przedziałów czasowych dla czternastu mierzonych pierwiastków. Przed wyznaczeniem składowych głównych PC1-PC4 przeprowadzono standaryzację danych pomiarowych, których dotyczyła analiza. Dalej, porównano także podobieństwo pierwszych, drugich składowych, przy pomocy podobieństwa kosinusowego r_C opisanego dla PC wzorem (2). Przy czym:

- PCn jest wektorem n-tej składowej głównej,
- a t1,t2 to dwie różne strefy czasowe.

r_C (PCn_t1,PCn_t2 )=|PCn_t1·PCn_t2 | (2)

We wszystkich badanych przedziałach czasowych największy wpływ na skład pierwiastkowy $PM_{10}$ miała emisja z transportu, czyli tzw. emisja komunikacyjna, co jest bezpośrednio związane z podmiejskim charakterem badanego obszaru i jego położeniem przy trasie do dużego ośrodka miejskiego. Dodatkowo, zaobserwowano emisję komunalną w tym przede wszystkim pochodzącą ze spalania węgla. Miała ona wyraźny wpływ na skład pierwiastkowy pyłu $PM_{10}$ w badanym okresie. Jest wysoce prawdopodobne, że jeśli podobna analiza pochodzenia $PM_{10}$ w tym samym okresie pomiarowym zostałaby przeprowadzona na podstawie dziennych danych o składzie pierwiastkowym $PM_{10}$, to wpływ takiego źródła jak elektrociepłownia (znacznie oddalona od receptora) nie byłby zauważony. Badania udowadniają, że przy użyciu danych o godzinowych stężeniach wybranych pierwiastków można ocenić pochodzenie pyłu $PM_{10}$ oraz zmienność udziału wybranych źródeł w kształtowaniu stężeń $PM_{10}$ w ciągu dnia, nawet przy wykorzystaniu danych z bardzo krótkiego okresu pomiarowego. Pokazuje to, że dużo lepszym, tańszym i wydajniejszym sposobem zbierania danych do oceny pochodzenia PM w obszarze miejskim czy podmiejskim jest próbkowanie z dużą rozdzielczością czasową.

(Publ. 11) Efektem współpracy z Instytutem Podstaw Inżynierii Środowiska Polskiej Akademii Nauk (IPIŚ PAN) w Zabrzu jest wspólna publikacja *„Concentration and elemental composition of quasi-ultrafine particles in Upper Silesia”*. Wiadomo, że cząstki ultradrobne (UFP), czyli takie, których średnica aerodynamiczna nie przekracza rozmiaru niż 0,1 μm ($PM_{0,1}$), stanowią niewielką część całkowitej masy pyłu atmosferycznego [20, 66, 141], jednak zwykle (zwłaszcza w obszarach miejskich) przewyższają liczebnością cząsteczki o rozmiarach średnicy aerodynamicznej powyżej 0,1 μm [142-144]. Biorąc pod uwagę ich duże stężenia liczbowe oraz niewielkie wymiary, to ich oddziaływanie związane z niekorzystnymi skutkami zdrowotnymi u człowieka, może być większe niż w przypadku grubszych frakcji PM. Ich toksyczność, a także duża efektywność depozycji płucnej UFP, mogą wywoływać poważne problemy płucne oraz kardiologiczne. Dlatego pomiar stężeń (zwykle liczbowych) UFP stał się standardowym monitoringiem w niektórych krajach Europy. Bardzo drobne cząsteczki są ubocznym produktem różnego rodzaju procesów wysokotemperaturowych lub też mogą powstawać w powietrzu jako cząstki wtórne. Pochodzą one głównie spalania paliw płynnych w silnikach Diesla (te o medianie średnicach od 20 do 100 nm), ze spalania węgla oraz oleju opałowego (35-100 nm), a także gazu ziemnego (15-30 nm) [139].

W niniejszej publikacji zaprezentowano wyniki pomiarowe przedstawiające cząsteczki o średnicach aerodynamicznych od 30 do 60 nm a także te o średnicach od 60 do 108 nm pobranych w trakcie kampanii pomiarowej przeprowadzonej w południowej części Polski. Celem badań było przedstawienie właściwości cząstek o średnicach aerodynamicznych od 60 do 108 nm (zwanych quasi-ultrafine particles, q-UFP). Próbki q-UFP zostały zebrane w dwóch górnośląskich miastach, Zabrzu oraz Katowicach, w

trzech miejscach pomiarowych w każdym z powyższych miast. Dla każdego z miast były to:

- stanowisko reprezentujące miejskie tło zanieczyszczeni powietrza,
- stanowisko reprezentujące silny wpływ transportu drogowego,

Próbki ultracząstek zostały pobrane za pomocą dwóch trzynastostopniowych impaktorów niskociśnieniowych DLPI firmy Dekati w których na każdym stopniu impaktora zostały zainstalowane filtry nylonowe. Skład pierwiastkowy q-UFPs określono metodą dyspersji energii fluorescencji rentgenowskiej (EDXRF). Urządzenie Epsilon 5 (PANalytical B.V.) jest urządzeniem wykorzystującym tą samą metodę pomiarową co stosowany przeze mnie w innych badaniach analizator Horiba PX-375, jednak nie umożliwia on pomiarów bezpośrednio w terenie. Uzyskane dane pomiarowe zostały wykorzystane do scharakteryzowania masowych stężeń w otoczeniu i składu pierwiastkowego ultradrobnych cząstek o średnicach aerodynamicznych od 30 a 108 nm (q-UFP) i pozwoliły na identyfikację źródeł ich pochodzenia. Na ich podstawie określono, że skład chemiczny q-UFP na Górnym Śląsku jest dość jednolity. Stężenia Zn, As, Pb, Cu, Sr w powietrzu atmosferycznym oraz ich udział w masie 24 pierwiastków związanych z q-UFP były porównywalne pomiędzy wszystkimi badanymi stanowiskami pomiarowymi. Działo się tak ze względu na fakt, że wpływ na powyższe stężenia pierwiastków miały te same źródła ich pochodzenia. Było to głównie spalanie węgla w celach ciepłowniczych oraz przy produkcji energii elektrycznej. Główny wpływ na kształtowanie się stężeń w powietrzu atmosferycznym takich pierwiastków, związanych z q-UFP, jak Al, Si, S, Cl, K, Sc, Ti, V, Cd, Cr, Mn, Co i Sb, mają lokalne źródła. Zdecydowana większość pierwiastków wchodzących w skład z q-UFP ma charakter antropogeniczny.

(Publ.12) Bardzo interesującą sesję pomiarową w okresie letnim 2020 r Jednostkach Ratowniczo-Gaśniczych zlokalizowanych w centralnej Polsce. Konsekwencją niniejszych badań jest publikacja: *"Elemental composition and origin of PM10 in selected Polish fire station: real time results from XRF analysis".*


*Rysunek 6. Zdjęcia miejsce usytuowania stanowiska pomiarowego w Jednostkach Ratowniczo-Gaśniczych (zdjęcia: zasoby własne)*

Ze względu na fakt, że niektóre z chorób nowotworowych, ale również choroby związane z układem krwionośnym, są bardzo powszechne wśród strażaków, istotne jest rozstrzygnięcie co powoduje wzrost zapadania na te choroby [145]. Strażacy są narażeni w trakcie wykonywania czynności zawodowych na emisję zanieczyszczeń będących efektem spalania, to znaczy: różne substancje chemiczne w stanie pary oraz w fazie cząstek stałych, głównie poprzez wdychanie, a także poprzez spożycie oraz drogą skórną [146-147]. Przy czym, dym pochodzący z pożarów może powodować nagłą śmierć zarówno strażaków, jak i ofiar pożarów. Powodem tego jest wdychanie toksycznych gazów. Dym pochodzący z pożarów zawiera cząstki stałe (PM) o różnym rozmiarze, różne związki w fazie gazowej, czy też substancje związane z PM, takie jak toksyczne i rakotwórcze wielopierścieniowe węglowodory aromatyczne (WWA), lotne związki organiczne (LZO) oraz metale ciężkie [148]. Toksyczne związki osadzać się również na środkach ochrony indywidualnej (PPE) oraz odzieży strażackiej [146, 148]. Co więcej, kluczowym problemem może być miejsce i sposób przechowywania PPE i odzieży w remizie strażackiej, oraz jakość jej prania, czy też dekontaminacji po użytkowania w trakcie akcji pożarniczej. Może to w istotnym stopniu powodować skażenia samych Jednostek Ratowniczo-Gaśniczych (popularnych remiz strażackich) [146, 149]. Ponadto spaliny silników Diesla z urządzeń pożarniczych mogą odgrywać znaczącą rolę w potencjalnym zagrożeniu zdrowia strażaków [150]. Dlatego też modele mogące przewidzieć zmienność składu pierwiastkowego i pochodzenie stężeń PM w Jednostkach Ratowniczo-Gaśniczych byłyby bardzo ważnym i kluczowym narzędziem dla ochrony życia ludzkiego. Co więcej, zaprojektowanie systemu ostrzegania mogłoby znacznie ułatwić osiągnięcie tego celu. W tym celu najskuteczniejszym narzędziem byłby szybki i kompleksowy pomiar. Następnie na podstawie stężenia pierwiastków uzyskanych z pomiarów uśrednionych w odstępach czasu dużo krótszych niż 24 godziny, ocena pochodzenia zmierzonego pyłu zawieszonego. Można ją uzyskać dzięki automatycznym pomiarom opartym na

technice X-ray fluorescence (XRF) w bezpośrednim miejscu występowania tychże zanieczyszczeń. Dane uzyskane za pomocą tego narzędzia mogłyby stanowić fragment wiarygodnej informacji, która pozwoli w przyszłości podjąć działania przeciwdziałające ewentualnemu zagrożeniu zdrowia wśród strażaków.

Celem przeprowadzonych badań (przy współpracy ze Szkołą Główną Służby Pożarniczej) była ocena składu pierwiastkowego i pochodzenia pyłu zawieszonego $PM_{10}$ w wybranych Jednostkach Ratowniczo-Gaśniczych w Polsce z zastosowaniem trzech różnych modeli receptorowych do aportacji źródeł oraz z wykorzystaniem analizatora Horiba PX-375. Nowością w badaniach, tak jak i w innych prowadzonych przeze mnie jest wysoka rozdzielczość czasowa pomiaru składu pierwiastkowego metali związanych z pyłem zawieszonym PM. W tym samym czasie mierzono stężenia pyłu $PM_{10}$ metodą tłumienia promieniowania beta. Badania takie nie były dotychczas prowadzone w Polsce i mogą posłużyć jako dane wejściowe do propozycji systemu ostrzegania o stężeniach $PM_{10}$ w Jednostkach Ratowniczo-Gaśniczych. Stężenia badanych metali charakteryzowały się dużą zmiennością czasową, natomiast stężenia pyłu $PM_{10}$ w garażu były niskie. Wzbogacenie pyłu $PM_{10}$ było bardzo wysokie lub wysokie, szczególnie w siarkę, cynk, arsen, nikiel, kadm i ołów. Analiza PCA oraz UNMIX i PMF wykazały duży wpływ czynnika związanego z siarką na zmienność. Świadczy to o tym, że wpływ spalania, w tym spalania paliw płynnych, w samochodach pożarniczych może mieć zasadniczy wpływ na zanieczyszczenie powietrza w Jednostkach Ratowniczo-Gaśniczych. Analiza PMF pozwoliła również na identyfikację czynnika odpowiedzialnego za wpływ zewnętrznej emisji antropogenicznej na stężenia wewnątrz garażu. Kolejnymi zidentyfikowanymi źródłami pyłu $PM_{10}$ i pierwiastków związanych z $PM_{10}$ są pyły mineralne oraz pyły drogowe związane z emisją poza spalinową, pochodzące zarówno z wnętrza jednostek, jak i z zewnątrz. Dodatkowo dane te posłużą mi w przygotowaniu modelu służącego do dokładniejszej identyfikacji źródeł emisji zanieczyszczenia pyłowego pochodzących ze spalania silników spalinowych Diesla (obsługujących ciężki sprzęt ratowniczy) oraz z emisji zanieczyszczeń pochodzących z pożarów. Zwłaszcza w sytuacjach gdy emisja z tych źródeł nałożona jest na emisję zanieczyszczeń innych źródeł.

# I. Podsumowanie i wnioski

Głównymi celami pracy doktorskiej były:

- ustalenie źródeł pochodzenia pyłu zawieszonego w powietrzu atmosferycznym,
- ustalenie aktualnej hierarchii źródeł pyłu zawieszonego w powietrzu atmosferycznym,
- wykazanie możliwości wykorzystania wyników o wysokiej rozdzielczości czasowej (0,5-1h), zmienności stężenia pyłu i związanych z nim pierwiastków do bardzo prostej i szybkiej oceny jakościowej wpływu konkretnego źródła emisji na ich stężenie w powietrzu.

Zasadniczymi problemami badawczymi, w trakcie prowadzonych badań, były:

- dobór odpowiedniego sprzętu pomiarowego, który umożliwia w sposób automatyczny, a dodatkowo z wysoką rozdzielczością czasową, prowadzić nie tylko pomiary koncentracji pobranego pyłu, ale również jego składu pierwiastkowego,
- dobór sprzętu pomocniczego wspomagającego pomiary parametrów środowiska i warunków otoczenia badanego receptora,
- wybór kilku reprezentatywnych z punktu widzenia różnorodności źródeł pochodzenia pyłu zawieszonego receptorów pomiarowych,
- zapewnienie wiarygodności danych (dobór referencyjnych metodyk pomiarowych, oraz badania porównawcze z innymi metodykami),
- dobór odpowiednich metodyk analizy danych (metody statystyczne),
- weryfikacja badań i walidacja wyników uzyskanych innymi metodami.

Na podstawie badań wykonanych w terenie, a następnie analizy pozyskanych w ten sposób wyników, wykazano że:

- w bardzo krótkim okresie pomiarowym, wykorzystanie spektrometru PX-375 lub dowolnie innego analizatora umożliwiającego pomiar stężenia masowego pierwiastków w cząstkach pyłu z bardzo dużą rozdzielczością czasową, pozwala na jakościowe powiązanie badanych pierwiastków śladowych w powietrzu z ich źródłami pochodzenia,
- zastosowanie badanego rozwiązania w systemie monitoringu jakości powietrza w Polsce pozwoli prowadzić w przyszłości ten monitoring znacznie wydajniej i efektywniej,
- zamiast wieloletnich pomiarów w pojedynczych, stałych receptorach można wykonywać pomiary w krótkich okresach czasowych (np. miesiąc w lecie i miesiąc w zimie) i na podstawie takich pomiarów z dobrą dokładnością ocenić pochodzenie pyłu i związanych z nim priorytetowych metali w wielu lokalizacjach,
- zastosowanie tego narzędzia pozwala wyznaczyć dużo precyzyjniej niż ma to miejsce obecnie, przestrzenne zmiany stężenia zanieczyszczeń w Polsce, a na tej podstawie oszacować narażenie zdrowotne na zanieczyszczenia powietrza mieszkańców wielu rejonów,

- biorąc pod uwagę, fakt bardzo dobrego zinwentaryzowania większości emitorów w Polsce (poprzez pomiary porównawcze, okresowe pomiary emisji na obiektach emisyjnych, ciągłe pomiary emisji AMS itp.) propozycja budowy automatycznego systemu szybkiego wykrywania i identyfikacji źródeł emisji, jest jak najbardziej uzasadniona,
- dodatkowo, dane porównawcze pozyskane przy pomocy bioindykatorów pozwoliły poszerzyć wiedzę na temat innych alternatywnych metod stosowanych do oceny źródeł i pochodzenia oraz identyfikacji zanieczyszczeń i umożliwiły efektywne wprowadzenie w szerzej rozumianą tematykę badawczą.

W dalszej perspektywie taki rozbudowany system z pewnością umożliwi stworzenie krajowej bazy danych (opartej na kilku lub kilkunastu automatycznych stacjach służących do szybkiej identyfikacji źródeł emisji pyłu zawieszonego)co z pewnością przyczyni się do redukcji zanieczyszczenia powietrza w Polsce. Dzięki takiemu systemowi także działania zmierzające do redukcji zanieczyszczenia powietrza będą koncentrować się w obszarach najbardziej zagrożonych i pilnie ich potrzebujących, a więc efekt działań będzie większy przy jednoczesnej redukcji kosztów z tym związanych.

Literatura:


[1] Praca zespołowa pod redakcją K. Juda-Rezler, B. Toczko, (2016) „Pyły drobne w atmosferze. Kompendium wiedzy o zanieczyszczeniu powietrza pyłem zawieszonym w Polsce", Inspekcja Ochrony Środowiska, Biblioteka Monitoringu Środowiska, Warszawa.

[2] W. Rogula-Kozłowska, G.Majewski, B. Błaszczak, K.Klejnowski, P. Rogula-Kopiec (2016) "Origin-oriented elemental profile of fine ambient particulate matter in central European suburban conditions", MDPI, International Journal of Environmental Research and Public Health 13 (7), 715, https://doi.org/10.3390/ijerph13070715.

[3] B. Błaszczak, W. Rogula-Kozłowska, B. Mathews, K. Juda-Rezler, K. Klejnowski, P. Rogula-Kopiec, (2016), "Chemical compositions of PM2. 5 at two non-urban sites from the polluted region in Europe", Aerosol and Air Quality Research 16 (10), 2333-2348, https://aaqr.org/articles/aaqr-15-09-oa-0538.

[4] G. Majewski, W. Rogula-Kozłowska, B. Szeląg, E. Anioł, P. Rogula-Kopiec, A. Brandyk, A. Walczak, M. Radziemska, (2022), „New insights into submicron particles impact on visibility, Environmental Science and Pollution Research 29 (58), 87969-87981.

[5] A.J. Cohen, H.R. Anderson, B. Ostro, K.D. Pandey i in., (2004), "Urban air pollution. W: M. Ezzati i in. (red.) Comparative quantification of health risks. Global and regional burden of disease attributable to selected major factors, Vol. 2, Chapter 17. World Health Organization Geneva, 1354–1433.

[6] S.S. Lim, T.Vos, A.D. Flaxman, G. Danaei i in, (2012), "A comparative risk assessment of burden of disease and injury attributable to 67 risk factors and risk factor clusters in 21 regions, 1990–2010: a systematic analysis for the Global Burden of Disease Study 2010, Lancet (380) 2224–2260, https://doi.org/10.1016/S0140-6736(12)61766-8.

[7] C.A. Pope III, D. Dockery, J. Spengler, M. Raizenne, (1991): "Respiratory health and PM-10 pollution", Am. Rev. Resp. Dis., 144, 668–674.

[8] J.E. Muscat, E.L. Wynder, (1995), "Diesel engine exhaust and lung cancer: an unproved association", Environmental Health Perspectives 103, 812–818.

[9] K. R. Spurny, (1996), "Chemical mixtures in atmospheric aerosols and their correlation to lung diseases and lung cancer occurrence in the general population", Toxicology Letters 88, 271–277.

[10] A. Zwozdziak, M.I. Gini, L. Samek, W. Rogula-Kozlowska, I. Sowka, (2017), „Implications of the aerosol size distribution modal structure of trace and major elements on human exposure, inhaled dose and relevance to the PM2.5 and PM10 metrics in a European pollution hotspot urban area", Journal of Aerosol Science 103, 38-52, https://doi.org/10.1016/j.jaerosci.2016.10.004.

[11] K. Widziewicz, W. Rogula-Kozłowska, K. Loska, (2016), "Cancer risk from arsenic and chromium species bound to PM2.5 and PM1 – Polish case study", Atmospheric Pollution Research 7 (5), 884-894, https://doi.org/10.1016/j.apr.2016.05.002.

[12] K. Widziewicz, W. Rogula-Kozłowska, K. Loska, K. Kociszewska, G. Majewski, (2018), "Health risk impacts of exposure to airborne metals and benzo(a)pyrene during episodes of high PM10 concentrations in Poland", Biomedical and Environmental Sciences 31 (1), 23-36, 2018, https://doi.org/10.3967/bes2018.003.

[13] Uchwała Nr 34 Rady Ministrów z dnia 29 kwietnia 2019 r. w sprawie przyjęcia Krajowego programu ograniczania zanieczyszczenia powietrza, https://isap.sejm.gov.pl/isap.nsf/download.xsp/WMP20190000572/O/M20190572.pdf.

[14] Ministerstwo Klimatu i Środowiska, BIP, Krajowy program ograniczania zanieczyszczenia powietrza, https://bip.mos.gov.pl/strategie-plany-programy/krajowy-program-ograniczania-zanieczyszczenia-powietrza/

[15] Ministerstwo Środowiska Departament Ochrony Powietrza, „Krajowy program ochrony powietrza do roku 2020 (z perspektywą do 2030)", Warszawa 2015, https://powietrze.gios.gov.pl/pjp/download.

[16] M. Kampa and E. Castanas, (2008), "Human health effects of air pollution," Environ. Pollut., vol. 151, no. 2, pp. 362–367, doi: 10.1016/j.envpol.2007.06.012.

[17] H. Effects Institute, (2020), "A special report on global exposure to air pollution and its health impact what is the state of global air?".

[18] J. C. Chow, (1995), "Measurement methods to determine compliance with ambient air quality standards for suspended particles", Journal of Air and Waste Management Association, 45, 320–382.

[19] J. C. Chow, J. G. Watson, D. H. Lowenthal, R.J. Countess, (1996), “Sources and chemistry of PM-10 aerosol in Santa Barbara county”, CA. Atmospheric Environment, 30, 1489–1499.

[20] W. Rogula-Kozłowska, (2015), “Size-segregated urban particulate matter: mass closure, chemical composition, and primary and secondary matter content”, Air Quality, Atmosphere & Health 9 (5), 533-550.

[21] W. Rogula-Kozłowska, K. Klejnowski, (2012), “Submicrometer aerosol in rural and urban backgrounds in southern Poland: primary and secondary components of PM1”, Bulletin of Environmental Contamination and Toxicology 90 (1), 103-109.

[22] D. Koch, D. Jacob, I. Te, D. Rind, M. Chin, (1999), Tropospheric sulfur simulation and sulfate direct radiative forcing in the Goddard Institute for Space Studies general circulation model, Journal Of Geophysical Research, 104, D19, 23799-23822.

[23] H.H. Lamb, (1970), Volcanic Dust in the Atmosphere; with a chronology and assessment of its meteorological significance, Royal Society , 266, 1178.

[24] M.O. Andreae, P. Metlet, (2001), “Emission of trace gases and aerosols from biomass burning”, Global Biogeochemical Cycles, 15, 955-966.

[25] Formenti P., Schutz L., Balkanski Y., Desboeufs K., Ebert M., Kandler K., Petzold A., Scheuvens D., Weinbruch S., Zhang D., (2011), Recent progress in understanding physical and chemical properties of African and Asian mineral dust, Atmospheric Chemistry and Physics, 11, 8231–8256.

[26] Zender C.S., Miller R.L.R.L.,Tegen I., (2011), Quantifying Mineral Dust Mass Budgets:Terminology, Constraints, and Current Estimates, Eos, 85, 48.

[27] Mahowald N.M., Kloster S., Engelstaedter S., Moore J.K., Mukhopadhyay S., McConnell J.R., Albani S., Doney S.C., Bhattacharya A., Curran M.A.J., Flanner M.G., Hoffman F.M., Lawrence D.M., Lindsay K., Mayewski P.A., Neff J., Rothenberg D., Thomas E., Thornton P.E., Zender C.S., (2010), Observed 20th century desert dust variability: impact on climate and biogeochemistry, Atmospheric Chemistry and Physics, 10, 10875–10893.

[28] Gazeta.pl, (2018) “Pył znad Sahary przyleciał do Polski. Brudne deszcze i pomarańczowe niebo”, http://wiadomosci.gazeta.pl/wiadomosci/7,114883,23281039,pyl-znad-sahary-zawital-do-polski-brudne-deszcze-i-pomaranczowe.html.

[29] V.R. Després, Huffman J., S.M. Burrows, C. Hoose, A.S. Safatov, G. Buryak, J. Fröhlich-Nowoisky, W. Elbert, M.O. Andreae, U. Pöschl, R. Jaenicke, (2012), “Primary biological aerosol particles in the atmosphere: a review”, Tellus B: Chemical and Physical Meteorology, 64, 1, 6195.

[30] G.J. Derevianko, C. Deutsch A. Hall, (2009), “On the relationship between ocean DMS and solar radiation”, Geophysical Research Letters, 36, L17606.

[31] C. Arsene, A. Bougiatiot, N. Mihalopoulos, (2009), “Sources and variability of non-methane hydrocarbons in the Eastern Mediterranean”, Global Nest Journal, 11, 333-340.

[32] R. Atkinson, J. Are, (2003), Atmospheric Degradation of Volatile Organic Compounds, Chemical Reviews, 103, 4605−4638.

[33] J.W. Fitz Fitzgerald, (1991), “Marine aerosols: a review”, Atmospheric Environment, 25A, 3-4, 533-545.

[34] C.D. Bl Blanchard, A.H. Woodcock A.H, (1957), “Bubble Formation and Modification in the Sea and its Meteorological Significance”, Svenska Geofysisra Foreningen 9, 2.

[35] A.U. Lewandowska, L.M. Falkowska, (2013), “Sea salt in aerosols over the Southern Baltic, Part 2. The neutralizing properties of sea salt and ammonia”, Oceanologia 55, 2, 299-318.

[36] A.U. Lewandowska, L.M. Falkowska (2013a), “Sea salt in aerosols over the southern Baltic. Part 1. The generation and transportation of marine particles”, 279-298.

[37] U. Schumann, H. Huntrieser H., (2007), “The global lightning-induced nitrogen oxides source”, Atmospheric Chemistry and Physics, 7, 3823–3907.

[38] L.J. Labrador, R. von Kuhlmann, M.G. Lawrence, (2005), "The effects of lightning-produced NOx and its vertical distribution on atmospheric chemistry: sensitivity simulations with MATCH-MPIC”, Atmospheric Chemistry and Physics, 5, 1815–1834.

[39] C.C. Chuang, J.E. Penner, K.E. Taylor, A.S. Grossman, J.J. Walton, (1997), “An assessment of the radiative effects of anthropogenic sulfate”, Journal of Geophysical Research, 102, D3, 3761-3778.

[40] J.M. Pacyna, E.G. Pacyna, (2001), “An assessment of global and regional emissions of trace metals to the atmosphere from anthropogenic sources world – wide”, Environmental Reviews, 9, 269–298.

[41] D. Shindell. G. Faluvegi, (2010), The net climate impact of coal-fired power plant emissions, Atmospheric Chemistry and Physics, 10, 3247–3260.

[42] A.M. Sánchez de la Campa, J.D. de la Rosa, Y. González-Castanedo, R. Fernández-Camacho, A. Alastuey, X. Querol, C. Piob, “High concentrations of heavy metals in PM from ceramic factories of Southern Spain”,(2010), Atmospheric Research, 96, 633–644.

[43] P.M. Lemieux, (2000), “Emissions of Polychlorinated Dibenzo-p-dioxins and Polychlorinated Dibenzofurans from the Open Burning of Household Waste in Barrels”, Environmental Science & Technology, 34, 377-384.

[44] CAFE Working Group on Particulate Matter, (2004), “Second Position Paper on Particulate Matter”, http://archiwum.ciop.pl/2863.html.

[45] A. Thorpe, R.M. Harrison, (2008), “Sources and properties of non-exhaust particulate matter from road traffic: A review”, Science Of The Total Environment, 400, 270–282.

[46] H.M. Prichard H.M., P.C. Fisher, (2012), “Identification of Platinum and Palladium Particles Emitted from Vehicles and Dispersed into the Surface Environment”, Environmental Science & Technology, 46, 3149−3154.

[47] D. Shindell, G. Faluvegi, (2010), “The net climate impact of coal-fired power plant emissions”, Atmospheric Chemistry and Physics, 10, 3247–3260.

[48] Ryua S.Y., Kwona B.G., Kima Y.J., Kimb H.H., Chun K.J.,(2007), Characteristics of biomass burning aerosol and its impact on regional air quality in the summer of 2003 at Gwangju, Korea, Atmospheric Research, 84, 4, 362-373.

[49] G.R. McMeeking, S.M. Kreidenweis, S. Baker, C.M. Carrico, J.C. Chow, J.L. Collett Jr., W.M. Hao, A.S. Holden, T. W. Kirchstetter, W.C. Malm, H. Moosmuller, A.P. Sullivan, C.E. Wold, (2009), “Emissions of trace gases and aerosols during the open combustion of biomass in the laboratory”, Journal of Geophysical Research, 114.

[50] C. Alvesa, A. Vicentea, T. Nunesa, C. Gonçalvesa, A. Patrícia, F.F. Mirantea, L. Tarelhoa, A.M. Sánchez de la Campab, X.Querol, A.Caseiroa, C. Monteiroa, M. Evtyuginaa, C. Pio, (2011), Summer 2009 wildfires in Portugal: Emission of trace gases and aerosol composition, Atmospheric Environment, 45, 641-649.

[51] W, Rogula-Kozłowska, J.S. Pastuszka, E. Talik, (2008), “Influence of Vehicular Traffic on Concentration and Particle Surface Composition of PM10 and PM2. 5 in Zabrze, Poland”, Environmental Science, Polish Journal of Environmental Studies, 17(4):539–548.

[52] G. Majewski, W. Rogula-Kozłowska, K. Rozbicka, P. Rogula-Kopiec, B. Mathews, A. Brandyk, (2018), “Concentration, chemical composition and origin of PM1: Results from the first long-term measurement campaign in Warsaw (Poland)”, Aerosol and Air Quality Research, 18: 636-654. https://doi.org/10.4209/aaqr.2017.06.0221.

[53] I. Sówka, A. Chlebowska-Styś, Ł. Pachurka, W. Rogula-Kozłowska, B. Mathews, (2019), “Analysis of Particulate Matter Concentration Variability and Origin in Selected Urban Areas in Poland”, Sustainability, vol. 11, no. 20, pp. 5735–5735, Oct. 2019, doi: 10.3390/su11205735.

[54] K. Widziewicz, W. Rogula-Kozłowska, (2017), “Urban environment as a factor modulating metals deposition in the respiratory tract and associated cancer risk”, Atmos. Pollut. Res. 9, 399–410.

[55] A. Chlebowska-Styś, D. Kobus, Ł. Pachurka, I. Sówka, (2017), “Analysis of concentrations trends and origins of PM 10 in selected European cities”, E3S Web Conf. 17, 13.

[56] A. Chlebowska-Styś, I. Sówka, Ł. Pachurka, (2016), “Analysis of air quality in selected Polish cities”, In Człowiek a Środowisko: Wzajemne Oddziaływanie = Man vs Environment: Interaction; Chmielewski, J., Żeber-Dzikowska, I., Gworek, B., Eds.; Instytut Ochrony Środowiska, Państwowy Instytut Badawczy: Warszawa, Poland, 2016; pp. 103–120.

[57] A. Chlebowska-Styś, D. Kobus, M. Zathey, I. Sówka, (2017), “The impact of road transport on air quality in selected Polish cities”, E3S Web Conf., 22, 1–8.

[58] W. Rogula-Kozłowska, K. Kuskowska, P. Ogrodnik, M. Penkała, (2018), “Traffic-generated changes in the elemental profile of urban coarse dust at a highway and crossroads”, E3S Web Conf. 45, 00074.

[59] W. Rogula-Kozłowska, K. Klejnowski, P. Rogula-Kopiec, L. Ośródka, E. Krajny, E. Błaszczak, B. Mathews, (2014), “Spatial and seasonal variability of the mass concentration and chemical composition of PM2.5 in Poland”, Air Qual. Atmos. Health 2014, 7, 41–58.

[60] J. Konieczyński, B. Kozielska, J. Żeliński, J. Staisz, Pasoń-Konieczyńska A. (2003), „Skład ziarnowy oraz profile wielopierścieniowych węglowodorów aromatycznych w pyłach emitowanych z obiektów energetyki komunalnej i zakładowej”, Wydawnictwo Politechniki Śląskiej, Gliwice, 9.

[61] J. Konieczyński, A. Pasoń, T. Kaczyńska, J. Szeliga, (1991), „Emisja substancji zanieczyszczających z domowych palenisk węglowych”, Archiwum Ochrony Środowiska, 1, 33–43.

[62] J. Konieczyński, (2005), „Emisja zanieczyszczeń z kotłów fluidalnych. IPIŚ PAN, Zabrze, s. 136.

[63] A. Kristensson, Ch. Johansson, R. Westerholm, E. Swietlicki, L. Gidhagenb, U. Wideqvist, V. Vesely, (2004), “Real-world traffic emission factors of gases and particles measured in a road tunnel in Stockholm, Sweden”, Atmospheric Environment 38, 657–673.

[64] A. Kocbach, B.V. Johansen, P.E. Schwarze, E. Namork, (2005), “Analytical electron microscopy of combustion particles: a comparison of vehicle exhaust and residential wood smoke”, Science of Total Environment 346, 231–243.

[65] G. Majewski, W. Rogula-Kozłowska, (2016), “The elemental composition and origin of fine ambient particles in the largest Polish conurbation: First results from the short-term winter campaign”, Theoretical and Applied Climatology 125 (1), 79-92.

[66] W. Rogula-Kozłowska, G. Majewski, P.O. Czechowski, (2015), “The size distribution and origin of elements bound to ambient particles: A case study of a Polish urban area”, Environmental Monitoring and Assessment 187 (5), 1-16, DOI:10.1007/s10661-015-4450-5.

[67] W. Rogula-Kozłowska, K. Barbara, K. Krzysztof, S. Szopa, (2013), „Hazardous compounds in urban PM in the central part of Upper Silesia (Poland) in winter”, Archives of Environmental Protection 39, 53-65.

[68] D.R. McCubbin, B.J. Apelberg, S. Roe, F. Divita, (2002), :Livestock Ammonia Management and Particulate-Related Health Benefits”, Environmental Science & Technology, 36, 6, 1141-1146.

[69] W.C. Hinds, (1998), “Aerosol technology. Properties, behavior, and measurement of airborne particles”. Second Edition. John Wiley & Sons, Inc. New York.

[70] J.C. Chow, (1995), “Measurement methods to determine compliance with ambient air quality standards for suspended particles”, J. Air Waste Manag. Assoc. 45:320–382.

[71] A. Calvo, C. Alves, A. Castro, V. Pont, A.M. Vicente, R. Fraile, (2013), “Research on aerosol sources and chemical composition: Past, current and emerging issues”, Atmos. Res. 120-121: 1–28.

[72] P. Sanderson, J.M. Delgado Saborit, R.M. Harrison, (2014), “A review of chemical and physical characterisation of atmospheric metallic nanoparticles”, Atmos. Environ. 94: 353-365.

[73] M. Kulmala, H. Vehkamäki, T. Petäjä, M. Dal Maso, A. Lauri, V.M. Kerminen, W. Birmili, P.H. Mcmurry, (2004), “Formation and growth rates of ultrafine atmospheric particles: a review of observations”, J. Aerosol Sci. 35:143–176.

[74] R. Zhang, A. Khalizov, L. Wang, M. Hu, W. Xu, (2012), “Nucleation and growth of nanoparticles in the atmosphere”, Chem. Rev. 112:1957–2011.

[75] P. Kumar, L. Pirjola, M. Ketzel, R. M.Harrison, (2013) “Nanoparticle emissions from 11 non-vehicle exhaust sources – A review”, Atmos Environ 67:252–277.

[76] R.M. Harrison, A.M. Jones, R.G. Lawrence, (2004): “Major component composition of PM10 and PM2,5 from roadside and urban background sites”, Atmospheric Environment 38, 4531–4538.

[77] M. Reizer, (2013), „Metodyka identyfikacji przyczyn występowania epizodów pyłowych w warunkach polskich”, Rozprawa doktorska, Oficyna Wydawnicza Politechniki Warszawskiej, Warszawa.

[78] G.D. Thurston, J.D. Spengler, (1985), “A quantitative assessment of source contributions to inhalable particulate matter pollution in metropolitan Boston”, Atmospheric Environment, 19 (1), 9-25.

[79] M.S. Callén, M.T. de la Cruz, J.M. López, M.V. Navarro, A.M. Mastral, (2009), "Comparison of receptor models for source apportionment of the PM10 in Zaragoza (Spain)", Chemosphere, 76(8):1120-9. doi: 10.1016/j.chemosphere.2009.04.015.

[80] S. Guo-Liang, L. Gui-Rong, P. Xing, W. Yi-Nan, T. Ying-Ze, W. Wei, F. Yin-Chang, (2014), A Comparison of Multiple Combined Models for Source Apportionment, Including the PCA/MLR-CMB, Unmix-CMB and PMF-CMB Models", Aerosol and Air Quality Research, 14: 2040–2050.

[81] P.K. Hopke. (ed.), (1991), "Receptor modeling for air quality management", Elsevier Science Publishing Company, Inc. New York, NY.

[82] M. Viana, T.A.J. Kuhlbusch, X. Querol, A. Alastuey, R.M. Harrison, P.K. Hopke, W. Winiwarter, M. Vallius, S. Szidat, A.S.H. Prevot, C. Hueglin, H. Bloemen, P. Wahlin, R. Zecchi, A. Kasper-Giebl, W. Maenhaut, R. Hitzenberger, (2008), "Source apportionment of particulate matter in Europe: A review of methods and results", J Aerosol Sci 39:827-849.

[83] J.P. Putaud, R. Van Dingenen, A. Alastuey, H. Bauer, W. Birmili, J. Cyrys, H. Flentje, S. Fuzzi, R. Gehrig, H.C. Hansson, R.M. Harrison, H. Herrmann, R. Hitzenberger, C. Hüglin, A.M. Jones, A. Kasper-Giebl, G. Kiss, A Kousa, T.A.J. Kuhlbush, G. Löschau, W. Maenhaut, A. Molnar, T. Moreno, J. Pekkanen, C. Perrino, M. Pitz, H. Puxbaum, X. Querol, S. Rodriguez, I. Salma, J. Schwarz, J. Smolik, J. Schneider, G. Spindler, H. ten Brink, J. Tursic, M. Viana, A. Wiedensohler, F. Raes, (2010), "A European aerosol phenomenology – 3: Physical and chemical characteristics of particulate matter from 60 rural, urban, and kerbside sites across Europe", Atmos. Environ. 44: 1308-1320.

[84] K. Juda-Rezler, M. Reizer, J-P. Oudinet, (2011), "Determination and analysis of PM10 source apportionment during episodes of air pollution in Central Eastern European urban areas: The case of wintertime 2006", Atmospheric Environment 45, 6557–6566, DOI:10.1016/j.atmosenv.2011.08.020.

[85] A. Zwozdziak, L. Samek, I. Sowka, L. Furman, M. Skrętowicz' (2012), "Aerosol Pollution from Small Combustors in a Village", The Scientific World Journal, 956401, https://doi.org/10.1100/2012/956401.

[86] I. Sówka, A. Zwoździak, K. Trzepla-Nabaglo, M. Skrętowicz, J. Zwoździak, (2012), "PM2.5 elemental composition and source apportionment in residential area of Wrocław, Poland", Environ Prot Eng 38:73–79.

[87] C.A. Belis, F. Karagulian, B.R. Larsen, P.K. Hopke, (2013), "Critical review and meta-analysis of ambient particulate matter source apportionment using receptor models in Europe", Atmos Environ 69: 94-108.

[88] A. Calvo, C. Alves, A. Castro, V. Pont, A.M. Vicente, R. Fraile, (2013), "Research on aerosol sources and chemical composition: Past, current and emerging issues"' Atmos. Res. 120-121: 1–28.

[89] W. Rogula-Kozłowska, G. Majewski, P.O. Czechowski, P. Rogula-Kopiec, (2017), "Analysis of the data set from a two-year observation of the ambient water-soluble ions bound to four particulate matter fractions in an urban background site in southern Poland", Environment Protection Engineering 43 (1). DOI:10.37190/epe170111.

[90] W. Rogula-Kozłowska, B. Błaszczak, S. Szopa, K. Klejnowski, I. Sówka, A. Zwoździak, M. Jabłońska, B. Mathews, (2012), "PM2. 5 in the central part of Upper Silesia, Poland: concentrations, elemental composition, and mobility of components", Environmental monitoring and assessment 185 (1), 581-601, DOI: 10.1007/s10661-012-2577-1.

[91] P.K. Hopke, K. Ito, T. Mar, W.F. Christensen, D.J. Eatough, R.C. Henry, (2006), "PM source apportionment and health effects: 1. Intercomparison of source apportionment results", Journal of Exposure Science and Environmental Epidemiology, 16: 275–286.

[92] S. Yatkin, A. Bayram, (2008), "Source apportionment of PM10 and PM2,5 using positive matrix factorization and chemical mass balance in Izmir, Turkey", Science of the Total Environment 390: 109–123.

[93] J.F. Fabretti, N. Sauret, J.F. Gal, P.C. Maria, U. Schärer, (2009), "Elemental characterization and source identification of PM2,5 using Positive Matrix Factorization: The Malraux road tunnel, Nice, France", Atmospheric Research 94: 320–329.

[94] Pallavi Pant, Jianxin Yin, Roy M. Harrison: Sensitivity of a Chemical Mass Balance model to different molecular marker traffic source profiles. Atmospheric Environment 82 (2014) 238e249.

[95] M.D. Gibson, J. Haelssig, J.R. Pierce, M. Parrington, J.E. Franklin, J. T. Hopper, Z. Li, T.J. Ward, (2015), "A comparison of four receptor models used to quantify the boreal wildfire smoke contribution to surface PM2.5 in

Halifax, Nova Scotia during the BORTAS-B experiment", Atmos. Chem. Phys., 15, 815-827, doi:10.5194/acp-15-815-2015.

[96] M. Pandolfi, Y. Gonzalez-Castanedo, A. Alastuey, J. D. de la Rosa, E. Mantilla, A. S. de la Campa, X. Querol, J. Pey, F. Amato, T. Moreno, (2010), "Source apportionment of PM(10) and PM(2.5) at multiple sites in the strait of Gibraltar by PMF: impact of shipping emissions", Environmental Science and Pollution Research 18, 260-269, doi: 10.1007/s11356-010-0373-4.

[97] E. Andriani, M. Caselli, G. de Gennaro, A. Giove, C. Tortorella, (2011), "Synergistic use of several receptor models (CMB, APCS and PMF) to interpret air quality data", Environmetrics 22, 789-797, https://doi.org/10.1002/env.1120.

[98] J. Nicolas, M. Chiari, J. Crespo, I. G. Orellana, F. Lucarelli, S. Nava, C. Pastor, E. Yubero, (2008), "Quantification of Saharan and local dust impact in an arid Mediterranean area by the positive matrix factorization (PMF) technique", Atmospheric Environment 42, 39, 8872-8882, https://doi.org/10.1016/j.atmosenv.2008.09.018.

[99] C. Thomas Coulter, (2004), "EPA-CMB8.2 Users Manual", Air Quality Modeling Group, Emissions, Monitoring & Analysis Division, Office of Air Quality Planning & Standards, Research Triangle Park, NC 27711, https://www.epa.gov/sites/default/files/2020-10/documents/epa-cmb82manual.pdf.

[100] G. Norris, R. Duvall, (2014), "EPA Positive Matrix Factorization (PM F) 5.0 Fundamentals and User Guide, U.S. Environmental Protection Agency, National Exposure Research Laboratory, Research Triangle Park, NC 27711, https://www.epa.gov/sites/default/files/2015-02/documents/pmf_5.0_user_guide.pdf.

[101] PN-EN 12341:2014 Standardowa grawimetryczna metoda pomiarowa do określania stężeń masowych frakcji PM10 lub PM2.5 pyłu zawieszonego, Polski Komitet Normalizacyjny.

[102] PN-EN 16450:2017 Automatyczne systemy pomiarowe do pomiarów stężenia pyłu zawieszonego (PM10; PM2.5), Polski Komitet Normalizacyjny.

[103] Shih Yu Pan, Hung Wei Chen, Shih Chieh Hsu, Charles C.-K. Chou, Yu Chi Lin, Yuan Wu Chen, Kai Hsien Chi, (2022), "Assessment of Atmospheric PM2.5 and PCDD/Fs Collected by Different High-volume Ambient Air Sampling Systems", Taiwan Association for Aerosol Research, https://doi.org/10.4209/aaqr.220116.

[104] F. Liu, S. Lai, K. Reinmuth-Selzle, J.F. Scheel, J. Fröhlich-Nowoisky, V.R. Després, T. Hoffmann, U. Pöschl, Ch.J. Kampf, (2016), "Metaproteomic analysis of atmospheric aerosol samples", Analytical and Bioanalytical Chemistry volume 408, p. 6337–6348.

[105] K. Imre, A. Molnar, V. Dézsi, A. Gelencsér, (2014), "Positive bias caused by residual water in reference PM10 measurements", Idojaras, Budapest, 1905, 119(3):207-216.

[106] K. Wadinga Fomba, K. Müller, J. Hofer, A.N. Makhmudov, D. Althausen, B.I. Nazarov, S.F. Abdullaev, H. Herrmann, (2019), "Variations of the aerosol chemical composition during Asian dust storm at Dushanbe, Tajikistan", E3S Web Conf., Volume 99, Central Asian Dust Conference (CADUC 2019), https://doi.org/10.1051/e3sconf/20199903007.

[107] A. Chlebowska-Styś, I. Sówka, Ł. Pachurka, (2016), „Analiza składu pyłu zawieszonego PM10 na stacji tła miejskiego w Pile", Eko-Dok, Interdyscyplinarne Zagadnienia w Inżynierii i Ochronie Środowiska, tom 8, str.36-53.

[108] A. Cabrerizo, P. Tejedo, L. Dachs, J. Benayas, (2016), "Anthropogenic and biogenic hydrocarbons in soils and vegetation from the South Shetland Islands (Antarctica)", Sci. Total Environ. https://doi.org/10.1016/j.scitotenv.2016.06.240.

[109] F. De Nicola, A. Alfani, G. Maisto, (2014), "Polycyclic aromatic hydrocarbon contamination in an urban area assessed by Quercus ilex leaves and soil", Environ. Sci. Pollut. Res. https://doi.org/10.1007/s11356-014-2665-6.

[110] H.G. Zechmeister, S. Dullinger, D. Hohenwallner, A. Riss, A. Hanus-Illnar, S. Scharf, (2006), "Pilot study on road traffic emissions (PAHs, heavy metals) measured by using mosses in a tunnel experiment in Vienna, Austria", Environmental Science and Pollution Research. pp. 398–405. https://doi.org/10.1065/espr2006.01.292.

[111] B.M.R. Appenzeller, A.M. Tsatsakis, (2012), "Hair analysis for biomonitoring of environmental and occupational exposure to organic pollutants: State of the art, critical review and future needs", Toxicol. Lett. https://doi.org/10.1016/j.toxlet.2011.10.0213.

[112] V.L.B. Jaspers, A. Covaci, D. Herzke, I. Eulaers, M. Eens, (2019), “Bird feathers as a biomonitor for environmental pollutants: Prospects and pitfalls. TrAC – Trends”, Anal. Chem. https://doi.org/10.1016/j.trac.2019.05.019.

[114] W. Bartz, M. Górka, J. Rybak, R. Rutkowski, A. Stojanowska, (2021), „The assessment of effectiveness of SEM- EDX and ICP-MS methods in the process of determining the mineralogical and geochemical composition of particulate matter deposited on spider webs”, Chemosphere 278, 130454, https://doi.org/https://doi.org/10.1016/j.chemosphere.2021.130454.

[115] J. Rybak, T. Olejniczak, (2014), „Accumulation of polycyclic aromatic hydrocarbons (PAHs) on the spider webs in the vicinity of road traffic traffic emissions”, Environ Sci Pollut Res Int. 2014; 21(3): 2313–2324, doi: 10.1007/s11356-013-2092-0.

[116] A, Stojanowska, T. Mach, T. Olszowski, J.S. Bihałowicz, M. Górka, J. Rybak, M. Rajfur, P. Świsłowski, (2021), „Air Pollution Research Based on Spider Web and Parallel Continuous Particulate Monitoring—A Comparison Study Coupled with Identification of Sources”, Minerals 11, 812. https://doi.org/https://doi.org/10.3390/min11080812.

[117] N. van Laaten, D. Merten, W. von Tümpling, T. Schäfer, M. Pirrung, (2020). “Comparison of Spider Web and Moss Bag Biomonitoring to Detect Sources of Airborne Trace Elements”, Water. Air. Soil Pollut. 231, 512, https://doi.org/10.1007/s11270-020-04881-8

[118] T. Mach, J.S. Bihałowicz (2022), “How to effectively analyse the impact of air quality on society – review of modern measurement techniques and apparaturus: particulates”, Zeszyty naukowe SGSP, ZN SGSP 2022, nr 84.

[119] R. Rutkowski, J. Rybak, W. Rogula-Kozłowska, M. Bełcik, K. Piekarska, I. Jureczko, (2019), “Mutagenicity of indoor air pollutants adsorbed on spider webs”, Ecotoxicol. Environ. Saf., 171, 549–557, DOI:10.1016/j.ecoenv.2019.01.019.

[120] J. Rybak, (2015), “Accumulation of major and trace elements in spider webs”, Water Air Soil Pollut., 226(4): 105, doi: 10.1007/s11270-015-2369-7.

[121] J. Rybak, I. Sówka, A. Zwozdziak, M. Fortuna, K. Trzepla-Nabagło, (2015), “Evaluation of the usefulness of spider webs as an air quality monitoring tool for heavy metals”. Ecological Chemistry and Engineering S, 22, 389–400, DOI: https://doi.org/10.1515/eces-2015-0021.

[122] S. Xiao-Li, P. Yu, G.C. Hose, C. Jian, L. Feng-Xiang, (2006), “Spider webs as indicators of heavy metal pollution in air. Bulletin of Environmental Contamination and Toxicology, vol. 76, 271–277.

[123] G.C. Hose, J.M. James, M.R. Gray, (2002), “Spider webs as environmental indicators”, Environ. Pollut. 120, 725–733, DOI: 10.1016/s0269-7491(02)00171-9.

[124] H.I. Abdel-Shafy, M.S.M. Mansour, (2018), “Solid waste issue: Sources, composition, disposal, recycling, and valorization”, Egyptian Journal of Petroleum, vol. 27, issue 4, p. 1275-1290, https://doi.org/10.1016/j.ejpe.2018.07.003.

[125] J.S. Bihałowicz, W. Rogula-Kozłowska, A. Krasuski, (2021), “Contribution of landfill fires to air pollution–An assessment methodology, Waste Management 125, 182-191, DOI: 10.1016/j.wasman.2021.02.046.

[126] W. Rogula-Kozłowska, J.S. Bihałowicz, (2022), “Alir Quality influence of selected pollutants emitted from a fire of 300 MG of municipal waste on ambient air quality: an example of modelling with hysplit”, Zeszyty Naukowe, 83 , 33-43, DOI: 10.5604/01.3001.0016.0222.

[127] World Health Organization, Regional Office for Europe, Copenhagen Air, Quality Guidelines for Europe Second Edition; WHO Regional Publications, European Series, No. 91, 2000; ISBN 92 890 1358 3.

[128] W. Rogula-Kozłowska, K. Barbara, K. Krzysztof, S. Szopa, (2013), „Hazardous compounds in urban PM in the central part of Upper Silesia (Poland) in winter”, Archives of Environmental Protection 39, 1, 53-65, DOI: 10.2478/aep-2013-0002.

[129] W. Rogula-Kozłowska, K. Klejnowski, P. Rogula-Kopiec, B. Mathews, (2012), „A study on the seasonal mass closure of ambient fine and coarse dusts in Zabrze, Poland”, Bulletin of Environmental Contamination and Toxicology 88(5):722-729, DOI:10.1007/s00128-012-0533-y.

[130] J.S. Pastuszka, W. Rogula-Kozłowska, E. Zajusz-Zubek, (2010), "Characterization of PM10 and PM2. 5 and associated heavy metals at the crossroads and urban background site in Zabrze, Upper Silesia, Poland, during the smog episodes", Environmental Monitoring and Assessment 168 (1), 613-627, doi: 10.1007/s10661-009-1138-8.

[131] G.C. Lough, J.J. Schauer, J.-S. Park, M.M. Shafer, J.T. DeMinter, J.P. Weinstein, (2005), "Emissions of Metals Associated with Motor Vehicle Roadways", Environ. Sci. Technol. 39, 826–836, doi:10.1021/es048715f.

[132] M. Barbieri, (2016) "The Importance of Enrichment Factor (EF) and Geoaccumulation Index (Igeo) to Evaluate the Soil Contamination", Journal of Geology & Geophysics 5 (1), https://doi.org/10.4172/2381-8719.1000237.

[133] H.K. Wedepohl, (1995), "The Composition of the Continental Crust." Geochimica et Cosmochimica Acta. https://doi.org/10.1016/0016-7037(95)00038-2.

[134] J. Rybak, M. Wróbel, J.S. Bihałowicz, W. Rogula-Kozłowska, (2020), "Selected Metals in Urban Road Dust: Upper and Lower Silesia Case Study", Atmosphere 11 (3): 290, https://doi.org/10.3390/atmos11030290.

[135] C. Reimann, P. de Caritat, (2000), "Intrinsic Flaws of Element Enrichment Factors (EFs) in Environmental Geochemistry", Environmental Science & Technology 34 (24): 5084–91, https://doi.org/10.1021/es001339o.

[136] H. Yongming, D. Peixuan, C. Junji, E. Posmentier, (2006). "Multivariate Analysis of Heavy Metal Contamination in Urban Dusts of Xi'an, Central China", Science of The Total Environment 355 (1–3): 176–86. https://doi.org/10.1016/j.scitotenv.2005.02.026.

[137] A. Bokwa, (2008), "Environmental Impacts of Long-Term Air Pollution Changes in Kraków, Poland", Polish Journal of Environmental Studies 17 (5), 673-686, bwmeta1.element.agro-article-9d3e6da9-cf29-43a8-9864-8b0a5de4065c.

[138] M. Qu, Y. Wang, B. Huang, Y. Zhao, (2018), "Source Apportionment of Soil Heavy Metals Using Robust Absolute Principal Component Scores-Robust Geographically Weighted Regression (RAPCS-RGWR) Receptor Model", Science of The Total Environment 626: 203–10. https://doi.org/https://doi.org/10.1016/j.scitotenv.2018.01.070.

[139] T. Kormoker, R.Proshad, Md. Saiful Islam, Md. Shamsuzzoha, A. Akter, T. Roy Tusher, (2021), "Concentrations, Source Apportionment and Potential Health Risk of Toxic Metals in Foodstuffs of Bangladesh." Toxin Reviews 40 (4): 1447–60. https://doi.org/10.1080/15569543.2020.1731551.

[140] I.E.A. Idriss, M. Abdel-Azim, K.I. Karar, S. Osman, A.M. Idris, (2021), "Isotopic and Chemical Facies for Assessing the Shallow Water Table Aquifer Quality in Goly Region, White Nile State, Sudan: Focusing on Nitrate Source Apportionment and Human Health Risk", Toxin Reviews 40 (4): 764–76. https://doi.org/10.1080/15569543.2020.1775255.

[141] W. Rogula-Kozłowska, (2014), "Traffic-generated changes in the chemical characteristics of size-segregated urban aerosols", Bulletin of Environmental Contamination and Toxicology, 93, 493–502, https://doi.org/10.1007/s00128-014-1364-9.

[142] P. Kumar, L. Morawska, W. Birmili, P. Paasonen, M. Hu, M. Kulmala, R.M. Harrison, L. Norford, R. Britter, (2014), "Ultrafine particles in cities", Environ Int., 66:1-10, DOI:10.1016/j.envint.2014.01.013.

[143] C. Dameto De Espana, A. Wonaschütz, G. Steiner, A. Rosati, A. Demattioa, H. Schueha, R. Hitzenberger, (2017), " Long-term quantitative field study of New Particle Formation (NPF) events as a source of Cloud Condensation Nuclei (CCN) in the urban background of Vienna", Atmospheric Environment, 164, 289-298, https://doi.org/10.1016/j.atmosenv.2017.06.001.

[144] I. Salma, T. Borsos, T. Weidinger T., P. Alto, T. Hussein, M. Dal Maso, M. Kulmala, (2011), "Production, growth and properties of ultrafine atmospheric aerosol particles in an urban environment", Atmos. Chem. Phys., 11, 1339–1353, https://doi.org/10.5194/acp-11-1339-2011.

[145] K.W. Fent, D.E. Evans, K. Babik, C. Striley, S. Bertke , S. Kerber, D. Smith, G.P. Horn, (2018), "Airborne contaminants during controlled residential fires", Journal of Occupational and Environmental Hygiene, 15, 5, 399–412, doi: 10.1080/15459624.2018.1445260.

[146] M. Engelsman, M.F. Snoek, A.P.W. Banks, P.Cantrel, X.Wang, L.-M. Tom, D. J. Koppel, (2019), "Exposure to metals and semivolatile organic compounds in Australian fire stations", Environmental research, 179, Pt A, 108745, doi: 10.1016/j.envres.2019.108745.

[147] B.H. Alharbi, M.J. Pasha, M.A.S. Al-Shamsi, (2021), "Firefighter exposures to organic and inorganic gas emissions in emergency residential and industrial fires", Science of the Total Environment, 770, pp. 1–9, 2021, doi: 10.1016/j.scitotenv.2021.145332.

[148] W. Rogula-Kozłowska, K. Bralewska, P. Rogula-Kopiec, R. Makowski, M. Majer-Łopatka, A. Łukawski, A. Brandyk, G. Majewski, (2020), "Respirable particles and polycyclic aromatic hydrocarbons at two Polish fire stations", Building and Environment, 184, 107255, doi: 10.1016/j.buildenv.2020.107255.

[149] M. Oliveira, K. Slezakova, M.J. Alves, A. Fernandes, J.P. Teixeira, C. Delerue-Matos, M. do Carmo Pereira, S. Morais, (2017), "Polycyclic aromatic hydrocarbons at fire stations: firefighters' exposure monitoring and biomonitoring, and assessment of the contribution to total internal dose", Journal of Hazardous Materials, 323, 184–194, doi: 10.1016/j.jhazmat.2016.03.012.

[150] R.C. Bott, K.M. Kirk, M.B. Logan, D.A. Reid, (2017), "Diesel particulate matter and polycyclic aromatic hydrocarbons in fire stations", Environmental science. Processes & Impacts, 19, 10, 1320–1326.

Zeszyty Naukowe SGSP 2022, Nr 84, s. 55–71
ISSN: 0239-5223; e-ISSN: 2720-0779

**DOI:** 10.5604/01.3001.0016.1801

**Tomasz Mach**
Department of Environmental Protection,
Wroclaw University of Science and Technology
e-mail: tomasz.mach@pwr.edu.pl
**ORCID:** 0000-0001-7371-3499

**Jan Stefan Bihałowicz**
The Main School of Fire Service
e-mail: jbihalowicz@sgsp.edu.pl
**ORCID:** 0000-0003-3465-5315

# HOW TO EFFECTIVELY ANALYSE THE IMPACT OF AIR QUALITY ON SOCIETY – REVIEW OF MODERN MEASUREMENT TECHNIQUES AND APPARATUS: PARTICULATES

## Abstract

The article discusses modern measurement techniques and equipment designed for air quality analysis. The problem of the quality of atmospheric and indoor air is strongly related to broadly understood public health. Modern measurement techniques allow faster and more effective assessments of the air quality condition in a given place. The paper discusses the structure, measurement method of solid pollutants and automatic measurement systems deploying the micro-oscillatory balance method, using the interaction of ionizing radiation with matter-suppression of beta radiation and gamma radiation spectrometry, optical methods based on light scattering on particulate matter and systems combining more than one method. Technical solutions introduced by manufacturers of measuring equipment, which allow more precise measurement of gaseous pollutants, were also discussed.

**Keywords:** Particulate matter, PM10, PM2.5, XRF spectrometry, PM concentration, elemental composition, PM automatic measurement.

# JAK SKUTECZNIE ANALIZOWAĆ WPŁYW JAKOŚCI POWIETRZA NA SPOŁECZEŃSTWO – PRZEGLĄD NOWOCZESNYCH TECHNIK I APARATURY POMIAROWEJ

## Abstrakt

W artykule omówiono nowoczesne techniki pomiarowe i urządzenia do analizy jakości powietrza. Problem jakości powietrza atmosferycznego i wewnętrznego jest silnie związany z szeroko rozumianym zdrowiem publicznym. Nowoczesne techniki pomiarowe pozwalają na szybszą i skuteczniejszą ocenę stanu jakości powietrza w danym miejscu. W artykule omówiono budowę, metodę pomiaru zanieczyszczeń stałych oraz automatyczne systemy pomiarowe wykorzystujące metodę wagi mikrosiłownikowej, wykorzystujące oddziaływanie promieniowania jonizującego z materią – tłumienie promieniowania beta i spektrometrię promieniowania gamma, metody optyczne oparte na rozpraszaniu światła na poszczególnych cząstkach pyłu zawieszonego oraz systemy łączące więcej niż jedną metodę. Omówiono również rozwiązania techniczne wprowadzone przez producentów sprzętu pomiarowego, które pozwalają na bardziej precyzyjny pomiar zanieczyszczeń gazowych.

**Słowa kluczowe:** pył zawieszony, PM10, PM2,5, spektrometria XRF, stężenie PM, skład pierwiastkowy, pomiar automatyczny PM.

## 1. Introduction

The problem of air quality is the subject of a wide social debate; however, effective environmental management requires the development and validation of new measurement techniques. Nowadays, when information is of great value and can contribute to a quick change of reality, reliable measurements and the speed of their acquisition are the key parameters. The public should have access to air quality data as part of environmental justice, and they must be informed quickly in the event of deterioration, in their quality of life, or a threat to their health. Previous measuring techniques are not always able to meet these requirements. This raises the need for measurement techniques that are able to provide the same air quality information faster, more accurately, or with less effort or resources. Thanks to this, it is possible to carry out measurements in real-time [1], and by connecting them with spatial information systems, make them available to the public [2], [3], and take into account new parameters in the assessment of social exposure [4], [5]. Thanks to new measurement techniques, public awareness about the dangers of air pollution is growing. Among other things, it is the data on air quality collected with the use of modern techniques, by enthusiasts and social activists, which can be the basis for new legal regulations [6]. The role of the R&D (research and development) sector is to ensure the accuracy of the information available to the public, i.a. by validating these techniques [7] and creating new ones. In this article, modern techniques for measuring solid pollutants will be discussed in the context of the current standards, along with the application of devices that use these techniques.

# 2. Measurement techniques and apparatus

## 2.1. Measurement of solid pollutants

### 2.1.1. PN-EN 12341:2014 Standard gravimetric measurement method for the determination of the PM10 or PM2.5 mass concentration of suspended particulate matter

First of all, let us quote a fragment of the PN-EN 12341: 2014 (PN-EN 12341: 2014) [8] standard that describes the gravimetric measurement method for the determination of mass concentrations of suspended particulate matter:

"In order for air quality throughout the European Union to be assessed in a consistent manner, Member States must use standard techniques and measurement procedures. The purpose of this European Standard is to provide a harmonized methodology for measuring the mass concentrations of particulate matter (PM10 and PM2.5 respectively) in the ambient air, in accordance with Directive 2008/50/EC on ambient air quality and cleaner air for Europe, which specifies parameters specific to assessment of the concentration levels of particulate matter in the air."

Particulate matter collection is carried out by taking a PM sample onto the filter and then weighing it on a filter equipped with a scale. The sampling itself is performed using the so-called PM collectors (or sequential PM collectors), furnished with a standardized inlet, i.e., a measuring head, the design of which is described in the above-mentioned standard. The PM collector works with a nominal flow rate of 2.3 $m^3$/h. This intensity is most often controlled with the help of built-in mass flow meters. The nominal sampling period is 24 hours (24-hour averages). Measurement results are expressed in $\mu g/m^3$, where the air volume corresponds to the volume at ambient conditions, near the inlet, at the time of sampling. Thanks to the changer and cassette with a minimum of 14 filters, the sequential PM collector allows the sampling for at least 2 weeks, without the need of replacing filters by the operator. However, the application of such a solution requires proper conditioning of the filters, which after 24 hours of exposure to the sample are found in a cassette with once-collected PM in a cassette, waiting to be taken for further analysis by the operator.

### 2.1.2. PN-EN 16450:2017 Automated measuring systems for the measurement of the concentration of particulate matter (PM10; PM2.5)

Moving on to the next standard, it is applicable to automatic measurement systems for suspended PM concentration; let us quote a fragment of the introduction to the standard (PN-EN 16450:2017) [9]: In order to comply with the requirements of the EU Air Quality Directive, the reference methods given in Directive 2008/50/EC for the measurement of particulate matter mass concentration are not widely used in automatic air pollution monitoring networks. Typically, these networks

use automated continuous measurement systems (AMS), e.g. based on the use of an oscillating microbalance, β-radiation absorption, or in situ optical methods. Such AMS systems are usually able to obtain 24-hour average measured values with a measurement range of up to 1,000 μg/m$^3$ and 1-hour average measured values up to 10,000 μg/m$^3$, if applicable, where air volume is the volume in ambient conditions near the inlet.

The PN-EN16450:2017 standard does not define a specific measurement methodology to be used for the automatic determination of mass concentration of solid particles in atmospheric air; therefore, various measurement methods can be used. Nevertheless, the measuring instrument should consist of:

- PM10 or PM2.5 selective measuring head. This head is used to selectively separate the PM fractions of interest from the total PM (in the case of optical analysers, such heads are not used, and a separation system is required instead);
- Sampling system/tube. Such an arrangement is usually of a length that corresponds to certain conditions regarding the height, from which the sample is to be taken. Most often it is equipped with "intelligent heating" depending on the external temperature and humidity. This heating is intended to eliminate the effect of volatile fractions released from the measuring filter. Another possible solution is a system of partial drying of the air sample;
- A vacuum pump responsible for sample collection;
- Flow sensors and controllers;
- Temperature and pressure sensors;
- Data recording system-logger: hardware and software for collecting and storing data and converting measurement results.

In addition, the automatic analyser for measuring solid particles can be equipped with moisture sensors or a compensation measurement system. Such a system is used to eliminate the influence of undesirable confounding factors or accidental changes in the determination of the mass of particulate matter.

Automatic devices for measuring particulate matter approved for operation in air pollution monitoring networks should obtain a certificate and a Type Approval report for compliance with the PN-EN 16450:2017 standard. Such tests and the report must be issued by an accredited laboratory, i.e. a laboratory with accreditation to the EN ISO / IEC 17025 standard for the tests performed. The methodology for the procedure, for confirming equivalence, must be in accordance with EN 16450:2017.

## 2.2. The method of oscillating microbalance

This methodology was invented in the 1990s by two Americans, Rupprecht and Patashnick [10]. This discovery resulted in the founding of a company that produces a number of instruments using the oscillating balance method.

The most popular representative of instruments using the oscillating microbalance method is the Teom 1400 series of PM meters (Thermo Fischer Scientific, Walthman, MA, USA), represented by: Teom 1400, Teom 1400a, Teom 1400ab, and Teom1405. The principles of mass measurement used by Teom instruments differ fundamentally from those on which most other measuring instruments have been based. The filter is mounted on a capillary, the so-called conical element (a thin, long, hollow glass tube). A capillary filter is placed in the sample flowing stream. The "fall" of individual PM particles onto the filter causes the capillary to vibrate. The conical element vibrates exactly at the natural frequency. The effect is similar to the vibration of a tuning fork. As the mass increases, the frequency of vibrations tends to decrease. The electronic control circuit senses these vibrations and, through positive feedback, adds sufficient energy to cover system losses. The automatic gain control circuit maintains a constant vibration amplitude. An accurate electronic counter measures the frequency in two-second sampling periods. The dependence of the frequency changes on the change of the mass of the vibrating element makes it possible to determine the mass gain over time [10].

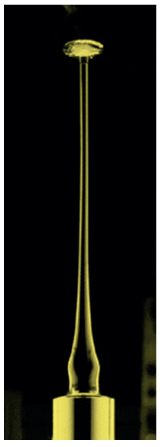

Fig. 1. Filter with a conical element induced to vibrations due to contact PM (3)

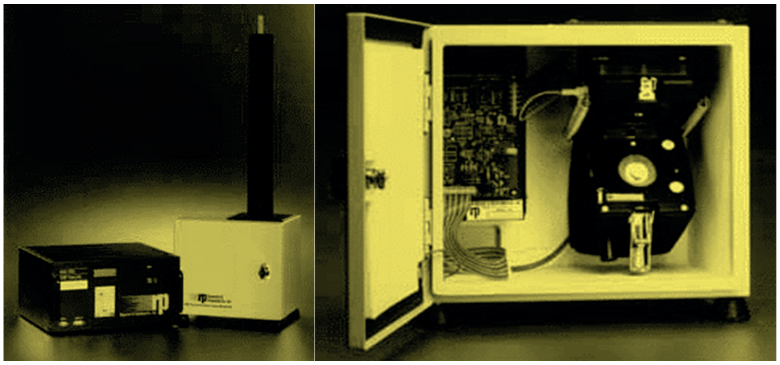

Fig. 2. Teom 1400ab (3)

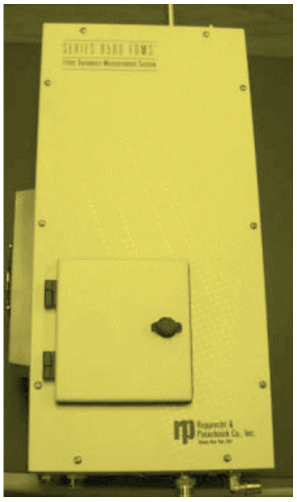

Fig. 3. Filter Dynamics Measurement System FDMS – system to eliminate the effect of the loss of volatile fractions (3)

The principle of mass measurement is described by the formula (1), where ΔM is the mass change, $K_0$ is the capillary stiffness (taking into account the mass conversion), $f_0$ – the initial frequency and $f_1$ – the final frequency [10].

$$\Delta M = K_0\left(\frac{1}{f_1^2} - \frac{1}{f_0^2}\right) \tag{1}$$

At the beginning of the 21st century, the so-called "effect of loss of volatile fractions" was worked out, which introduced a large error in the measurement of the oscillatory microbalance method, which means that this method is susceptible to the above-mentioned problem. The essence of the "volatile fraction loss effect" is the deposition of PM, including volatile fractions, on the measuring filter, which

causes vibrations. With time, volatile particles deposited on the filter will once again transform into a volatile form, which disturbs the actual vibration value. To eliminate the above-mentioned effect, an additional component installed in the sampling path was constructed, called FDMS (Filter Dynamics Measurement System). This system divides the measuring cycle into two stages of 6 minutes each. In the first stage, the sample flows through the instrument along the "old path" and is deposited on the measuring filter. In the second stage, the sample additionally flows through the FDMS system, where it is heated to evaporate volatile fractions. Thanks to this, the device not only eliminates the evaporative effect of volatile fractions but also has the ability to measure the mass of solid particles, with the separation into volatile and non-volatile fractions. This device is widely used in air quality monitoring [11] and in connection with other parameters of the atmosphere quality [12].

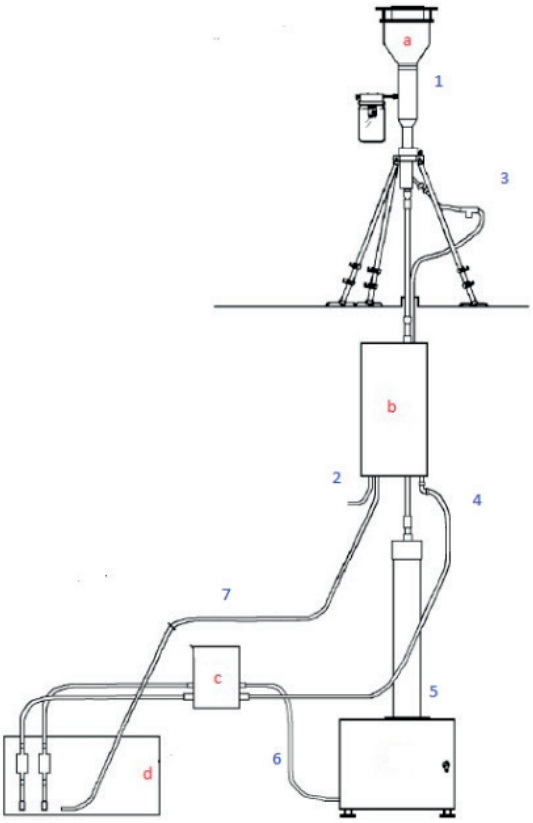


Fig. 4. Scheme of Teom 1400ab FDMS: a – measuring head PM10, b – FDMS (Filter Dynamics Measurement System), c – module SES, d – control unit, e – measurement unit, 1 – main flow, 2 – pump, 3 – by-pass flow, 4 – by-pass flow, 5 – baseline/reference flow, 6 – baseline/reference flow, 7 – rinsing flow (3)

One of the interesting facts about automatic measurement systems is that when, at the turn of the 20th and 21st centuries, the European Union started to devise a standard describing automatic PM measurement, the concept of describing the oscillatory microbalance method as the required measurement method has won. As Rupprecht & Patashnick (the company was founded to commercialize the invention) patented its method, negotiations with the manufacturer began. The EU imposed a condition that the patent would be made available free of charge to all interested parties. After long negotiations, the agreement has not been concluded, and we had to wait until 2017 for the standard describing automatic measurement systems, for measuring the concentration of particulate matter.

### 2.3. β radiation suppression method

The β-radiation absorption method is known and very well-tested. A number of measuring instruments make use of this method to measure the concentration of PM in the atmospheric air [13].

It is known that high-energy electrons from the radioactive decay of carbon $^{14}C$ react with nearby molecules, as a rule losing their energy. Sometimes they are also absorbed by it. These electrons are called β rays, and the process that takes place is called β radiation suppression [14].

Let us imagine a system, in which between the source of radioactive carbon $^{14}C$ and the β-ray detector a material is placed (e.g. a filter tape), on which a sample of solid particles is then deposited. This sample would absorb the beta rays emitted by the source and their energy would be reduced. As a result, the detector receives less β radiation than has been emitted by the source.

The difference between what has been emitted and what has been measured by the detector (and thus the degree of particle number reduction) is a function of the mass, of the absorbing material in the path of the beta rays.

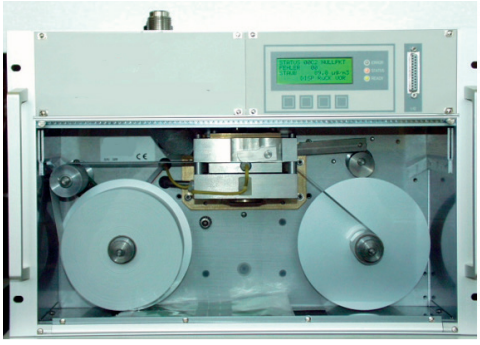

Fig. 5. Example of the construction of a PM meter using the β-radiation attenuation method (3)

The number of β rays passing through the absorbing material decreases exponentially with the mass of the material, through which they pass according to equation (2), where $I$ is the measured radiation $\beta$ intensity, $I_0$ the measured intensity of undamped beta radiation (measurement made on a clean measuring tape), $\mu$ cross-section of beta-ray absorbing material ($cm^2/g$), $x$ the density of the absorbing substance ($g/cm^2$) [14].

$$I = I_0 e^{-\mu x} \tag{2}$$

This equation is very similar to those describing the attenuation of gamma particles, however, in the case of gamma radiation, the radiation spectrum is continuous and the rate of loss of free electrons is higher than the faster electrons, which causes deviations from the linear dependence in the exponent. Equation (2) is an idealizing simplification of the actual process to simplify the related mathematical apparatus. Nevertheless, the manufacturers' research has shown that in properly designed devices deploying β radiation suppression, the use of the above-described formula does not cause the appearance of significant differences.

## 2.4. Optical method

In recent years, optical methods have been gaining more and more importance, both in simple applications (simple, cheap, installed in hundreds of pieces, measuring systems informing more about the level of contamination - so-called indicators) and in "reference" applications, i.e., instruments fully certified for compliance with the applicable EN 16450:2017 standard.

There are several varieties of optical methods used in the measurement of PM, the most popular of which are nephelometry and spectrometry.

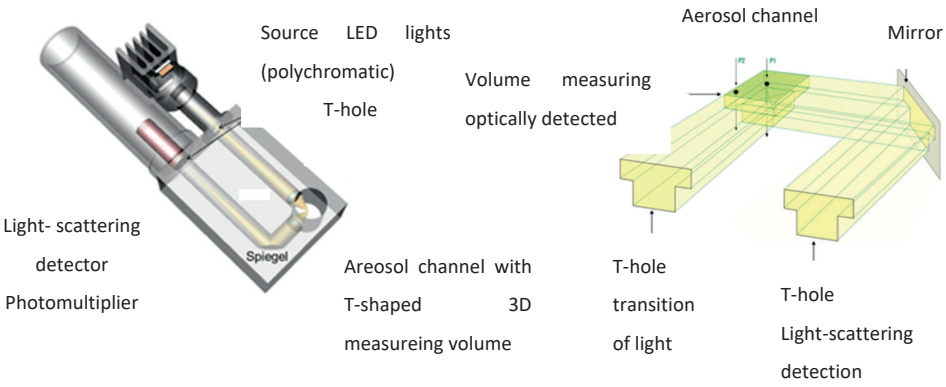


Fig. 6. Example of a particulate spectrometer measuring system (1)

In general, the main principle of all optical instruments is the diffusion of light onto solid particles. In the case of nephelometry, the detector placed most often at an angle of 90° from the light source, which may be, for example, a LED diode, laser, etc., measures the intensity of light reflected from solid particles.

In the case of spectrometry, it is more complicated, yet the measurement is much more accurate. Spectrometers count particles and determine the particle size for each, individual molecule using scattered light, e.g., according to the Lorenz-Mie law. The source of light (usually polychromatic) is a laser or LED diode. Scattered light reflected from the particle passes through the laser beam and is then reflected by the mirror at an angle of 90° to the detector. The determination of the optical particle size is performed by assigning the scattered light signal to the particle diameter with a calibration curve. The use of a polychromatic light source makes it possible to obtain an accurate calibration curve, without ambiguities in the Mie range. This enables a high resolution of the method to be obtained.

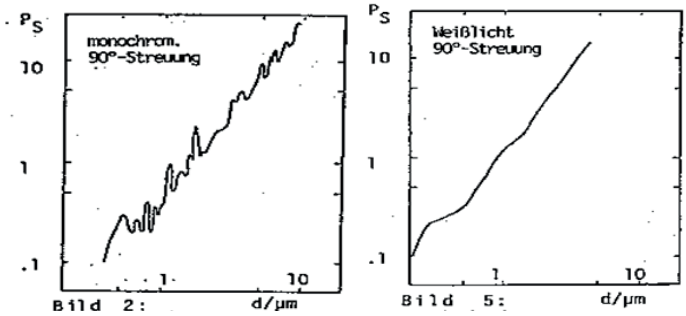


Fig. 7. Example of a calibration curve for the detection of 90° scattered light with a monochromatic light source (left) and a polychromatic light source (right)(1)


Fig. 8. An example of a Fidas200 optical aerosol spectrometer (1)

The main advantage of optical analysers - spectrometers is the identification of fractions for each molecule. As a result, it is possible to simultaneously measure many PM fractions with a single measuring instrument. No other methodology for measuring solid particles offers such a possibility. Another important advantage

is the practical lack of consumables, such as filters or measuring tapes (which significantly reduces operating costs).

In recent years, optical instruments (not only reference ones) have gained enormous popularity. Due to the fact that several fractions are measured simultaneously, especially PM10 and PM2.5, these instruments dominate the atmospheric pollution monitoring networks, both domestic (in Poland: the SEM network belonging to the Chief Inspectorate of Environmental Protection CIEP, and managed by the Central Research Laboratory CRL) and local ones (e.g. city, company, etc.).

The main advantage of measuring several fractions with a single instrument is that it eliminates "electronic noise" emitted by the instruments. Each analyser emits a noise on a different level. For example: when measuring PM10 and PM2.5 fractions with the use of two independent analysers, an effect was observed at very low concentrations when the analyser concentration of PM10 fraction (this fraction includes the PM2.5 fraction) measured at lower concentrations of particulate matter than the analyser measuring the PM2.5 fraction. An example of such an effect is a higher indication of PM2.5 than PM10 (which happens relatively often), measured at a single measuring point by two different instruments. By using one device, the above problem is eliminated. Another aspect is the purchase and operating costs, which are lower for one instrument measuring several fractions than for a bank of analysers measuring one fraction each. Another advantage are smaller dimensions and one sampling system, which facilitates the preparation of the measuring point, but also enables comprehensive measurement of many fractions in places inaccessible to single-fraction instruments. This method allowed a more precise analysis of the distribution of the number of particles as a function of diameter, in order to more precisely compare different measurement points [15], and to analyse these distributions in places where the emission from wood combustion is dominant [16].

### 2.5. Other measurement methods

In addition to the basic (most commonly used) measurement methodologies described in the EN 16450: 2017 standard used in instruments for particulate matter, there are additional instruments that use at least two methods simultaneously, so-called hybrid devices.

An example of such a solution is the device called the Synchronized Hybrid Ambient Realtime Particulate Monitor SHARP 5030, of one of the most renowned manufacturers, combining the optical nephelometry method with the β radiation absorption method. The advantage of the nephelometer is the short measurement time, while its disadvantage is the accuracy of the measurement. The opposite is the

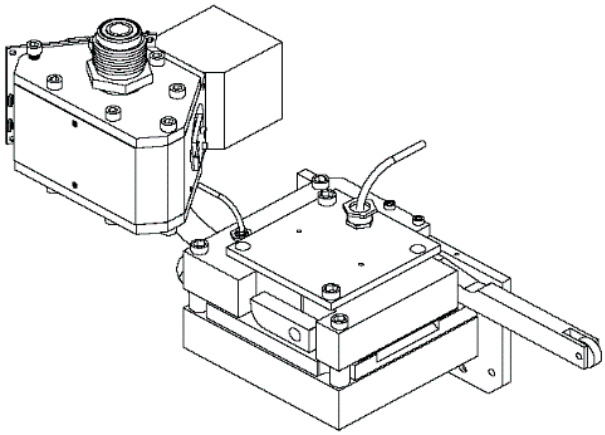

Fig. 9. Synchronized Hybrid Ambient Realtime Particulate Monitor (3)

case with the beta radiation suppression method, where we obtain high accuracy, but unfortunately, the shortest measurement time is 1h. Thanks to the use of both methods in parallel (the nephelometer carries out the measurement and is permanently and automatically calibrated with the β radiation suppression system), the device benefits from the advantages of each method (and also eliminates their disadvantages) and is able to make measurements very precisely, providing at the same time one-minute results, while ensuring a high detection threshold. It was used inter alia for the analysis of PM2.5 sources during the episodes of atmospheric turbidity [17] and for the analysis of aerosol formation [18].

Another interesting instrument is the ELPI+ (Electrical Low Pressure Impactor). The analysed gas, which contains PM, passes through a device that gives the particles an electric charge in the process of a corona discharge. Then the sample containing the charged PM particles is placed in a multi-stage impactor, the stages of which are electrically isolated from each other. PM with a decreasing aerodynamic diameter from 10 μm to 0.006 μm are deposited on the individual stages (14 elements) of the impactor. When a particle falls on the impactor stage, the charge of the PM particle is collected on the impactor stage. The charge is measured in real-time by a highly sensitive multi-channel electrometer. The electrical signal from each of the impactor stages is converted into data on the distribution of the number and mass of particles according to their size, i.e. the aerodynamic diameter. An additional advantage of this solution is the collection of individual PM fractions on measuring filters. The collected sample can be used not only to confirm (using gravimetric methods) the correctness of the automatic measurement indication but also for further laboratory analyses. In such a way, we can obtain information, for example, on the elemental composition of the collected sample [19].

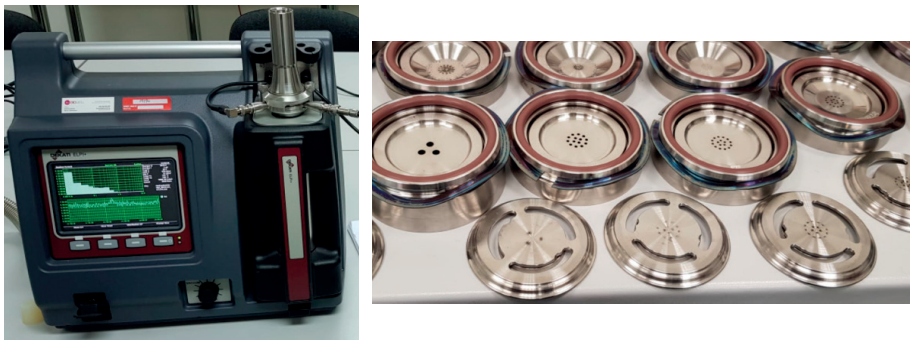

Fig. 10. Electric Low Pressure Impactor ELPI+ (3)

Thanks to its real-time measurement, ELPI+ is an ideal tool for PM analyses in conditions of unstable concentrations and variable fractional distribution. A durable and solid construction allows the device to be used also in difficult environmental conditions; it was used inter alia in determining the parameters of emissions from low-emission coal power plants [20], aerosol analysis in dental offices in the context of SARS-CoV-2 virus transmission [21] or in the analysis of emissions from waste fires [22]. The latest versions of the above solution, although a bit simplified, and consequently also miniaturized, provide a wide range of possibilities for its use in measuring air pollution in buildings [23]. The aspect of air pollution we breathe in buildings (homes, shops, offices, etc.) is becoming increasingly importan, especially since indoor time has drastically increased in recent decades. Miniaturization also allows the use of these devices in mobile air quality monitoring [24].

Another device, an even more interesting one, is the Horiba PX-375 analyser. This instrument combines β radiation absorption with XRF spectrometry. Thanks to the innovative combination of these two measurement methodologies, the manufacturer has gained the unique possibility of automatic, practically in real-time, measurement of the concentration of PM10 or PM2.5 solid particles, with the simultaneous spectral analysis, thanks to which the user obtains information about the elemental composition of the measured PM.

There is a need for simultaneous measurement of PM and its chemical properties in order to quickly adjust process parameters and identify emission sources. This proves to be particularly useful in areas where PM emissions from different sources overlap or where there is only one dominant source and the problem is to correctly identify the origin of the PM. The use of the PX-375 analyser in the research enables the acquisition and use of data (PM concentration, but most of all the exact elemental composition of the tested PM) from averaging measurements at time intervals shorter than 24 hours. The use of traditional measurement methodologies excludes capturing short-term elevated concentrations of elements in the atmosphere. Long-term measurement allows both the definition of short-term changes and


Fig. 11. Horiba PX-375 analyzer with a measurement screenshot (2)

the characteristics of pollutants at the regional level, as well as the use of recorded concentrations of inorganic elements as indicators in the identification of pollution sources [25], [26], a comparison of actual concentrations with environmental indicators [27], even if it is known that in rural ones, low emission can significantly worsen air quality. Hence, cheap and easily accessible methods of monitoring are needed. Recently, spider webs biomonitoring is getting popular, however, there is no information about its comparison with active methods. In this study, PTEs accumulated on spider webs were compared with results from continuous particulate monitor (CPM) and environment monitoring [28], [29].

## 3. Conclusions

The apparatus is a key element in air quality measurements. The measurement of solid pollutants can be performed by various technical solutions, which should be compliant with standards for automatic measurement systems. Equipment manufacturers are devising modern solutions and techniques aimed at providing society with better access to more reliable data on air quality. It is important that the recipients of information on airborne pollutants be aware of the various methods of measuring parameters, and hence the differences between them and the advantages of individual methods. Due to the flexibility presented in the EN 16450 standard, the methods used in various devices differ from each other.

The measuring instruments described in this publication and the methodologies they use can be deployed successfully in diverse applications.

Manual methodologies (gravimetric samplers) are applicable when measurements should meet the requirements described in the European Union regula-

tions, i.e., for example all official settlements of the PM concentration occurring in the atmospheric air. Due to the long analysis time manual methodologies are unsuitable for hot-spot measurements, where results are expected immediately or almost immediately.

If, in addition to the concentration of PM, we are also interested in the separation of volatile and non-volatile fractions, the only possible solution are instruments that use the oscillatory microbalance method together with the FDMS system.

Optical methods are ideal for hot-spot, fast, short-term measurement applications. However, for example, to detect the sources of PM emissions, an excellent solution is to measure its elementary composition of PM are XRF methodologies.

## Acknowledgments

This work was carried out as a part of the Implementation Doctorate, 2nd edition, W-7 (03DW/0001/18), financed by the National Centre for Research and Development, Poland.

All photos, figures, and schemes used are the property of the authors or have been used courtesy and with the consent of the following companies:

1. *Palas GmbH, Karlsruhe, Germany,*
2. *Horiba GmbH, Tulln, Austria,*
3. *MLU Sp. z o. o., Katowice, Poland.*

### References

[1] Bell M.L., Dominici F., Ebisu K., Zeger S L., Samet J M., *Spatial and Temporal Variation in PM2.5 Chemical Composition in the United States for Health Effects Studies*, "Environmental Health Perspectives" 2007, 115(7), pp. 989–995, https://doi.org/10.1289/ehp.9621.

[2] Bihałowicz J.S., Rogula-Kozłowska W., Krasuski A., Majder-Łopatka M., Walczak A., Fliszkiewicz M., Rogula-Kopiec P., Mach T., *Characteristics of Particles Emitted from Waste Fires—A Construction Materials Case Study*, "Materials" 2021, 15(1), p. 152–152, https://doi.org/10.3390/ma15010152.

[3] Chatain M., Alvarez R., Ustache A., Rivière E., Favez O., Pallares C., *Simultaneous Roadside and Urban Background Measurements of Submicron Aerosol Number Concentration and Size Distribution (in the Range 20–800 nm), along with Chemical Composition in Strasbourg, France*, "Atmosphere" 2021. https://doi.org/10.3390/atmos12010071.

[4] Ehtezazi T., Evans D.G., Jenkinson I.D., Evans P.A., Vadgama V.J., Vadgama J., Jarad F., Grey N., Chilcott R.P., *SARS-CoV-2: characterisation and mitigation of risks associated with aerosol generating procedures in dental practices*, "British Dental Journal" 2021, doi:10.1038/s41415-020-2504-8, https://doi.org/10.1038/s41415-020-2504-8.

[5] GIOŚ, *Portal Jakość Powietrza GIOŚ*, 2021.
[6] Grivas G., Athanasopoulou E., Kakouri A., Bailey J., Liakakou E., Stavroulas I., Kalkavouras P., Bougiatioti A., Kaskaoutis D., Ramonet M., Mihalopoulos N., Gerasopoulos E., *Integrating in situ Measurements and City Scale Modelling to Assess the COVID–19 Lockdown Effects on Emissions and Air Quality in Athens, Greece*, "Atmosphere" 2020, 11(11), p. 1174, https://doi.org/10.3390/atmos11111174.
[7] Heal M., Kumar P., Harrison R.M., *Particles, air quality, policy and health*, "Chemical Society Reviews" 2012, 41(19), pp. 6606–6630, https://doi.org/10.1039/C2CS35076A.
[8] Herrmann E., Ding A.J., Kerminen V-M., Petäjä T., Yang X.Q., Sun J.N., Qi X.M., Manninen H., Hakala J., Nieminen T., Aalto P.P., Kulmala M., Fu C.B., *Aerosols and nucleation in eastern China: first insights from the new SORPES-NJU station*, "Atmos. Chem. Phys." 2014, 14(4), pp. 2169–2183, https://doi.org/10.5194/acp-14-2169-2014.
[9] Kang Y., Aye L., Ngo T.D., Zhou J., *Performance evaluation of low-cost air quality sensors: A review*, "Science of The Total Environment" 2022, 818, p. 151769–151769, https://doi.org/10.1016/j.scitotenv.2021.151769.
[10] Kuula J., Friman M., Helin A., Niemi J.V., Aurela M., Timonen H., Saarikoski S., *Utilization of scattering and absorption-based particulate matter sensors in the environment impacted by residential wood combustion*, "Journal of Aerosol Science" 2020, 150, p. 105671, https://doi.org/10.1016/j.jaerosci.2020.105671.
[11] Li L., Tan Q., Zhang Y., Feng M., Qu Y., An J., Liu X., *Characteristics and source apportionment of PM2.5 during persistent extreme haze events in Chengdu, southwest China*, "Environmental Pollution" 2017, 230, pp. 718–729, https://doi.org/10.1016/j.envpol.2017.07.029.
[12] Li Y., Chang M., Ding S., Wang S., Ni D., Hu H., *Monitoring and source apportionment of trace elements in PM2.5: Implications for local air quality management*, "Journal of Environmental Management" 2017, 196, pp. 16–25, https://doi.org/10.1016/j.jenvman.2017.02.059.
[13] Lyu R., Zhang J., Wu J., Feng Y., *Primary Carbonaceous Particle Emission from Four Power Plants with Ultralow Emission in China*, "ACS Omega" 2021, 6(2), pp. 1309–1315, https://doi.org/10.1021/acsomega.0c04754.
[14] Mach T., Rogula-Kozłowska W., Bralewska K., Majewski G., Rogula-Kopiec P., Rybak J., *Impact of Municipal, Road Traffic, and Natural Sources on PM10: The Hourly Variability at a Rural Site in Poland*, "Energies" 2021, 14(9), p. 2654, https://doi.org/10.3390/en14092654.
[15] Mahajan S., Chung M-K., Martinez J., Olaya Y., Helbing D., Chen L-J., *Translating citizen-generated air quality data into evidence for shaping policy*, "Humanities and Social Sciences Communications" 2022, 9(1), p. 122, https://doi.org/10.1057/s41599-022-01135-2.
[16] Majewski G., Szeląg B., Mach T., Rogula-Kozłowska W., Anioł E., Bihałowicz J., Dmochowska A., Bihałowicz J.S., *Predicting the Number of Days with Visibility in a Specific Range in Warsaw (Poland) Based on Meteorological and Air Quality Data*, "Frontiers in Environmental Science" 2021, https://doi.org/10.3389/fenvs.2021.623094.
[17] Mitreska E., Davcev D., Mitreski K., *A Mobile Environmental Air Quality Information System as a Support for m-Health BT – Mobile Computing, Applications, and Servi-*

*ces* [in:] Memmi G., Blanke U. (eds), Cham, Springer International Publishing: 2014, pp. 277–281.
[18] Oksanen L-M., Virtanen J., Sanmark E., Venkat V., Soeva S., Aaltonen K., Kivistö I., Svirskaite J., Pérez A., Kuula J., Levanov L., Hyvärinen A-P., Maunula L., Atanasova N., Laitinen S., Anttila V-J., *SARS-CoV-2 air and surface contamination on a COVID-19 ward and at home*, "Research Square" 2021, pp. 1–25, https://doi.org/10.21203/rs.3.rs-1002547/v2.
[19] Patashnick H., Rupprecht E.G., *Continuous PM-10 Measurements Using the Tapered Element Oscillating Microbalance*, "Journal of the Air & Waste Management Association" 1991, 41(8), pp. 1079–1083, https://doi.org/10.1080/10473289.1991.10466903.
[20] PKN, *PN-EN 12341:2014 Powietrze atmosferyczne – Standardowa grawimetryczna metoda pomiarowa do określania stężeń masowych frakcji PM10 lub PM2,5 pyłu zawieszonego*, 2014.
[21] PKN, *PN-EN 16450:2017 Powietrze atmosferyczne – Automatyczne systemy pomiarowe do pomiarów stężenia pyłu zawieszonego (PM10; PM2,5)*, 2017.
[22] Rogula-Kozłowska W., Sówka I., Mathews B., Klejnowski K., Zwoździak A., Kwiecińska K., *Size-Resolved Water-Soluble Ionic Composition of Ambient Particles in an Urban Area in Southern Poland*, "Journal of Environmental Protection" 2013, 04(04), pp. 371–379, https://doi.org/10.4236/jep.2013.44044.
[23] Schwab J.J., Felton H.D., Rattigan O.V., Demerjian K.L., *New York State Urban and Rural Measurements of Continuous PM 2.5 Mass by FDMS, TEOM, and BAM*, "Journal of the Air & Waste Management Association" 2006, 56(4), pp. 372–383, https://doi.org/10.1080/10473289.2006.10464523.
[24] Shukla K., Aggarwal S.G., *A Technical Overview on Beta-Attenuation Method for the Monitoring of Particulate Matter in Ambient Air*, "Aerosol and Air Quality Research" 2022, 22, p. 220195, https://doi.org/10.4209/aaqr.220195.
[25] Skrzypczak E., Szefliński Z., *Wstęp do fizyki jądra atomowego i cząstek elementarnych*, PWN, Warsaw 2012.
[26] Snyder E.G., Watkins T.H., Solomon P.A., Thoma E.D., Williams R.W., Hagler G.S.W., Shelow D., Hindin D.A., Kilaru V.J., Preuss P.W., *The Changing Paradigm of Air Pollution Monitoring*, "Environmental Science & Technology" 2013, 47(20), pp. 11369–11377, https://doi.org/10.1021/es4022602.
[27] Stojanowska A., Mach T., Olszowski T., Bihałowicz J.S., Górka M., Rybak J., Rajfur M., Świsłowski P., *Air Pollution Research Based on Spider Web and Parallel Continuous Particulate Monitoring—A Comparison Study Coupled with Identification of Sources*, "Minerals" 2021, 11(8), p. 812, https://doi.org/10.3390/min11080812.
[28] Tu R., Li T., Meng C., Chen J., Sheng Z., Xie Y., Xie F., Yang F., Chen H., Li Y., Gao J., Liu Y., *Real-world emissions of construction mobile machines and comparison to a non-road emission model*, "Science of The Total Environment" 2021, 771, p. 145365, https://doi.org/10.1016/j.scitotenv.2021.145365.
[29] Xia T., Catalan J., Hu C., Batterman S., *Development of a mobile platform for monitoring gaseous, particulate, and greenhouse gas (GHG) pollutants*, "Environmental Monitoring and Assessment" 2021, 193(1), p. 7, https://doi.org/10.1007/s10661-020-08769-2.

# Spider webs in monitoring of air pollution

*Radosław* Rutkowski[1,*] *Justyna* Rybak[1] , *Tomasz* Mach[2] , and *Wioletta* Rogula–Kozłowska[3]

[1]Wrocław University of Science and Technology, Department of Environmental Protection, 27 Wybrzeże Wyspiańskiego St., 50-370 Wrocław, Poland
[2]MLU-Recordum, 16 Połomińska St., 40-585 Katowice, Poland
[3]The Main School of Fire Service, Faculty of Fire Safety Engineering, 52/54 Słowackiego St., 01-629 Warsaw, Poland

**Abstract.** Biomonitoring is a significant tool of environmental protection strategies. Variety of bioindicators are used worldwide, particularly mosses, lichens and tree leaves. However, they revile many considerable disadvantages, e.g. limitation to vegetative season, moisture demand, exposition to severe weather conditions, limited time of monitoring. Classical impactors, on the other hand, are expensive, cannot be used without supervision and allow only for short-term monitoring. Spider webs, however, reveal features of extraordinary bioindicators. Webs are abundant, easy to collect, costless and can be found all year round, despite vegetative season. Spider silk is a very efficient, non-selective accumulator of contaminants, that allows for long-term monitoring. Thanks to this characteristics, spider webs proved to be immensely useful bioindicators of air pollution. They allow for monitoring of heavy metals, Polycyclic Aromatic Hydrocarbons (PAHs), dioxins, so as assessment of mutagenic activity and anthropopression assessment and indication of dominant source of pollutants. Most of the researches concerning application of spider webs as bioindicators have been conducted in Wrocław, Poland. This paper reviews current knowledge on spider webs in monitoring of air pollution.

## 1 Introduction

Air pollution is a rising concern of modern society. In 2015, over 4 million people died all over the world because of the exposure to atmosphere pollutants. According to Institute for Health Metrics and Evaluation (IHME), the main causes of these deaths were: chronic obstructive pulmonary disease (27.1%), lower respiratory infections (24.7%), ischemic heart disease (17.1%), lung cancer (16.5%) and stroke (14.2%) [1]. Sources of these threats are mostly industrial, which include: power generation, road transport, waste disposal and variety of domestic sources. Agriculture, along with burning of agricultural waste, is also a source of pollution, which must not be overlooked.

Consistent development of industries, urbanization and transport demand efficient, cheap and universal tools for monitoring their impact on the environment. For this purpose, new

* Corresponding author: radoslaw.rutkowski@pwr.edu.pl

methods of biomonitoring are being developed and refined, among which, spiders usage steps out of the line.

Biological monitoring term was defined in 1980 Luxemburg seminar, organized by the European Economic Community (EEC), National Institute for Occupational Safety and Health (NIOSH) and Occupational Safety and Health Association (OSHA). The aim of the seminar was to examine the roles of ambient and biological monitoring in protecting the health of workers exposed to toxic agents and to define a multidisciplinary approach to this monitoring. The biological monitoring was defined as the measurement and assessment of workplace agents or their metabolites either in tissues, secreta, excreta, expired air on any combination of these to evaluate exposure and health risk compared to an appropriate reference [2]. In most common comprehension, biological monitoring is the usage of the living organisms to estimate and track changes in the environment.

Biomonitoring is typically employed either as a complementary method or as an alternative method for accurate large-scale studies when the extensive use of equipment on-site is expensive or impractical. The advantage of this methods is that they can substantiate the physical and chemical data by physiological data referring to the viability of this material. A wide variety of species are known as useful bioindicators in aquatic and terrestrial ecosystems. Depending on the type of organisms used for monitoring, they are classified into plants (e.g. mosses, lichens, tree leafs, algae), animals and microorganisms.

Many of them revile considerable disadvantages. For example: lichens, which are considered to be a textbook bioindicators might be rare in urban areas due to their vulnerability to $SO_2$, sulphur and nitrogen based pollutants, which confounds their bioaccumulative properties. Content of lichens and mosses depends on surface they grow, hence finding specimens in different areas with similar composition might be hindered. These organisms are very moisture-dependent, so utilized “bags” must be precisely prepared in order to preserve drying process [3]. Because of the moisture issue, short term exposition might be recommended.

Spiders are the largest order of arachnids that lately have proved to be extraordinary bioindicators - vastly thanks to a spider silk – a unique device in Animalia kingdom, which guaranteed them evolutionary success.

Spiders inhabit almost any kind of environment and dwell readily in urbanized areas, which makes their silk a greatly available sampling material. Many spider species reside households and are well tolerated by humans (e.g. Pholcidae family). Spiders web are thus vastly accessible, easy to collect and costless. There are independent of vegetative season factors like sunlight or temperature. Webs are protected from severe weather conditions like rain or wind, hence the accumulation rates depends on the site location. Sample collection is non-invasive and does not require killing animal itself [4, 5, 6].

Webs efficiently accumulate toxins, which enables a long-term monitoring of air pollution level in contrast to standard measurements, which allow only for short-term studies. What is more, passive samplers use mostly selective sorbents, which cannot be applied for wide range of air pollutants.

## 2 Heavy metals

Heavy metals are non-biodegradable compounds which can bind to ecosystem’s trophic chain, many of them exhibit toxic and carcinogenic properties. There are many anthropogenic sources of heavy metals emission to the atmosphere, among which vehicular traffic rises increasing concern. Metals which pose particular threat for the environment are: chromium (Cr), lead (Pb), mercury (Hg), cadmium (Cd), arsenic (As), copper (Cu), manganese (Mn), nickel (Ni), zinc (Zn) and silver (Ag).

Hose at al. investigated application of spider webs in biological monitoring at the beginning of XXI century [4]. Research proved usefulness of this material as bioaccumulative environmental indicators. Analysis of spider webs sampled from limestone arches in New South Wales (Australia) displayed several times higher levels of Pb and Zn at Jenolan Caves compared to reference sites at Abercrombie and Wombeyan Caves. The high concentrations at Jenolan was explained by vehicular traffic emissions that travelled through the arch [4].

Xiao-li et al. [5] tested practicality of spider webs for detecting motor vehicle emission in urban area in China. Webs from two common spiders (*Achaearanea tepidariorum* and *Araneus ventricosus*) were tested for concentration of Pb, Zn, Cu and Cd and data was compared to the proximity and volume of motor vehicle traffic at the sites. Beside significant differences in heavy metal concentrations between polluted and references sites, the study showed also distance-, and like Hose at al. [4], age-related differentials.

Since Xiao-li et al. [5], research on spider webs have been conducted in Poland by Rybak at al. and focused mainly on road traffic emissions [7-11]. Rybak investigated cumulative ability of spider webs to heavy metals across Wrocław, Lower Silesia. First preliminary study incorporated two species of Agelenidae family (*Malthonica silvestris* and *Malthonica ferruginea*) [6].

Agelenids, known as funnel weavers, build non-sticky, dense, horizontal webs with a funnel retreat on, or above the ground. Spiders from this family do not eat their webs. They are commonly found in urbanized areas like road tunnels, bridges, parking lots and homesteads. Webs of Agelenidae, Pholcidae and Linyphiidae family proved to be excellent bioindicators of atmospheric pollutants [7-11].

Study displayed significant differences between samples collected at investigated sites in case of Pb, Zn and Pt concentrations, indicating their potential usefulness as bioindicators [6]. Study conducted by Rybak in 2015 on several elements revealed varying concentrations of all elements at sites, with a following general descending order of concentration: Fe>K>Al>Zn>Mg>Ti>Mn>Cu>Pb>Ni>Cr>V>Co>Pt>W [10]. Principal component analysis (PCA) of data done on *Malthonica silvestris* webs revealed two contamination sources: road traffic emissions and industrial.

Rybak et al. also evaluated whether data obtained from webs reflect the level of air pollution measured with conventional methods [11]. The airborne particulate matter (PM) and associated heavy metals (Pb, Zn) collected in Wrocław were analysed with the use of classic method of air pollution assessment (impactors) and with webs of *Malthonica silvestris*. Study revealed correlation between average heavy metals concentrations on spider webs and average concentrations of Pb and Zn bound to submicron particles (PM1). Results conclude that content of heavy metals found on spider silk may not match the composition of corresponding elements present in bioaerosol. Overall, study confirmed usefulness of spider webs in monitoring of traffic emission as they are able to capture PM in a manner similar to flora-based bioindicators that have been used up to date, but spider silk have additional advantages like long time of exposition

## 3 Polycyclic Aromatic Hydrocarbons

Polycyclic Aromatic Hydrocarbons (PAHs) and their derivatives are formed mostly during incomplete combustion or pyrolysis of organic material [12]. Diesel engines are one of the main sources of this organic particles. PAHs pose substantial threat to humans due to their mutagenic and carcinogenic properties. Rybak and Olejniczak for the first time investigated possible use of spider webs as indicators of polycyclic aromatic hydrocarbons (PAHs) pollution [9].

Results from Wroclaw displayed a significantly higher mean concentrations of PAHs in samples collected at a heavy traffic sites compared to samples from reference/background

sites. Data indicated a positive correlation between PAHs content and close vicinity to the roads, confirming the contribution of pollution emissions from vehicular traffic. Agelenidae webs proved to be efficient indicators of PAHs. Interesting finding was, that in case of outdoor air, spider webs are more suitable for detecting PAHs of high molecular mass, rather than low molecular mass due to direct deposition of this compounds [9].

## 4 Dioxins

Dioxins compounds are persistent environmental pollutants, which can accumulate in the food chain, mainly in the fatty tissue of animals. They are mainly by-products of industrial processes and combustion of industrial compounds including improper municipal waste incineration and burning of trash. They are known for mutagenic and carcinogenic properties.

Spider silk displays suitable properties to determine the environmental exposure to polichlorinated dibenzo-para-dioxins (PCDDs). Preliminary study of Rybak et al. [13] showed that samples of spider webs collected in Lower Silesia adsorbed dioxins from air. Concentration of PCDDs was dependent on proximity to medical solid waste incinerator, major roadways and on municipal waste/garbage burning at backyards and in stoves. Spider webs displayed characteristics of fine PCDDs indicator and revealed exposure of inhabitants to this highly toxic pollutants.

## 5 Mutagenic activity

In order to assess environmental threats of air pollution, complex chemical analysis of air samples might not be efficient enough due to complex composition of the mixture and cholinergic interactions between individual compounds [14]. For obtaining reliable information about biological activity of pollutants, bacterial test for mutagenicity, e.g. the one proposed by Ames [15] are now commonly used. Studies by Rybak at al. and Rutkowski at al. [16, 17] proved successful application of spider webs in Ames mutagenicity assessment of both indoor and outdoor air pollution. Spiders dwell readily in human buildings, where adults of Pholcidae and Agelenidae family can be observed for whole year. As they naturally occur at homes or in outdoor localities such us road tunnels we can use them for cheap, long term monitoring of air pollutants, what is particularly utile in case of indoor monitoring. Study of Rybak at al. [16] has shown mutagenic activity of web samples collected from rooms exposed to pyrogenic and petrogenic emission (boiler room, garage, bedroom in a house nearby traffic road). Houses at sites without this potential threats did not display mutagenic activity.

## 6 Mineralogical composition

Application of spider webs in identification of various inorganic particles by SEM-EDX (Scanning Electron Microscope with Energy Dispersive X-Ray Analyser) technique was studied by Górka at al. [18]. This technique allows chemical and morphological characteristics of geological and trace elements particles identified on webs surface. Spider silk revealed its potential to be a tool for anthropopression assessment and indication of dominant source of pollutants. The extent of adsorbed particles on webs, so as their size and mineralogical composition varied largely depending on spider taxa and exposure time. Identified inorganic particles were mostly a derivatives of soil deflation or buildings/monuments weathering. Analysis of blank laboratory spider webs indicated that this material transported to real environment may serve as passive sampler both for mineralogical characteristics of atmospheric dust, as well as their chemical and isotopic

signature. Webs of Pholcidae family were recommended for this kind of studies in comparison to Agelenidae family, as the former resembled better particle accumulation property.

## 7 Magnetic susceptibility

Magnetic susceptibility is an interesting method of environmental pollution study in which spider webs also found application since they are diamagnetic. Exposure of pollutants containing metallic particles on spider silk increases value of its magnetic susceptibility, thus variation of this property should reflect the level of ambient air pollution. Rachwał et al. [19] applied this method for monitoring of both outdoor and indoor dust samples. Samples collected in rural and urban areas in Poland displayed significant increase in magnetic susceptibility compared to clean laboratory spider webs. It indicated serious contamination of PM containing ferromagnetic particles, presumably of anthropogenic source. Based on that, biomagnetic investigation of spider webs may be recommended as a method for monitoring of airborne pollution.

## 8 Disscusion

Ubiquity of major pollutants, mainly heavy metals, PAHs and dioxins in environment, despite venue of their identification (environmental component, e.g. air, water, soil, sludge) depends mostly on scale of their emission. In different areas, distinct emission sources determine scale of pollution in qualitative and quantitative sense. Each technological emission origin, e.g. exhaustion pipes, power plant chimneys, or brazier batteries have its own chemical profiles, hence proportions of pollutants types of that source are generally determined. This knowledge is used worldwide for: associating pollutants in a given area with specific sources, which ultimately allows for; identification of priority pollution sources and environmental issues of this area; evaluating environmental threats on this area, especially for the local living organisms; taking rational actions leading to elimination of threats associated with emission of pollutants to the environment [20].

Physical and chemical forms of which various pollutants enter environment, especially the air, determine their onward migration in this environment, so as manner and range of contamination by other components [21]. It is necessary to develop methods of monitoring, which allow for accurate, extensive and common monitoring at the same time. Principally, this applies to air, from which pollutants migrate to remaining components. Classical methods are restricted to many limitations. Apart from mainly technical ones, like costs, localization characteristics and selectivity, that limit their universality, there are methodical limitations, as well. In example, in monitoring of air pollution by PAHs, dioxins and heavy metals, it is necessary to extract PM from air first and afterwards, to determine its components [22, 23]. There are some principle problems related to this methodology. First of all, only PM contaminants are assumed, thus only solid and liquid formed. It is commonly known that some metals and definitely most of PAHs, exist in air in gaseous and semi-gaseous forms [24]. What is more, depending on PM components, which are being analysed, variety of filters and collecting materials are used. They are determined by chemical composition of filtering material, therefore by content of substances in so called black samples, so as by analytical methods limitations used in laboratories [25].

What is more, application of only one filtering material usually implies indication of only one group of compounds. To detect many compounds simultaneously, it is necessarily to use several PM samplers containing several types of filters [26]. Another issue is application of different samplers types indoor and outdoor due to technicalities [27, 28]. Despite the

necessity of appliance of both types of devices for this kind of monitoring, there is also the limitation due to impossibility of direct comparison of indoor and outdoor pollutants as different methods of measurement are applied.

There are more similar problem and restrictions related to classical methods of measurements of PM and other pollutants. The limitation scarcely mentioned before, but presumably most important, is the expense issue, which induces applying of conventional methods only in prechosen, neuralgic locations, or if it serves scientific researches, it is only temporal and short-term. It seems that yet mentioned, along with other issues related to contaminants identification may be overcome by application of medium in a form of spider webs. Nevertheless, before common praxis of spider webs, precise systematization of their application is necessary, along with design and acceptance of uniformed units in description of contamination. Sampling of heavy metals, PAHs or dioxins by spider webs is too distinct in comparison to street/urban dust, wet and dry deposition or other biological samplers (e.g. mosses and lichens), which are now widely used. Nonetheless, similarly to spider webs, information gathered by those methods are difficult to compare and to relate to concentrations of pollutants in air. Therefore, it is necessary to investigate the relationship between data collected by spider webs and quality of air in research field. Simultaneous measurements of contaminants assembled on spider webs and/or passive sampler must be performed. The key parameter in this kind of research would be the determination of optimal time of monitoring.

There are also other aspects that need further investigations. One of the most challenging facets of spider webs utilization is the mechanism of accumulation of pollutants.

Hose et al. [4] analyzing non-sticky cribellate spiders webs (*Badumna socialis* and *Stiphidion facetum*) demonstrated that washing webs with diluted acid reduced heavy metal concentrations up to 80% and concluded that contaminants do not incorporate into web matrix but bind to web surface. Nevertheless, webs of different families may display distinct efficiency in trapping contaminants.

Spiders tolerate high concentration of metals in environment and their bodies are efficient accumulators of this elements, so the content of metals in their bodies may reflect the metal amount in the environment [29]. For sake of reliable air monitoring, it is essential to distinguish external deposition of contaminants from incorporation of chemical particles passed from spiders hemolymph via spinnerets. Study of Rybak at al. [30] (paper under review) on *Eratigena atrica* fed with food contaminated by Cu and Pb proved the correlation between levels of Cu and Pb in webs and spiders. Research displayed that washing webs with shampoo and organic solvents decreased the concentration of heavy metals nearly by 70%, which is in accordance with Hose et al. [4] and suggests the dominance of external pathway of pollution (presumably by excreta or remains of the consumed prey). Remaining contamination must have been caused by internal incorporation.

Next step in research of application of spider webs in biomonitoring, that seems to be very interesting would be comparison of levels of PAHs displayed on spider webs and in body of spiders.

The concern that is frequently expressed in case of research on spider webs is the estimation of time of exposition to pollutants. In fact, it is easy to date the time of the web exposition by removing the old web and using only a new construction or to apply transferred webs derived from the laboratory [7, 18].

## 9 Conclusions

Spider webs reflect many features of perfect bioindicator. They are abundant, cheap, easy to collect and identify. Webs are usually woven in secluded places preventing them from destroying by weather conditions. Cumulative ability of spider webs as a consequence of their chemical structure, and independence from vegetation period, allow for unique

opportunity of assessment of air pollution level in a long-term period, contrary to the classic measurements. Classic samplers are also expensive and need continuous supervision. Spider silk is a non-selective and highly efficient natural passive sampler material, thus it can be used for monitoring of vast range of air pollutants, like heavy metals, PAHs, dioxins.

The investigations were co-financed within the framework of the order No. 0401/0004/17 with the specific subsidy granted for the Faculty of Environmental Engineering Wroclaw University of Science and Technology (W-7) by the Minister of Science and Higher Education

## References

1. Health Effects Institute. 2017. State of Global Air 2017. Data source: Global Burden of Disease Study 2015. IHME (2016)
2. A. Berlin, R.E. Yodaiken, D.C Logan, Int Arch Occup Environ Health **50** (1982)
3. H.G Zechmeiste, S. Dullinger, D. Hohenwallner, A.Riss, A. Hanus-Illnar, S. Sharf, Environ. Sci. Pollut. Res. **13** (2006)
4. G.C. Hose, J.M. James, M.R. Gray. Environ Pollut, **120**, 725-733 (2002)
5. S. Xiao-Li, P. Yu, G.C. Hose, C. Jian, L, Feng-Xiang, Bul Environ Contam Toxicol, **76**, 271-277 (2006)
6. J. Rybak, OCHR SR. **34**, 47-50 (2012)
7. J. Rybak, I. Sówka, A. Zwoździak, Environ. Prot. Eng. **38**, 175 (2012)
8. J. Rybak, Ecol. Eng. **15**, 39 (2014)
9. J. Rybak, T. Olejniczak, Environ. Sci. Pollut. Res. **21**, 2313 (2014)
10. J. Rybak, Water. Air. Soil Pollut. **224** (2015)
11. J. Rybak, I. Sówka, A. Zwoździak, M. Fortuna, K. Trzepla-Nabagło, Ecol. Chem. Eng. S, **22**, 389 (2015).
12. K. Widziewicz, W. Rogula- Kozłowska, G. Majewski, Int. J. Environ Res. **11** (2017)
13. J. Rybak, R. Rutkowski, E3S WEB CONF, **28** (2018)
14. L.D. Claxton, P.P. Matthews, S.H. Warren, Mutat. Res. **567**, 347 (2004)
15. B.N. Ames, J. McCann, E. Yamasaki, Mutat. Res., **31**, 347 (1975)
16. J. Rybak, R. Rutkowski, K. Piekarska, M. Bełcik, W: 2nd Symposium "Air Quality and Health", book of abstracts, 79-79 (2017)
17. R. Rutkowski, P. Jadczyk, J. Rybak, E3S WEB CONF, **44** (2018)
18. M. Górka, W. Bartz, J. Rybak, J AEROSOL SCI, 123, 63–75 (2018)
19. M. Rachwał, J. Rybak, W. Rogula- Kozłowska, Environ. Pollut., **234**, 543–551 (2018)
20. J.H. Seinfeld, S.N. Pandis, *Atmospheric chemistry and physics: from air pollution to climate change*, John Wiley & Sons (2012)
21. E. Sarti, L. Pasti, M. Rossi, M. Ascanelli, A. Pagnoni, M. Trombini, M. Remelli, Environ Sci Pollut Res, **6**(4), 708-71 (2015)
22. J.C. Chow, J. Air Waste Manage. Assoc., **45**, 320–382 (1995)
23. B. Brunekreef, R.L. Maynard, Atmos Environ, **42**(26), 6425-6430 (2018)
24. A. Dvorská, G. Lammel, J. Atmos. Environ., **45**(2), 420-427 (2011)
25. C.S. Davis, P. Fellin, R. Otson, JAPCA, **37**(12), 1397-1408 (1987)
26. W. Rogula-Kozłowska, K. Widziewicz, G. Majewski, Microchemical J, **132**, 327-332 (2017)

27. L. Morawska, Control of Particles Indoors - State of the Art. Proceedings of Healthy Buildings 2000, **2**, 9-20, Espoo, Finland (2000)
28. L. Morawska, T. Salthammer, *Indoor environment: airborne particles and settled dust*, Wiley-VCH (2013)
29. M.P. Jung, J.H. Lee, Environ. Monit. Assess. **184**, 1773–1779 (2012)
30. J. Rybak, B.E. Hanus-Lorenz, W. Rogula-Kozłowska, K. Loska, K. Widziewicz, R. Rutkowski, W: International Conference on Advances in Energy Systems and Environmental Engineering (ASEE17), book of abstracts / ed. by Bartosz Kaźmierczak. Wrocław : Oficyna Wydawnicza Politechniki Wrocławskiej, 121-122 (2017)

minerals

MDPI

*Article*

# Air Pollution Research Based on Spider Web and Parallel Continuous Particulate Monitoring—A Comparison Study Coupled with Identification of Sources

**Agnieszka Stojanowska [1,*], Tomasz Mach [1], Tomasz Olszowski [2], Jan Stefan Bihałowicz [3], Maciej Górka [4], Justyna Rybak [1], Małgorzata Rajfur [5] and Paweł Świsłowski [6]**

1 Department of Environmental Protection, Wroclaw University of Science and Technology, Wybrzeże Wyspiańskiego 27, 50-370 Wrocław, Poland; tomasz.mach@pwr.edu.pl (T.M.); justyna.rybak@pwr.edu.pl (J.R.)
2 Department of Thermal Engineering and Industrial Facilities, Opole University of Technology, 45-271 Opole, Poland; t.olszowski@po.edu.pl
3 Institute of Safety Engineering, The Main School of Fire Service, 52/54 Słowackiego St., 01-629 Warsaw, Poland; jbihalowicz@sgsp.edu.pl
4 Faculty of Earth Science and Environmental Management, University of Wrocław, Cybulskiego 32, 50-205 Wrocław, Poland; maciej.gorka@uwr.edu.pl
5 Institute of Environmental Engineering and Biotechnology, University of Opole, 45-032 Opole, Poland; mrajfur@o2.pl
6 Institute of Biology, University of Opole, 45-022 Opole, Poland; pawel.swislowski@uni.opole.pl
* Correspondence: agnieszka.stojanowska@pwr.edu.pl

**Abstract:** Air pollution is monitored mainly in urban or industrial areas, even if it is known that in rural ones, low emission can significantly worsen air quality. Hence, cheap and easily accessible methods of monitoring are needed. Recently, spider webs biomonitoring is getting popular, however, there is no information about its comparison with active methods. In this study, PTEs accumulated on spider webs were compared with results from continuous particulate monitor (CPM). Generally, higher potentially toxic elements concentrations were noted in spider web, with exception in the case of Zn. Zn may be present rather in smaller fractions, hence it needs more time for accumulation on spider web while it is easily collected by CPM. Higher concentrations of other elements on spider webs may result from formation of aggregates which could not be reported in $PM_{10}$ sampling (CPM). What is more, the order of the most and the least accumulated elements were similar and the percentage share of studied elements was coherent in most cases, proving that this new tool prospers to become commonly used in biomonitoring. Additionally, to identify possible sources of pollution air backward trajectories and trajectory frequencies for Kotórz were prepared based on the HYSPLIT model.

**Keywords:** biomonitoring; potentially toxic elements; spider web; PM; continuous particulate monitor



**Citation:** Stojanowska, A.; Mach, T.; Olszowski, T.; Bihałowicz, J.S.; Górka, M.; Rybak, J.; Rajfur, M.; Świsłowski, P. Air Pollution Research Based on Spider Web and Parallel Continuous Particulate Monitoring—A Comparison Study Coupled with Identification of Sources. *Minerals* **2021**, *11*, 812. https://doi.org/10.3390/min11080812

Academic Editors: Romain Millot, Jiubin Chen and David Widory

Received: 25 June 2021
Accepted: 23 July 2021
Published: 27 July 2021



## 1. Introduction

Particulate matter (PM) is a mixture of solid and liquid particles, suspended in the air, originating from both natural and anthropogenic sources [1,2]. In Europe, PM is considered one of the major air pollutants [3] and according to WHO, it is responsible for causing respiratory diseases often leading to premature deaths [4]. Considering the hazardous impact of PM, the monitoring of the particles in the air is essential issue nowadays, especially in urbanized areas, where people are exposed to higher PM levels, which are of great focus [5–7]. For instance, in Poland, the annual air quality assessment in terms of $PM_{10}$ and $PM_{2.5}$ concentrations is carried out mainly in big cities or areas where industries suspected of emitting hazardous pollution are located. However, the air quality in the nearby, usually rural, areas, situated on the leeward side, are often not considered in the monitoring but might be contaminated as well.

Another thing is that usually, to obtain very accurate information about air quality, the specific instrumentation is used, i.e., active samplers. However, in some cases where their

use is impossible due to financial issues or limitations in the study area, bioindicators can be applied. In bioindication, the assessment of environmental pollution can be conducted with the use of living organisms, like lichens [8], mosses [9,10], tree leaves [11] or their products, e.g., spider web [12]. The use of spider webs in biomonitoring is quite a new idea, but it has been already proved that this tool can give good results in the case of potentially toxic elements (PTEs) accumulation. Spiders build their webs in various places (both natural and polluted). With this feature, spider webs can be used regardless of air pollution and hence the way to obtain them is easy and cheap. There is also a possibility to determine the exact time of exposition by destroying the old web and observing the moment of new construction. Another idea is to use the clean web, obtained from laboratory-bred spiders, which facilitates the determination of exposure time. Additionally, the method is noninvasive and can be considered no waste. The possibility of the use of spider webs in assessing air quality has been performed before, and satisfying results were obtained [13–17]. The webs have already proved to be a good passive sampler in the case of potentially toxic elements [13,16,18,19] or polycyclic aromatic hydrocarbons (PAHs) [20,21].

The papers mentioned above prove that spider webs are nowadays a subject of interest for many scientists. The results from spider webs were once compared with lichens [15] and once with mosses [22] proving that the element mass fractions are significantly higher for spider web which might suggest that webs could be used in all cases where the results for lichens or mosses are under the detection limit. There was also one intent aiming at the comparison of two selected metals with different fractions of PM obtained by cascade impactors of Harvard type. However, the comparison of the usefulness of spider webs has never been checked regarding an active PM sampling by a continuous particulate monitor (CPM) equipped with metal concentration in $PM_x$ online analyzer.

In the present study, the comparison of metal concentration obtained from spider web monitoring using atomic absorption flame spectrometry (F-AAS) with the results of $PM_{10}$ elemental composition measured online using energy-dispersive X-ray fluorescence (EDXRF) was conducted. Then the relations between results from both methods were checked. Additionally, enrichment factor was calculated to indicate which element is the most problematic in the study area and then backward trajectories and trajectory frequencies were presented in order to verify from which areas the pollution could come from. The major goal was a verification and validation of results from the bioindicator (spider web) method with EDXRF data. The bioindicators are used widely but the question about quantity and quality of environmental answers is still open. Therefore, in this paper, the investigation on such comparison should yield new valuable and methodically confirmed universal data, interesting for other international readers.

## 2. Study Area

Kotórz Mały is a small village (approx. 1000 inhabitants) in the Opolskie Voivodship, southwestern Poland (Figure 1). According to the report from 2019 presented by Wojewódzki Inspektorat Ochrony Środowiska—Regionalny Wydział Monitoringu Środowiska (Province Inspectorate of Environmental Protection—Regional Department of Environmental Monitoring) [23] the concentrations of given elements (Pb, As, Cd, Ni) in $PM_{10}$ (particulate matter with a diameter of 10 microns or less) did not exceed the limits in the area of Opolskie Voivodship. In terms of the concentration of $PM_{10}$, the measurements carried out in 2019 revealed that the annual average value remained below the permissible level. However, the daily average values were exceeded, considering the criteria defined for the protection of health (50 $\mu g/m^3$), at five measuring stations [23]. We suppose that in this area in winter the local pollution originating from house heating dominate, or long-range transport can have a significant role in here, bringing the pollution from outside the locality. According to Olszowski in Kotórz Mały we can distinguish two zones in terms of dominating heating system [24]. In the first zone, predominated by rural buildings, 91% of the households use coal for heating processes. The second one is the modern building zone, where the production of heat energy is based on fuel gas (73%). Therefore, we can

distinguish local sources of pollution, originating from the area of the village, i.e., coal burning for home heating purposes but also railway tracks, polish industry pollution sources (Figure 1A–I), and cross-border sources of pollution.

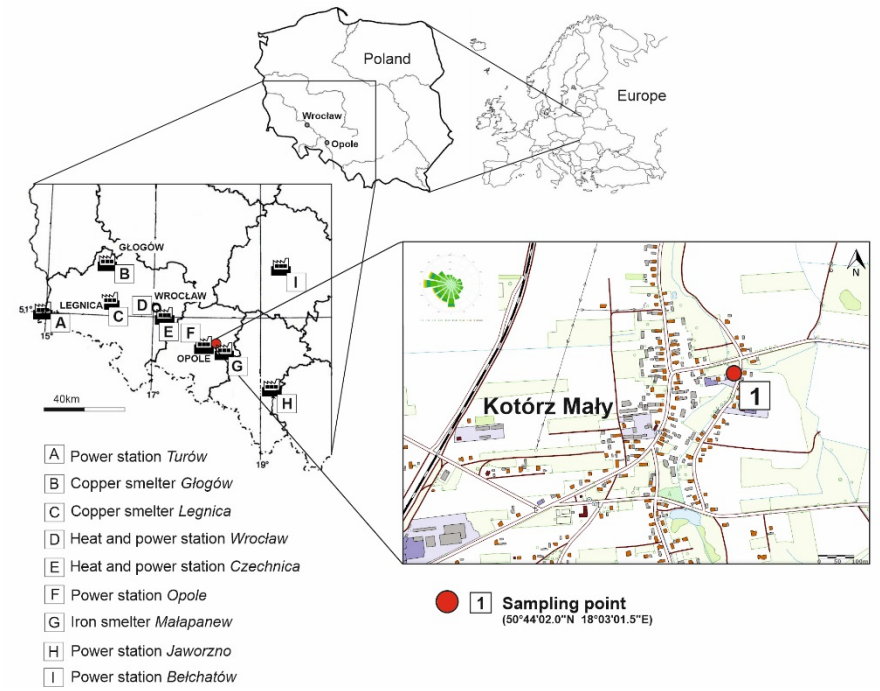


**Figure 1.** Location of the study area.

As presented on Figure 1, in the nearby voivodships many power stations are located i.e., Turów, Jaworzno, Bełchatów, and Opole. About 220 km west from Kotórz Mały lies Turów power plant which is known to be the second most polluting industry in Poland [25] and it is responsible for 40% of the dust pollution in the whole voivodship [26]. Other power stations are located in Jaworzno (100 km, southeast), Bełchatów (115 km, northeast), and Opole, only about 10 km southwest from Kotórz. What is more, heat and power stations in Wrocław (80 km, northeast) and Czechnica in Siechnice (70 km, northwest) are located nearby. As Opole and Jaworzno power stations and Wrocław and Czechnica heat and power stations are coal-fired, produced emissions are strictly connected with the process of coal burning. Coals from the Upper Silesian Coal Basin are known to contain Cr, Ni, Pb, and Zn [27], which by the combustion process are accumulated in the bottom and fly ash and then can be released to the atmosphere [28,29]. On the other hand, power stations Turów and Bełchatów are based on the lignite-burning for power production [30]. The amounts of potentially toxic elements in the ashes from lignite combustion in Poland are similar to the world-averages concentrations [31]. The ashes, produced in the process of lignite burning, contain following elements, presented in descending order Sr, Ba, Cr, Zn, Cu, Ni, As, Pb, Co [31]. Additionally, Cu smelters are situated in the area of Legnica and Głogów 140 and 170 km away from Kotórz Mały, respectively. In this region atmospheric aerosols can be characterized by the presence of Cu, Pb, Ni, Zn sulphides but also of metallurgical alloys varying in composition (Cu-Zn, Pb, Pb-Cu) [32]. Additionally, recent biomonitoring studies also provided the information about air contamination by Cu, Zn, and Pb in both of these regions [15,17]. In addition, an iron smelter—Małapanew in Ozimek can contribute to the air pollution by emitting the Fe particles to the atmosphere, however, from what is known for authors, now the activities in this area are much limited than in the past. Nowadays it deals mostly with the $PM_{10}$ and $PM_{2.5}$ exceeding [33]. Apart from this, a few cross-border sources of pollution exist, located in the neighboring countries, i.e., Czech Republic (Ostravsko-karvinská Basin and North Bohemian Basin) or in Slovakia (Košice). In Košice region coke and steel production and iron metallurgy are placed. A

confirmation of their negative impact on air pollution, especially on Fe emission, is the fact that high concentrations of studied elements (i.e., Fe, Mn, Cr, Pb, Zn) were found in the proximity of the ironworks [34]. In eastern part of Czech Republic steel manufacturing conurbation is located, which in known from emissions of high amounts of Fe, but also Zn, Cr, Pb and Mn in smaller quantity [35]. On the other hand, North Bohemian Basin is a part of Europe, known by the name of "black triangle", where high amounts of pollution are emitted [36]. This region is connected with electromechanical and metallurgical activities and brown coal mines and power plants are located there [36]. From this region following pollution may origin: e.g., Fe from industrial combustion of lignite, Pb connected with chemical works and lignite combustion and also Cu, due to the activity of a non-ferrous smelter in Príbram [37].

## 3. Meteorological/Environmental Parameters

The year 2019 was considered one of the warmest in comparison to previous years. In general, the annual average temperature in Poland amounted to 10.2 °C. In terms of precipitation, 2019 was classified as normal. Annual precipitation in Poland in this period amounted to 556 mm while in Opole to only 469.5 mm. During the samples collection, the average temperature in February amounted to 4 °C while in March about 6 °C [23]. The voivodship where Kotórz Mały is located the dominant winds blow from west and south [38] as also presented on the Figure 1.

## 4. Methods

### *4.1. Monitoring with Continuous Particulate Monitor*

Samples Collection

CPM with EDXRF (PX-375 Horiba analyzer, HORIBA ltd., Kyoto, Japan) was used in this study to obtain the results concerning the elemental composition of $PM_{10}$. The PX-375 analyzer provides rapid air pollution measurements by conducting online automatic PM sampling characterized by excellent sensitivity and precise performance. The PM mass is measured continuously utilizing beta ray attenuation and then using nondestructive energy-dispersive X-ray fluorescence (EDXRF) spectroscopic analysis the quantitative and qualitative elemental composition can be obtained already in the field. Uncertainty of this method for given elements is as follows: $\pm 1.1$ ng/m$^3$ for Mn, $\pm 153.2$ ng/m$^3$ for Fe, $\pm 4$ ng/m$^3$ for Cu, $\pm 12.4$ ng/m$^3$ for Zn, $\pm 5.2$ ng/m$^3$ for Pb, $\pm 50.7$ ng/m$^3$ for Al.

In the process of PM collection, a two-layer nonwoven polytetrafluoroethylene (PTFE) fabric filter (HORIBA TFH-01 membrane), in the form of roll, was used as a filter tape. The manufacturer ensures collection rate up to 99.97%. Each roll has a length of 21 m and 40 mm width. The filters are characterized by thickness of 140 µm and the pore size in the filter was equal to 1 µm [39]. In general PTFE material is a fluoropolymer, characterized by an excellent chemical inertness and thermal stability, hydrophobicity, low surface energy and also low friction coefficient [40] after [41,42].

The air samples acquisition was characterized by the flow rate equal to 16.7 dm$^3$·min$^{-1}$. Every sixty minutes beta ray attenuation analysis was conducted to assess the exact mass quantity. This measurement is based on law which says that absorbed radiation is exponentially dependent only on the mass of filtered material [43]. According to that at first beta radiation was emitted at empty filter, then there was time for sample acquisition and the particles were adsorbed on the filter tape. Considering the difference between these two measurements the result, in the form of collected $PM_{10}$, was given. After that the filter tape is moved, the new measurement begins. The analysis was performed for 500 s, operated at 15 kV or 50 kV voltage (depending on the studied element). At the same time, continuously, a subsequent sample was collected.

A standard reference material SRM 2738 (air particulate on filter media), certified by NIST, was used to acquire a quality control for the machine and to define the elemental quantification of X-ray spectra. To calibrate the machine, the blank tape was checked three times and finally the mean value was taken. The calibration of the CPM was done two

times by the qualified Horiba employees: at the beginning of the experiment and at the end, however, a few times during the sampling DryCal Defender 530 was used to make sure the flow did not change. The lowest detection limits (LDL) taken as a double the standard deviation of the analyzed blank samples were as follows: Al (56.7 ng/m$^3$), Cu (1.85 ng/m$^3$), Fe (7.00 ng/m$^3$), Mn (1.45 ng/m$^3$), Pb (1.05 ng/m$^3$), and Zn (1.25 ng/m$^3$). The repeatability of the obtained results was within ±2% of the equivalent film value. Additionally, in the information provided by the producer, it was shown that a strong correlation exists between the metal results given by CPM EDXRF (Horiba, PX-375, HORIBA Ltd., Kyoto, Japan) and conventional wet mineralization and measurement using ICP-MS.

CPM was placed in Kotórz Mały (Figure 1) and during about one month (7 February–17 March 2020), the hourly measurements were carried out continuously. Then the daily average values for this period were calculated.

### 4.2. Air-Mass Back Trajectory Analysis

To identify the possible sources of pollution, connected with long-range transport, movements of air masses concerning 24-h backward trajectories for Kotórz were constructed based on NOAA HYSPLIT model [44,45]. In addition, the meteorological data were acquired by the access to Gridded Meteorological Data Archives from National Oceanic and Atmospheric Administration (NOAA; www.ready.noaa.gov, accessed on 21 July 2021). Back trajectories of air masses were calculated for chosen days of spider web sampling period (7 February–17 March 2020) where higher than normal episodes of $PM_{10}$ and selected metal concentrations were found (Figure 2). For each selected day, four 6-hourly trajectories at 500, 1000, and 1500 m.a.s.l. were calculated taking into account the following ending times: 00:00, 06:00, 12:00, and 18:00 UTC + 1 h.

Additionally, for long-term analysis, the maps of trajectory frequencies were constructed. Different colors indicate different frequencies [%] of the air mass movement crossing over a given geographical sampling point.

### 4.3. Enrichment Factor

Since the Horiba PX-375 was also analyzing the concentration of the aluminum in the ambient air, we were able to calculate the enrichment factor EF of elements collected in the air samples. The EF is defined [46]:

$$EF = \frac{\frac{C_{x,m}}{C_{Al,m}}}{\frac{C_x}{C_{Al}}} \quad (1)$$

where $C_{x,m}$ and $C_{Al,m}$ are concentrations of element $x$ and aluminum in $PM_{10}$ measured in our experiment while $C_x$ and $C_{Al}$ are concentrations in the upper crust according to [47]. According to [48] the EF values can be divided into 5 classes representing the level of enrichment (Table 1).

**Table 1.** EF classes according to [48].

| EF Value | Level of Enrichment |
|---|---|
| $EF \leq 2$ | minimal |
| $EF \in [2,5]$ | moderate |
| $EF \in [5,20]$ | significant |
| $EF \in [20,40]$ | very high |
| $EF > 40$ | extremely high |

### 4.4. The Concentrations of Metals in $PM_{10}$

The PX-375 was analyzing concentrations of selected metals $x$ in $PM_{10}$ fraction in the atmospheric air $C_{x,V,i}$ in $\frac{ng}{m^3}$, the concentration of $PM_{10}$ $C_{PM_{10},V,i}$ and total mass of the sample $M_{PM_{10},i}$ in 1 h intervals numbered by index $i$. The spider webs were collecting

metals constantly, in the same total period as PX-375 so we had to find the total mass of $PM_{10}$ collected during the whole experiment and masses of metals. The mass of $PM_{10}$ collected in the whole experiment was simply the sum of masses of all $n$ samples.

$$M_{PM_{10}} = \sum_{i=1}^{n} M_{PM_{10},i} \tag{2}$$

The calculation of the masses of metals is more tricky since as a result, we obtain the volumetric concentration $C_{x,V,i}$, firstly the volume of the analyzed air in sample number $i$ have to be found:

$$V_i = \frac{M_{PM_{10},i}}{C_{PM_{10},V,i}} \tag{3}$$

And then the mass of the metal $x$ in sample $i$ can be expressed as:

$$M_{x,i} = C_{x,V,i} \cdot V_i \tag{4}$$

It leads to the formula for the mass of the metal in the whole experiment:

$$M_x = \sum_{i=1}^{n} \frac{C_{x,V,i}}{C_{PM_{10},V,i}} M_{PM_{10},i} \tag{5}$$

Therefore, we were able to calculate the content of these metals per mass of $PM_{10}$.

$$C_{x,m} = \frac{M_x}{M_{PM_{10}}} \tag{6}$$

We recalculated these values to determine the content of the selected metals in mg of the metal per kg of particulate matter. The mass concentration of metal $x$ denoted as $C_{x,m}$ was determined as the ratio of atmospheric air volumetric concentration $C_{x,V}$ and concentration of $PM_{10}$ $C_{PM_{10},V}$:

$$C_{x,m} = \frac{C_{x,V}}{C_{PM_{10},V}} \tag{7}$$

### *4.5. Biomonitoring with Spider Webs*

Sampling Collection and Characteristic

Two species from the family Agelenidae, *Tegenaria agrestis* (WALCKENAER, 1802) and *Eratigena atrica* (C.L. KOCH, 1843), have been chosen for studies. In previous studies [20], we found that agelenids are the best choice for biomonitoring as they weave large and dense webs known as funnel webs which are not sticky and stretch out horizontally like a carpet with tubular retreat inside of spiders. In general, spider web is a silk material, which is made up from protein named spidroin (spider fibroin). Spidroin is built of 100–400 amino acids (mostly glycine 30.2% and alanine 24.3%). Glycine is responsible for elasticity of the web while alanine gives it the strength. Other amino acids building the web are as follows: serine, proline, glutamine, leucine, valine, tyrosine and arginine. The exact composition of these proteins is dependent on e.g., species and diet [49]. The deposition of heavy metals on webs has been studied in following researches [19,50]. Hose et al. [50] showed that heavy metals (Pb, Zn) are deposited mainly on web surfaces in cribellate spiders (*Badumna socialis* and *Stiphidion facetum*). The authors proved that washing webs with diluted acid reduced metal concentrations up to 80%. Cribellate webs are not sticky and trap prey and particulates in the dense network of silk fibers. The way of trapping air contaminants by spider webs of another family of spiders (Agelenidae) has been studied by Rybak et al. [19]. The webs of Agelenidae are also not sticky. The authors compared unwashed webs with washed once (shampoo and organic solvent acetone from MERCK) and noted a significant decrease in the of heavy metals' concentration (nearly up to 70%) which also suggests that heavy metals are mainly deposited with dust particles on the web surface [19]. However,

in both studies, some parts of studied metals were not removed by the washing which could be attributed to internal contamination or other types of deposition mechanisms might be possible.

The newly woven webs (after the removal of an old web) were often visited and observed in the place of study, and therefore, after a defined exposure time for the creation of the new construction, they were removed and preserved for further analyses. These in situ samples of spider webs were collected from secluded locations which provided them the protection from unfavorable weather conditions. Additionally, we used webs derived from laboratory breeding of spiders. The already woven webs (from breeding containers) were deployed on plastic Petri dishes and closed in order to protect them from pre-exposure pollution. Spider webs of similar age, size and weight were used in this study. Then the dishes with spider webs were fixed at sampling sites with hot glue. The 10 prepared samples were placed in the close proximity to Horiba apparatus, on about 1.5 m height. After the exposition to pollutants for a defined period of time (approx. one month: 7 February–17 March 2020), the samples were collected with the use of glass, sterile baguettes and placed in sterile glass vials until further analyses (methodology according to [14,16,20,50]. Firstly, the webs were cleaned to remove accidental artefacts. Then they were conditioned for 24 h at the temperature of 20 ± 2 °C and 40 ± 5% humidity and next they were weighted three times using analytical balance Radwag AS 60/C/2 (minimum weight 1 mg, readability 0.01 mg, repeatability 0.04 mg). The samples were weight at a temperature of 23 ± 2 °C and relative humidity of 40 ± 5%). The average weight of the spider web sample was equal to 9 mg. The preexposure control webs, obtained from laboratory breeding, were previously analyzed in terms of chosen element concentration and revealed negligible values. According to the fact that most of the webs were collected from laboratory breeding spiders, we suppose that the concentration of selected by us elements on clean webs (before exposition) was negligible.

### *4.6. Metal Concentration Analyses*

The mineralization and analyses of mineralized spider web samples were performed at the Institute of Environmental Engineering and Biotechnology, University of Opole (Opole, Poland).

Concentrations of Mn, Fe, Ni, Cu, Zn, Cd and Pb were determined in spider webs. After exposure, the research material was transported to the laboratory, homogenized, and digested in Teflon vessels. The webs were mineralized in a mixture of 5 $cm^3$ of nitric acid $HNO_3$ (65%, Merck) and 3 $cm^3$ of $H_2O_2$ (30%, Merck) at 180 °C for 20 min using a Speedwave Four closed microwave system from BERGHOF, DE. This process was carried out at 220 °C for 20 min and was performed twice to ensure complete digestion of all dust samples according to [51].

Samples were transferred quantitatively, after mineralization, into a 25 $cm^3$ (class A) volumetric flask with deionized water. Metals were determined using an atomic absorption flame spectrometer (F-AAS) type iCE 3500 (series 3000) made by Thermo Scientific, USA. The F-AAS method was used previously in analyses of potentially toxic elements collected on spider web and satisfying results were obtained [15].

### *4.7. Quality Assurance and Control*

In Table 2, the instrumental detection limits (*IDL*) and instrumental quantification limits (*IQL*) for the spectrometer iCE 3500 are presented [52,53].

The values of the highest concentrations of the models used for calibration (2.0 $mg/dm^3$ for Cd, 5 $mg/dm^3$ for Ni, Cu, Zn, Pb, 7.5 $mg/dm^3$ for Mn and 10 $mg/dm^3$ for Fe) were approved as linear limits to signal dependence on concentration. Calibration of the spectrometer was performed with an internal standard solution from ANALYTIKA Ltd. (CZ). Additionally, in Table S3, concentrations of heavy metals in certified reference materials BCR-482 lichen, produced at the Institute for Reference Materials and Measurements, Belgium, were shown.

**Table 2.** The instrumental detection limits (*IDL*) and instrumental quantification limits (*IQL*) for the spectrometer iCE 3500 (mg/dm$^3$) [52,53].

| Metal | *IDL* (mg/dm$^3$) | *IQL* (mg/dm$^3$) |
|---|---|---|
| Mn | 0.0016 | 0.020 |
| Fe | 0.0043 | 0.050 |
| Ni | 0.0043 | 0.050 |
| Cu | 0.0045 | 0.033 |
| Zn | 0.0033 | 0.010 |
| Cd | 0.0028 | 0.013 |
| Pb | 0.0130 | 0.070 |

## 5. Results

### *5.1. Spider Webs Monitoring*

The monitoring with the use of spider webs revealed various concentrations of seven selected PTEs (Fe, Pb, Zn, Cu, Mn, Cd, and Ni; Table S2). The concentrations of Cd and Ni in the spider web were below the detection limit, hence their exact determination was impossible and they were omitted in the later part of the paper. The most abundant element on the spider web was Fe, which concentrations varied greatly with min. 1805 mg/kg and max. 2.4191 mg/kg. The next one was Pb and its concentrations were about one order of magnitude smaller than for Fe. In the case of Pb, the results differed from 173 to 2245 mg/kg. Two times smaller results were obtained for Mn, ranging from 168 to 1418 mg/kg. As the least abundant turned out to be Zn (min. 212 mg/kg, max. 687 mg/kg) and Cu (min. 60 mg/kg, max. 136 mg/kg).

### *5.2. Continuous Particulate Monitor*

To confront the information obtained by spider webs monitoring CPM was used. Air quality monitoring with the use of CPM provided hourly results of $PM_{10}$ concentrations which were then averaged. The minimal value of daily average amounted to 10.47 μg/m$^3$ while the maximum was 36.8 μg/m$^3$. In the sampling period, the exceeding of the maximum daily level for $PM_{10}$ (i.e., 50 μg/m$^3$) was not observed during the whole period, and the average value of $PM_{10}$ collected by CPM during sampling amounted to 20.53 μg/m$^3$. However, in the collected $PM_{10}$ the presence of potentially toxic elements such as: Fe, Mn, Cu, Zn and Pb were noted.

### *5.3. Enrichment of Samples*

The assessment of the enrichment in the studied elements was considered to be very important as the study site was located in the inhabited area. The enrichment factor (EF) shows a value enabling the quantitative determination of the anthropogenic influence on element concentration in PM. We calculated this factor for the samples collected by Horiba PX-375 and aluminum was used as the reference element. The reference concentrations in the upper crust were taken from [47]. The results are presented in Table 3. According to Table 1, the results for Zn and Pb indicated extremely high enrichment while EF for Cu is very high. In the case of Fe, there is only minimal enrichment whereas Mn shows moderate enrichment.

**Table 3.** EF for the elements in $PM_{10}$.

| Element | Cu | Zn | Pb | Mn | Fe |
|---|---|---|---|---|---|
| EF | 30.4 | 192 | 225 | 2.33 | 0.853 |

### *5.4. Backward Trajectories and Trajectory Frequencies*

After indication of the possible problematic elements it was crucial to determine their origin. The concentrations of $PM_{10}$, Zn, Pb, and Fe were presented in Figure 2 and daily variation of these concentrations was observed depending on the specific day of

the measurements. Such differentiation can occur when local air quality is influenced by regional or long-range transport. However, during a few days noted concentrations were much higher than in others. According to the most distinctive peaks, as can be seen in Figure 2, six episodes (A—08.02, B—17.02, C—28.02, D—04.03, E—09.03, F—16.03) were distinguished. Then, for each of these days, the maps of backward trajectories were constructed and presented in Figure 2. Creating these graphs can help us to indicate the potential source of pollution during each selected day.

In Episode A, noted concentration of Fe was the highest in the whole sampling period and it was shown that Fe was the predominant air pollutant during this day. According to air mass backward trajectories, this high Fe concentration might be enhanced by the transport of air mass from the Małapanew iron smelter, the activity of which, related to steel casting, classified the plant as very harmful to the environment in previous years [54]. Nowadays, however, the plant is known to work to a much lesser extent but possibly it is still emitting pollution. Another thing is that part of the winds pass through Hungary and could also bring the pollution from over there. According to [55] and the studies conducted in the area of Budapest in the total measured trace element concentrations, Fe was the most abundant (accounted for about 87%) and was followed by Zn, Pb, Cu and Mn. Additionally, in general, the Fe presence can be also ascribed to rail-wheel-brake interactions [56] as the railway tracks are located nearby.

High concentrations of PM, Fe, and Zn were noted in Scenario B and the air mass back trajectories indicated that the pollution could be possibly brought from the parts of Hungary, transporting the elements as listed above in Scenario A. However, according to the fact that the pollution during this day was relatively not high when compared to other episodes, hence, possibly the pollution may rather originate from local pollutants like railway tracks (Fe) or car traffic (Zn).

Episode C was characterized by quite high concentrations of Zn, Pb, and PM. Considering the prevailing wind directions during this day, we can assume that the pollution comes from the power station Turów (from west), which is lignite-fired and known to contribute to pollution with Zn, Cu, and Pb [31]. The observed winds can also cross by Wrocław heat and power station and Opole power station, which are coal-fired, leading to production of Pb and Zn. What is more, Zn as well as Pb, generated in the coal combustion processes, mostly accumulate in the fly ashes [29,57] which enhance their transport. Hence, it is understandable that in the case of Episode C, where the winds coming through this regions, relatively high values of Zn and Pb can be observed. Moreover, the high peak of $PM_{10}$ could be also connected with the transport of pollution from further regions (i.e., Ústí nad Labem region, north-western Czech Republic) from where particles of Fe, Pb but also Cu can be transported [37].

In Episode D, high concentrations of $PM_{10}$, Fe, Zn and Pb were found. As we can notice, the structure of the highest points in this episode is a little more complicated—at first, high Fe and Zn concentrations are observed, while PM maximum point during this episode is the next day just right after the maximum of Fe and Zn. The day in which high Fe and Zn concentrations are found with relatively not high PM concentrations may indicate the observation of Fe and Zn rich air mass inflow. Having a look at the map of air masses backward trajectories, it can be seen that at first air masses could be brought from the area of the eastern Czech Republic where steel manufacturing conurbation of Ostrava is located, which is known for episodes of high pollutant concentrations [58]. In this region, the problem of contaminated air pollution results from different sources, such as steel and coke plants, low emission, coming from the burning of waste or coal powder, and traffic [59]. It was also shown that raw iron production contributes to about 30% of the coarse aerosol mass during the post-smog period [59]. In another study, the pollution produced in this area was recognized to contain high amounts of Fe (stating about 75–87% of the total sum of monitored potentially toxic elements). Other important elements were as follows: Zn (7.1–11%), Cr (2.3–6.8%), Pb (0.3–5.8%), and Mn (1.4–2.4%) [35]. This information confirms the hypothesis that elevated PTEs amounts can result from transboundary

pollution. However, similarly to Scenario C, high concentration of Pb simultaneously with high concentration of Zn can be also an indication of the pollution brought from Turów and Opole power stations, coming from the west direction. Even though, it is supposed to be in smaller quantities, according to the fact that in the second day of this episode dominating wind direction change (south to west), a decrease of Fe, and, Pb concentration can be noted.

High PM and high Fe concentrations were found in the case of Episode E. Moreover, a peak in the case of Zn concentration was observed and a small peak of Pb. In this case, air masses could be brought mainly from the area of north western Czech Republic but also from the region of Ostrava. Both of these regions can be suspected of Fe, Pb and Zn pollution [35,37]. Some of the trajectories pass also through the region of polish Cu-smelters (Legnica and Głogów), from which transport of PM bearing Cu, Zn, Pb can be suspected [32]. In this episode, as well as C and D, the possibility of transport of pollution from Turów occurs, where lignite-fired power station is located. Hence, emitted pollution are supposed to be strictly connected with the process of lignite burning, which is proved to introduce Pb and Zn to the atmosphere [31].

Episode F presents high Fe concentrations and slightly lower PM when compared to other episodes. Considering that, we suppose that similarly to Episode A, collected sample must correspond to air masses enriched in Fe particles. In this case, the map of air masses backward trajectories indicates on emission originating from an industrial complex (composed of coke and steel production and iron metallurgy), located in the area of Košice (Slovakia). This region is known to be the dominant industrial source of air pollution, characterized by exceeding of daily limits for $PM_{10}$ [60]. Additionally, according to [34] the maximum concentrations of all studied elements (especially Fe) were recorded at sites localized in the proximity of the ironworks, indicating its impact on air quality. Hence, it is supposed that in the case of favorable direction of wind, as in Episode F, the pollution could be also brought from there to Poland. Additionally, some of the winds reach the Hungary. Hence, it is supposed that pollution like Fe accounting for almost 90% of the total measured trace element concentrations [55] but also Zn, Pb, Cu, and Mn could be transported from over there.

What is more, the map of trajectory frequencies for this period presents that most of the occurring winds come from the S/SW/SE parts, which is in accordance with the general dominant wind directions in this region [38] also presented as wind rose in Figure 1. This could enhance not only the transport of air masses from polish industry sources located in the proximity of Kotórz Mały but also from the cross-border sources of pollution. These wind directions are the main factor determining elemental composition of pollution on spider web during this sampling period.

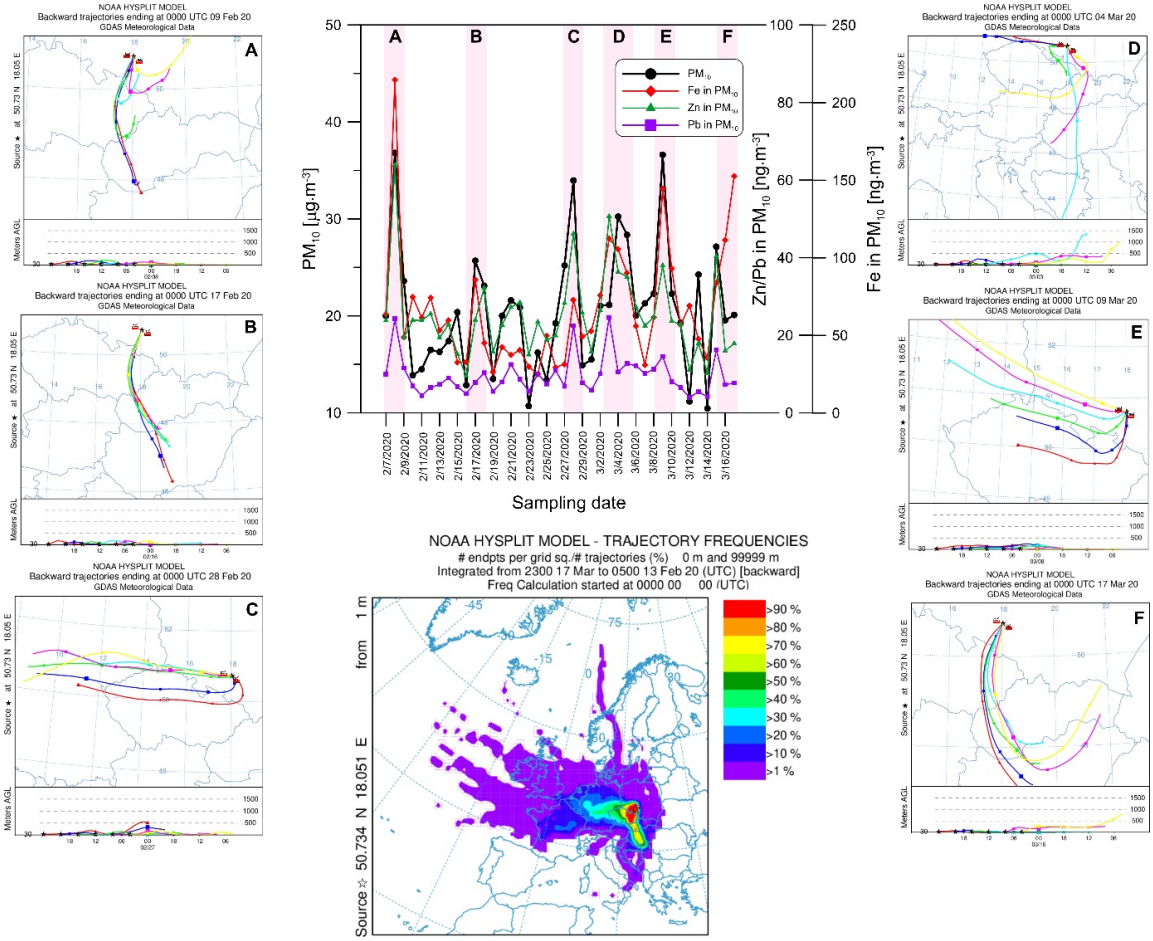


**Figure 2.** HYSPLIT trajectory frequencies and 24 h air backward trajectories in Kotórz calculated for given episodes (**A**–**F**).

## 6. Comparison of Methods

### *6.1. Concentration of PM-Bound Elements Obtained by Two Methods*

The PM was sampled with the use of 10 spider webs and $PM_{10}$ was collected by Horiba PX-375 CPM then the results from both methods were compared. Here we present the concentrations of selected elements in spider webs as violin plots (Figure 3). The horizontal coordinates of the violins are located at the positions corresponding to the concentrations measured with the Horiba PX-375. The values obtained by using CPM were intentionally recalculated to obtain the concentrations of given elements in $PM_{10}$ and expressed in $mg \cdot kg^{-1}$. By this, the comparison of these results with particles adsorbed on spider webs was possible.

The amounts of accumulated PTEs in the case of both methods differed. Figure 3 shows that the most commonly accumulated element was Fe as well on spider web as in the results from CPM, while the least abundant was Cu also for both methods. Concentrations of Mn, Pb, and Zn revealed similar orders of magnitude for spider webs, but for Horiba PX-375 these values differed. In general, the order of accumulated elements for webs was as follows: Fe > Pb > Mn > Zn > Cu while for particulate monitor: Fe > Zn > Pb > Mn > Cu. However, for all PTEs (except Zn), the results obtained for spider webs were higher than for CPM. It needs to be remembered that the Horiba PX-375 CPM collected the selected $PM_{10}$ fraction, which contains particles smaller than 10 µm while on the spider web also bigger particles are accumulated. There is also a possibility that fine particles bearing some elements will not be able to accumulate on web threads according to the threads arrangement (too big meshes).

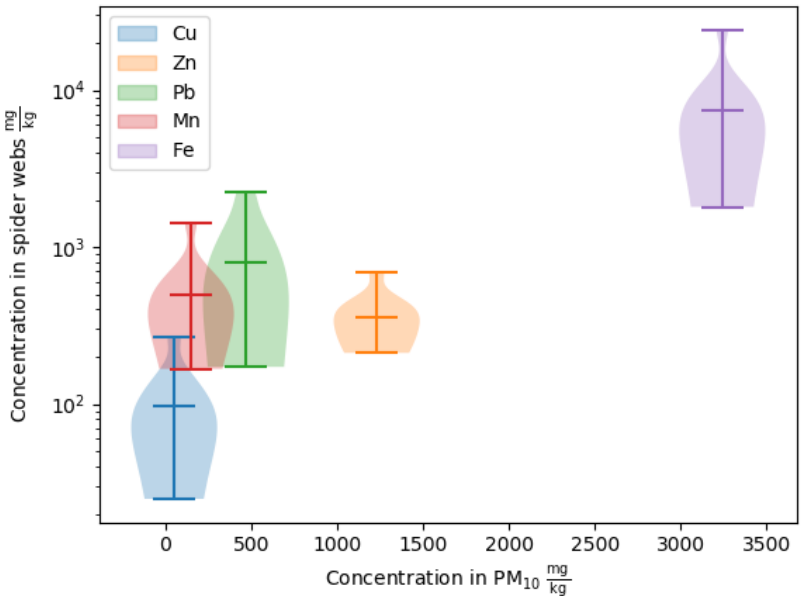


**Figure 3.** Concentrations in spider webs with relation to the concentration measured by Horiba PX-375. The horizontal position of the violin is the total concentration of $PM_{10}$ while in the vertical direction the violin represents the distribution of concentration.

### *6.2. Percentage Contribution of Given Element*

According to the fact that the exact number of concentrated elements for these two methods of air pollution monitoring varies due to different mechanisms responsible for PM collection, we wanted also to check the frequency of occurrence for selected metals in the total amount of studied atmospheric aerosols. For this purpose, obtained results for spider webs (expressed in μg/g; Table S2) and for CPM (in ng/$m^3$; Table S1) were converted into percentage contribution. As shown on the Figure 4, the view on the results in this manner enables the information about agreement of both methods given in percentage of difference. It can be noticed, that for Pb almost complete agreement was found, having about 10% share in both methods. In the case on Mn and Cu, their contribution in total aerosols was very small for both tools. There was about 30% difference in the answer between spider web and CPM for Mn, showing bigger Mn input on spider web, while Cu contribution differed in less than 50%, however its input in total metals is so small (about 1%) so that it is very hard to give precise answer. For the most abundant element, which was Fe, the result is satisfying, revealing about 25% difference between methods and bigger contribution of this element on spider webs. The highest difference was observed for Zn which was commonly found in the particles from CPM but its contribution on spider web was very poor. It resulted in bigger than 50% difference between these methods.

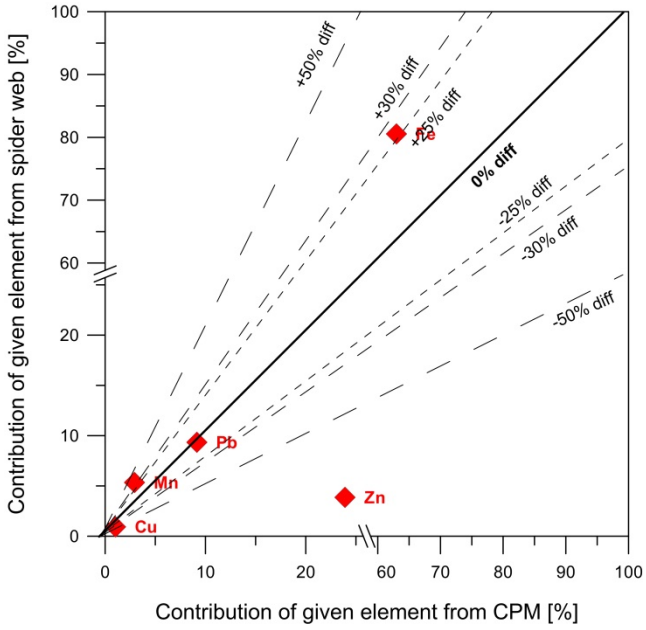


**Figure 4.** The comparison of both applied methods (spider web and CPM) for assessing the air pollution (% of difference).

## 7. Discussion

In the study by Olszowski [61] it was shown that the average mass concentrations of particulate matter were significantly higher in Kotórz Mały than in other rural regions in Poland and Czech Republic which indicates that the problem of air quality in the study area is relevant and current. Therefore, the dynamic situation in terms of air pollution in Poland, also in small villages, requires cheap, easy, and simple tools to monitor air quality. Considering that, we focused on validating the method of air pollution monitoring with the use of spider webs and its comparison with CPM.

The spider web is easily accessible, low cost and not complicated in use material [18]. What is more, monitoring with this indicator can be considered non-invasive and zero-waste as no extra waste is produced. Spider webs are supposed to collect total suspended particulate matter (TSP) and the obtained results could indicate the specific elements that seem to be problematic in the study area and give a simple overall and qualitative information whether more specific, more precise monitoring is needed. In order to check the reliability of the obtained results from spider web monitoring a comparison of our results with other studies was conducted. For the purposes of this article, the most relevant seems to be a comparison with the results obtained also in Poland and preferably with the use of the web produced by the same spider family. Additionally, the values of element concentrations were recalculated into a one-month exposition (Table 4), which allowed us to easily compare the obtained results. The elemental composition and the concentrations of specific elements varied depending on the study area. For instance, in the paper by Rybak [13] a similar experiment was conducted, however, the concentration of Fe was almost four times lower in there (7469 μg/g in this study, 2058 μg/g in paper by Rybak; Table 4) which can indicate much higher emission of this element in the area of Kotórz Mały due to close location of railway tracks and long-range transport (Figure 2). Moreover, the concentrations of Pb and Mn were a few times higher than reported for Wrocław [13] (Table 4). In the case of Zn, similar values were found in the present study and Stojanowska et al. [15] or Bartz et al. [17], however, when comparing it with the results from Wrocław we could notice an almost two times higher results for the study by Rybak [13] and nearly ten times higher value in the paper by Rybak et al. [18] which is not that surprising as three out of the five tested locations were located just right next to road with very intensive road traffic [18]. In addition, this might be a case in the study by Rybak [13]. Both of Rybak's studies were conducted in a big polish city characterized by heavy motor traffic.

On the other hand, the amount of collected Cu in the area of Kotórz is small, especially when compared to areas where copper smelting dominates [15,17] but the influence of Cu smelting in this region cannot be excluded. The observations of visibly higher Cu concentrations in areas with the proximity of Cu smelters and the information listed above prove that the spider web can be considered a good bioindicator. Hence, it can be concluded that this comparison of PTEs content on webs with other researches indicated that the results obtained in this study are reasonable. Additionally, elevated values for some elements can be easily explained by the analysis of the dominating sources of pollution in this area (Figure 2).

**Table 4.** Concentrations of average PTEs in this study and selected other researches (for easier comparison it was recalculated to one month of exposition).

| Parameter | This Study | Stojanowska et al. (2020) | Rybak (2015) | Rybak et al. (2015) | Bartz et al. (2021) |
|---|---|---|---|---|---|
| Study area | Kotórz Mały | Smelter in Legnica | Wrocław | Wrocław | Smelter in Głogów |
| Fe [µg/g] | 7469 | | 2058 | | |
| Mn [µg/g] | 494 | | 146 | | |
| Pb [µg/g] | 797 | 307 | 87 | 738 (2011)<br>790 (2012) | 357 |
| Zn [µg/g] | 357 | 500 | 738 | 3666 (2011)<br>1919(2012) | 479 |
| Cu [µg/g] | 98 | 706 | 109 | | 226 |
| Exposition time | 1 month | 1 month (recalculated from 2 months) | 1 month (recalculated from 2 months) | 1 month | 1 month (recalculated from 3 months) |

Aware of the fact that results obtained with CPM are very accurate it has to be remembered that it is rather an expensive device and its use is limited due to high costs. On the contrary, spider web is non-expensive, easily accessible material. Hence, the webs may seem in this case to be promising alternative for the air quality monitoring. Above mentioned confrontation of results verified that identified elements concentrations on webs are reasonable and could be suspected to comparison with CPM. As it is commonly known, CPM provide very precise information about PTEs concentrations and hence, as it presents the actual air pollution, it seems to be good point of reference for spider webs. It needs to be mentioned that the spider web was exposed to the air pollution, the same time in which CPM constantly worked. As presented on Figure 2, the results were recalculated to enable the comparison between these two methods and given in the total amount of selected elements in the whole sampling period. However, CPM collected only one selected fraction ($PM_{10}$), while on the spider web, also bigger particles were adsorbed and according to that the correlations were not found. What is more, finer particles could possibly not be able to accumulate on web threads as the threads arrangement is very specific (possibly too big meshes for some particles).

As presented in our research, noticeable amounts of chosen PTEs were found in the air samples, mostly revealing higher amounts for the particles collected on spider webs (Figure 3) with an exception for Zn. Both methods (CPM and spider web) clearly indicated that the most commonly found element was Fe, clearly distinguishable from the other elements. However, for Fe particles collected by CPM, only minimal enrichment in this element was found, hence its origin should be rather assigned to natural sources and occasionally to anthropogenic activities (long range transport as hypothesized based on Figure 2 or rail-wheel-brake interactions [12,56]). As a confirmation, in the paper by Mach et al. [62] also a low EF value (2.5 average for the period) was found, indicating rather natural sources of Fe in $PM_{10}$ in this region. However, it needs to be remembered that the EF value was calculated based on the CPM results (reporting only $PM_{10}$). Observing the comparison of the Fe values collected on spider web in this study (rural area) and the other study conducted in urban area [13] it could be seen that the result here was much higher (Table 4). This is surprising but might only indicate that in this rural area there are some additional sources of Fe pollution as indicated by air backward trajectories (Figure 2). Since EF, based on CPM results, showed small enrichment in anthropogenic Fe it can be

supposed that it probably occurred in the form of aggregates, which easily settled on the web threads but were not reported by CPM.

As mentioned above, Zn was the only element, which concentration was slightly higher in CPM results than in webs. It can be supposed that Zn was present in a big part in the fine fraction (similarly to the results from the study by Bartz et al. [17]) or even ultrafine fraction [63] which could complicate the accumulation on web due to too big meshes (specific threads arrangement) or the limitation of wet deposition. According to [64] some of finer fractions might be favorably deposited by wet deposition rather than that gravitational settling. Hence, as in this study the webs were protected from rain or snow, the wet deposition could be limited. As the EF showed extremely high enrichment in Zn, the impact of anthropopressure in this area is of much concern. The air masses with Zn can be transported from abroad, originating from steel manufacturing conurbation of Ostrava (Czech Republic) as it was shown by HYSPLIT trajectories (Figure 2). The emission of Zn in this can be also connected with polish industry pollution sources e.g., Cu smelting in Legnica and Głogów, from which Zn, co-appearing with Cu and Pb can be brought. However, the influence of vehicle emissions cannot be omitted as, since the time that leaded fuels were banned, it was chosen to be a new tracer of traffic emissions instead of Pb [65]. As additional sources of Zn, tailpipe emissions of motor oil [66] and tire wear [67] are considered. The sampling point (Figure 1) was located within a few kilometers of two national roads: Road No. 46 (southeast from the sampling point, approx. 9500 vehicles/day) and Road No. 45 (northwest from the sampling point, approx. 8000 vehicles/day) [68] and what is more, A4 highway, connecting east and west parts of southern Poland, pass through this region. Kotórz Mały lies about 80 km away from the most heavily loaded part of the route, which is in Katowice (100,983 vehicles/day) [68] and it is known to be a big source of Zn pollution [69]. Hence, the high value of EF for this element is not that surprising and the differentiation from spider webs results can be understood.

In the case of Pb, its concentration on spider web was also higher than reported by CPM. Even if the leaded fuel is not so commonly used anymore it seems that there is still a problem with the contamination by this element. This situation was confirmed by elevated EF value, indicating extremely high enrichment, and the fact that the results for spider webs, obtained in our study, exceeded the values from other studies (Table 4). Pb presence is often connected with high usage of motor vehicles in the urban area (i.e., lead wheel weights dropped from car wheels can be then pulverized by intensive traffic [70]. What is more, the origin of Pb particles in the air can be also connected with coal burning for home heating purposes, and it can be found in varying quantities in low-rank coals and high-rank coals and their corresponding ashes [71]. Combining this information with the fact that more than 90% of the households in the village use coal for heating processes [24] a big part of the identified pollution can be attributed to this sector. From the polish local sources, as a contributor to Pb emission, we can also mention A4 highway [69] and regions with Cu smelting (Legnica and Głogów) [32]. Another source of pollution with Pb in this area can be long range transport bringing pollution from steel manufacturing conurbation of Ostrava (Czech Republic) as shown in Figure 2.

Even if Cu was not that commonly found, comparing to other elements, neither on spider web nor in case of CPM sampling, the EF shows that the enrichment was very high (Table 3). This could be the result of bringing the pollution from the polish Cu smelting regions or Czech non-ferrous smelter in Príbram [37], as showed by air mass backward trajectories on Figure 2. Cu, as well as Zn, can be also a marker of brake lining wear [67,69] which could be the case here according to the fact of proximity of national roads and A4 highway. The presence of this element on spider webs shows similarity in term of quantity to results from Wrocław but observed amount was visibly lower than those from Cu smelting regions (Table 4). However, the impact of Cu smelters cannot be excluded, as particles from over there could be also brought in here but in smaller amounts.

In the case of Mn, the EF value was low indicating lower anthropogenic impact, hence the attention was focused on the other, more interesting, above-mentioned elements. As

anthropogenic sources of Mn particles petrol combustion [72] and coal combustion in power plants [73] can be considered. On the other hand, in the natural environment, it also commonly occurs in most iron ores [74]. In this study, it was rather negligible and as showed by EF its origin could be mainly connected with natural processes.

Consideration of this study in terms of various elements and their origin helped us to explain the differences that could be noted while comparing the spider webs and CPM monitoring. What is more, the observed variance can be possibly connected with the different materials used in the case of spider web biomonitoring (natural product, protein) and CPM with PTFE membrane (fluoropolymer). Despite different materials in these two methods the similarity can be found in the structure as both of them are characterized by irregular structure of threads arrangement which creates tortuous routes through the material. As presented by Lindsley [75] these tortuous paths through which particles have to pass through greatly increase the probability of particle deposition. The observed differences may also result from different mechanisms responsible for particles accumulation. While for PTFE filters the accumulation mechanisms are well known (interception, impaction, diffusion, electrostatic attraction and sedimentation [75]) for spider webs it is more complicated. As it is considered a passive method sedimentation obviously occurs. It has been previously proposed that electrostatic forces could play an important role in silk adhesion [76,77] however experimental evidence concerning cribellar silk shows that it has non-electrostatic adhesive properties [78] after [79]. Then according to Vollrath and Edmonds [80] it is the specific glue that coats orb spider's webs which is responsible for electrostatic properties causing enhanced collection of charged particles (i.e., pollens, pollutants particles and flying insects). For instance, for orb webs the capture effectiveness is attributed to mechanical, adhesive, hygroscopic features of the constituent silk but also to architectural structure and the distortions of the entire structure induced by wind [78]. Apart from the fact that Agelenidae webs are non-sticky (not covered with glue) the rest of the mechanisms responsible for particles capture might be similar. According to this unclear situation, it is very difficult to compare these two materials.

Considering the different mechanisms occurring in these two methods (active method and biomonitoring-based passive method) it was expected that CPM could collect more particles. However, due to the selective collection of particles, and the other reasons mentioned above, the opposite situation was observed (generally higher PTEs in spider webs). Additionally, the percentage contribution of selected elements in total atmospheric particles, analyzed by us with the use of spider web and CPM, was presented (Figure 4). It was shown that only input of Zn in total amount of metals revealed no agreement between both methods (>50% difference). For the rest of elements, the difference between methods varied, giving 0–40% of difference. The most accurate result was obtained for Pb which showed almost complete agreement, indicating that even if the concentrations were different the percentage share in total aerosols was the same.

## 8. Conclusions

To summarize, spider webs and CPM can give satisfying results, but their comparison is not always clear due to different mechanisms of particles accumulation. It was shown that most elements concentrations, except Zn, were higher for spider webs indicating that some of the particles could occur in sizes bigger than $PM_{10}$ due to formation of aggregates. As CMP collected only $PM_{10}$, these big aggregates were not reported and it lead to the differentiation of results between both methods. However, the percentage share of selected elements is very similar in both methods and the differences in the results are somehow understandable and can be explained considering the origin of the particles and the occurrence of given elements in different fractions. Additionally, we observed that the order of occurrence of elements was similar (at least in the case of the most abundant and the least abundant PTEs). In addition, obtained results are somehow comparable with other biomonitoring studies based on the use of spider webs which confirms the reliability of this results. This in turn, proves that this new bioindicator can be a good tool in air

pollution monitoring. However, the issue needs to be studied in more details in the future and the correlation between PTEs in other fractions ($PM_{2.5}$ and especially TSP) obtained by active sampling and accumulation of PTEs on spider webs should be checked.

**Supplementary Materials:** The following are available online at https://www.mdpi.com/article/10.3390/min11080812/s1, Table S1: Results obtained in monitoring with the use of Continuous Particulate Monitor, Table S2: Results obtained in monitoring with the use of spider website, Table S3: Comparison of measured and certified concentrations in BCR-482 lichen.

**Author Contributions:** Conceptualization: A.S., T.M., T.O., J.R., M.G. and J.S.B.; methodology: T.M., M.R., P.Ś., J.S.B.; validation: A.S.; formal analysis: J.S.B., M.G. and A.S.; investigation: A.S., T.M., T.O., M.R. and P.Ś. resources: A.S., T.M., M.R. and P.Ś.; data curation: M.G. and J.S.B.; writing—original draft preparation, A.S.; writing—review and editing, T.O., J.R. and M.G.; visualization, M.G., J.S.B.; supervision, J.R.; project administration: J.R., A.S.; funding acquisition: J.R. and M.G. All authors have read and agreed to the published version of the manuscript.

**Funding:** This paper was co-financed within the "Excellent Science" program of the Polish Ministry of Science and Higher Education. This research was carried out as a part of the "Implementation doctorate-edition II Faculty W-7 (03DW/0001/18)" project, financed by the National Centre for Research and Development. The funders had no role in the design of the study, in the collection, analyses, or interpretation of data; in the writing of the manuscript, or in the decision to publish the results.


**Institutional Review Board Statement:** Not applicable.

**Informed Consent Statement:** Not applicable.

**Acknowledgments:** The authors gratefully acknowledge the NOAA Air Resources Laboratory (ARL) for the provision of the HYSPLIT transport and dispersion model and/or READY website (https://www.ready.noaa.gov accessed on 21 July 2021) used in this publication.

**Conflicts of Interest:** The authors declare no conflict of interest.

## References

1. Ukaogo, P.O.; Ewuzie, U.; Onwuka, C.V. Environmental Pollution: Causes, Effects, and the Remedies. In *Microorganisms for Sustainable Environment and Health*, 1st ed.; Chowdhary, P., Raj, A., Vermna, D., Akhter, Y., Eds.; Elsevier: Amsterdam, The Netherlands, 2020; pp. 419–429.
2. Yadav, I.C.; Devi, N.L. Biomass Burning, Regional Air Quality, and Climate Change. In *Encyclopedia of Environmental Health*, 2nd ed.; Nriagu, J., Ed.; Elsevier: Amsterdam, The Netherlands, 2019; pp. 386–391.
3. European Environment Agency. *Air Quality in Europe—2019 Report*; European Environmental Agency: Copenhagen, Denmark, 2019.
4. World Health Organization. *Health Effects of Particulate Matter*; WHO: Geneva, Switzerland, 2013.
5. Braniš, M.; Domasová, M.; Řezáčová, P. Particulate air pollution in a small settlement: The effect of local heating. *Appl. Geochem.* **2007**, *22*, 1255–1264. [CrossRef]
6. Furusjö, E.; Sternbeck, J.; Cousins, A.P. PM10 source characterization at urban and highway roadside locations. *Sci. Total Environ.* **2007**, *387*, 206–219. [CrossRef] [PubMed]
7. Landrigan, P.J.; Fuller, R.; Acosta, N.J.R.; Adeyi, O.; Arnold, R.; Basu, N.N.; Baldé, A.B.; Bertollini, R.; Bose-O'Reilly, S.; Boufford, J.I.; et al. The Lancet Commission on pollution and health. *Lancet* **2018**, *391*, 462–512. [CrossRef]
8. Ciężka, M.M.; Górka, M.; Modelska, M.; Tyszka, R.; Samecka-Cymerman, A.; Lewińska, A.; Łubek, A.; Widory, D. The coupled study of metal concentrations and electron paramagnetic resonance (EPR) of lichens (Hypogymnia physodes) from the Świętokrzyski National Park—Environmental implications. *Environ. Sci. Pollut. Res.* **2018**, *25*, 25348–25362. [CrossRef] [PubMed]
9. Kłos, A.; Ziembik, Z.; Rajfur, M.; Dołhańczuk-Śródka, A.; Bochenek, Z.; Bjerke, J.W.; Tømmervik, T.; Zagajewski, B.; Ziółkowski, D.; Jerz, D.; et al. Using moss and lichens in biomonitoring of heavy-metal contamination of forest areas in southern and north-eastern Poland. *Sci. Total Environ.* **2018**, *627*, 438–449. [CrossRef] [PubMed]
10. Świsłowski, P.; Kosior, G.; Rajfur, M. The influence of preparation methodology on the concentrations of heavy metals in Pleurozium schreberi moss samples prior to use in active biomonitoring studies. *Environ. Sci. Pollut. Res.* **2021**, *28*, 10068–10076. [CrossRef]

11. Wang, L.; Gong, H.; Liao, W.; Wang, Z. Accumulation of particles on the surface of leaves during leaf expansion. *Sci. Total Environ.* **2015**, *532*, 420–434. [CrossRef]
12. Górka, M.; Bartz, W.; Rybak, J. The mineralogical interpretation of particulate matter deposited on Agelenidae and Pholcidae spider webs in the city of Wrocław (SW Poland): A preliminary case study. *J. Aerosol Sci.* **2018**, *123*, 63–75. [CrossRef]
13. Rybak, J. Accumulation of Major and Trace Elements in Spider Webs. *Water Air Soil Pollut.* **2015**, *226*, 1–12. [CrossRef] [PubMed]
14. Rybak, J.; Sówka, I.; Zwoździak, A. Preliminary assessment of use of Spider webs for the indication of air contaminants. *Environ. Prot. Eng.* **2012**, *38*, 175–181. [CrossRef]
15. Stojanowska, A.; Rybak, J.; Bożym, M.; Olszowski, T.; Bihałowicz, J.S. Spider webs and lichens as bioindicators of heavy metals: A comparison study in the vicinity of a copper smelter (Poland). *Sustainability* **2020**, *12*, 8066. [CrossRef]
16. Xiao-Li, S.; Yu, P.; Hose, G.C.; Jian, C.; Feng-Xiang, L. Spider webs as indicators of heavy metal pollution in air. *Bull. Environ. Contam. Toxicol.* **2006**, *76*, 271–277. [CrossRef] [PubMed]
17. Bartz, W.; Górka, M.; Rybak, J.; Rutkowski, R.; Stojanowska, A. The assessment of effectiveness of SEM- EDX and ICP-MS methods in the process of determining the mineralogical and geochemical composition of particulate matter deposited on spider webs. *Chemosphere* **2021**, *278*, 130454. [CrossRef]
18. Rybak, J.; Sówka, I.; Zwozdziak, A.; Fortuna, M.; Trzepla-Nabagło, K. Evaluation of the Usefulness of Spider Webs as an Air Quality Monitoring Tool for Heavy Metals. *Ecol. Chem. Eng.* **2015**, *22*, 400. [CrossRef]
19. Rybak, J.; Rogula-Kozłowska, W.; Loska, K.; Widziewicz, K.; Rutkowski, R. The concentration of Cu and Pb in the funnel spider Eratigena atrica (CL Koch 1843) (Araneae: Agelenidae) and its web. *Chem. Ecol.* **2019**, *35*, 1–12. [CrossRef]
20. Rybak, J.; Olejniczak, T. Accumulation of polycyclic aromatic hydrocarbons (PAHs) on the spider webs in the vicinity of road traffic emissions. *Environ. Sci. Pollut. Res.* **2014**, *21*, 2313–2324. [CrossRef]
21. Rybak, J.; Rogula-Kozłowska, W.; Jureczko, I.; Rutkowski, R. Monitoring of indoor polycyclic aromatic hydrocarbons using spider webs. *Chemosphere* **2019**, *218*, 758–766. [CrossRef] [PubMed]
22. van Laaten, N.; Merten, D.; von Tümpling, W.; Schäfer, T.; Pirrung, M. Comparison of Spider Web and Moss Bag Biomonitoring to Detect Sources of Airborne Trace Elements. *Water Air Soil Pollut.* **2020**, *231*, 1–17. [CrossRef]
23. Regionalny Wydział Monitoringu Środowiska w Opolu. *Roczna Ocena Jakości Powietrza w Województwie Opolskim—Raport Wojewódzki za Rok 2019*; Regionalny Wydział Monitoringu Środowiska w Opolu: Opole, Poland, 2020.
24. Olszowski, T. The concentration of PM10 in a rural area during episodes of tropospheric inversion occurring in the cool months. *ProScience* **2014**, *1*, 387–392.
25. European Environment Agency. *Costs of Air Pollution from European Industrial Facilities 2008–2012—An Updated Assessment. EEA Technical Report No 20/2014*; European Environmental Agency: Copenhagen, Denmark, 2014.
26. WIOŚ. *Raport o Stanie Środowiska Województwa Dolnośląskiego w 2007*; WIOS: Wrocław, Poland, 2008.
27. Parzentny, H.R.; Róg, L. Potentially hazardous trace elements in ash from combustion of coals in limnic series (Upper Carboniferous) of the Upper Silesian Coal Basin. *Górnictwo Geol.* **2007**, *3*, 81–91.
28. Srogi, K. Pierwiastki śladowe w węglu. *Wiadomości Górnicze* **2007**, *2*, 87–96.
29. Wierońska, F.; Makowska, D.; Strugała, A.; Bytnar, K. Analysis of the Content of Nickel, Chromium, Lead and Zinc in Solid Products of Coal Combustion (CCPs) Coming From Polish Power Plants. In *IOP Conference Series: Earth and Environmental Science*; IOP Publishing: Bristol, UK, 2019.
30. Widera, M.; Kasztelewicz, Z.; Ptak, M. Lignite mining and electricity generation in Poland: The current state and future prospects. *Energy Policy* **2016**, *92*, 151–157. [CrossRef]
31. Czech, T.; Marchewicz, A.; Sobczyk, A.T.; Krupa, A.; Jaworek, A. Śliwiński, Ł.; Rosiak, D. Heavy metals partitioning in fly ashes between various stages of electrostatic precipitator after combustion of different types of coal. *Process. Saf. Environ. Prot.* **2020**, *133*, 18–31. [CrossRef]
32. Muszer, A. *Charakterystyka Sferul i Minerałów Akcesorycznych z Wybranych Utworów Fanerozoicznych i Antropogenicznych*; Fundacja Ostoja: Wrocław, Poland, 2007.
33. Podgórska, B.; Synowiec, P.; Górniak, J.; Podgórska, S. *Program Ochrony Środowiska dla Gminy Ozimek na Lata 2017–2020 wraz z Perspektywą na Lata 2021–2024*; ALBEKO: Opole, Poland, 2017.
34. Hanculak, J.; Kurbel, T.; Spaldon, T.; Sestinova, O.; Findorakova, L.; Fedorova, E. Influence of Iron and Steel Industry on Selected Elements of Atmospheric Deposition in the Urban and Suburban Area of Košice (Slovakia). *J. Pol. Miner. Eng. Soc.* **2005**, *16*, 95–102. [CrossRef]
35. Sýkorová, B.; Kucbel, M.; Raclavská, H.; Raclavský, K.; Matýsek, D. Heavy metals in air nanoparticles in affected industry area. *J. Sustain. Dev. Energy Water Environ. Syst.* **2017**, *5*, 58–68. [CrossRef]
36. Hykyšová, S.; Brejcha, J. Monitoring of PM10 air pollution in small settlements close to opencast mines in the North-Bohemian Brown Coal Basin. *WIT Trans. Ecol. Environ.* **2009**, *123*, 387–398. [CrossRef]
37. Suchara, I.; Sucharová, J. Distribution of sulphur and heavy metals in forest floor humus of the Czech Republic. *Water Air Soil Pollut.* **2002**, *136*, 289–316. [CrossRef]
38. GIOŚ. *The State of the Environment in the Opolskie Voivodship*; GIOŚ: Opole, Poland, 2020. (In Polish)
39. HORIBA. New Construction Resolves Many of the Problems Associated with the Demanding Usage Environment for PM Sampling Filters. Available online: http://www.horiba.com/fileadmin/uploads/Process-Environmental/Documents/Downloads_Catalog/Catalog_Ambient/TFH-01_47_brochure_HRE2423B_uploaded_on_20140619.pdf (accessed on 20 June 2021).

40. Zhang, Y.; Yin, M.; Xia, O.; Zhang, A.P.; Tam, H.Y. Optical 3D μ-printing of polytetrafluoroethylene (PTFE) microstructures. In Proceedings of the IEEE International Conference on Micro Electro Mechanical Systems (MEMS), Belfast, Northern Ireland, 21–25 January 2018; pp. 37–40.
41. Ebnesajjad, S. Introduction to Fluoropolymers: Materials, Technology, and Applications. In *Introduction to Fluoropolymers: Materials, Technology, and Applications*; Elsevier LTD: Oxford, UK, 2013.
42. Teng, H. Overview of the development of the fluoropolymer industry. *Appl. Sci.* **2012**, *2*, 496–512. [CrossRef]
43. Liberti, A. Modern methods for air pollution monitoring. *Pure Appl. Chem.* **1975**, 519–534. [CrossRef]
44. Rolph, G.; Stein, A.; Stunder, B. Real-time Environmental Applications and Display sYstem: READY. *Environ. Model. Softw.* **2017**, *95*, 210–228. [CrossRef]
45. Stein, A.F.; Draxler, R.R.; Rolph, G.D.; Stunder, B.J.B.; Cohen, M.D.; Ngan, F. Noaa's hysplit atmospheric transport and dispersion modeling system. *Bull. Am. Meteorol. Soc.* **2015**, *96*, 2059–2077. [CrossRef]
46. Zoller, W.H.; Gladney, E.S.; Duce, R.A. Atmospheric concentrations and sources of trace metals at the South Pole. *Science* **1974**, *183*, 198–200. [CrossRef] [PubMed]
47. Wedepohl, K.H. The composition of the continental crust. *Geochim. et Cosmochim. Acta* **1995**, *59*, 1217–1239. [CrossRef]
48. Yongming, H.; Peixuan, D.; Junji, C.; Posmentier, E.S. Multivariate analysis of heavy metal contamination in urban dusts of Xi'an, Central China. *Sci. Total Environ.* **2006**, *355*, 176–186. [CrossRef]
49. Al-Azawii, Z.N. Study on chemical composition and designing web patterns of Iraqi spider silk. *Biochem. Cell. Arch.* **2020**, *20*, 1397–1400. [CrossRef]
50. Hose, G.C.; James, J.M.; Gray, M.R. Spider webs as environmental indicators. *Environ. Pollut.* **2002**, *120*, 725–733. [CrossRef]
51. Gerboles, M.; Buzica, D.; Brown, R.J.C. Interlaboratory comparison exercise for the determination of As, Cd, Ni and Pb in $PM_{10}$ in Europe. *Atmos. Environ.* **2011**, *45*, 3488–3499. [CrossRef]
52. Konopka, Z.; Swisłowski, P.; Rajfur, M. Biomonitoring of Atmospheric Aerosol with the use of Apis mellifera and Pleurozium schreberi. *Chem. Didact. Ecol. Metrol.* **2020**, *24*, 107–116. [CrossRef]
53. Spectro-Lab. *Instrukcja Obsługi Aparatu AAS iCE 3500 Firmy Thermo Scientific*; Spectro-Lab: Warszawa, Poland, 2013.
54. Tychowska-Jankowska, A. *Environmental Impact Forecast*; Burmistrz Ozimka: Ozimek, Poland, 2013. (In Polish). Available online: https://ozimek.pl/static/img/k01/obwieszczenia_burmistrza/2013/04_Prognoza_oddzialywania_na_srodowisko.pdf (accessed on 20 June 2021).
55. Muránszky, G.; Ovari, M.; Virág, I.; Csiba, P.; Dobai, R.; Záray, G. Chemical characterization of PM10 fractions of urban aerosol. *Microchem. J.* **2011**, *98*, 1–10. [CrossRef]
56. Byeon, S.H.; Willis, R.; Peters, T.M. Chemical characterization of outdoor and subway fine (PM2.5–1.0) and coarse (PM10–2.5) particulate matter in Seoul (Korea) by computer-controlled scanning electron microscopy (CCSEM). *Int. J. Environ. Res. Public Health* **2015**, *12*, 2090–2104. [CrossRef]
57. Nalbandian, H. *Trace Element Emissions from Coal*; IEA Clean Coal Centre: Paris, France, 2012. Available online: https://usea.org/sites/default/files/092012_Trace%20element%20emissions%20from%20coal_ccc203.pdf (accessed on 20 June 2021).
58. Vossler, T.; Cernikovsky, L.; Novak, J.; Placha, H.; Krejci, B.; Nikolova, I.; Chalupnickova, E.; Williams, R. An investigation of local and regional sources of fine particulate matter in Ostrava, the Czech Republic. *Atmos. Pollut. Res.* **2015**, *6*, 454–463. [CrossRef]
59. Pokorná, P.; Hovorka, J.; Klán, M.; Hopke, P.K. Source apportionment of size resolved particulate matter at a European air pollution hot spot. *Sci. Total Environ.* **2015**, *502*, 172–183. [CrossRef]
60. Slovak Hydrometeorological Institute. *Air Pollution in the Slovak Republic*; Slovak Hydrometeorological Institute: Bratislava, Slovakia, 2019.
61. Olszowski, T. Influence of individual household heating on PM2.5 concentration in a rural settlement. *Atmosphere* **2019**, *10*, 782. [CrossRef]
62. Mach, T.; Rogula-Kozłowska, W.; Bralewska, K.; Majewski, G.; Rogula-Kopiec, P.; Rybak, J. Impact of Municipal, Road Traffic, and Natural Sources on PM10: The Hourly Variability at a Rural Site in Poland. *Energies* **2021**, *14*, 2654. [CrossRef]
63. Juda-Rezler, K.; Kowalczyk, D. Size distribution and trace elements contents of coal fly ash from pulverized boilers. *Pol. J. Environ. Stud.* **2013**, *22*, 25–40.
64. Miler, M.; Gosar, M. Assessment of metal pollution sources by SEM/EDS analysis of solid particles in snow: A case study of Žerjav, Slovenia. *Microsc. Microanal.* **2013**, *19*, 1–14. [CrossRef] [PubMed]
65. Goix, S.; Resongles, E.; Point, D.; Oliva, P.; Duprey, J.L.; de la Galvez, E.; Ugarte, L.; Huayta, C.; Prunier, J.; Zouiten, C.; et al. Transplantation of epiphytic bioaccumulators (Tillandsia capillaris) for high spatial resolution biomonitoring of trace elements and point sources deconvolution in a complex mining/smelting urban context. *Atmos. Environ.* **2013**, *80*, 330–341. [CrossRef]
66. Cadle, S.H.; Mulawa, P.A.; Hunsanger, E.C.; Nelson, K.; Ragazzi, R.A.; Barrett, R.; Gallagher, G.L.; Lawson, D.R.; Knapp, K.T.; Snow, R. Composition of light-duty motor vehicle exhaust particulate matter in the Denver, Colorado area. *Environ. Sci. Technol.* **1999**, *33*, 2328–2339. [CrossRef]
67. Pant, P.; Harrison, R.M. Estimation of the contribution of road traffic emissions to particulate matter concentrations from field measurements: A review. *Atmos. Environ.* **2013**, *77*, 78–97. [CrossRef]
68. GDDKiA. *Generalny Pomiar Ruchu w 2015 Roku*; GDDKiA: Warsaw, Poland, 2016. (In Polish)
69. Adamiec, E.; Jarosz-Krzemińska, E.; Wieszała, R. Heavy metals from non-exhaust vehicle emissions in urban and motorway road dusts. *Environ. Monit. Assess.* **2016**, *188*, 369. [CrossRef]

70. Root, R.A. Lead loading of urban streets by motor vehicle wheel weights. *Environ. Health Perspect.* **2000**, *108*, 937. [CrossRef]
71. Bartoňová, L.; Raclavská, H.; Čech, B.; Kucbel, M. Behavior of Pb during coal combustion: An overview. *Sustainability* **2019**, *11*, 6061. [CrossRef]
72. Moore, K.; Polidori, A.; Sioutas, C. *Toxicological Assessment of Particulate Emissions From the Exhaust of Old and New Model Heavy- and Light-Duty Vehicles*; METRANS: Los Angeles, CA, USA, 2011.
73. Deng, S.; Shi, Y.; Liu, Y.; Zhang, C.; Wang, X.; Cao, Q.; Zhang, F. Emission characteristics of Cd, Pb and Mn from coal combustion: Field study at coal-fired power plants in China. *Fuel Process. Technol.* **2014**, *126*, 469–475. [CrossRef]
74. WHO. Chapter 6.8—Manganese. In *Air Quality Guidelines*, 2nd ed.; WHO: Geneva, Switzerland, 2001; pp. 1–13.
75. Lindsley, W.G. Filter Pore Size and Aerosol Sample Collection. In *NIOSH Manual of Analytical Methods*, 5th ed.; Kevin, A., O'Connor, P.F., Eds.; National Institute for Occupational Safety and Health: Washington, DC, USA, 2016; pp. 2–14.
76. Opell, B.D. What forces are responsible for the stickiness of spider cribellar threads? *J. Exp. Zool.* **1993**, *265*, 469–476. [CrossRef]
77. Opell, B.D. Do static electric forces contribute to the stickiness of a spider's cribellar prey capture threads? *J. Exp. Zool.* **1995**, *273*, 186–189. [CrossRef]
78. Ortega-Jimenez, V.M.; Dudley, R. Spiderweb deformation induced by electrostatically charged insects. *Sci. Rep.* **2013**, *3*, 1–4. [CrossRef] [PubMed]
79. Peters, H.M. The spinning apparatus of Uloboridae in relation to the structure and construction of capture threads (Arachnida, Araneida). *Zoomorphology* **1984**, *104*, 96–104. [CrossRef]
80. Vollrath, F.; Edmonds, D. Consequences of electrical conductivity in an orb spider's capture web. *Naturwissenschaften* **2013**, *100*, 1163–1169. [CrossRef] [PubMed]

# ANALYSIS OF THE HOURLY VARIABILITY IN THE PM10 ELEMENTAL COMPOSITION AND ITS SOURCES: THE CASE STUDY OF A RURAL AREA IN THE SOUTHERN PART OF POLAND

Tomasz Mach[1], Wioletta Rogula-Kozłowska[2], Justyna Rybak[1], Patrycja Rogula-Kopiec[3], Grzegorz Majewski[4]

[1] Wroclaw University of Technology
[2] Main School of Fire Service in Warsaw
[3] Institute of Environmental Engineering of the Polish Academy of Sciences in Zabrze
[4] Warsaw University of Life Sciences

The elemental composition of particulate matter (PM) is one of its critical features determined in order to characterize the impact of PM on the environment and health as well as to assess the origin of PM at a specific receptor.

It's well known that the assessment of PM origin by using data on the elemental composition of PM supported by various approaches and mathematical models is more effective in areas where the elemental profiles of PM emitted from various sources are highly diverse and repeatable over a longer period of time [1].

In areas where PM emissions from different sources overlap or one source clearly dominates, it may be very difficult or impossible to determine its origin correctly [2,3]. In such regions, to assess the origin of PM based on the elemental composition of PM, its more appropriate to use concentration data from averaging periods shorter than 24 hours [4]. This study presents and analyze data on PM10 elemental composition collected during monthly measurement campaign and measured automatically in one-hour samples using the Horiba PX-375 analyzer (Fig 1.). In addition, during the measurement campaign, hourly variability of PM2.5, SO2, NO, NO2 and O3 concentrations together with meteorological parameters (temperature and humidity, wind speed and direction as well as precipitation) were examined. This data was further used to assess the hourly variability of the contribution of individual sources in modulating PM10 concentrations in a specific receptor. Sampling site lying in a close proximity to a moderately inhabited rural area (Kotórz Mały, Opolskie Voivodeship), surrounded by meadows and low bushes was used as a receptor (Fig. 2).

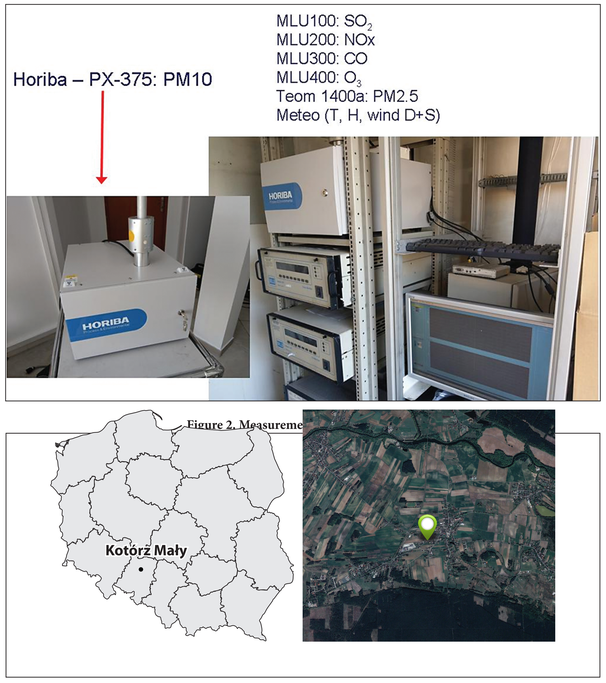


**Figure 1. Location and surroundings of the sampling site**

When considering air concentrations averaged over the entire monthly measurement period, the analyzed PM10-bound elements can be ordered as follows: As<V<Ni<Pb<Cr<Mn <Cu<Ti<Zn<K<Fe<Ca<Al<Si< S. Generally, trace elements, including toxic ones, such as As, V, Ni, Pb, Cr, Mn were present in very low concentrations, not exceeding 10 ng/m3 (average daily value); they were therefore significantly lower than previously registered in other regions of the country [2,3].

These elements had fairly even concentrations when comparing both - daily and hourly averaged concentrations (Table 1). A slight increase in the concentration of most trace elements as well as PM10 concentrations was observed at 12.00-14.00 (for few elements also between 18.00-20.00, Fig. 3).

**Table 1. Descriptive statistics of the daily concentrations of tested parameters**

| Variable | Descriptive statistics | | | | |
|---|---|---|---|---|---|
| | N | Average | Minimum | Maximum | Std. Dev. |
| $PM_{10}$, µg/m³ | 29 | 20,8 | 7,1 | 48,4 | 7,5 |
| Al, ng/m³ | 29 | 357,2 | 76,4 | 675,0 | 154,9 |
| As, ng/m³ | 29 | 0,5 | 0,0 | 4,5 | 1,0 |
| Ca, ng/m³ | 29 | 256,2 | 64,6 | 517,5 | 134,1 |
| Cr, ng/m³ | 29 | 6,1 | 5,2 | 7,3 | 0,5 |
| Cu, ng/m³ | 29 | 11,2 | 7,1 | 22,8 | 3,1 |
| Fe, ng/m³ | 29 | 195,2 | 63,9 | 355,4 | 77,1 |
| K, ng/m³ | 29 | 76,7 | 5,4 | 132,5 | 34,3 |
| Mn, ng/m³ | 29 | 6,9 | 3,0 | 12,7 | 2,5 |
| Ni, ng/m³ | 29 | 5,4 | 4,5 | 8,5 | 0,9 |
| NO, µg/m³ | 29 | 1,0 | 0,5 | 2,8 | 0,5 |
| $NO_2$, µg/m³ | 29 | 6,2 | 3,1 | 8,2 | 1,3 |
| $O_3$, µg/m³ | 16 | 25,1 | 19,3 | 33,1 | 3,8 |
| Pb, ng/m³ | 29 | 6,1 | 1,4 | 14,9 | 3,9 |
| S, ng/m³ | 29 | 1485,5 | 556,7 | 2352,4 | 487,4 |
| Si, ng/m³ | 29 | 770,3 | 98,5 | 1722,8 | 455,8 |
| $SO_2$, µg/m³ | 29 | 3,4 | 1,8 | 4,9 | 0,9 |
| Ti, ng/m³ | 29 | 12,8 | 0,3 | 54,8 | 11,7 |
| V, ng/m³ | 29 | 2,1 | 1,8 | 2,5 | 0,2 |
| Zn, ng/m³ | 29 | 14,5 | 4,4 | 37,6 | 7,7 |
| CO, µg/m³ | 16 | 0,4 | 0,2 | 0,5 | 0,1 |
| Temperatura max., st. C | 29 | 27,8 | 19,0 | 32,6 | 3,4 |
| Temperatura min., st. C | 29 | 14,8 | 10,5 | 18,6 | 2,2 |
| Temperatura śr., st. C | 29 | 21,1 | 16,8 | 25,6 | 2,3 |
| Wilg. powietrza, % | 29 | 67,6 | 47,7 | 97,7 | 13,8 |
| Prędkość wiatru, m/s | 29 | 7,1 | 4,2 | 11,7 | 1,9 |
| Ciśnienie atmosferyczne, hPa | 29 | 1013,7 | 1008,2 | 1017,4 | 2,4 |
| Opad atmosferyczny, mm | 29 | 1,7 | 0,0 | 12,0 | 3,6 |

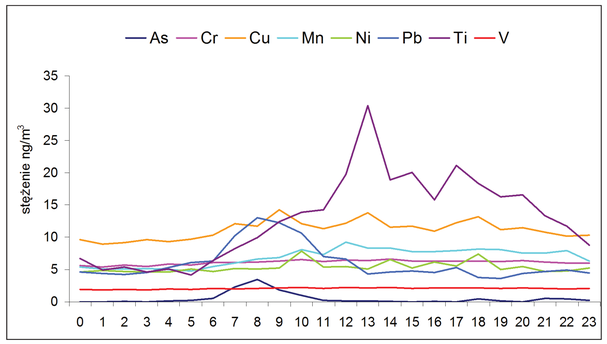


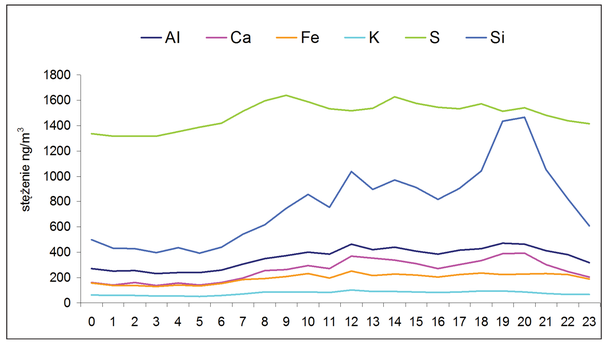


**Fig. 3. The course of the average hourly concentrations of selected PM10-bound elements at the sampling point in the Kotórz Mały village. Data averaged over July 3rd-31st, 2018.**

PC1

| H | V | Cr | Mn | Ni | Cu | Zn | As | Pb | Al | Si | S | K | Ca | Fe | Ti | War. | Udział % |
|---|---|---|---|---|---|---|---|---|---|---|---|---|---|---|---|---|---|
| 0 | | | 0,92 | | | | | | 0,94 | 0,98 | | | 0,94 | 0,93 | 0,85 | 6,2 | 44,2 |
| 1 | | | 0,85 | | | | | | 0,94 | 0,97 | | | 0,92 | 0,91 | 0,90 | 5,9 | 42,0 |
| 2 | | | 0,79 | | | | 0,76 | | 0,86 | 0,93 | | | 0,95 | 0,90 | 0,89 | 6,0 | 40,2 |
| 3 | | | 0,70 | | | | | | 0,90 | 0,97 | | | 0,92 | 0,92 | 0,86 | 5,4 | 38,5 |
| 4 | | | 0,86 | | | | | | 0,84 | 0,95 | | | 0,83 | 0,95 | 0,87 | 5,5 | 36,5 |
| 5 | | | 0,72 | | | | | | 0,95 | 0,93 | | 0,76 | 0,83 | 0,91 | 0,81 | 5,6 | 37,2 |
| 6 | | | 0,78 | | | | | | 0,92 | 0,93 | | 0,82 | 0,85 | 0,91 | 0,82 | 6,1 | 40,3 |
| 7 | | | 0,73 | | | | | | 0,87 | 0,87 | | 0,84 | 0,86 | 0,82 | 0,91 | 5,9 | 39,3 |
| 8 | | | 0,84 | | | | | | 0,92 | 0,95 | | 0,81 | 0,81 | 0,88 | 0,90 | 6,3 | 42,3 |
| 9 | | | 0,83 | 0,75 | | | | | 0,94 | 0,95 | | 0,82 | 0,83 | 0,76 | 0,91 | 6,1 | 40,6 |
| 10 | | | 0,75 | | | | | | 0,91 | 0,81 | | 0,76 | 0,87 | | 0,88 | 5,2 | 34,3 |
| 11 | | | 0,90 | | 0,72 | | | | 0,87 | 0,92 | | 0,85 | 0,89 | 0,93 | 0,94 | 6,8 | 45,5 |
| 12 | 0,77 | 0,76 | 0,98 | | 0,89 | | | | 0,97 | 0,99 | | 0,96 | 0,98 | 0,98 | 0,97 | 9,4 | 63,0 |
| 13 | 0,71 | | 0,73 | | 0,92 | 0,83 | 0,95 | 0,92 | | | | 0,79 | | 0,92 | | 6,8 | 45,2 |
| 14 | | | 0,87 | | | | | | 0,97 | 0,97 | | 0,93 | 0,96 | 0,97 | 0,95 | 7,4 | 49,4 |
| 15 | | | 0,93 | | 0,91 | | | | 0,92 | 0,97 | | 0,90 | 0,94 | 0,96 | 0,83 | 7,6 | 53,6 |
| 16 | | | 0,91 | | 0,75 | | | | 0,92 | 0,99 | | 0,88 | 0,97 | 0,98 | 0,93 | 6,9 | 46,2 |
| 17 | | | 0,87 | 0,86 | 0,91 | | | | 0,82 | 0,91 | | 0,77 | 0,94 | 0,92 | 0,92 | 8,2 | 54,5 |
| 18 | | | 0,94 | | | | | | 0,98 | 0,93 | | 0,92 | 0,93 | 0,93 | 0,90 | 7,5 | 50,2 |
| 19 | | | 0,84 | 0,71 | 0,83 | | | | 0,92 | 0,87 | | 0,83 | 0,91 | 0,91 | 0,89 | 6,9 | 45,9 |
| 20 | | | 0,77 | | 0,84 | | | | 0,95 | 0,91 | | 0,95 | 0,95 | 0,91 | 0,89 | 6,7 | 48,1 |
| 21 | | | 0,71 | | 0,76 | | | | 0,91 | 0,95 | | 0,91 | 0,98 | 0,76 | 0,88 | 6,6 | 44,1 |
| 22 | | | 0,94 | | | | | | 0,94 | 0,97 | | 0,87 | 0,92 | 0,95 | 0,93 | 7,0 | 46,7 |
| 23 | | | 0,89 | | | | | | 0,94 | 0,96 | | 0,75 | 0,95 | 0,93 | 0,84 | 6,1 | 40,8 |

PC2

| H | V | Cr | Mn | Ni | Cu | Zn | As | Pb | Al | Si | S | K | Ca | Fe | Ti | War. | Udział % |
|---|---|---|---|---|---|---|---|---|---|---|---|---|---|---|---|---|---|
| 0 | 0,95 | 0,97 | | | | | | | | | | | | | | 2,4 | 17,2 |
| 1 | 0,96 | 0,97 | | | | | | | | | | | | | | 2,3 | 16,4 |
| 2 | 0,95 | 0,95 | | | | | | | | | | | | | | 2,7 | 17,7 |
| 3 | 0,96 | 0,97 | | | | | | | | | | | | | | 2,6 | 18,5 |
| 4 | | | | | 0,76 | | 0,81 | 0,90 | | | | | | | | 2,4 | 16,0 |
| 5 | 0,96 | 0,95 | | | | | | | | | | | | | | 2,4 | 16,1 |
| 6 | | | | | | | 0,85 | 0,95 | | | | | | | | 2,2 | 14,7 |
| 7 | | | | | 0,81 | | 0,82 | 0,95 | | | | | | | | 2,5 | 16,9 |
| 8 | | | | | | | 0,90 | 0,93 | | | | | | | | 2,3 | 15,1 |
| 9 | | | | | 0,80 | 0,89 | 0,92 | | | | | | | | | 2,7 | 18,1 |
| 10 | | | | 0,79 | 0,73 | 0,93 | 0,87 | 0,94 | | | | | | 0,71 | | 4,6 | 30,9 |
| 11 | | | | | | | -0,93 | -0,96 | | | | | | | | 2,1 | 14,1 |
| 12 | | | | | | | 0,92 | 0,72 | | | | | | | | 2,1 | 14,0 |
| 13 | | | | | | | | | 0,91 | 0,90 | | 0,91 | | 0,88 | | 5,2 | 34,5 |
| 14 | 0,73 | 0,74 | | | | | 0,93 | 0,91 | | | | | | | | 3,6 | 23,7 |
| 15 | 0,97 | 0,94 | | | | | | | | | | | | | | 2,2 | 15,6 |
| 16 | 0,92 | 0,93 | | | | | | | | | | | | | | 2,6 | 17,2 |
| 17 | | | | | 0,78 | | | | | | | | | | | 1,9 | 12,7 |
| 18 | | | | | | | 0,88 | 0,96 | | | | | | | | 2,0 | 13,2 |
| 19 | | | | | | 0,90 | | 0,84 | | | 0,71 | | | | | 2,1 | 14,2 |
| 20 | | | | | | 0,93 | 0,94 | | | | 0,72 | | | | | 2,4 | 17,1 |
| 21 | | | | | | 0,72 | 0,70 | 0,94 | | | | | | | | 2,8 | 18,9 |
| 22 | 0,94 | 0,93 | | | | | | | | | | | | | | 2,3 | 15,4 |
| 23 | 0,96 | 0,96 | | | | | | | | | | | | | | 2,2 | 14,5 |

PC3

| H | V | Cr | Mn | Ni | Cu | Zn | As | Pb | Al | Si | S | K | Ca | Fe | Ti | War. | Udział % |
|---|---|---|---|---|---|---|---|---|---|---|---|---|---|---|---|---|---|
| 0 | | | | | | 0,83 | | 0,77 | | | | | | | | 1,9 | 13,6 |
| 1 | | | | | | 0,87 | | | | | | | | | | 1,8 | 13,1 |
| 2 | | | | | | 0,81 | | | | | | | | | | 1,7 | 11,1 |
| 3 | | | | | | 0,84 | | 0,87 | | | | | | | | 2,0 | 14,5 |
| 4 | 0,97 | 0,97 | | | | | | | | | | | | | | 2,4 | 15,9 |
| 5 | | | | | | | | 0,88 | | | | | | | | 2,2 | 14,7 |
| 6 | 0,95 | 0,95 | | | | | | | | | | | | | | 2,2 | 14,8 |
| 7 | 0,90 | 0,91 | | | | | | | | | | | | | | 2,5 | 16,7 |
| 8 | 0,96 | 0,97 | | | | | | | | | | | | | | 2,2 | 14,7 |
| 9 | 0,86 | 0,89 | | | | | | | | | | | | | | 2,5 | 16,4 |
| 10 | | | | | | | | | | | 0,96 | | | | | 1,3 | 8,5 |
| 11 | | | | | | | | | | | 0,85 | | | | | 1,7 | 11,3 |
| 12 | | | | | | 0,74 | | | | | 0,87 | | | | | 1,4 | 9,5 |
| 13 | | | | | | | | | | | -0,91 | | | | | 1,3 | 8,9 |
| 14 | | | | | | 0,79 | | | | | 0,90 | | | | | 2,0 | 13,2 |
| 15 | | | | | | 0,74 | | | | | 0,82 | | | | | 1,5 | 10,9 |
| 16 | | | | | | 0,80 | | | | | | | | | | 2,0 | 13,2 |
| 17 | | | | | | | 0,76 | | | | | | | | | 2,1 | 13,7 |
| 18 | 0,71 | | | | | | | | | | -0,75 | | | | | 1,8 | 11,8 |
| 19 | 0,93 | 0,91 | | | | | | | | | | | | | | 2,3 | 15,3 |
| 20 | 0,92 | 0,93 | | | | | | | | | | | | | | 2,2 | 15,4 |
| 21 | 0,90 | 0,91 | | | | | | | | | | | | | | 3,0 | 19,9 |
| 22 | | | | | | | 0,95 | 0,75 | | | | | | | | 1,7 | 11,0 |
| 23 | | | | | | | 0,95 | 0,85 | | | | | | | | 1,7 | 11,3 |

PC4

| H | V | Cr | Mn | Ni | Cu | Zn | As | Pb | Al | Si | S | K | Ca | Fe | Ti | War. | Udział % |
|---|---|---|---|---|---|---|---|---|---|---|---|---|---|---|---|---|---|
| 0 | | | | 0,82 | | | | | | | | | | | | 1,6 | 11,4 |
| 1 | | | | 0,83 | | | | | | | | | | | | 1,5 | 10,4 |
| 2 | | | | 0,74 | | | | | | | | | | | | 1,7 | 11,2 |
| 3 | | | | | | | | | | | 0,91 | | | | | 1,4 | 10,3 |
| 4 | | | | | | | | | | | 0,89 | | | | | 1,7 | 11,6 |
| 5 | | | | 0,79 | | | | | | | | | | | | 1,4 | 9,1 |
| 6 | | | | | | | | | | | -0,72 | | | | | 1,3 | 9,0 |
| 7 | | | | | | | | | | | 0,87 | | | | | 1,2 | 8,0 |
| 8 | | | | | 0,83 | | | | | | 0,72 | | | | | 1,5 | 10,2 |
| 9 | | | | | | | | | | | 0,88 | | | | | 1,5 | 9,8 |
| 10 | 0,87 | 0,88 | | | | | | | | | | | | | | 2,2 | 14,7 |
| 11 | 0,78 | 0,76 | | 0,78 | | | | | | | | | | | | 2,2 | 14,9 |
| 15 | | | | -0,88 | | | | | | | | | | | | 1,2 | 8,3 |
| 18 | | | | 0,76 | 0,71 | 0,74 | | | | | | | | | | 2,1 | 13,9 |
| 19 | | | | | | | -0,86 | | | | | | | | | 1,3 | 8,7 |
| 22 | | | | | 0,88 | | | | | | 0,74 | | | | | 2,2 | 14,5 |
| 23 | | | | 0,93 | 0,83 | | | | | | | | | | | 2,0 | 13,2 |

PC5

| H | V | Cr | Mn | Ni | Cu | Zn | As | Pb | Al | Si | S | K | Ca | Fe | Ti | War. | Udział % |
|---|---|---|---|---|---|---|---|---|---|---|---|---|---|---|---|---|---|
| 23 | | | | | | 0,89 | | | | | 0,77 | | | | | 1,9 | 12,7 |

**Fig. 4. Collective summary of the results from PCA performed for hourly data concerning elemental composition of PM10. For each hour, altogether 29 results, while in tables we listed only those elements that were each time correlated with new pc1-pc5 variables (correlation coefficient r> 0.7).**

The results obtained from the Principal Component Analysis (PCA) for this period revealed that in the afternoon the receptor may be intensively affected by traffic emission (Fig. 4).

Generally, the concentrations of major elements in PM10 in the tested receptor are subjected to a strong hourly variations. These fluctuations are associated not only with the changes in the profile of the emission sources identified by statistical analysis but mainly with the changes in the speed and direction of the wind (Fig. 5).

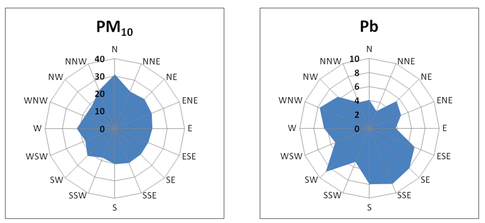


**Fig. 5. The course of the average hourly concentrations of selected PM10-bound elements and PM10-bound Pb at the sampling point in the Kotórz Mały village. Data averaged over July 3rd-31st, 2018.**

[1] W. Rogula-Kozłowska, G. Majewski, P.O. Czechowski. Environmental Monitoring and Assessment 187 (5), 240, 2015.
[2] G. Majewski, W. Rogula-Kozłowska. Theoretical and Applied Climatology 125 (1-2), 79-92, 2016.
[3] M. Schaap, E.P. Weijers, D. Mooibroek, L. Nguyen, R. Hoogerbrugge. BOP – report (https://www.pbl.nl/sites/default/files/cms/publicaties/500099007.pdf; dostęp 10.07.2019).
[4] Y. Li, M. Chang, S. Ding, S. Wang, D. Ni, H. Hu. Journal of Environmental Management 196, 16-25, 2017.

*This study was financed partly from the Ministry of Science and Higher Education funds granted to the Faculty of Environmental Engineering of the Wroclaw University of Technology and related to the realization of the implementation doctorate No. 0015/DW/2018*

INSTYTUT PODSTAW INŻYNIERII ŚRODOWISKA
POLSKIEJ AKADEMII NAUK

## XI KONFERENCJA NAUKOWA
## OCHRONA POWIETRZA W TEORII I PRAKTYCE

# KSIĄŻKA POSZERZONYCH ABSTRAKTÓW

pod redakcją Marianny Czaplickiej, Jacka Gębickiego,
Wioletty Rogula-Kozłowskiej, Izabeli Sówki, Grzegorza Majewskiego

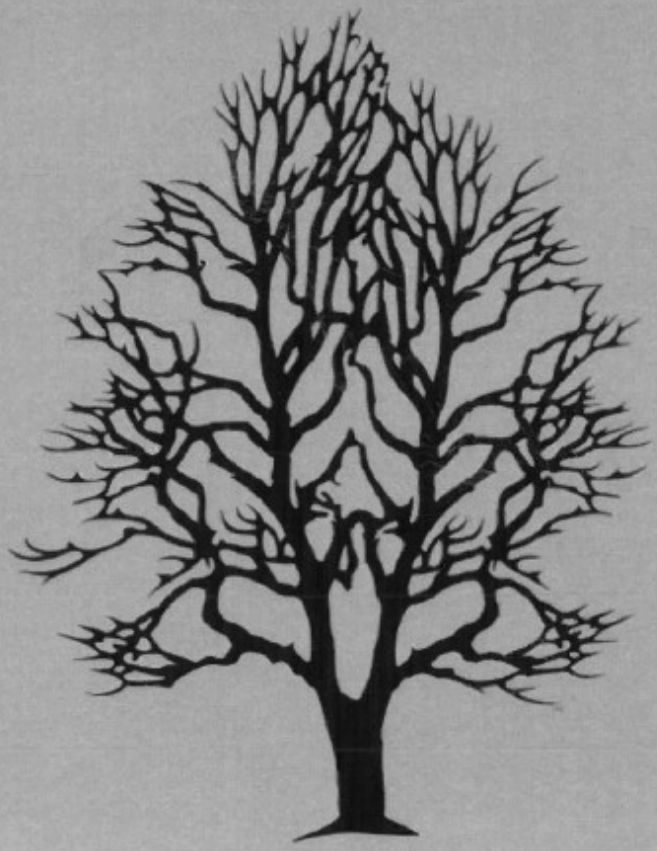

ZABRZE 2019

# Analiza godzinowej zmienności składu pierwiastkowego i źródeł $PM_{10}$: stadium przypadku obszaru wiejskiego w południowej części Polski

Tomasz Mach[1], Wioletta Rogula-Kozłowska[2], Justyna Rybak[1], Patrycja Rogula-Kopiec[3], Grzegorz Majewski[4]

[1] Politechnika Wrocławska
[2] Szkoła Główna Służby Pożarniczej w Warszawie
[3] Instytut Podstaw Inżynierii Środowiska PAN w Zabrzu
[4] Szkoła Główna Gospodarstwa Wiejskiego w Warszawie

**Streszczenie**

Skład pierwiastkowy pyłu zawieszonego (PM) jest jedną z jego krytycznych cech wyznaczaną zarówno w celu scharakteryzowania wpływu PM na środowisko i zdrowie jak również w celu określenia pochodzenia PM w konkretnym receptorze. Obecnie wiadomo już, że ocena pochodzenia PM wykorzystująca dane o składzie pierwiastkowym PM i różnego rodzaju podejścia i modele matematyczne jest bardziej efektywna w obszarach, w których profile pierwiastkowe PM emitowanego z różnych źródeł są mocno zróżnicowane i powtarzalne w dłuższym okresie czasu (Rogula-Kozłowska i in. 2015). W obszarach gdzie emisje PM z różnych źródeł nakładają się na siebie lub jedno źródło jest wyraźnie dominujące, prawidłowe określenie pochodzenia PM może być bardzo trudne lub wręcz niemożliwe (Majewski i Rogula-Kozłowska 2016, Schaap i in. 2019). W takich rejonach do oceny pochodzenia PM w oparciu o skład pierwiastkowy PM bardziej przydatne są dane pochodzące z uśredniania pomiarów w krótszych niż doba odcinkach czasu (Li i in. 2017). W tej pracy przedstawiono i przeanalizowano dane pochodzące z miesięcznej kampanii pomiarowej składu pierwiastkowego $PM_{10}$ mierzonego automatycznie w próbkach jednogodzinowych z wykorzystaniem analizatora PX-375 firmy Horiba. Dodatkowo podczas kampanii pomiarowej badano godzinową zmienność stężeń $PM_{2,5}$, $SO_2$, NO, $NO_2$, $O_3$ oraz parametrów meteorologicznych (temperatura i wilgotność powietrza, prędkość i kierunek wiatru oraz opad atmosferyczny). Dane wykorzystano do oceny godzinowej zmienności udziału poszczególnych źródeł w stężeniach $PM_{10}$ w konkretnym receptorze. Jako receptor wybrano punkt pomiarowy znajdujący się w pobliżu umiarkowanie zamieszkałego obszaru wiejskiego (Kotórz Mały, województwo opolskie), otoczonego łąkami i niskimi krzewami.

Średnio w całym miesięcznym okresie pomiarowym badane w pracy pierwiastki związane z $PM_{10}$ można uszeregować następująco pod względem stężenia w powietrzu: As<V<Ni<Pb<Cr<Mn<Cu<Ti<Zn<K<Fe<Ca<Al<Si<S. Generalnie pierwiastki śladowe, w tym toksyczne, takie jak As, V, Ni, Pb, Cr, Mn występowały w bardzo niskich stężeniach, nie przekraczających 10 ng/m$^3$ (średniodobowa wartość); były zatem znaczni niższe niż rejestrowane wcześniej w innych rejonach kraju (Majewski i Rogula-Kozłowska 2016, Schaap i in. 2019). Pierwiastki te miały dość wyrównane stężenia zarówno średniodobowe jak i średniogodzinowe. Niewielki wzrost stężeń większości pierwiastków

śladowych, jak i stężeń $PM_{10}$ (uśredniona dla okresu 12.00–13.00 stężenie $PM_{10}$ było na poziomie 34 µg/m³, uśrednione w pozostałych godzinach było w zakresie 19–22 µg/m³), obserwowano w godzinach 12.00–14.00 (Rys. 1). Wyniki z przeprowadzonej analizy składowych głównych (PCA) dla tego okresu wskazują na to, że w godzinach popołudniowych na receptor oddziaływać może intensywnie emisja komunikacyjna. Generalnie stężenia pierwiastków głównych w pyle $PM_{10}$ w badanym receptorze podlegają silnym zmianom godzinowym. Wahania te związane są nie tylko ze zmianami w strukturze zidentyfikowanych w analizie statystycznej źródeł ale głównie ze zmianami w prędkości i kierunku wiatru.

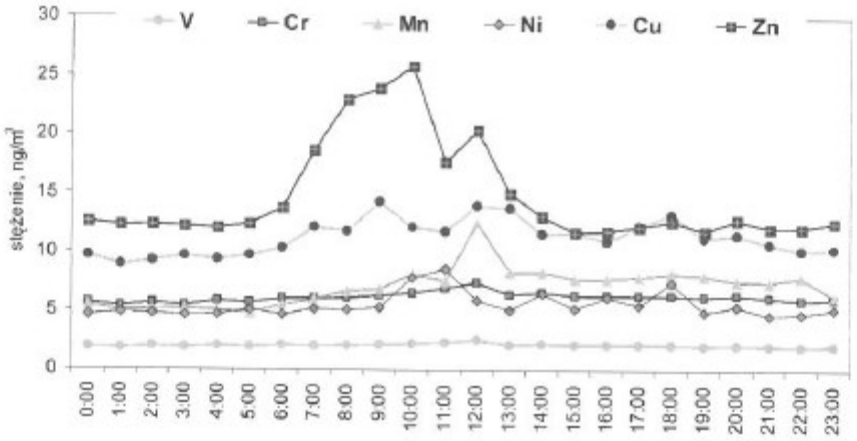


Rys. 1. Przebieg średniogodzinowych stężeń wybranych pierwiastków związanych z $PM_{10}$ na stacji pomiarowej we wsi Kotórz Mały. Dane uśredniono w okresie 3–31 lipca 2018 roku

Praca została sfinansowana częściowo ze środków Ministerstwa Nauki i Szkolnictwa Wyższego przyznanych Wydziałowi Inżynierii Środowiska Politechniki Wrocławskiej w związku z realizacją projektu Doktorat Wdrożeniowy nr 0015/DW/2018.

## Literatura

Li, Y., Chang, M., Ding, S., Wang, S., Ni, D. & Hu. H. (2017). *Journal of Environmental Management*, 196, pp. 16–25.

Majewski, G. & Rogula-Kozłowska, W. (2016). *Theoretical and Applied Climatology*, 125, 1–2, pp. 79–92.

Rogula-Kozłowska, W., Majewski, G. & Czechowski, P.O. (2015). *Environmental Monitoring and Assessment*, 187, 5, 240.

Schaap, M., Weijers, E.P., Mooibroek, D., Nguyen, L. & Hoogerbrugge. R. BOP – report (https://www.pbl.nl/sites/default/files/cms/publicaties/500099007.pdf; dostęp 10.07.2019).

ISBN 978-83-60877-11-1

energies

MDPI

*Article*

# Impact of Municipal, Road Traffic, and Natural Sources on $PM_{10}$: The Hourly Variability at a Rural Site in Poland

**Tomasz Mach [1], Wioletta Rogula-Kozłowska [2], Karolina Bralewska [2], Grzegorz Majewski [3], Patrycja Rogula-Kopiec [4] and Justyna Rybak [1,*]**

1 Faculty of Environmental Engineering, Wrocław University of Science and Technology, Wybrzeże Wyspiańskiego 27, 50-370 Wrocław, Poland; tomasz.mach@pwr.edu.pl
2 Institute of Safety Engineering, The Main School of Fire Service, 52/54, Słowackiego St., 01-629 Warsaw, Poland; wrogula@sgsp.edu.pl (W.R.-K.); kbralewska@sgsp.edu.pl (K.B.)
3 Institute of Environmental Engineering, Warsaw University of Life Sciences, 02-787 Warszawa, Poland; grzegorz_majewski@sggw.edu.pl
4 Institute of Environmental Engineering, Polish Academy of Sciences, 34 M. Skłodowska-Curie St., 41-819 Zabrze, Poland; patrycja.rogula-kopiec@ipis.zabrze.pl
* Correspondence: justyna.rybak@pwr.edu.pl

**Abstract:** The paper presents data from a monthly campaign studying the elemental composition of $PM_{10}$, as measured by a specific receptor in Kotórz Mały (Opole Voivodeship)—located in the vicinity of a moderately inhabited rural area—measured in one-hour samples using a Horiba PX-375 analyzer. The hourly variability of $SO_2$, NO, $NO_2$, CO, and $O_3$ concentrations, as well as the variability of meteorological parameters, was also determined. On average, during the entire measurement period, the elements related to $PM_{10}$ can be arranged in the following order: As < V < Ni < Pb < Cr < Mn < Cu < Ti < Zn < K < Fe < Ca < Al < Si < S. Trace elements, including toxic elements—such as As, V, Ni, Pb, Cr, and Mn—were present in low concentrations, not exceeding 10 ng/m$^3$ (average daily value). These elements had fairly even concentrations, both daily and hourly. The concentrations of the main elements in the $PM_{10}$, as measured by the receptor, are subject to strong hourly changes related not only to changes in the structures of the sources identified in the statistical analysis, but also to wind speed and direction changes (soil and sand particle pick-up and inflow of pollutants from coal combustion). It has been shown that the transport emissions measured by the receptor can have an intense effect on $PM_{10}$ in the afternoon.

**Keywords:** atmospheric aerosol; municipal and traffic emissions; natural sources; enrichment factor; coal and gasoline combustion; 24-h concentrations; diurnal variability; PX-375; XRF analysis



**Citation:** Mach, T.; Rogula-Kozłowska, W.; Bralewska, K.; Majewski, G.; Rogula-Kopiec, P.; Rybak, J. Impact of Municipal, Road Traffic, and Natural Sources on $PM_{10}$: The Hourly Variability at a Rural Site in Poland. *Energies* **2021**, *14*, 2654. https://doi.org/10.3390/en14092654

Academic Editor: Luisa F. Cabeza

Received: 3 April 2021
Accepted: 26 April 2021
Published: 6 May 2021



## 1. Introduction

Particulate matter (PM)'s elemental composition is one of its critical characteristics, determined to characterize the environmental and health effects of the PM, as well as to define the PM's origin at a particular receptor. Taking advantage of the fact that the elemental composition of PM leaving the emission source is more or less defined, the information about it can be used to define the origin of PM in almost any area. Various types of mathematical models are used for this purpose [1–5]. Data on element concentrations of PM are used to evaluate the origin of PM for two main reasons: First, excluding light elements—mainly carbon, nitrogen, and sulfur—most of the elements that form PM, under atmospheric conditions, occur in chemically stable compounds. These compounds, along with PM particles, are transported from the emitters to the receptor in more or less the same chemical form, and in amounts that strictly depend on the number of PM particles emitted by the emitters containing these elements [6–9]. The situation is different with carbon, sulfur, and nitrogen compounds, as their presence in PM at a specific receptor depends not only on the number of stable compounds in PM emitted

from sources affecting this receptor, but also on the presence of gaseous organic and inorganic precursors of secondary aerosols in the atmosphere, as well as meteorological factors determining the intensity and direction of changes of volatile and semi-volatile compounds in the atmosphere [10–13]. The second reason why the knowledge of elemental composition facilitates the understanding of the temporal and spatial variability of PM origin in different regions is that some elements are effective markers of specific PM sources. More specifically, we can say that there are elements characteristic of only one source/emitter, or of a group of similar PM sources, that allow us to distinguish a given source/group of sources from others. For example, the presence of silicon or aluminum are characteristic of PM emitted from soil erosion or sand, while potassium suggests PM derived from biomass combustion [7,14–16]. Until recently, lead has been successfully applied as a marker for PM emissions from petrol combustion in car engines [17–19]. Sometimes the mass ratios of trace elements contained in PM are used to assess the origin of PM in a given area, as their characteristic values for PM emitted from different sources are known [1,20]. Today, it is known that the assessment of the origin of PM on the basis of its elemental content, and with the employment of various approaches and mathematical models, is more effective in areas where the elemental profiles of PM emitted from different sources are highly varied and approximately repeatable long term [1–3,21].

For the correct use of these models, and in order to obtain the right conclusions from the results, it is necessary to collect a large amount of data. Their number depends on many factors; in addition to the meteorological and emission characteristics of the area, it also depends on the model used.

In areas where PM emissions from different sources overlap and/or one source is clearly dominant, the correct determination of the origin of the PM may be very difficult or even impossible [22–25]. Presumably, in such regions, data from averaging measurements over time intervals shorter than 24 h could be more useful in assessing the origin of PM, determined by the elemental concentrations of the PM. Previous studies have shown, for example, that concentrations and chemical composition, including the elemental profiles of PM, dynamically change throughout the day, hour by hour, and that the main causes of this variability are road and municipal emissions. Unfortunately, it is often technically impossible to determine the composition of various elements of PM in samples taken over one hour. Such data come almost exclusively from studies conducted with automatic measurements using the XRF technique. So far, such research has never been conducted in Poland. Meanwhile, in almost all regions of Poland, in terms of PM origin, difficulties have been noted in performing such an analysis (PM origin analysis) based on daily data on the elemental composition of PM. This paper presents and analyses data from a monthly measurement campaign studying the elemental composition of $PM_{10}$ measured in one-hour samples (averaged every hour). The data were used to assess the origins of $PM_{10}$ in a rural area in southern Poland. The variability of the elemental composition of $PM_{10}$, determining the variability of the participation of individual sources in the concentrations of $PM_{10}$ at a specific receptor, was examined.

## 2. Materials and Methods

### *2.1. Sampling Site*

As the receptor, the measurement point in the northern part of the village was selected, which is situated near a moderately inhabited rural area (Kotórz Mały, Opolskie Voivodeship; Figure 1) surrounded by meadows, low shrubs, and trees (50°43′66.02″ N; 18°02′06.80″ E, 162 m. a. s. l.). Kotórz Mały is a village with around 1000 inhabitants, which is located 15 km northeast of Opole, with 122,000 inhabitants. In this village three car services, two metal surface varnishing services, and two carpentries are situated, all of which are equipped with high-efficiency dust collection systems. Apart from these, there are no local sources of air contamination in Kotórz Mały. As is typical for Poland, natural emissions are the main sources of aerosol during the warm seasons, while domestic heating systems are the main local source of air contamination during the cold season [26].

Two national roads are situated within a few kilometers of the village: Road No. 45 to the northwest, with a traffic load of approx. 8000 vehicles/day, and Road No. 46 to the southeast, with approx. 9500 vehicles/day (data from General Director for National Roads and Motorways https://www.gddkia.gov.pl/userfiles/articles/g/generalny-pomiar-ruchu-w-2015_15598//SYNTEZA/WYNIKI_GPR2015_DK.pdf) (access date: 28 April 2021).

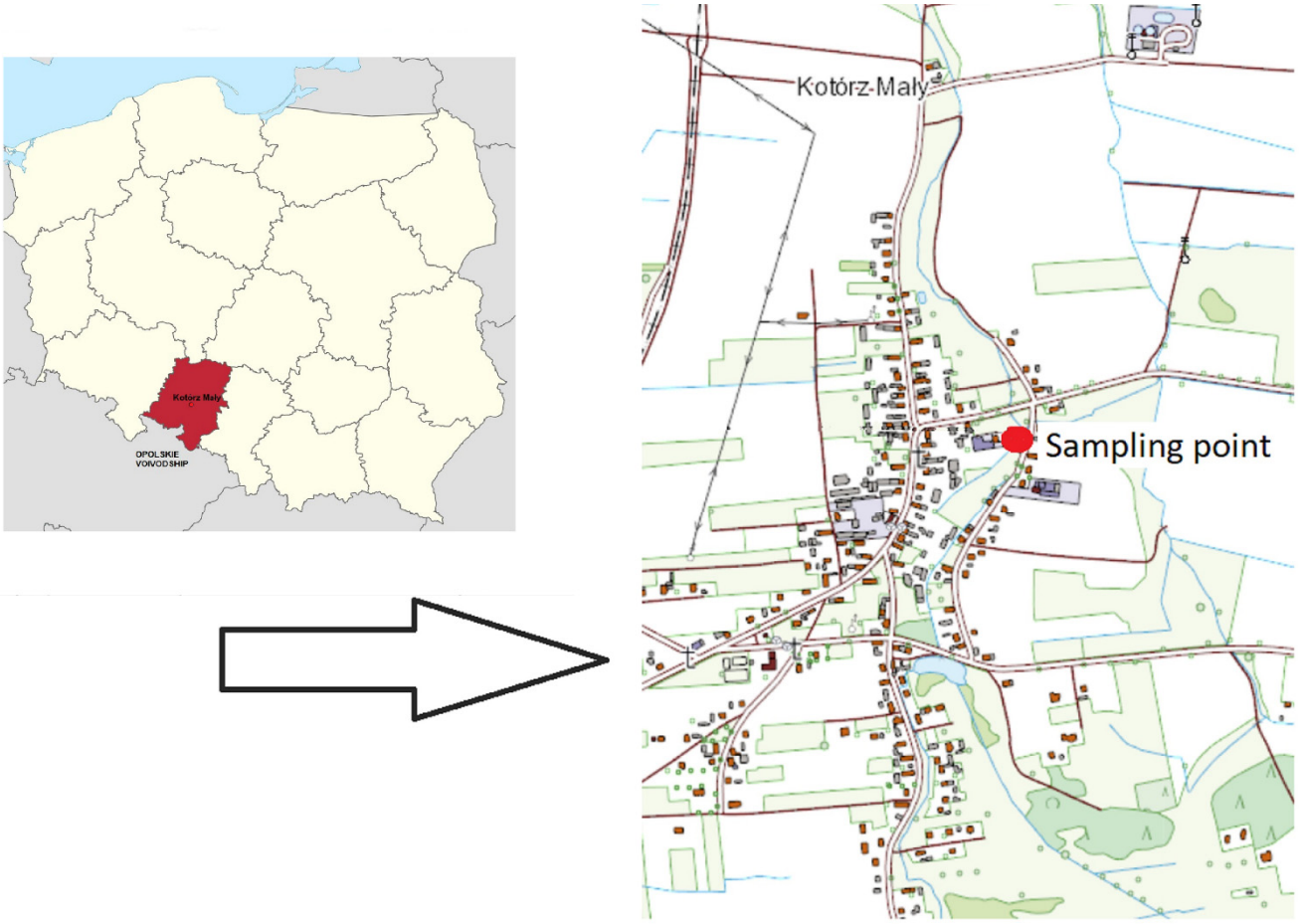


**Figure 1.** Location of the measuring point in Kotórz Mały.

### 2.2. Measurement Method

$PM_{10}$ mass and elemental concentrations of Al, As, Ca, Cr, Cu, Fe, K, Mn, Ni, Pb, S, Si, Ti, V, and Zn were measured hourly with an online XRF (Horiba PX-375, HORIBA ltd., Kyoto, Japan). This monitor applies reel-to-reel filter tape sampling, with analysis of beta ray attenuation, in order to determine the total $PM_{10}$ mass. A nondestructive energy-dispersive X-ray fluorescence (EDXRF) spectroscopic analysis was applied to assess the selected elements' concentrations. The EDXRF contains a complementary metal–oxide–semiconductor (CMOS) camera for sample images. A two-layer non-woven PTFE fabric filter was applied in order to stop the PM from passing onto the opposite side. $PM_{10}$ inlet and filter tape was used for air, at a flow rate of 16.7 L/min, assuming a deposit of approx. 11.1 mm in diameter. After the collection of single samples every 60 min, beta ray attenuation EDXRF analyses were performed for 500 s (15 kV or 50 kV depending on the element per hourly sample) together with the collection of the subsequent sample. In addition, we could check the color of the samples, which gives more reliable results.

NIST-certified standard material, SRM 2783 (air particulate matter on filter media), was applied to determine the elemental quantification of X-ray spectra, and to obtain a quality control measure. Additionally, the lowest detection limits (LLD as double the standard deviation of the blank analyzed) were Al (56.7 ng/m$^3$), As (3.7 ng/m$^3$), Ca (1.1 ng/m$^3$),

Cr (2.05 ng/m$^3$), Cu (1.85 ng/m$^3$), Fe (7.00 ng/m$^3$), K (4.8 ng/m$^3$), Mn (1.45 ng/m$^3$), Ni (0.9 ng/m$^3$), Pb (1.05 ng/m$^3$), S (1.55 ng/m$^3$), Si (8.85 ng/m$^3$), Ti (0.25 ng/m$^3$), V (1.7 ng/m$^3$), and Zn (1.25 ng/m$^3$).

The measurements lasted from 3 to 31 July 2018. In addition to the concentration of $PM_{10}$ and the elemental composition of $PM_{10}$, the hourly variability of the concentrations was also examined during the measurement campaign:

- $SO_2$ (Monitoring für Leben und Umwelt API-MLU100 automatic analyzer; in accordance with PN-EN 14212 (Atmospheric air quality. Standard fluorescent UV method for determining the concentration of sulfur dioxide); the limit of detection and measurement accuracy is 2.850 μg/m$^3$). This analyzer ranges from 0–50 ppb to 0–20 ppm, and is based on the UV fluorescence principle. The optical shutter and a reference detector provide high stability;
- $NO/NO_2$ (Monitoring für Leben und Umwelt MLU200E automatic analyzer; in accordance with PN-EN 14211 (Atmospheric air quality. Standard chemiluminescent method for measuring the concentration of monoxide and nitrogen dioxide); the limit of detection and measurement accuracy is 1.025 μg/m$^3$). This analyzer ranges from 0–50 ppb to 0–20 ppm, and has independent ranges for NO, $NO_2$, and $NO_x$. The analyzer is based on the chemiluminescence detection principle. Measurements are compensated for temperature, pressure, and flow changes. An auto-zero circuit provides a true zero reference, which gives good stability;
- $O_3$ (Monitoring für Leben und Umwelt MLU400E automatic analyzer; in accordance with PN-EN 14625 (Atmospheric air quality. Standard method for measuring ozone concentration using UV photometry); the limit of detection and measurement accuracy is 4.280 μg/m$^3$). This analyzer ranges from 0–100 ppb to 0–10, ppm and has single-path ultraviolet absorption. The analyzer is based on the Beer–Lambert law for measuring low ranges of ozone in ambient air. The idea is that a 254 nm signal of UV light passes through the sample cell, where it is absorbed in proportion to the concentration of ozone present;
- CO (Monitoring für Leben und Umwelt MLU400E automatic analyzer; in accordance with PN-EN 14626 (Ambient air quality. Standard method for the determination of carbon monoxide using non-dispersive infrared spectroscopy); the limit of detection and measurement accuracy is 0.125 mg/m$^3$). This analyzer ranges from 0–1ppm to 0–1000 ppm, and has a gas filter wheel for CO-specific measurement, and a 14 m path length for sensitivity. The idea of measurement is based on the comparison of infrared energy absorbed by a sample to a reference sample according to the Beer–Lambert law. This is accomplished with a gas filter correlation wheel, which allows a high-energy light source to pass through both a CO-filled chamber and one with no CO. The light path passes through the sample cell, and the energy loss through this cell is compared with the zero reference signal provided by the gas filter to produce a signal proportional to concentration, with little effect from interfering gases within the sample;

Meteorological parameters—e.g., air temperature, humidity, wind speed, wind direction, atmospheric pressure, and precipitation—were measured with a Gill Instruments Windsonic 2D wind speed and direction sensor, and an LSI DMA572 temperature and humidity sensor, according to the instructions of the network of state weather stations operated by the Institute of Meteorology and Water Management (IMWM).

### *2.3. Data Analyses*

First, the hourly data on each measured day were averaged. Descriptive statistics of all of the parameters tested during the measurement period, averaged to the 24-h value, are presented in Table 1.

**Table 1.** Descriptive statistics of a series of 24-h concentrations of $PM_{10}$, $PM_{10}$-bound elements, gaseous pollutants, and meteorological parameters, as measured by the receptor.

| Parameter | Statistics | | | | |
|---|---|---|---|---|---|
| | N | Average | Minimum | Maximum | Standard Deviation |
| $PM_{10}$, μg/m$^3$ | 29 | 20.8 | 7.1 | 48.4 | 7.5 |
| $PM_{10}$-bound elements | | | | | |
| Al, ng/m$^3$ | 29 | 357.2 | 76.4 | 675.0 | 154.9 |
| As, ng/m$^3$ | 29 | 0.5 | <LLD | 4.5 | 1.0 |
| Ca, ng/m$^3$ | 29 | 256.2 | 64.6 | 517.5 | 134.1 |
| Cr, ng/m$^3$ | 29 | 6.1 | 5.2 | 7.3 | 0.5 |
| Cu, ng/m$^3$ | 29 | 11.2 | 7.1 | 22.8 | 3.1 |
| Fe, ng/m$^3$ | 29 | 195.2 | 63.9 | 355.4 | 77.1 |
| K, ng/m$^3$ | 29 | 76.7 | 5.4 | 132.5 | 34.3 |
| Mn, ng/m$^3$ | 29 | 6.9 | 3.0 | 12.7 | 2.5 |
| Ni, ng/m$^3$ | 29 | 5.4 | 4.5 | 8.5 | 0.9 |
| Pb, ng/m$^3$ | 29 | 6.1 | 1.4 | 14.9 | 3.9 |
| S, ng/m$^3$ | 29 | 1485.5 | 556.7 | 2352.4 | 487.4 |
| Si, ng/m$^3$ | 29 | 770.3 | 98.5 | 1722.8 | 455.8 |
| Ti, ng/m$^3$ | 29 | 12.8 | 0.3 | 54.8 | 11.7 |
| V, ng/m$^3$ | 29 | 2.1 | 1.8 | 2.5 | 0.2 |
| Gaseous pollutants | | | | | |
| $SO_2$, μg/m$^3$ | 29 | 3.4 | 1.8 | 4.9 | 0.9 |
| NO, μg/m$^3$ | 29 | 1.0 | 0.5 | 2.8 | 0.5 |
| $NO_2$, μg/m$^3$ | 29 | 6.2 | 3.1 | 8.2 | 1.3 |
| $O_3$, μg/m$^3$ | 29 | 25.1 | 19.3 | 33.1 | 3.8 |
| CO, μg/m$^3$ | 29 | 0.4 | 0.2 | 0.5 | 0.1 |
| Meteorological parameters | | | | | |
| Temperature max. °C | 29 | 27.8 | 19.0 | 32.6 | 3.4 |
| Temperature min. °C | 29 | 14.8 | 10.5 | 18.6 | 2.2 |
| Temperature average. °C | 29 | 21.1 | 16.8 | 25.6 | 2.3 |
| Humidity % | 29 | 67.6 | 47.7 | 97.7 | 13.8 |
| Wind speed m/s | 29 | 7.1 | 4.2 | 11.7 | 1.9 |
| Atmospheric pressure, hPa | 29 | 1013.7 | 1008.2 | 1017.4 | 2.4 |
| Precipitation, mm | 29 | 1.7 | 0.0 | 12.0 | 3.6 |

In the case of the concentrations of $PM_{10}$ and $PM_{10}$-bound elements, the hourly variability of the concentrations during the day was also tested (Figures 2 and 3). For this purpose, the average concentrations determined for each hour were averaged over the entire measurement period (29 concentrations for 0.00 h; 29 for 01.00 h, etc.).

The enrichment factor (EF) was estimated for each element, measured separately for the average concentration of the element in each hour of the day, and for the averaged concentration of the element over the whole campaign. The method of calculating the EF for the elements, and the assumptions for the calculations, were done in the same way as in previous works [22–24,27–29]. The enrichment factor allowed us to determine quantitatively the influence of anthropogenic effects on the $PM_{10}$-bound elements' concentrations.

Additionally, principal component analysis (PCA) was applied to the 15 × 29 data matrix [23,24] representing the 1-h $PM_{10}$-bound elements' concentrations.

All calculations were done using Statistica 8.0 software (StatSoft, Tulsa, OK, USA).

All documentation photos of the experiment and the research are available in the Supplementary Materials (Figures S1–S5).

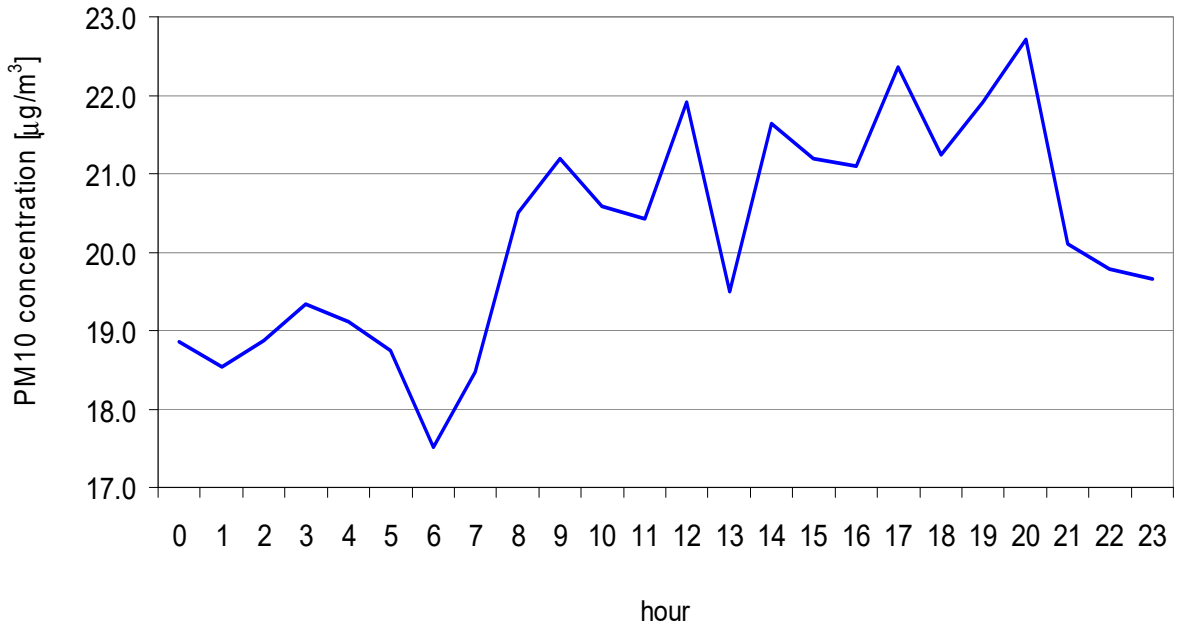


**Figure 2.** The average hourly $PM_{10}$ concentrations averaged for the entire measurement period (03–31.07.2019), as measured by the receptor.

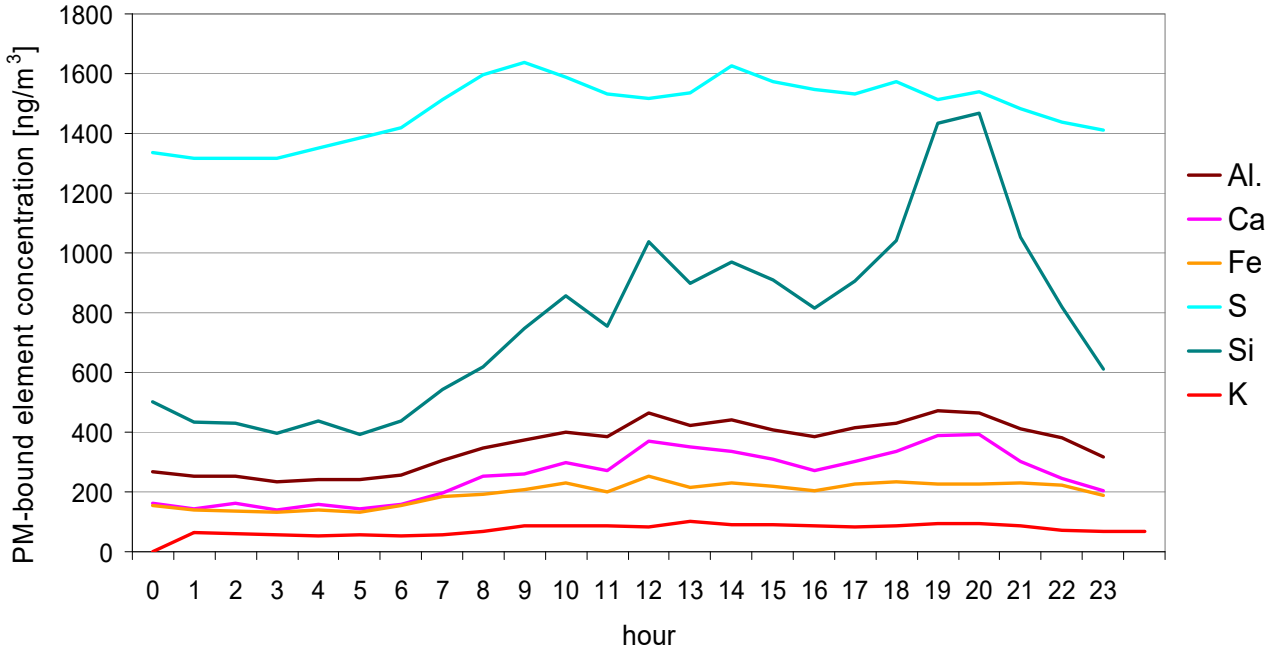


(**a**)

**Figure 3.** *Cont.*

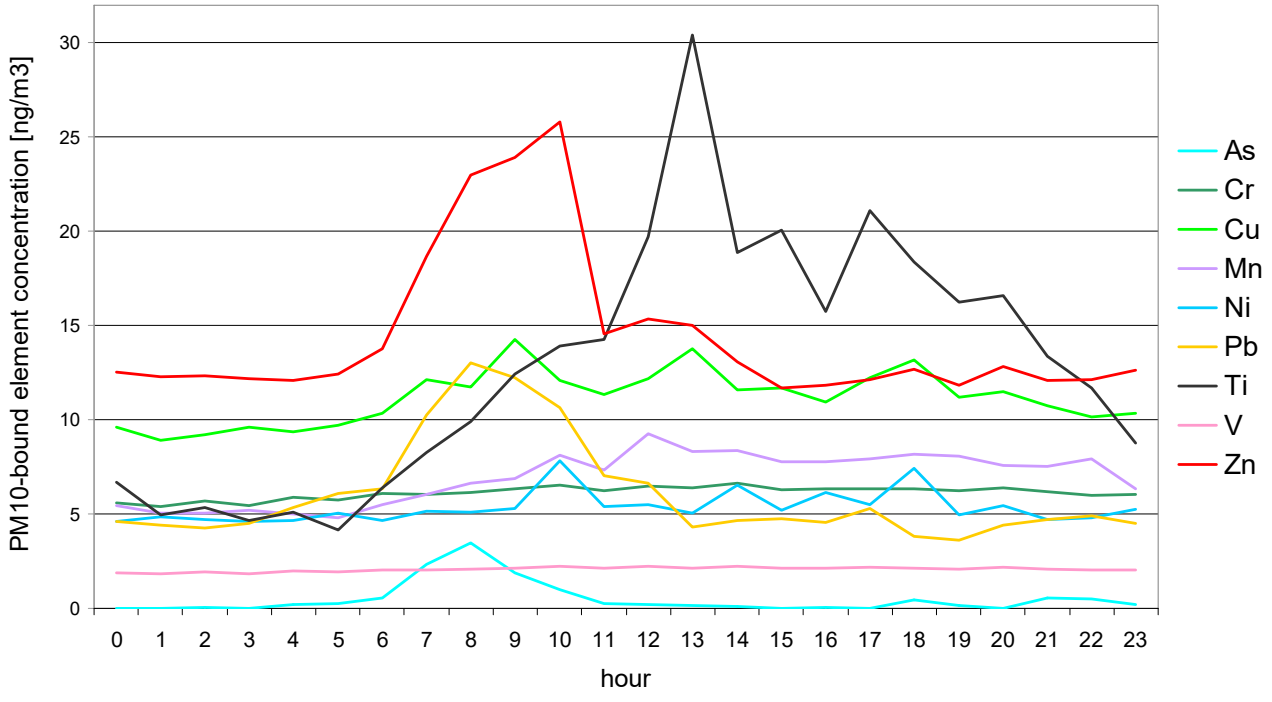


(**b**)

**Figure 3.** The average hourly concentrations of (**a**) Al, Ca, Fe, S, Si and K, and (**b**) As, Cr, Cu, Mn, Ni, Pb, Ti, V and Zn, averaged for the entire measurement period (03–31.07.2019), as measured by the receptor.

## 3. Results and Discussion

### *3.1. Concentrations of $PM_{10}$*

The 24-h concentrations of $PM_{10}$ in Kotórz Mały ranged from 7.1 to 48.4 μg/m$^3$ (Table 1). The mean $PM_{10}$ concentration over the whole measurement campaign was 20.8 μg/m$^3$. This is below the daily $PM_{10}$ concentration limit established by the European Commission (50 μg/m$^3$; not to be exceeded on more than 35 days per year) [30]. $PM_{10}$ concentrations fluctuated throughout the day, although the changes were relatively small (±5 μg/m$^3$) (Figure 2). The lowest concentrations of $PM_{10}$ were recorded between 00.00 a.m. and 06.00 a.m., and the highest between 02.00 p.m. and 09.00 p.m. The fact that the measurements were conducted in the summer, the slight variability of $PM_{10}$ concentrations during the day, and the location of the receptor between two national roads—i.e., Road No. 45, with a traffic density of approx. 8000 vehicles/day (approx. 3 km in a straight line to the northwest), and Road No. 46, with a traffic volume of approx. 9500 vehicles/day (approx. 6 km in a straight line to the southeast) (data from 2015 data from General Director for National Roads and Motorways https://www.gddkia.gov.pl/userfiles/articles/g/generalny-pomiar-ruchu-w-2015_15598//SYNTEZA/WYNIKI_GPR2015_DK.pdf access date: 28 April 2021), allow us to assume that the $PM_{10}$ concentrations at the receptor were mainly determined by traffic emissions, and their peaks in the afternoon hours were caused by the increased traffic intensity related to movement to and from work (2nd shift). This is also indicated by the wind distribution of $PM_{10}$ pollution (Figure 4), according to which the highest concentrations of $PM_{10}$ were observed at the inflow of air masses from the north–northwest and the northeast, where the above routes run. $PM_{10}$ concentrations above the average (>20 μg/m$^3$) were also recorded, with air masses appearing from the southeast. This may also indicate the impact $PM_{10}$ of emission sources present in the Opole agglomeration, located 15 km southeast of the receptor, on the $PM_{10}$ concentration at the receptor. Although the measurements were carried out in the summer, the so-called low-stack emissions related to the combustion of solid fuels in individual home furnaces (e.g., to heat bathwater and satisfy heating needs) can be taken into account as an additional

source of $PM_{10}$ in the evenings, especially since in the analyzed measurement period there were days when the air temperature was below 15 °C.

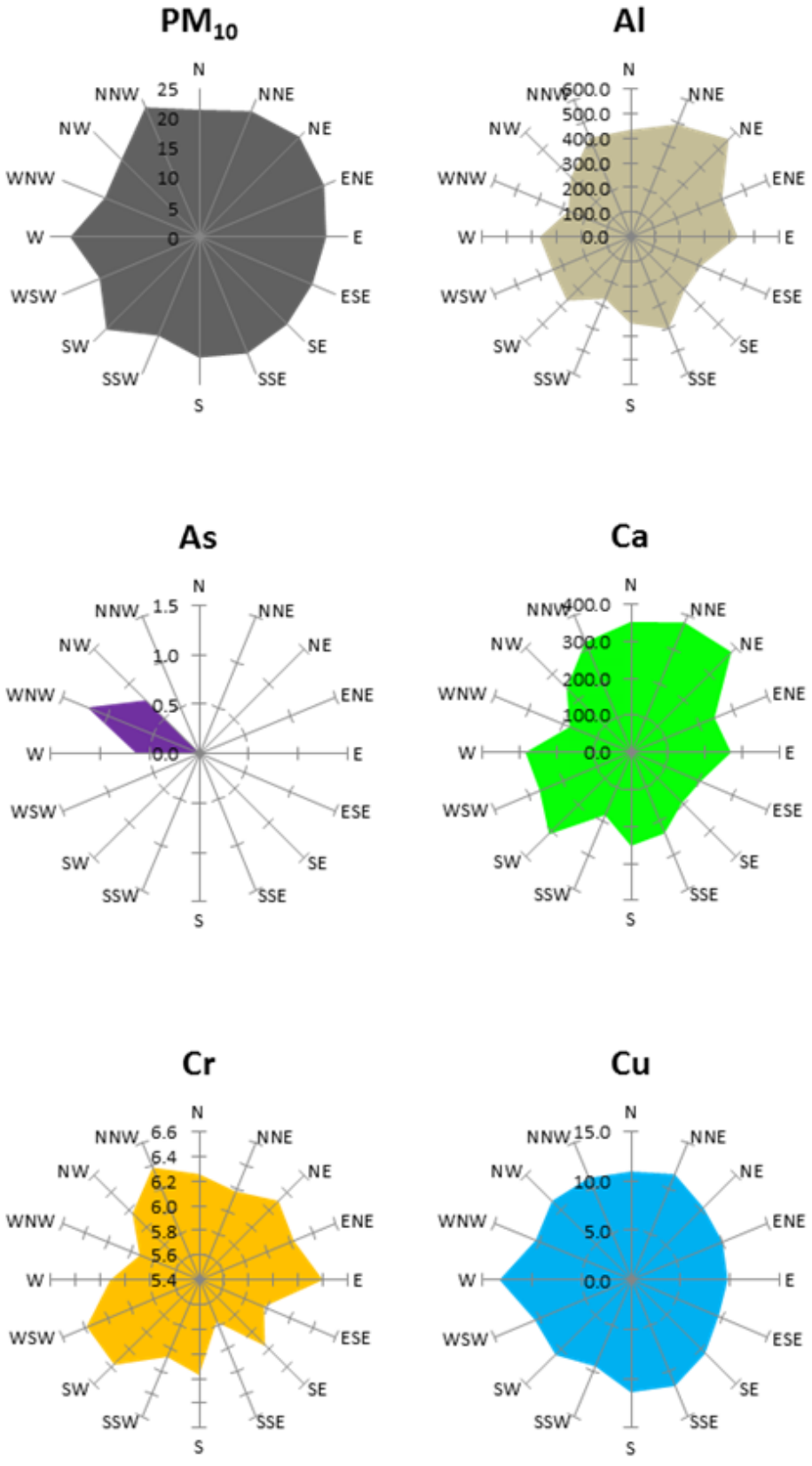


**Figure 4.** *Cont.*

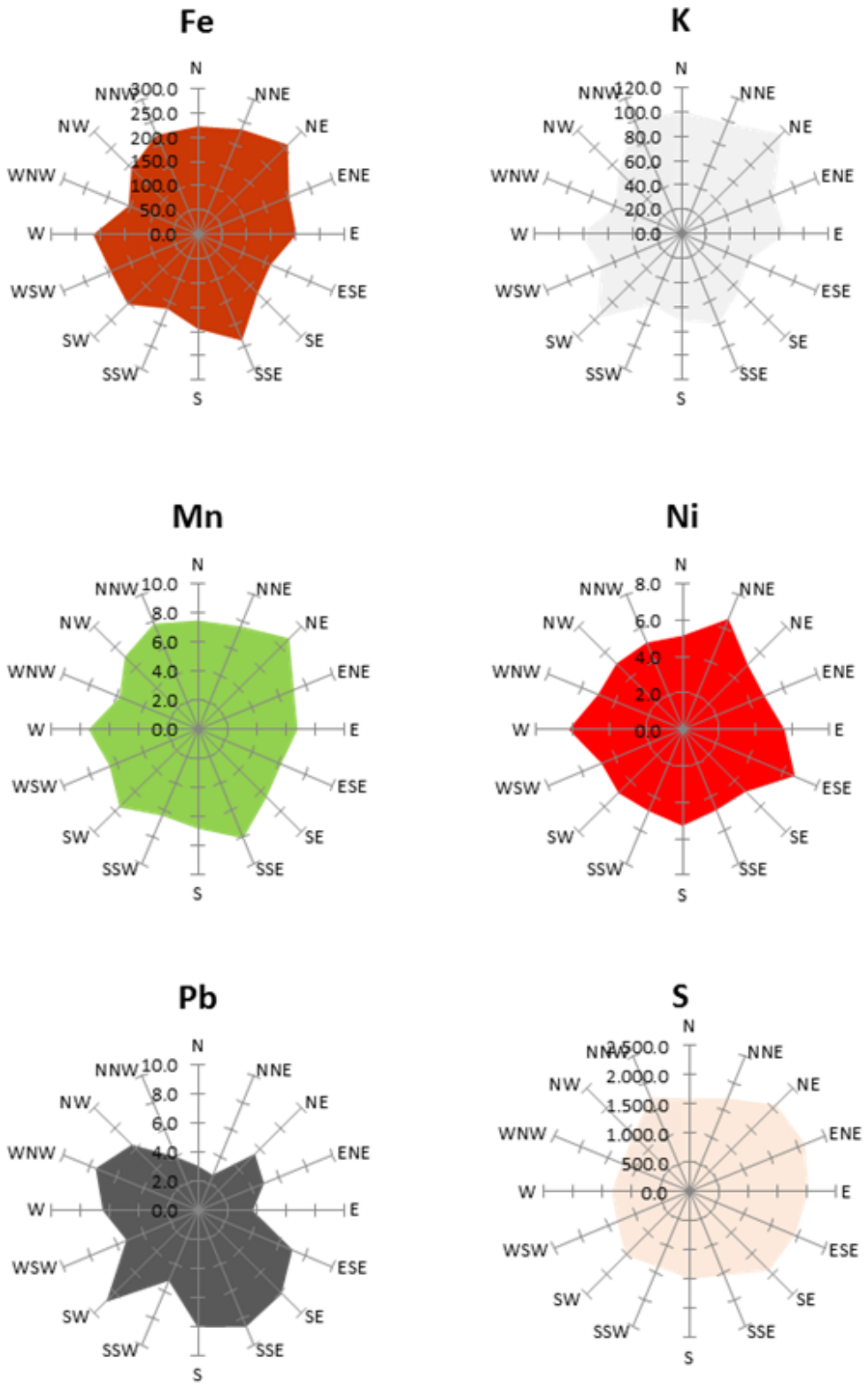


**Figure 4.** *Cont.*

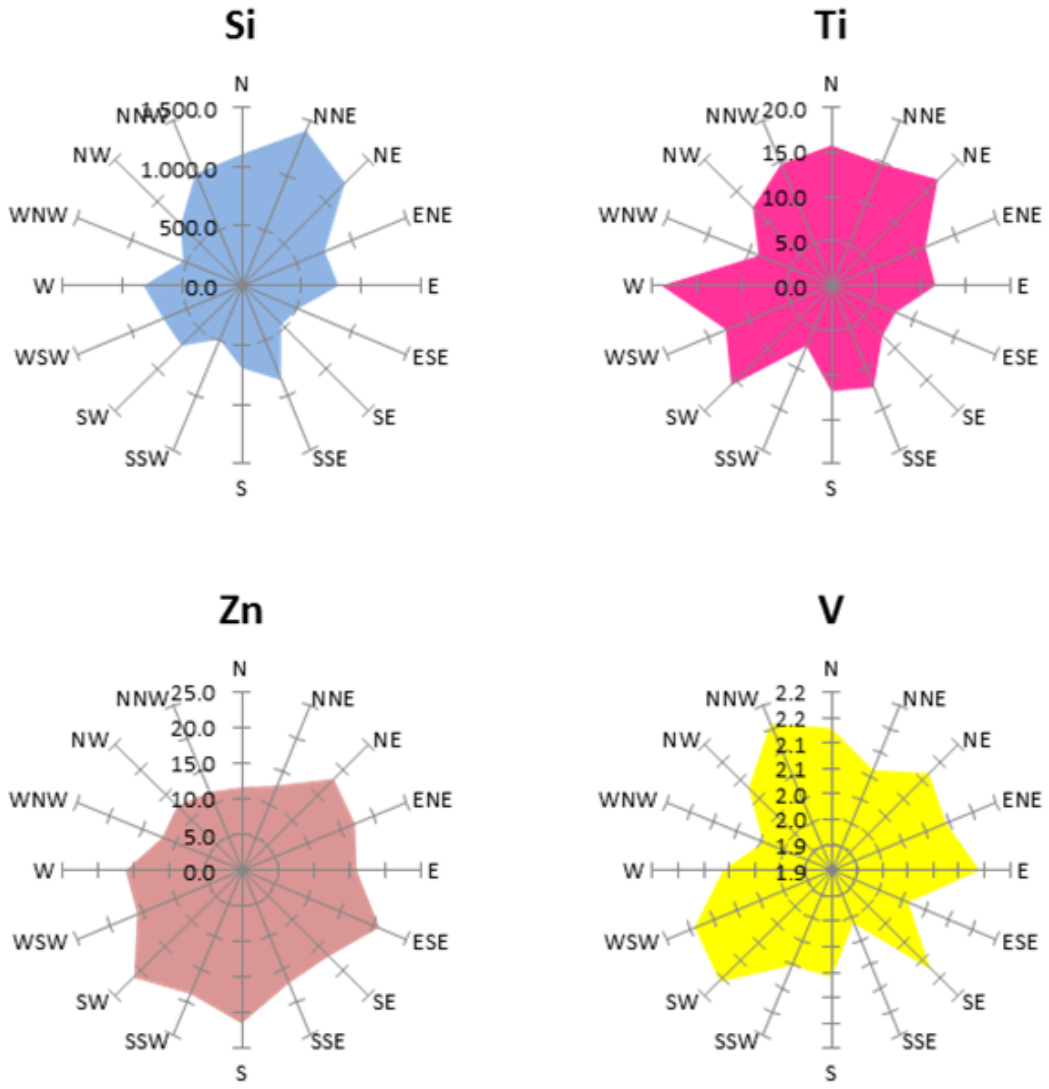


**Figure 4.** Average concentrations of $PM_{10}$ and $PM_{10}$-bound elements related to wind direction during the measurement period.

The mean concentration of $PM_{10}$ at the receptor did not differ much from the $PM_{10}$ concentrations registered in the in the non-heating season eason in other locations in Poland, e.g., at two rural sites in Upper Silesia (2013; 16.14–27.89 μg/m$^3$) [31], in the industrial district of the city of Sosnowiec (2017, 20 μg/m$^3$) [32], in a health resort in Krynica Zdrój (2016, 15.2 μg/m$^3$) [33], in small cities around the Kraków agglomeration (2017, 23.31 μg/m$^3$) [34], and in urban areas of Wrocław and Poznań (2016, approx. 18 μg/m$^3$ in both cities) [35]. The mean $PM_{10}$ concentration in Kotórz Mały was comparable to the concentration of $PM_{10}$ recorded in summer in agricultural areas of the Netherlands (2011, 21 μg/m$^3$), and to the mean annual concentrations of $PM_{10}$ in selected European cities (Vienna, Brussels, London; 2014, 23–25 μg/m$^3$) [36]; however, it was low in relation to the values registered at various European locations, such as Istanbul, Turkey (2014, 58 μg/m$^3$) [37], and Žilina, Slovakia (2017, 86 μg/m$^3$) [38]. The relatively low concentration of $PM_{10}$ at the receptor was probably influenced by the existence of a natural forest barrier (approx. 0.8 km in a straight line), the lack of local industries or enterprises that influence air quality (closest industrial activity approx. 13 km from the receptor), and the high average wind speed (7.1 m/s), which in the analyzed measurement period was more than twice as high as the average annual wind speed in Poland (2.6 m/s in summer; 3.8 m/s in winter). High wind speeds could stimulate the air mixing processes, causing the migration

of pollutants from the receptor to other areas, but it should also be taken into account that they could favor the inflow of pollutants from neighboring areas, e.g., the Opole agglomeration, especially resulting from the activities of industrial plants operating in Opole, i.e., over 15 km from measurement devices (power and heating plants, food and construction industry plants).

In this study, the concentrations of gaseous PM precursors—i.e., nitrogen oxides ($NO_x$), sulfur oxides ($SO_2$), ozone ($O_3$), and carbon monoxide (CO)—were also analyzed (Table 1). The average concentrations of NO, $NO_2$, $SO_2$, $O_3$, and CO in the receptor take values were 1.0 μg/m$^3$, 6.2 μg/m$^3$, 3.4 μg/m$^3$, 25.1 μg/m$^3$, and 0.4 μg/m$^3$, respectively, and these were lower than the concentrations recorded in different parts of Poland, e.g., in the central agglomeration of Silesia (summer 2017, $NO_x$ approx. 30 μg/m$^3$) [39], in the Warsaw agglomeration (summer 2014, $NO_2$ = 18.5 μg/m$^3$, $NO_x$ = 22.5 μg/m$^3$, $SO_2$ = 4 μg/m$^3$, $O_3$ = 62.2 μg/m$^3$) [40], and two cities in northern Poland (Tczew and Sopot) (warm season 2014; $NO_2$ = 10.3 μg/m$^3$ (Tczew) and 10.0 μg/m$^3$ (Sopot); $SO_2$ = 3.9 μg/m$^3$ (Tczew) and 3.6 μg/m$^3$ (Sopot); CO = 225 μg/m$^3$ (Tczew) and 247 μg/m$^3$ (Sopot)) [41]. The growing intensity of photochemical reactions caused by UV in the sunny months, the utilization of petrol cars in summer, and the lack of the need to heat most of the buildings, could have resulted in low concentrations of gaseous pollutants at the receptor [42]. The concentrations of the considered gaseous pollutants were also below the limit values set out in European law [30].

It is important to study the relationship between the concentrations of the gaseous substances and $PM_{10}$, but this was not the subject of this study. Moreover, it would be necessary to collect data from a longer period. Herein, the studies on gaseous pollutants, as well as the knowledge of the average meteorological parameters during the research period, served to assess the aero-sanitary air conditions during the research period. These were typical for the summer period in Poland, and taking into account the air quality in other regions of southern Poland during the summer, they can be assessed as having been even better [40,43–45].

### *3.2. $PM_{10}$-Bound Elements*

The average concentrations of the selected $PM_{10}$-bound elements fluctuated within wide limits, and took values ranging from 0.5 ng/m$^3$ (As) to 1485.5 ng/m$^3$ (S). The masses of 15 $PM_{10}$-bound elements collectively accounted on average for 15% of the $PM_{10}$ mass. S, Si, and Al were the most abundant among the determining elements. Their average mass percentages in the total $PM_{10}$ mass were 7%, 4%, and 2%, respectively. On average, during the entire monthly measurement period, the elements related to the $PM_{10}$ tested in the study could be arranged in the following order: As < V <Ni < Pb < Cr < Mn < Cu < Ti < Zn < K < Fe < Ca < Al < Si < S (Table 1). Most of these elements had fairly even concentrations, both daily and hourly (Table 1; Figure 3). Slight increases in the concentrations of most of the elements were observed between 12.00 p.m. and 02.00 p.m., and between 06.00 p.m. and 08.00 p.m. (Figure 3), except for Si, Zn, Ti, As, and Pb, for which the concentration jumps were higher compared to the other elements. For Zn and Ti, almost twofold increases in concentration were recorded during the hours of 06.00–10.00 a.m. and 11.00 a.m.–01.00 p.m., respectively; for Si the increase was recorded between 06.00 p.m. and 08.00 p.m., and for As and Pb at 08.00 a.m. In general, the trace elements, including the toxic ones—such as As, V, Ni, Pb, Cr, and Mn—were present in very low concentrations, not exceeding 10 ng/m$^3$ (mean daily value); the average concentrations of As, Ni, and Pb in Kotórz Mały did not exceed the permissible values of annual concentrations recommended by the European Commission (6 ng/m$^3$, 20 ng/m$^3$, and 0.5 μg/m$^3$, respectively) [30]. The concentrations of the majority of tested $PM_{10}$-bound elements were much lower than those previously recorded in other regions of Poland (Table 2). The concentrations of $PM_{10}$-bound Si, K, Al, Ti, Fe, Ca, and Mn were determined by natural sources. This is indicated by the EF values which, regardless of the time of day, did not exceed 10 for the whole period of study (Table 3). Si, K, Al, Ti, Fe, and Ca are typical crustal elements, therefore it can be assumed that they were derived from the resuspension of crustal and

soil matter [22,24,25,46]. When analyzing the changes in EF values during the day, it should be noted that the EF values for Al, Fe, and Mn at 11.00 p.m.–08.00 a.m, and for Ti at 01.00 p.m, were higher than the EF values averaged over the entire measurement period. This may indicate the impact of an additional source of contamination in the considered hours. This will be explained in detail later in the manuscript using the PCA. The concentrations of the remaining $PM_{10}$-bound elements—i.e., S, Cu, Pb, Ni, Zn, As, and Cr—were strongly influenced by anthropogenic sources ($EF_x > 10$; Table 3). EF values for these elements changed during the day, with the highest values (higher than the average over the whole measurement period) recorded between 12.00 a.m and 11.00 a.m. This may indicate a strong impact of several anthropogenic sources during this time period, e.g., combustion of fuels by vehicles, abrasion of vehicle elements (wheels, brakes) and road surfaces, the influx of contaminated air masses from urbanized areas, and low-stack emissions [47–50]. An interesting case is that of V and As. The EFs for these elements indicate that at certain times of the day (V 07.00 p.m.–08.00 p.m.; As at 05.00 p.m.) their concentrations were strongly influenced by natural sources, and at others by anthropogenic sources. EFs greater than 10 for these elements in the rest of the day do not exclude the possibility that during these hours they also came from natural sources—e.g., soil resuspension—but that the impact of anthropogenic sources (such as road traffic or coal combustion) was more intensive [47,51,52].

**Table 2.** The mean concentrations of $PM_{10}$ and $PM_{10}$-bound elements at various sites in Poland.

| Sampling Site (City, Type) | Measurement Period | $PM_{10}$ ($\mu g/m^3$) | Concentration ($ng/m^3$) | | | | | | | | | | | |
|---|---|---|---|---|---|---|---|---|---|---|---|---|---|---|
| | | | As | Ca | Cr | Cu | Fe | K | Mn | Ni | Pb | Ti | V | Zn |
| Kotórz Mały, this study | Summer 2018 | 21 | 0.5 | 256.2 | 6.1 | 11.2 | 195.2 | 76.7 | 6.9 | 5.4 | 6.1 | 12.8 | 2.1 | 14.5 |
| Warsaw, urban area [53] | Summer 2017 | 40 | | 228.9 | 52.5 | 16.2 | 145.9 | | 21.4 | 10.8 | 17.2 | | | |
| Wadowice, urban area [54] | Winter 2017 | 174 | 11.0 | 590.0 | 4.0 | 27.0 | 760.0 | 1400.0 | 27.0 | 4.2 | 120.0 | 56.0 | 15.0 | 360.0 |
| Poznań, urban area [35] | Summer 2017 | 17 | | 2611.0 | | | | 48.0 | | | | | | |
| Wrocław, urban area [35] | Summer 2016 | 17 | | 1080.0 | | | | 300.0 | | | | | | |
| Poznań, urban area [55] | 2010–2016 | 17 | 1.0 | | | | | | | 1.2 | | | | |
| Upper Silesia, rural area [56] | Spring 2014 | 23 | 0.8 | | 239.4 | 2.5 | 217.3 | | 12.3 | 6.2 | 20.4 | | | 72.7 |
| Kraków, urban area [57] | Winter 2015 | 30–95 | | 580.0 | 10.1 | 23.6 | | 160.0 | 22.5 | 3.2 | 45.7 | 73.5 | 3.9 | 148.6 |

**Table 3.** The enrichment factors (EFs) for the $PM_{10}$-bound elements, averaged for each hour of the day and the measurement period.

| Period | Element | | | | | | | | | | | | | |
|---|---|---|---|---|---|---|---|---|---|---|---|---|---|---|
| | Al | As | Ca | Cr | Cu | Fe | K | Mn | Ni | Pb | S | Si | Ti | V | Zn |
| 0 | 2.1 | 0.0 | 3.3 | 97.3 | 406.8 | 3.1 | 1.3 | 6.2 | 150.3 | 164.2 | 849.0 | 1.0 | 1.3 | 21.6 | 146.3 |
| n1 | 2.3 | 0.0 | 3.4 | 108.2 | 437.1 | 3.2 | 1.5 | 6.7 | 182.4 | 181.3 | 969.3 | 1.0 | 1.1 | 24.1 | 165.6 |
| 2 | 2.3 | 24.2 | 3.9 | 114.5 | 454.3 | 3.1 | 1.4 | 6.8 | 179.2 | 176.1 | 976.8 | 1.0 | 1.2 | 25.6 | 167.3 |
| 3 | 2.3 | 0.0 | 3.6 | 119.1 | 515.5 | 3.3 | 1.4 | 7.5 | 189.4 | 203.7 | 1057.8 | 1.0 | 1.1 | 26.4 | 179.2 |
| 4 | 2.2 | 64.2 | 3.7 | 116.8 | 454.3 | 3.2 | 1.4 | 6.6 | 174.2 | 217.7 | 985.9 | 1.0 | 1.1 | 26.0 | 161.2 |
| 5 | 2.4 | 92.0 | 3.7 | 127.1 | 526.0 | 3.4 | 1.4 | 7.1 | 210.9 | 278.5 | 1128.0 | 1.0 | 1.0 | 28.6 | 185.1 |
| 6 | 2.3 | 195.7 | 3.8 | 120.2 | 500.3 | 3.4 | 1.4 | 7.2 | 174.0 | 258.4 | 1029.0 | 1.0 | 1.4 | 26.8 | 183.5 |
| 7 | 2.2 | 655.8 | 3.7 | 97.0 | 474.9 | 3.3 | 1.4 | 6.4 | 155.0 | 337.2 | 889.0 | 1.0 | 1.5 | 21.4 | 201.2 |
| 8 | 2.2 | 855.5 | 4.2 | 86.3 | 403.1 | 3.1 | 1.5 | 6.2 | 134.6 | 376.5 | 821.5 | 1.0 | 1.6 | 19.1 | 216.8 |
| 9 | 2.0 | 382.2 | 3.6 | 73.7 | 406.2 | 2.7 | 1.2 | 5.3 | 115.4 | 292.6 | 699.0 | 1.0 | 1.6 | 16.4 | 187.0 |

**Table 3.** *Cont.*

| Period | Element | | | | | | | | | | | | | | |
|---|---|---|---|---|---|---|---|---|---|---|---|---|---|---|---|
| | **Al** | **As** | **Ca** | **Cr** | **Cu** | **Fe** | **K** | **Mn** | **Ni** | **Pb** | **S** | **Si** | **Ti** | **V** | **Zn** |
| 10 | 1.8 | 179.0 | 3.6 | 65.9 | 299.1 | 2.7 | 1.1 | 5.4 | 148.9 | 221.3 | 590.0 | 1.0 | 1.6 | 14.7 | 175.6 |
| 11 | 2.0 | 46.3 | 3.7 | 71.7 | 318.6 | 2.6 | 1.2 | 5.6 | 116.5 | 166.7 | 646.1 | 1.0 | 1.8 | 16.0 | 112.8 |
| 12 | 1.8 | 26.9 | 3.7 | 54.4 | 248.6 | 2.4 | 1.1 | 5.1 | 86.3 | 114.0 | 465.7 | 1.0 | 1.8 | 12.2 | 86.5 |
| 13 | 1.8 | 24.6 | 4.0 | 61.7 | 326.5 | 2.4 | 1.1 | 5.4 | 92.0 | 85.9 | 545.7 | 1.0 | 3.3 | 13.6 | 97.8 |
| 14 | 1.8 | 17.8 | 3.6 | 59.2 | 253.5 | 2.3 | 1.0 | 5.0 | 109.6 | 85.3 | 534.2 | 1.0 | 1.9 | 13.2 | 78.5 |
| 15 | 1.8 | 0.0 | 3.5 | 60.0 | 272.3 | 2.4 | 1.0 | 4.9 | 93.5 | 93.7 | 550.3 | 1.0 | 2.1 | 13.3 | 74.8 |
| 16 | 1.9 | 11.7 | 3.4 | 67.5 | 284.3 | 2.5 | 1.1 | 5.5 | 123.3 | 100.2 | 603.2 | 1.0 | 1.9 | 14.9 | 84.8 |
| 17 | 1.8 | 3.3 | 3.4 | 60.7 | 286.4 | 2.4 | 1.0 | 5.0 | 99.4 | 104.7 | 539.3 | 1.0 | 2.3 | 13.7 | 78.3 |
| 18 | 1.6 | 67.6 | 3.3 | 52.7 | 268.7 | 2.2 | 0.9 | 4.5 | 116.2 | 65.3 | 480.5 | 1.0 | 1.7 | 11.8 | 71.0 |
| 19 | 1.3 | 16.5 | 2.8 | 37.7 | 165.8 | 1.5 | 0.7 | 3.2 | 56.6 | 45.2 | 335.9 | 1.0 | 1.1 | 8.3 | 48.1 |
| 20 | 1.2 | 0.0 | 2.7 | 37.8 | 166.6 | 1.5 | 0.6 | 3.0 | 60.5 | 53.9 | 334.2 | 1.0 | 1.1 | 8.4 | 51.0 |
| 21 | 1.5 | 79.7 | 3.0 | 50.9 | 216.7 | 2.2 | 0.7 | 4.1 | 72.6 | 79.9 | 448.1 | 1.0 | 1.2 | 11.4 | 66.9 |
| 22 | 1.8 | 91.1 | 3.1 | 63.3 | 263.2 | 2.7 | 0.9 | 5.6 | 95.5 | 107.3 | 558.3 | 1.0 | 1.4 | 14.1 | 86.3 |
| 23 | 2.0 | 50.6 | 3.5 | 85.8 | 359.7 | 3.1 | 1.2 | 6.0 | 140.6 | 131.5 | 738.2 | 1.0 | 1.4 | 19.3 | 120.7 |
| 3–31.07 (average) | 1.8 | 98.5 | 3.4 | 68.7 | 308.6 | 2.5 | 1.1 | 5.2 | 114.4 | 141.4 | 614.1 | 1.0 | 1.6 | 15.6 | 109.9 |

### *3.3. Source Apportionment of $PM_{10}$*

Principal component analysis (PCA) was employed in order to assess the correlations between different $PM_{10}$-bound elements, and to identify the main sources of $PM_{10}$ in Kotórz Mały. Fifteen variables (Al, As, Ca, Cr, Cu, Fe, K, Mn, Ni, Pb, S, Si, Ti, V, and Zn) were included in this analysis. This analysis was divided into individual hours of the day due to the different hourly trends observed in these constituents (Figure 5).

As a result of the PCA, five principal components (PC1–PC5) were identified with eigenvalues higher than 1.0 (according to the Kaiser criterion). Together they explain on average 97.4% of the cumulative variance in the dataset (Figure 5). The most important is the first principal component, which explains on average 42.7% of the variability; the second component explains 17.6% of the variability; the third 13.3%; the fourth 12.7%; and the fifth 11.1%. It should be noted that the above variances are not the same as the percentage source contributions to the $PM_{10}$ concentrations at the sampling site. An additional analysis—i.e., principal component analysis (PCA), combined with multi-linear regression analysis (MLRA)—should be performed in order to determine the above contributions. In the case under study, the application of these analyses was difficult, because at certain times of the day the concentrations of $PM_{10}$ were simultaneously influenced by several sources. However, to make the interpretation of the PCA results easier, the enrichment factors (EFs) for the $PM_{10}$-bound elements (Table 3), the division of the studied element concentrations according to wind direction (Figure 4), and conclusions drawn by the authors of previous studies [24,29,58] were all taken into account.

Fourteen elements—i.e., V, Cr, Mn, Ni, Cu, Zn, As, Pb, Al, Si, K, Ca, Fe, and Ti—were strongly correlated (factor loadings $\geq$ 0.7) with PC1. The vast majority of these elements (Al, Ca, K, Mn, Fe, Si, and Ti) were of natural origin (EFs < 10, Table 3), and their highest concentrations were observed when there was an inflow of air masses from the north–northeast and the northeast (Figure 4). Crops, forest, and a lake are located in these directions at distances of 0.2 km, 1.3 km, and 2.9 km, respectively. The above premises and the conclusions of other researchers [19,38,59–61] indicate that the Al, Ca, K, Mn, Fe, Si, and Ti came from the resuspension of soil and the mechanical abrasion processes of crustal materials. Moreover, following the work of Gustafsson et al. [62] and Li et al. [63], it can be concluded that Al, Si, and K could also have been derived from the abrasion of the pavement. Research [22,64–67] shows that the remaining elements correlated with PC1—i.e., V, Cr, Ni, Cu, Zn, As, and Pb—were likely traffic-related pollutants deposited in soils, whose particles have been entrained by wind or field work. Therefore, it can be assumed that the $PM_{10}$ identified in PC1 came from mineral matter. As shown by the hourly

correlations of these elements with PC1, this source affected $PM_{10}$ concentrations in the receptor throughout the day, with the more intensive interactions occurring at 12.00 a.m., 03.00 p.m., and 05.00 p.m.–06.00 p.m.

PC1

| H | V | Cr | Mn | Ni | Cu | Zn | As | Pb | Al | Si | S | K | Ca | Fe | Ti | Eigenvalue | Variance % |
|---|---|---|---|---|---|---|---|---|---|---|---|---|---|---|---|---|---|
| 0 | | | 0.92 | | | | | | 0.94 | 0.98 | | | 0.94 | 0.93 | 0.85 | 6.2 | 44.2 |
| 1 | | | 0.85 | | | | | | 0.94 | 0.97 | | | 0.92 | 0.91 | 0.9 | 5.9 | 42 |
| 2 | | | 0.79 | | | | 0.76 | | 0.86 | 0.93 | | | 0.95 | 0.9 | 0.89 | 6 | 40.2 |
| 3 | | | 0.7 | | | | | | 0.9 | 0.97 | | | 0.92 | 0.92 | 0.86 | 5.4 | 38.5 |
| 4 | | | 0.86 | | | | | | 0.84 | 0.95 | | | 0.83 | 0.95 | 0.87 | 5.5 | 36.5 |
| 5 | | | 0.72 | | | | | | 0.95 | 0.93 | | 0.76 | 083 | 0.91 | 0.81 | 5.6 | 37.2 |
| 6 | | | 0.78 | | | | | | 0.92 | 0.93 | | 0.82 | 0.85 | 0.91 | 0.82 | 6.1 | 40.3 |
| 7 | | | 0.73 | | | | | | 0.87 | 0.87 | | 0.84 | 0.86 | 0.82 | 0.91 | 5.9 | 39.3 |
| 8 | | | 0.84 | | | | | | 0.92 | 0.95 | | 0.81 | 0.81 | 0.88 | 0.9 | 6.3 | 42.3 |
| 9 | | | 0.83 | 0.75 | | | | | 0.94 | 0.95 | | 0.82 | 0.83 | 0.76 | 0.91 | 6.1 | 40.6 |
| 10 | | | 0.75 | | | | | | 0.91 | 0.81 | | 0.76 | 0.87 | | 0.88 | 5.2 | 34.3 |
| 11 | | | 0.9 | | 0.72 | | | | 0.87 | 0.92 | | 0.85 | 0.89 | 0.93 | 0.94 | 6.8 | 45.5 |
| 12 | 0.77 | 0.76 | 0.98 | | 0.89 | | | | 0.97 | 0.99 | | 0.96 | 0.98 | 0.98 | 0.97 | 9.4 | 63 |
| 13 | 0.71 | | 0.73 | | 0.92 | 0,83 | 0,95 | 0,92 | | | | | 0.79 | | 0.92 | 6.8 | 45.2 |
| 14 | | | 0.87 | | | | | | 0.97 | 0.97 | | 0.93 | 0.96 | 0.97 | 0.95 | 7.4 | 49.4 |
| 15 | | | 0.93 | | 0.91 | | | | 0.92 | 0.97 | | 0.9 | 0.94 | 0.96 | 0.83 | 7.5 | 53.6 |
| 16 | | | 0.91 | | 0.75 | | | | 0.92 | 0.99 | | 0.88 | 0.97 | 0.98 | 0.93 | 6.9 | 46.2 |
| 17 | | | 0.87 | 0.86 | 0.91 | | | | 0.82 | 0.91 | | 0.77 | 0.94 | 0.92 | 0.92 | 8.2 | 54.5 |
| 18 | | | 0.94 | | | | | | 0.98 | 0.93 | | 0.92 | 0.93 | 0.93 | 0.9 | 7.5 | 50.2 |
| 19 | | | 0.84 | 0.71 | 0.83 | | | | 0.92 | 0.87 | | 0.83 | 0.91 | 0.91 | 0.89 | 6.9 | 45.9 |
| 20 | | | 0.77 | | 0.84 | | | | 0.95 | 0.91 | | 0.95 | 0.95 | 0.91 | 0.89 | 6.7 | 48.1 |
| 21 | | | 0.71 | | 0.76 | | | | 0.91 | 0.95 | | 0.91 | 0.98 | 0.76 | 0.88 | 6.6 | 44.1 |
| 22 | | | 0.94 | | | | | | 0.94 | 0.97 | | 0.87 | 0.92 | 0.95 | 0.93 | 7 | 46.7 |
| 23 | | | 0.89 | | | | | | 0.94 | 0.96 | | 0.75 | 0.95 | 0.93 | 0.84 | 6.1 | 40.8 |

**Figure 5.** *Cont.*

PC2

| H | V | Cr | Mn | Ni | Cu | Zn | As | Pb | Al | Si | S | K | Ca | Fe | Ti | Eigenvalue | Variance % |
|---|---|---|---|---|---|---|---|---|---|---|---|---|---|---|---|---|---|
| 0 | 0.95 | 0.97 | | | | | | | | | | | | | | 2.4 | 17.2 |
| 1 | 0.96 | 0.97 | | | | | | | | | | | | | | 2.3 | 16.4 |
| 2 | 0.95 | 0.95 | | | | | | | | | | | | | | 2.7 | 17.7 |
| 3 | 0.96 | 0.97 | | | | | | | | | | | | | | 2.6 | 18,5 |
| 4 | | | | | 0.76 | | 0.81 | 0.9 | | | | | | | | 2.4 | 16 |
| 5 | 0.96 | 0.95 | | | | | | | | | | | | | | 2.4 | 16.1 |
| 6 | | | | | | | 0.85 | 0.95 | | | | | | | | 2.2 | 14.7 |
| 7 | | | | | 0.81 | | 0.82 | 0.95 | | | | | | | | 2.5 | 16.9 |
| 8 | | | | | | | 0.9 | 0.93 | | | | | | | | 2.3 | 15.1 |
| 9 | | | | | | 0.8 | 0.89 | 0.92 | | | | | | | | 2.7 | 18.1 |
| 10 | | | | 0.79 | 0.73 | 0.93 | 0.87 | 0.94 | | | | | | 0.71 | | 4.6 | 30.9 |
| 11 | | | | | | | 0.93 | 0.96 | | | | | | | | 2.1 | 14.1 |
| 12 | | | | | | | 0.92 | 0.72 | | | | | | | | 2.1 | 14 |
| 13 | | | | | | | | | 0.91 | 0.9 | | 0.91 | | 0.89 | | 5.2 | 34.5 |
| 14 | 0.73 | 0.74 | | | | | 0.93 | 0.91 | | | | | | | | 3.6 | 23.7 |
| 15 | 0.97 | 0.94 | | | | | | | | | | | | | | 2.2 | 15.6 |
| 16 | 0.92 | 0.93 | | | | | | | | | | | | | | 2.6 | 17.2 |
| 17 | | | | | | 0.78 | | | | | | | | | | 1.9 | 12.7 |
| 18 | | | | | | | 0.88 | 0.96 | | | | | | | | 2 | 13.2 |
| 19 | | | | | | 0.9 | | 0.84 | | | 0.71 | | | | | 2.1 | 14.2 |
| 20 | | | | | | 0,93 | 0,94 | | | | 0,72 | | | | | 2.4 | 17.1 |
| 21 | | | | | | 0,72 | 0,70 | 0,94 | | | | | | | | 2.8 | 18.9 |
| 22 | 0.94 | 0.93 | | | | | | | | | | | | | | 2.3 | 15.4 |
| 23 | 0.96 | 0.96 | | | | | | | | | | | | | | 2.2 | 14.5 |

**Figure 5.** *Cont.*

PC3

| H | V | Cr | Mn | Ni | Cu | Zn | As | Pb | Al | Si | S | K | Ca | Fe | Ti | Eigenvalue | Variance % |
|---|---|---|---|---|---|---|---|---|---|---|---|---|---|---|---|---|---|
| 0 | | | | | | 0.83 | | 0.77 | | | | | | | | 1.9 | 13.6 |
| 1 | | | | | | 0.87 | | | | | | | | | | 1.8 | 13.1 |
| 2 | | | | | | 0.81 | | | | | | | | | | 1.7 | 11.1 |
| 3 | | | | | | 0.84 | | 0.87 | | | | | | | | 2 | 14.5 |
| 4 | 0.97 | 0.97 | | | | | | | | | | | | | | 2.4 | 15.9 |
| 5 | | | | | | | | 0.88 | | | | | | | | 2.2 | 14.7 |
| 6 | 0.95 | 0.95 | | | | | | | | | | | | | | 2.2 | 14.8 |
| 7 | 0.9 | 0.91 | | | | | | | | | | | | | | 2.5 | 16.7 |
| 8 | 0.96 | 0.97 | | | | | | | | | | | | | | 2.2 | 14.7 |
| 9 | 0.86 | 0.89 | | | | | | | | | | | | | | 2.5 | 16.4 |
| 10 | | | | | | | | | | | 0.96 | | | | | 1.3 | 8.5 |
| 11 | | | | | | | | | | | 0.85 | | | | | 1.7 | 11.3 |
| 12 | | | | | | 0.74 | | | | | 0.87 | | | | | 1.4 | 9.5 |
| 13 | | | | | | | | | | | 0.91 | | | | | 1.3 | 8.9 |
| 14 | | | | | | 0.79 | | | | | 0.9 | | | | | 2 | 13.2 |
| 15 | | | | | | 0.74 | | | | | 0.82 | | | | | 1.5 | 10.9 |
| 16 | | | | | | 0.8 | | | | | | | | | | 2 | 13.2 |
| 17 | | | | | | | 0.76 | | | | | | | | | 2.1 | 13.7 |
| 18 | 0.71 | | | | | | | | | | 0.75 | | | | | 1.8 | 11.8 |
| 19 | 0.93 | 0.91 | | | | | | | | | | | | | | 2.3 | 15.3 |
| 20 | 0.92 | 0.93 | | | | | | | | | | | | | | 2.2 | 15.4 |
| 21 | 0.9 | 0.91 | | | | | | | | | | | | | | 3 | 19.9 |
| 22 | | | | | | | 0.95 | 0.75 | | | | | | | | 1.7 | 11 |
| 23 | | | | | | | 0.95 | 0.85 | | | | | | | | 1.7 | 11.3 |

**Figure 5.** *Cont.*

PC4

| H | V | Cr | Mn | Ni | Cu | Zn | As | Pb | Al | Si | S | K | Ca | Fe | Ti | Eigenvalue | Variance % |
|---|---|---|---|---|---|---|---|---|---|---|---|---|---|---|---|---|---|
| 0 | | | | 0.82 | | | | | | | | | | | | 1.6 | 11.4 |
| 1 | | | | 0.83 | | | | | | | | | | | | 1.5 | 10.4 |
| 2 | | | | 0.74 | | | | | | | | | | | | 1.7 | 11.2 |
| 3 | | | | | | | | | | | 0.91 | | | | | 1.4 | 10.3 |
| 4 | | | | | | | | | | | 0.89 | | | | | 1.7 | 11.6 |
| 5 | | | | 0.79 | | | | | | | | | | | | 1.4 | 9.1 |
| 6 | | | | | | | | | | | 0.72 | | | | | 1.3 | 9 |
| 7 | | | | | | | | | | | 0.87 | | | | | 1.2 | 8 |
| 8 | | | | | | 0.83 | | | | | 0.72 | | | | | 1.5 | 10.2 |
| 9 | | | | | | | | | | | 0.88 | | | | | 1.5 | 9.8 |
| 10 | 0.87 | 0.88 | | | | | | | | | | | | | | 2.2 | 14.7 |
| 11 | 0.78 | 0.76 | | 0.78 | | | | | | | | | | | | 2.2 | 14.9 |
| 15 | | | | 0.88 | | | | | | | | | | | | 1.2 | 8.3 |
| 18 | | | | 0.76 | 0.71 | 0.74 | | | | | | | | | | 2.1 | 13.9 |
| 19 | | | | | | | 0.86 | | | | | | | | | 1.3 | 8.7 |
| 22 | | | | | | 0.88 | | | | | 0.74 | | | | | 2.2 | 14.5 |
| 23 | | | | 0.93 | 0.83 | | | | | | | | | | | 2 | 13.2 |

PC5

| H | V | Cr | Mn | Ni | Cu | Zn | As | Pb | Al | Si | S | K | Ca | Fe | Ti | Eigenvalue | Variance% |
|---|---|---|---|---|---|---|---|---|---|---|---|---|---|---|---|---|---|
| 23 | | | | | | 0.89 | | | | | 0.77 | | | | | 1.9 | 12.7 |

**Figure 5.** A summary of the results of the principal component analysis (PCA) performed on hourly data on the elemental composition of $PM_{10}$. For each hour, 29 data were used, and the tables summarized only those elements that were always correlated with the variables PC1–PC5 (correlation coefficient $r > 0.7$).

Elements such as V, Cr, Ni, Cu, Zn, As, Pb, Al, Si, S, K, and Fe were strongly correlated with PC2. The concentrations of Cr and V during the day were at a relatively constant level (Figure 3), and their slight increases were observed with the inflow of air from the north–northwest, southwest, west–southwest, and east (Figure 4). The highest mean concentrations of Pb were observed when there was an inflow of air masses from the southeast, south, southwest, and south–southeast; Zn from the southwest, south, and east–southeast; As from the west–northwest; Cu from the west; and Ni from the east–southeast (Figure 4). Within 3 km to the north–northwest, southwest, and west–southwest is National Road No. 45, and within 6 km to the south, south–southeast, and southeast is National Road No. 46; the Opole agglomeration is located to the southwest and west–southwest (10 km to the northern border of the city, 15 km to the center). Taking into account that the group of Pb, Cu, Zn, Cr, and Ni is mostly representative of vehicle exhausts and road dust [46,68–70], Cu and Zn are characteristic markers of brake lining wear, and Zn of tire wear [19,71], and that zinc compounds are also used as antioxidants and detergents to improve the quality of automotive grease, it can be assumed that the $PM_{10}$ identified in PC2 originates from traffic emissions. This source had the most intense influence on the concentrations of $PM_{10}$ at the receptor at 12.00 a.m., 03.00 p.m., and 05.00 p.m.–06.00 p.m. These are the times of the day when traffic is usually the heaviest, due to the movement

of city inhabitants to work, schools, kindergartens, etc. During these hours, PC2 explains most—approx. 30%—of the variance in $PM_{10}$ emissions.

Six elements were strongly correlated with PC3, i.e., S, V, Cr, Zn, As, and Pb (Figure 5). S is a characteristic PM component in areas where coal and fine coal are used for energy purposes [25,63]. It is also a characteristic element released during biomass, waste, and garbage burning in small-scale installations, i.e., domestic stoves and local boiler houses [25,72,73]. Moreover, the source of S may be secondary inorganic aerosols (sulphates), also released from the above-mentioned sources [74]. Zn and Pb associated with coarse dust, apart from traffic emissions, may come from biomass burning [25,60]. According to the research described in [64,75], another source of Cr and V is fossil fuel and fuel oil combustion. The highest concentrations of S were recorded between 10.00 a.m. and 06.00 p.m., with air inflow from the northeast and north–northeast (Figure 4). Zn and Pb concentrations between 10.00 p.m. and 03.00 a.m.—i.e., in the hours when these elements showed a strong correlation with PC3—also corresponded to the inflow of air masses from the northeast (Figure 4), where the neighboring village Turawa (about 1000 inhibitants) is located approximately 2.5 km from the receptor. Furthermore, the village of Kotórz Mały is divided into two zones: northern and southern. The northern part of the village is characterized by rural development, which predominantly uses obsolete individual heating systems (IHS), while the southern part is characterized by modern construction [26]. Fuel for IHS is mainly hard coal, in a proportion of share equal to 81%. All IHS are used during the cold season (from October until April). In the summer, local people use IHS for hot water supply and for preparing food. During the measurement campaign, in the neighborhood of the sampling point, 74 out of 85 individual point emitters (IPEs) were active (Figure 1). The activity of emission sources was indicated on the basis of the individual responses of IHS owners and the authors' own observations. The emission of pollutants was periodical, and depended on the needs of users. The average daily time of IPE activity was 3 h. It can be noted that, even in the summer, a great number of old stoves are used, and almost 70% of the heating systems use fossil fuels. Of course, the quantity of burned fuel, and its relatively short daily time of use, were not hugely significant, but did influence the local air quality. The above observations allow us to conclude that the $PM_{10}$ identified in PC3 came from low-stack emissions from sources located to the northeast of the receptor, and that these sources explain the largest amount of variation in the early morning hours (04.00 a.m.–07.00 a.m.). The effect of municipal emissions, which can be represented by PC3, in Kotórz Mały during this period was not large compared to the impact of natural sources (soil/mineral matter) and road traffic (exhaust and non-exhaust emission). This is to be expected, as the research was carried out in the summer period, when there is no strong low-stack emissions impact related to home heating [26]. Nevertheless, due to the strong correlation of PC3 with the characteristic elements, it can be noted that in households in suburban areas these types of emissions are still important, even during the summer period. Taking into account the variability of the importance of PC3 during the day, it can be suggested that it is also associated with the burning of various types of biomass waste and other organic materials and their derivatives, either when cleaning gardens and fields or during recreation activities (grilling, bonfires, etc.) [76–79].

PC4 explains a smaller amount of variance (12.7%) compared to PC1; its variances ranged from 8.0% (at 07.00 a.m.) to 14.9% (at 11.00 a.m.). PC4 was the most strongly correlated with V, Cr, Ni, Cu, Zn, As, and S. Concentrations recorded in hours corresponding to the correlations of individual elements with PC4 indicate the inflow of air masses mainly from the southeast, south–southeast, southwest, and west–southwest. Local sources, such as smaller economic activities, could also contribute to PC4—e.g., services in the field of vehicle mechanics (3 services) and metal surface varnishing (2 services) are located more than 1 km from the receptor. In addition, 12 km in a straight line from the receptor towards the southwest there is an open-cast mine of carbonate rocks called the Odra Quarry, while the Mala Panew ironworks in Ozimek is located 13.5 km in a straight line towards the

southeast. These observations allow us to assume that PC4 reflects the industrial sources of the $PM_{10}$ at the receptor. Additionally, this is supported by the strong correlations of PC4 with Ni—which is a component of metal products [80,81]—and with As, Cu, V, and Cr, which are related to the production of ceramics, cement, and metal smelting [81–83].

The last extracted principal component is PC5. Only two elements (Zn and S) were strongly correlated with PC5. The source identified in PC5 explains approx. 13% of the variance in $PM_{10}$ emissions, and only at 11.00 p.m. At that time, the mean Zn and S concentrations were 12.5 ng/m$^3$ and 1400 ng/m$^3$, respectively. Such values of these two elements were recorded when there was an air inflow from the northwest. In the northern part of the village, as described above, there are mainly low-rise coal and biomass-heated buildings. In addition, in the same direction, at a distance of 2.3 km, lies the neighboring village of Węgry, with about 1000 inhabitants, also characterized by rural development. This allows us to assume that the $PM_{10}$ identified in PC5 probably originated from fossil fuel and/or biomass combustion in local households [73]. Most probably, the hourly variability of the concentrations of the examined elements, for Zn and S as opposed to the other elements correlated with PC3, resulted in the isolation of an additional component of PC5. This component, however, similarly to PC3, is undoubtedly related to municipal emissions.

## 4. Conclusions

Regardless of the fact that in this study we used data from the summer period, it was shown that at a receptor in a typical rural area in the southern part of Poland, the impact of carbon emissions on the elemental composition of $PM_{10}$ can be noticed almost every hour of the day. During the measurement period, especially at night and in the early morning hours, an evident influence of municipal emissions on the elemental composition of $PM_{10}$ was observed. However, natural emissions (soil, sand) and exhaust and non-exhaust emissions from vehicle traffic had a stronger and more dominant influence on the elemental composition of $PM_{10}$ during the research period. It is highly probable that if the analysis of the origins of $PM_{10}$ during this measurement period was carried out on the basis of daily data on the elemental composition of the $PM_{10}$, as is usually the case, the influence of other sources would not be noticed. Thus, it has been shown that using hourly concentrations of selected elements, it is possible to assess the origins of $PM_{10}$ dust and the variability of the share of selected sources in shaping $PM_{10}$ concentrations over the course of a day, even with the use of data from a relatively short measurement period.

As shown by the conducted PCA, the number of variances explained by particular main components varies by the hour, which suggests the variability of the impact of various sources of emissions during the day. Furthermore, the conducted research and observations allow us to conclude that the PCs are characterized by $PM_{10}$ sources whose efficiency changed with not only the wind's direction but also its speed, which determines the distances to which pollutants are transferred.

**Supplementary Materials:** The following are available online at https://www.mdpi.com/article/10.3390/en14092654/s1, Figure S1: An example of a filter for measurements, Figures S2 and S3: Measuring equipment PX-375 Horiba, Figure S4: Sampling site in Kotórz Mały, Figure S5: The examples of obtained results. The concentrations of individual elements and $PM_{10}$.

**Author Contributions:** Conceptualization, W.R.-K. and T.M.; methodology, G.M., P.R.-K., K.B.; validation, T.M., P.R.-K. and G.M.; formal analysis, G.M.; investigation, T.M.; resources, K.B.; writing—original draft preparation, W.R.-K. and K.B.; writing—review and editing, J.R.; supervision, J.R., W.R.-K. All authors have read and agreed to the published version of the manuscript.

**Funding:** This research was carried out as a part of the "Implementation doctorate-edition II Faculty W-7 (03DW/0001/18)" project, financed by the National Centre for Research and Development. The funders had no role in the design of the study, in the collection, analyses, or interpretation of data; in the writing of the manuscript, or in the decision to publish the results.

**Institutional Review Board Statement:** Not applicable.

**Informed Consent Statement:** Not applicable.

**Data Availability Statement:** The data presented in this study are available on request from the corresponding author.

**Acknowledgments:** The authors acknowledge the companies HORIBA and MLU-recordum Environmental Monitoring Solutions GmbH for supplying the measurement equipment (PX-375 Horiba, Japan). We also acknowledge Tomasz Olszowski for valuable comments on the manuscript and study arrangements.

**Conflicts of Interest:** The authors declare no conflict of interest.

## References

1. Pant, P.; Harrison, R.M. Critical review of receptor modelling for particulate matter: A case study of India. *Atmos. Environ.* **2012**, *49*, 1–12. [CrossRef]
2. Belis, C.; Karagulian, F.; Larsen, B.; Hopke, P. Critical review and meta-analysis of ambient particulate matter source apportionment using receptor models in Europe. *Atmos. Environ.* **2013**, *69*, 94–108. [CrossRef]
3. Viana, M.; Kuhlbusch, T.; Querol, X.; Alastuey, A.; Harrison, R.; Hopke, P.; Winiwarter, W.; Vallius, M.; Szidat, S.; Prévôt, A.; et al. Source apportionment of particulate matter in Europe: A review of methods and results. *J. Aerosol Sci.* **2008**, *39*, 827–849. [CrossRef]
4. Hopke, P.K. *Receptor Modeling for Air Quality Management*; Elsevier: Amsterdam, The Netherlands, 1991. [CrossRef]
5. Hopke, P.K. Review of receptor modeling methods for source apportionment. *J. Air Waste Manag. Assoc.* **2016**, *66*, 237–259. [CrossRef] [PubMed]
6. Thorpe, A.; Harrison, R.M. Sources and properties of non-exhaust particulate matter from road traffic: A review. *Sci. Total. Environ.* **2008**, *400*, 270–282. [CrossRef]
7. Pernigotti, D.; Belis, C.A.; Spanò, L. SPECIEUROPE: The European data base for PM source profiles. *Atmos. Pollut. Res.* **2016**, *7*, 307–314. [CrossRef]
8. Zhu, Y.; Huang, L.; Li, J.; Ying, Q.; Zhang, H.; Liu, X.; Liao, H.; Li, N.; Liu, Z.; Mao, Y.; et al. Sources of particulate matter in China: Insights from source apportionment studies published in 1987–2017. *Environ. Int.* **2018**, *115*, 343–357. [CrossRef]
9. Bi, X.; Dai, Q.; Wu, J.; Zhang, Q.; Zhang, W.; Luo, R.; Cheng, Y.; Zhang, J.; Wang, L.; Yu, Z.; et al. Characteristics of the main primary source profiles of particulate matter across China from 1987 to 2017. *Atmos. Chem. Phys. Discuss.* **2019**, *19*, 3223–3243. [CrossRef]
10. Ervens, B.; Turpin, B.J.; Weber, R.J. Secondary organic aerosol formation in cloud droplets and aqueous particles (aqSOA): A review of laboratory, field and model studies. *Atmos. Chem. Phys.* **2011**, *11*, 11069–11102. [CrossRef]
11. Zhang, Y.; Seigneur, C.; Seinfeld, J.H.; Jacobson, M.; Clegg, S.L.; Binkowski, F.S. A comparative review of inorganic aerosol thermodynamic equilibrium modules: Similarities, differences, and their likely causes. *Atmos. Environ.* **2000**, *34*, 117–137. [CrossRef]
12. Hallquist, M.; Wenger, J.C.; Baltensperger, U.; Rudich, Y.; Simpson, D.; Claeys, M.; Dommen, J.; Donahue, N.M.; George, C.; Goldstein, A.H.; et al. The formation, properties and impact of secondary organic aerosol: Current and emerging issues. *Atmos. Chem. Phys.* **2009**, *9*, 5155–5236. [CrossRef]
13. Schaap, M.; Van Loon, M.; Brink, H.M.T.; Dentener, F.J.; Builtjes, P.J.H. Secondary inorganic aerosol simulations for Europe with special attention to nitrate. *Atmos. Chem. Phys. Discuss.* **2004**, *4*, 857–874. [CrossRef]
14. Liang, S.Y.; Cui, J.L.; Bi, X.Y.; Luo, X.S.; Li, X. Deciphering source contributions of trace metal contamination in urban soil, road dust, and foliar dust of Guangzhou, southern China. *Sci. Total Environ.* **2019**, *695*, 133596. [CrossRef]
15. Pachon, J.E.; Weber, R.J.; Zhang, X.; Mulholland, J.A.; Russell, A.G. Revising the use of potassium (K) in the source apportionment of PM2.5. *Atmos. Pollut. Res.* **2013**, *4*, 14–21. [CrossRef]
16. Chow, J.C.; Lowenthal, D.H.; Chen, L.-W.A.; Wang, X.; Watson, J.G. Mass reconstruction methods for PM2.5: A review. *Air Qual. Atmos. Health* **2015**, *8*, 243–263. [CrossRef] [PubMed]
17. Richter, P.; Griño, P.; Ahumada, I.; Giordano, A. Total element concentration and chemical fractionation in airborne particulate matter from Santiago, Chile. *Atmos. Environ.* **2007**, *41*, 6729–6738. [CrossRef]
18. Lammel, G.; Röhrl, A.; Schreiber, H. Atmospheric lead and bromine in Germany. *Environ. Sci. Pollut. Res.* **2002**, *9*, 397–404. [CrossRef] [PubMed]
19. Pant, P.; Harrison, R.M. Estimation of the contribution of road traffic emissions to particulate matter concentrations from field measurements: A review. *Atmos. Environ.* **2013**, *77*, 78–97. [CrossRef]
20. Pervez, S.; Bano, S.; Watson, J.G.; Chow, J.C.; Matawle, J.L.; Shrivastava, A.; Tiwari, S.; Pervez, Y.F. Source Profiles for PM10-2.5 Resuspended Dust and Vehicle Exhaust Emissions in Central India. *Aerosol Air Qual. Res.* **2018**, *18*, 1660–1672. [CrossRef]
21. Pokorná, P.; Hovorka, J.; Hopke, P.K. Elemental composition and source identification of very fine aerosol particles in a European air pollution hot-spot. *Atmos. Pollut. Res.* **2016**, *7*, 671–679. [CrossRef]

22. Rogula-Kozłowska, W.; Błaszczak, B.; Szopa, S.; Klejnowski, K.; Sówka, I.; Zwoździak, A.; Jabłońska, M.; Mathews, B. PM2.5 in the central part of Upper Silesia, Poland: Concentrations, elemental composition, and mobility of components. *Environ. Monit. Assess.* **2012**, *185*, 581–601. [CrossRef] [PubMed]
23. Rogula-Kozłowska, W.; Majewski, G.; Czechowski, P.O. The size distribution and origin of elements bound to ambient particles: A case study of a Polish urban area. *Environ. Monit. Assess.* **2015**, *187*, 240. [CrossRef] [PubMed]
24. Rogula-Kozłowska, W.; Majewski, G.; Błaszczak, B.; Klejnowski, K.; Rogula-Kopiec, P. Origin-Oriented Elemental Profile of Fine Ambient Particulate Matter in Central European Suburban Conditions. *Int. J. Environ. Res. Public Health* **2016**, *13*, 715. [CrossRef] [PubMed]
25. Majewski, G.; Rogula-Kozłowska, W. The elemental composition and origin of fine ambient particles in the largest Polish conurbation: First results from the short-term winter campaign. *Theor. Appl. Clim.* **2015**, *125*, 79–92. [CrossRef]
26. Olszowski, T. Influence of Individual Household Heating on PM2.5 Concentration in a Rural Settlement. *Atmosphere* **2019**, *10*, 782. [CrossRef]
27. Rogula-Kozłowska, W. Size-segregated urban particulate matter: Mass closure, chemical composition, and primary and secondary matter content. *Air Qual. Atmos. Health* **2016**, *9*, 533–550. [CrossRef]
28. Rogula-Kozłowska, W.; Klejnowski, K.; Rogula-Kopiec, P.; Mathews, B.; Szopa, S. A Study on the Seasonal Mass Closure of Ambient Fine and Coarse Dusts in Zabrze, Poland. *Bull. Environ. Contam. Toxicol.* **2012**, *88*, 722–729. [CrossRef]
29. Rogula-Kozłowska, W.; Klejnowski, K. Submicrometer Aerosol in Rural and Urban Backgrounds in Southern Poland: Primary and Secondary Components of PM1. *Bull. Environ. Contam. Toxicol.* **2012**, *90*, 103–109. [CrossRef]
30. European Parliament. European Council Directive 2008/50/EC on ambient air quality and cleaner air for Europe. *Off. J. Eur. Communities* **2008**. (OJ L 152, 11.6.2008, p. 1). Available online: http://extwprlegs1.fao.org/docs/pdf/eur80016.pdf (accessed on 29 April 2021).
31. Zajusz-Zubek, E.; Mainka, A.; Korban, Z.; Pastuszka, J.S. Evaluation of highly mobile fraction of trace elements in PM10 collected in Upper Silesia (Poland): Preliminary results. *Atmos. Pollut. Res.* **2015**, *6*, 961–968. [CrossRef]
32. Jabłońska, M.; Janeczek, J. Identification of industrial point sources of airborne dust particles in an urban environment by a combined mineralogical and meteorological analyses: A case study from the Upper Silesian conurbation, Poland. *Atmos. Pollut. Res.* **2019**, *10*, 980–988. [CrossRef]
33. Klejnowski, K.; Janoszka, K.; Czaplicka, M. Characterization and Seasonal Variations of Organic and Elemental Carbon and Levoglucosan in PM10 in Krynica Zdroj, Poland. *Atmosphere* **2017**, *8*, 190. [CrossRef]
34. Furman, P.; Styszko, K.; Skiba, A.; Zięba, D.; Zimnoch, M.; Kistler, M.; Kasper-Giebl, A.; Gilardoni, S. Seasonal Variability of PM10 Chemical Composition Including 1,3,5-triphenylbenzene, Marker of Plastic Combustion and Toxicity in Wadowice, South Poland. *Aerosol Air Qual. Res.* **2021**, *21*, 200223. [CrossRef]
35. Sówka, I.; Chlebowska-Styś, A.; Pachurka, Ł.; Rogula-Kozłowska, W.; Mathews, B. Analysis of Particulate Matter Concentration Variability and Origin in Selected Urban Areas in Poland. *Sustainability* **2019**, *11*, 5735. [CrossRef]
36. Chlebowska-Styś, A.; Sówka, I.; Kobus, D.; Pachurka, Ł. Analysis of concentrations trends and origins of PM 10 in selected European cities. In Proceedings of the E3S Web of Conferences, Les Ulis, France, 24 May 2017; Volume 17, p. 13. Available online: https://www.e3s-conferences.org/articles/e3sconf/abs/2017/05/e3sconf_eko2017_00013/e3sconf_eko2017_00013.html (accessed on 29 April 2021).
37. Kindap, T.; Ünal, A.; Chen, S.-H.; Hu, Y.; Odman, M.; Karaca, M. Long-range aerosol transport from Europe to Istanbul, Turkey. *Atmos. Environ.* **2006**, *40*, 3536–3547. [CrossRef]
38. Jandacka, D.; Durcanska, D. Differentiation of Particulate Matter Sources Based on the Chemical Composition of PM10 in Functional Urban Areas. *Atmosphere* **2019**, *10*, 583. [CrossRef]
39. Kowalska, M.; Skrzypek, M.; Kowalski, M.; Cyrys, J. Effect of NOx and $NO_2$ Concentration Increase in Ambient Air to Daily Bronchitis and Asthma Exacerbation, Silesian Voivodeship in Poland. *Int. J. Environ. Res. Public Health* **2020**, *17*, 754. [CrossRef] [PubMed]
40. Majewski, G.; Rogula-Kozłowska, W.; Rozbicka, K.; Rogula-Kopiec, P.; Mathews, B.; Brandyk, A. Concentration, Chemical Composition and Origin of PM1: Results from the First Long-term Measurement Campaign in Warsaw (Poland). *Aerosol Air Qual. Res.* **2018**, *18*, 636–654. [CrossRef]
41. Marć, M.; Bielawska, M.; Simeonov, V.; Namieśnik, J.; Zabiegała, B. The effect of anthropogenic activity on BTEX, NO2, SO2, and CO concentrations in urban air of the spa city of Sopot and medium-industrialized city of Tczew located in North Poland. *Environ. Res.* **2016**, *147*, 513–524. [CrossRef]
42. Marć, M.; Zabiegała, B.; Simeonov, V.; Namieśnik, J. The Relationships Between BTEX, NOx, and O3Concentrations in Urban Air in Gdansk and Gdynia, Poland. *CLEAN Soil Air Water* **2014**, *42*, 1326–1336. [CrossRef]
43. Rogula-Kozłowska, W.; Majewski, G.; Czechowski, P.O.; Rogula-Kopiec, P. Analysis of the data set from a two-year observation of the ambient water-soluble ions bound to four particulate matter fractions in an urban background site in Southern Poland. *Environ. Prot. Eng.* **2017**, *43*. [CrossRef]
44. Samek, L. Overall human mortality and morbidity due to exposure to air pollution. *Int. J. Occup. Med. Environ. Health* **2016**, *29*, 417–426. [CrossRef]
45. Błaszczyk, E.; Rogula-Kozłowska, W.; Klejnowski, K.; Kubiesa, P.; Fulara, I.; Mielżyńska-Švach, D. Indoor air quality in urban and rural kindergartens: Short-term studies in Silesia, Poland. *Air Qual. Atmos. Health* **2017**, *10*, 1207–1220. [CrossRef] [PubMed]

46. Rodríguez, S.; Querol, X.; Alastuey, A.; Viana, M.-M.; Alarcón, M.; Mantilla, E.; Ruiz, C. Comparative PM10–PM2.5 source contribution study at rural, urban and industrial sites during PM episodes in Eastern Spain. *Sci. Total Environ.* **2004**, *328*, 95–113. [CrossRef]
47. Juda-Rezler, K.; Reizer, M.; Maciejewska, K.; Błaszczak, B.; Klejnowski, K. Characterization of atmospheric PM2.5 sources at a Central European urban background site. *Sci. Total Environ.* **2020**, *713*, 136729. [CrossRef] [PubMed]
48. Siudek, P. Seasonal variability of trace elements in fine particulate matter (PM2.5) in a coastal city of northern Poland – profile analysis and source identification. *Environ. Sci. Process. Impacts* **2020**, *22*, 2230–2243. [CrossRef]
49. Wang, W.; Zhang, W.; Dong, S.; Yonemachi, S.; Lu, S.; Wang, Q. Characterization, Pollution Sources, and Health Risk of Ionic and Elemental Constituents in $PM_{2.5}$ of Wuhan, Central China. *Atmosphere* **2020**, *11*, 760. [CrossRef]
50. Dytłow, S.; Górka-Kostrubiec, B. Concentration of heavy metals in street dust: An implication of using different geochemical background data in estimating the level of heavy metal pollution. *Environ. Geochem. Health* **2021**, *43*, 521–535. [CrossRef]
51. Cong, Z.; Kang, S.; Luo, C.; Li, Q.; Huang, J.; Gao, S.; Li, X. Trace elements and lead isotopic composition of PM10 in Lhasa, Tibet. *Atmos. Environ.* **2011**, *45*, 6210–6215. [CrossRef]
52. Lim, J.-M.; Lee, J.-H.; Moon, J.-H.; Chung, Y.-S.; Kim, K.-H. Airborne PM10 and metals from multifarious sources in an industrial complex area. *Atmos. Res.* **2010**, *96*, 53–64. [CrossRef]
53. Bralewska, K.; Rogula-Kozłowska, W. Health exposure of users of indoor sports centers related to the physico-chemical properties of particulate matter. *Build. Environ.* **2020**, *180*, 106935. [CrossRef]
54. Turek-Fijak, A.; Brania, J.; Styszko, K.; Zięba, D.; Stęgowski, Z.; Samek, L. Chemical characterization of PM10 in two small towns located in South Poland. *Nukleonika* **2021**, *66*, 29–34. [CrossRef]
55. Sówka, I.; Chlebowska-Styś, A.; Pachurka, Ł.; Rogula-Kozłowska, W. Seasonal variations of PM2.5 and PM10 concentrations and inhalation exposure from PM-bound metals (As, Cd, Ni): First studies in Poznań (Poland). *Arch. Environ. Prot.* **2018**, *44*, 86–95. [CrossRef]
56. Mainka, A.; Zubek, E.Z.; Kaczmarek, K. PM10 composition in urban and rural nursery schools in Upper Silesia, Poland: A trace elements analysis. *Int. J. Environ. Pollut.* **2017**, *61*, 98. [CrossRef]
57. Styszko, K.; Samek, L.; Szramowiat, K.; Korzeniewska, A.; Kubisty, K.; Rakoczy-Lelek, R.; Kistler, M.; Giebl, A.K. Oxidative potential of PM10 and PM2.5 collected at high air pollution site related to chemical composition: Krakow case study. *Air Qual. Atmos. Health* **2017**, *10*, 1123–1137. [CrossRef]
58. Rogula-Kozłowska, W.; Klejnowski, K.; Rogula-Kopiec, P.; Ośródka, L.; Krajny, E.; Błaszczak, B.; Mathews, B. Spatial and seasonal variability of the mass concentration and chemical composition of PM2.5 in Poland. *Air Qual. Atmos. Health* **2014**, *7*, 41–58. [CrossRef]
59. Wang, Z.-S.W.; Wu, T.; Shi, G.-L.; Fu, X.; Tian, Y.-Z.; Feng, Y.-C.; Wu, X.-F.; Wu, G.; Bai, Z.-P.; Zhang, W.-J. Potential Source Analysis for PM10 and PM2.5 in Autumn in a Northern City in China. *Aerosol Air Qual. Res.* **2012**, *12*, 39–48. [CrossRef]
60. Pan, Y.; Wang, Y.; Sun, Y.; Tian, S.; Cheng, M. Size-resolved aerosol trace elements at a rural mountainous site in Northern China: Importance of regional transport. *Sci. Total Environ.* **2013**, *461-462*, 761–771. [CrossRef]
61. Kim, M.-K.; Jo, W.-K. Elemental composition and source characterization of airborne PM10 at residences with relative proximities to metal-industrial complex. *Int. Arch. Occup. Environ. Health* **2006**, *80*, 40–50. [CrossRef]
62. Gustafsson, M.; Blomqvist, G.; Gudmundsson, A.; Dahl, A.; Jonsson, P.; Swietlicki, E. Factors influencing PM10 emissions from road pavement wear. *Atmos. Environ.* **2009**, *43*, 4699–4702. [CrossRef]
63. Li, J.-D.; Deng, Q.-H.; Lu, C.; Huang, B.-L. Chemical compositions and source apportionment of atmospheric PM10 in suburban area of Changsha, China. *J. Central South Univ. Technol.* **2010**, *17*, 509–515. [CrossRef]
64. Sówka, I.; Zwoździak, A.; Trzepla-Nabaglo, K.; Skrętowicz, M.; Zwoździak, J. PM2.5 elemental composition and source apportionment in a residential area of wrocŁaw, POLAND. *Environ. Prot. Eng.* **2012**, *38*, 73–79.
65. Samek, L.; Zwoździak, A.; Sówka, I. Chemical characterization and source identification of particulate matter PM10 in a rural and urban site in Poland. *Environ. Prot. Eng.* **2013**, *39*. [CrossRef]
66. Kulshrestha, A.; Satsangi, P.G.; Masih, J.; Taneja, A. Metal concentration of PM2.5 and PM10 particles and seasonal variations in urban and rural environment of Agra, India. *Sci. Total Environ.* **2009**, *407*, 6196–6204. [CrossRef] [PubMed]
67. Song, Y.; Xie, S.; Zhang, Y.; Zeng, L.; Salmon, L.G.; Zheng, M. Source apportionment of PM2.5 in Beijing using principal component analysis/absolute principal component scores and UNMIX. *Sci. Total Environ.* **2006**, *372*, 278–286. [CrossRef] [PubMed]
68. Toscano, G.; Moret, I.; Gambaro, A.; Barbante, C.; Capodaglio, G. Distribution and seasonal variability of trace elements in atmospheric particulate in the Venice Lagoon. *Chemosphere* **2011**, *85*, 1518–1524. [CrossRef] [PubMed]
69. Chakraborty, A.; Gupta, T. Chemical Characterization and Source Apportionment of Submicron (PM1) Aerosol in Kanpur Region, India. *Aerosol Air Qual. Res.* **2010**, *10*, 433–445. [CrossRef]
70. Kuo, C.-Y.; Wang, J.-Y.; Liu, W.-T.; Lin, P.-Y.; Tsai, C.-T.; Cheng, M.-T. Evaluation of the vehicle contributions of metals to indoor environments. *J. Expo. Sci. Environ. Epidemiol.* **2012**, *22*, 489–495. [CrossRef]
71. Sternbeck, J.; Sjödin, Å.; Andréasson, K. Metal emissions from road traffic and the influence of resuspension—results from two tunnel studies. *Atmos. Environ.* **2002**, *36*, 4735–4744. [CrossRef]
72. Samek, L.; Gdowik, A.; Ogarek, J.; Furman, L. Elemental composition and rough source apportionment of fine particulate matter in air in Cracow, Poland. *Environ. Prot. Eng.* **2016**, *42*. [CrossRef]

73. Khare, P.; Baruah, B. Elemental characterization and source identification of PM2.5 using multivariate analysis at the suburban site of North-East India. *Atmos. Res.* **2010**, *98*, 148–162. [CrossRef]
74. Cesari, D.; Amato, F.; Pandolfi, M.; Alastuey, A.; Querol, X.; Contini, D. An inter-comparison of PM10 source apportionment using PCA and PMF receptor models in three European sites. *Environ. Sci. Pollut. Res.* **2016**, *23*, 15133–15148. [CrossRef] [PubMed]
75. Rajšić, S.; Mijić, Z.; Tasić, M.; Radenković, M.; Joksić, J. Evaluation of the levels and sources of trace elements in urban particulate matter. *Environ. Chem. Lett.* **2008**, *6*, 95–100. [CrossRef]
76. Badyda, A.; Krawczyk, P.; Bihałowicz, J.S.; Bralewska, K.; Rogula-Kozłowska, W.; Majewski, G.; Oberbek, P.; Marciniak, A.; Rogulski, M. Are BBQs Significantly Polluting Air in Poland? A Simple Comparison of Barbecues vs. Domestic Stoves and Boilers Emissions. *Energies* **2020**, *13*, 6245. [CrossRef]
77. Yu, K.-P.; Chen, Y.-C.; Miao, Y.-J.; Siregar, S.; Tsai, Y.W.; Lee, W.-M.G. Effects of Oil Drops and the Charcoal's Proximate Composition on the Air Pollution Emitted from Charcoal Barbecues. *Aerosol Air Qual. Res.* **2020**, *20*, 1480–1494. [CrossRef]
78. Chen, C.; Luo, Z.; Yu, C.; Chunjiang, Y. Release and transformation mechanisms of trace elements during biomass combustion. *J. Hazard. Mater.* **2019**, *380*, 120857. [CrossRef] [PubMed]
79. Iqbal, M.A.; Kim, K.-H. Sampling, pretreatment, and analysis of particulate matter and trace metals emitted through charcoal combustion in cooking activities. *TrAC Trends Anal. Chem.* **2016**, *76*, 52–59. [CrossRef]
80. Zhou, S.; Yuan, Q.; Li, W.; Lu, Y.; Zhang, Y.; Wang, W. Trace metals in atmospheric fine particles in one industrial urban city: Spatial variations, sources, and health implications. *J. Environ. Sci.* **2014**, *26*, 205–213. [CrossRef]
81. Fernández-Camacho, R.; Rodríguez, S.; De La Rosa, J.; De La Campa, A.S.; Alastuey, A.; Querol, X.; González-Castanedo, Y.; Garcia-Orellana, I.; Nava, S. Ultrafine particle and fine trace metal (As, Cd, Cu, Pb and Zn) pollution episodes induced by industrial emissions in Huelva, SW Spain. *Atmos. Environ.* **2012**, *61*, 507–517. [CrossRef]
82. Viana, M.; Querol, X.; Alastuey, A.; Gil, J.; Menéndez, M. Identification of PM sources by principal component analysis (PCA) coupled with wind direction data. *Chemosphere* **2006**, *65*, 2411–2418. [CrossRef]
83. Negral, L.; Moreno-Grau, S.; Moreno, J.; Querol, X.; Viana, M.M.; Alastuey, A. Natural and Anthropogenic Contributions to PM10 and PM2.5 in an Urban Area in the Western Mediterranean Coast. *Water Air Soil Pollut.* **2008**, *192*, 227–238. [CrossRef]

*energies*

MDPI

*Article*

# Comparative Study of PM10 Concentrations and Their Elemental Composition Using Two Different Techniques during Winter–Spring Field Observation in Polish Village

**Tomasz Mach [1], Tomasz Olszowski [2,*], Wioletta Rogula-Kozłowska [3], Justyna Rybak [1], Karolina Bralewska [3], Patrycja Rogula-Kopiec [4], Marta Bożym [5], Grzegorz Majewski [6], Zbigniew Ziembik [7] and Anna Kuczuk [2]**

1 Faculty of Environmental Engineering, Wroclaw University of Science and Technology, Wybrzeże Wyspiańskiego 27, 50-370 Wrocław, Poland; tomasz.mach@pwr.edu.pl (T.M.); justyna.rybak@pwr.edu.pl (J.R.)
2 Department of Thermal Engineering and Industrial Facilities, Opole University of Technology, 45-271 Opole, Poland; a.kuczuk@po.edu.pl
3 Safety Engineering Institute, The Main School of Fire Service, Slowackiego Street 52/54, 01-629 Warsaw, Poland; wrogula@sgsp.edu.pl (W.R.-K.); kbralewska@sgsp.edu.pl (K.B.)
4 Institute of Environmental Engineering of the Polish Academy of Sciences, 41-819 Zabrze, Poland; patrycja.rogula@ipispan.edu.pl
5 Department of Environmental Engineering, Opole University of Technology, 45-271 Opole, Poland; m.bozym@po.edu.pl
6 Institute of Environmental Engineering, Warsaw University of Life Sciences, 02-787 Warsaw, Poland; grzegorz_majewski@sggw.edu.pl
7 Institute of Environmental Engineering and Biotechnology, University of Opole, 6a Kominka Str., 45-032 Opole, Poland; ziembik@uni.opole.pl
* Correspondence: t.olszowski@po.edu.pl

**Abstract:** The aims of this study were to determine the concentrations and elemental composition of PM10 in the village of Kotórz Mały (Poland), to analyse their seasonal variability, to determine the sources of pollutant emissions and to compare the consistency of the results obtained using different methods. Sampling and weather condition measurements were carried out in the winter (January–February) and spring (April) of 2019. Two combinations of different techniques were used to examine PM10 concentrations and their chemical composition: gravimetric method + atomic absorption spectrometry (GM+AAS) and continuous particle monitor + energy dispersive X-ray fluorescence (CPM+EDXRF). In winter, the average concentrations of PM10 measured by the GM and CPM were similar (GM 44.3 μg/m$^3$; CPM 34.0 μg/m$^3$), while in spring they were clearly different (GM 49.5 μg/m$^3$; CPM 29.8 μg/m$^3$). Both AAS and EDXRF proved that in both seasons, Ca, K and Fe had the highest shares in the PM10 mass. In the case of the lowest shares, the indications of the two methods were slightly different. Factor analysis indicated that air quality in the receptor was determined by soil erosion, coal and burning biomass, and the combustion of fuels in car engines; in the spring, air quality was also affected by gardening activities.

**Keywords:** continuous particle monitor; reference method; PX-365; EDXRF; AAS; factor analysis



**Citation:** Mach, T.; Olszowski, T.; Rogula-Kozłowska, W.; Rybak, J.; Bralewska, K.; Rogula-Kopiec, P.; Bożym, M.; Majewski, G.; Ziembik, Z.; Kuczuk, A. Comparative Study of PM10 Concentrations and Their Elemental Composition Using Two Different Techniques during Winter–Spring Field Observation in Polish Village. *Energies* **2022**, *15*, 4769. https://doi.org/10.3390/en15134769

Academic Editor: Boris Igor Palella

Received: 20 May 2022
Accepted: 27 June 2022
Published: 29 June 2022



## 1. Introduction

Particulate matter (PM) released from primary sources or generated and transformed in the atmosphere by reactions can be toxic and may contribute to adverse environmental effects [1,2]. It is well recognised that the presence of above-normal amounts of aerosol in the air is associated with morbidity and mortality as well as annoyance and psychological stress [3,4]. The current research looked at specific locations, seasonal trends, dust properties and relevant control factors [5–11]. Most research is conducted in highly urbanised

areas, mainly cities and agglomerations; the amount of air quality recognition work in rural settlement areas is much less [12].

Particulate matter is a mixture of solid and liquid particles, suspended in the air, originating from both natural and anthropogenic sources [13,14]. The sources of PM in the atmosphere which are then enriched with toxic elements or compounds have been widely investigated in many works, including Rodríguez et al. [15], Majewski et al. [16], Rogula-Kozłowska et al. [17] and Mach et al. [18]. Over the last decade, the number of papers reporting results of studies conducted in the areas of compact rural buildings and small villages has increased. In several papers [19–25] it was remarked that, in the cold season, the principal source of PM emission is associated with the combustion of conventional fuels in domestic heating systems. Concentrations of aerosol particles within local air sheds are affected also by meteorological parameters [19]. An occasional increase in rural aerosol concentrations was mostly attributed to the transportation of particles from polluted urban or industrial areas and remote natural sources [18,26].

Many methods are used in aerosol testing, including direct measurements, indirect measurements or mathematical modelling [18]. For the study of the mass concentration of particulate matter and its constituents, the reference methods should be the gravimetric method (GM) followed by an analysis by atomic absorption spectrometry (AAS), while other methods may be used if their equivalence to the reference method has been demonstrated [27].

In addition to the AAS technique (and the equivalent ICP-MS technique (Inductively Coupled Plasma Mass Spectrometry)), non-destructive techniques are applicable and are generally referred to as X-ray fluorescence (XRF) [28–32]. The detailed characterisation and application of AAS and XRF were presented in a paper by Galvão et al. [33]. There are many works which confirm the usefulness of XRF as an effective technique to determine the elements in various research materials, for example, soil, mollusc tissues and fish tissues [4,34–36]. In addition, authors often focus their attention on studies which compare XRF indications with AAS. Comparative XRF and AAS studies of the same samples (first using non-destructive techniques and then those that require mineralisation of the test material) are usually carried out under laboratory conditions, including an analysis of the Pb content in the same dust samples [37,38], the measurement of metals in ash following the combustion of petroleum oil [39], the detection of metal content in soils [34,36] and a determination of the elements in the previously mentioned animal tissues [4,35]. The results of Bizo et al. [34] clearly showed that there were no statistically significant differences in the elemental concentrations determined by AAS and XRF, noting that AAS had a lower limit of detection (LOD) and limit of quantification (LOQ). Gerboles et al. [40] has also presented interesting research. The authors described the results of inter-laboratory measurements on five samples of identical composition. The measurements used for comparison were graphite furnace atomic absorption spectrometry (GF-AAS), inductively coupled plasma with mass spectrometry (ICP-MS), energy dispersive X-ray fluorescence (EDXRF) and inductively coupled plasma-atomic emission spectrometry (ICP-AES). The results of this research indicated significant agreement between EDXRF and the other techniques. The results of inter-laboratory comparative studies using XRF, ICP-MS and PIXE (particle-induced X-ray emission) to measure elemental loads of Al, K, Ca, Ti, V, Cu, Sr, Fe, Zn and Pb, among others, in PM10 samples were also presented [41]. With the exception of Fe and Zn, the authors showed consistency of results (also between laboratories). Gupta et al. [42] also used AAS and XRF to carry out a comparative study of the metal concentrations of Zn, Ca, Fe, K, Mn, Ni, Pb, Al, Na and Cr in PM2.5 retained on quartz filters. The authors obtained a high correlation coefficient for Al, K and Na.

Portable, fully automatic XRF analysers are also increasingly used in field studies [43,44]. The previously mentioned authors point to the functionality of these instruments, the important compatibility with reference or reference-equivalent methodologies and the possibility to carry out in situ measurements, even for short periods of time. However, it seems that there is still a need to improve knowledge on non-destructive techniques, despite the

considerable amount of research work dedicated to their verification that has been carried out with various environmental components. The need for such studies is particularly apparent with regard to the determination of air quality in terms of dust and trace elements present in dust, especially in areas that are hardly monitored. Such areas include dense rural development where, for example, significant anthropogenic emissions take place in the cold season and thus significant local degradation of aero-sanitary parameters occurs. So far, only a few measurement campaigns of particulate matter PM in rural areas have been carried out in Poland [18,19,45–48]. At the same time, automatic on-line XRF measurement was used only once in a study by Mach et al. [18].

This paper presents and analyses data on PM10 concentrations and their chemical composition. The data were obtained in two measurement campaigns carried out in the winter and spring. The concentration and elemental composition of PM10 were determined using two methods (techniques), that is, GM+AAS and CPM+EDXRF. In addition to checking the air quality in the rural area, the main aim of the study was to compare the aforementioned methods in terms of the possible compatibility of the results. In addition, potential differences in air quality over the two seasons were checked and an attempt to determine the contribution of individual emission sources was made.

The scope, type, place, apparatus and conditions of observation enabled the verification of the following hypotheses:

1. Concentration levels of PM10 are identical regardless of the method of sampling and analysis;
2. Concentration levels of PM10-bound elements are identical regardless of the method of analysis; and
3. Concentration levels of PM10 and PM10-bound elements are identical regardless of the season (winter-spring relation).

## 2. Materials and Methods

### *2.1. Observation Site Description*

#### 2.1.1. Characteristic of the Village—Location and Sources of Air Pollution

The study was conducted in the village of Kotórz Mały, Opole Voievodeship, Poland (50°73′66.02″ N; 18°05′06.80″ E, 162 m.a.s.l.). Kotórz Mały is a small settlement (with a population of approx. 1100). The location of the sampling point is shown in Figure 1. There are more than 300 buildings within the village, of which 295 are permanently inhabited. The village is characterised by compact development, consisting mainly of storey buildings, and within its boundaries, new buildings (located mainly in the western part) and old buildings (in the eastern part) can be distinguished. The houses are heated individually. A railroad and a district road pass through the village. In close proximity (<10 km), there are two national roads, DK45 and DK46, with a traffic density of approx. 8000 and 9500 vehicles per day, respectively [18]. The village has an agricultural character, although several businesses prosper within its borders, including two carpenter's shops, two locksmith's shops, two car painting shops and three motor vehicle workshops. All of these plants are equipped with highly efficient dedusting equipment. There are several significant emitters associated with the cement, food, mining and metals industries in the region where the village is located. Emitters from plants located in the voivodeship's capital of Opole, which is also the largest city in the region (with 122,000 inhabitants), are also significant. Opole is located 15 km southwest of the village.

During the warm season, the main source of tropospheric organic and inorganic matter is connected with natural emissions from surrounding areas and anthropogenic emissions from agriculture, traffic, hard coal, wood, biomass, waste and garbage burning in small-scale installations, for example, domestic stoves and local boiler houses [18]. During the cold season, the main local source of air pollution is associated with domestic heating [19].

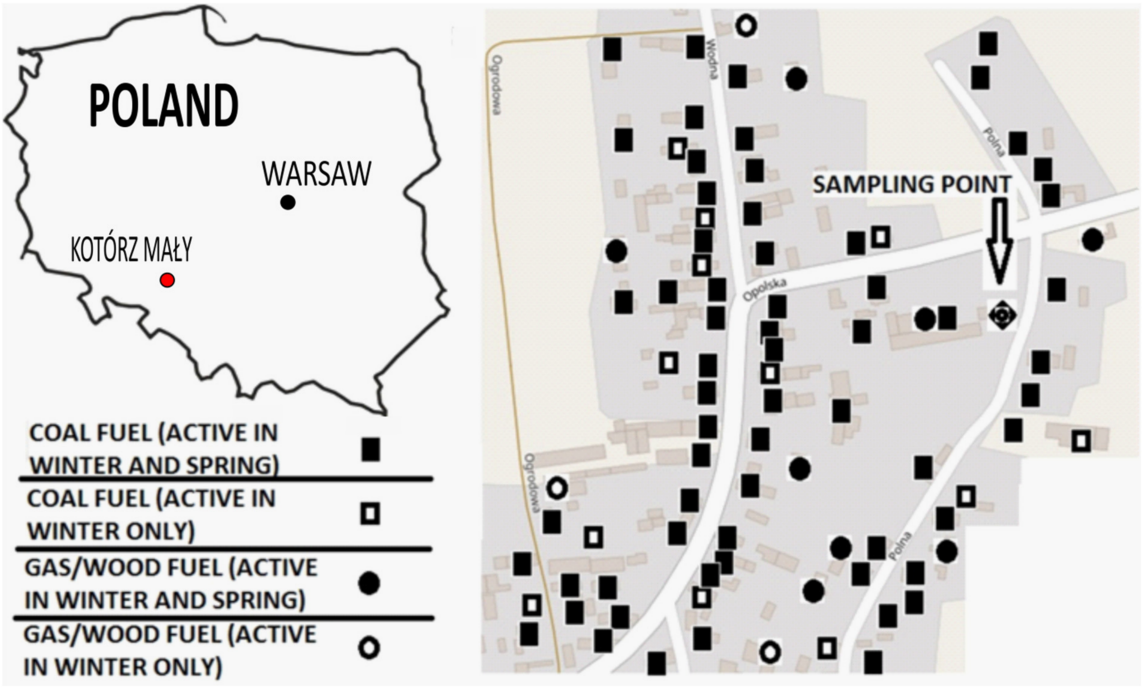


**Figure 1.** Location of sampling point with arrangement of point emission sources within a radius of 300 m from the sampling point (without a Renewable Energy Systems-RES; n = 11).

#### 2.1.2. Characteristics of the Village—Emitters and Fuel Consumption

The sampling point was situated in the dense building area and close to the district road in the old part of the village. As previously mentioned, the study area was characterised by storey rural houses, which predominantly used obsolete individual heating systems (IHS). Coal was mainly used throughout Kotórz Mały in a proportionate share equal to 81% (Table 1). All IHS are usually used during the cold season (form October until April). In the summer, local peoples also use IHS for hot water supply and food preparation, but the number of IHS in use is significantly lower. In the neighbourhood of the sampling point during the measurement campaigns, 86 individual point emitters (IPE) from 97 IHS were active in the winter and 71 in the spring. The location of IPE is shown in Figure 1. The exact number of specific emission sources was determined based on the results of surveys conducted among the residents. The activity of emission sources was indicated on the basis of individual responses of IHS owners and the authors' own observations. The activity of emitters was periodic and dependent on the needs of users. The average daily time of IPE activity was 17 h in the winter and 14 h in the spring.

**Table 1.** Characteristics of Individual Point Emitters (IPE) related to the individual hot water supply and energy for cooking.

| **No of IPE = 86, Total Energy Sources = 97** | **Heating Systems Share (%); (Number in the Bracket)** | | | | | |
|---|---|---|---|---|---|---|
| | coal | fuel gas | wood | RES | eco-coal | pellets |
| Active during winter campaign | **55** (52) | **4** (4) | **2** (2) | **11** (11) | **24** (23) | **5** (5) |
| Active during spring campaign | **50** (41) | **4** (3) | **1** (1) | **13** (11) | **27** (22) | **5** (4) |

A large number of old stoves were in use. More than 80% of heating systems were connected with the burning of fossil fuels or wood. Only 11 items were emission free. Comparing winter and spring fuel consumption, no significant differences were observed related to a single day (Table 2). The large differences in fuel consumption between the winter and spring were related to the different periods of sampling. The relatively high fuel consumption also corresponds to inefficient stoves and the low energy efficiency of the

buildings themselves. Of course, the quantity of burned fuel and the relatively long daily use times of fuel source exploitation seems to have influenced local air quality.

**Table 2.** Average fuel consumption (Mg) in the single village households during periods of sampling.

| Season | Hard Coal | Eco-Coal | Wood | Pellets | Gas |
|---|---|---|---|---|---|
| Winter | 0.87 | 0.56 | 0.94 | 0.61 | 2.74 |
| Single day in winter | 0.018 | 0.011 | 0.019 | 0.012 | 0.06 |
| Spring | 0.27 | 0.17 | 0.28 | 0.21 | 1.17 |
| Single day in spring | 0.018 | 0.011 | 0.018 | 0.14 | 0.06 |
| Year 2019 | 6.9 | 4.2 | 5.8 | 3.6 | 4.08 |

Apart from that and agricultural activity typical for rural areas, the local sources of anthropogenic emission were smaller economic activities with services in the fields of woodwork (2 items), vehicle mechanics (2 items) and metal surface varnishing (2 items). These activities were located less than 1 km from the sampling point.

### *2.2. Sampling and Analysis*

The measuring point was equipped with two instruments which realised two different methods of PM10 data collection. First, a reference gravimetric method (GM) with LVS aspirator was used. Samples were collected at 24 h intervals. Second, PM10 mass concentration was measured hourly with an online continuous particle monitor (CPM) which applies reel-to-reel filter tape sampling with beta ray attenuation analysis to determine the total PM10 mass. Both methods were applied at the same time, that is, for 49 consecutive days during the winter period (January–February 2019) and 15 consecutive days during the spring period (April 2019). Because of the need to meet technical conditions, apparatuses were located at a distance of 18 m from each other, with PM10 sampling heads all at the same height above the ground (2.4 m).

#### 2.2.1. PM10 Mass Concentration

In the case of the reference gravimetric method, the mass concentration of PM10 was determined in accordance with the European Standard [49]. The aspiration of the PM10 from the air was provided using low-volume automatic dust sampler Atmoservice PNS-15 aspirator (produced in Poland under the licence for the low-volume sampler LVS 3.1, Comde-Derenda GmbH, Stahnsdorf, Germany). The airflow rate passed filters was 2.3 $m^3$/h. The PM separator applied Whatman QMA quartz air filters with a diameter of 47 mm. Prior to and after aspiration, the filters were seasoned for a minimum 24 h under conditions of constant temperature and humidity and, subsequently, their weight was determined using a differential scale RADWAG XA 52/2X ® (Radwag Balances and Scales, Radom, Poland). The expanded concentration measurement uncertainty, which was calculated on the basis of the guidebook [50], did not exceed 15.2%.

The PX-375 monitor CPM+EDXRF (PX-375 Horiba, Osaka, Japan) was applied for CPM assessment. A two-layer nonwoven Polytetrafluoroethylene (PTFE) fabric filter was used as a filter tape during PM10 collection. The air samples acquisition was achieved by a flow rate equal to 1.002 $m^3$/h. The beta ray attenuation analysis was conducted every 60 min, assessing the exact mass quantity which was based on a rule that absorbed radiation is exponentially dependent only on the mass of filtered material [51]. At the beginning, beta radiation was emitted at an empty filter which gave enough time for sample acquisition and for adsorption of particles on the filter tape. Taking into account the difference between these two measurements, the collected PM10 was given as a result, and then the filter tape was moved to allow for the new measurement. The conditions of the analysis were as follows: 500 s at 15 kV or 50 kV voltage (depending on the element). Samples were collected continuously. For further data comparison, the average daily mass concentration was adopted.

#### 2.2.2. Elements

All samples obtained by GM were analysed by AAS in the laboratory. A microwave oven was used (Start D, Millestone) to digest the quartz filters in Teflon vessels containing a mixture of 8 mL of nitric acid (65%, Merck, Darmstadt, Germany) and 2 mL of hydrogen peroxide (30%, Avantor, Gliwice, Poland). The temperature programme for sample digestion was: 20 min of linearly increasing temperature between ambient and 220 °C, 25 min of constant temperature (220 °C) and 20 min of cooling with 1000 W of power. As suggested by Gerboles et al. [40], this process was performed twice to ensure full digestion of all the dust samples. The mass concentration of metals (Cu, Zn, Cr, Ni, Fe, Mn, K and Ca) was determined by the AAS method, whereas Pb was determined by the GF-AAS method using the Solaar 6M spectrometer (Waltham, MA, USA). The samples after digestion were filtered through a cellulose filter into 25 mL graduated flasks. For high concentrations of metals, the samples were diluted.

Certified material (ERM-CZ120) was prepared and analysed as samples, in triplicate. The recovery (%) from the ERM analysis and LOQ and LOD are presented in Table 3.

**Table 3.** Results of the analysis of certified material 'Fine Dust (PM10-LIKE)' No. ERM-CZ120 and detection limits for dust with mass from 0.1 g and volume 25 mL.

| Material | Pb | Cu | Zn | Ni | Cr | Mn | Fe | Ca | K |
|---|---|---|---|---|---|---|---|---|---|
| Certified | 113 | 462 | 1240 | 58 | 201 | 611 | 38,144 | 63,043 | 10,998 |
| [mg/kg] | ±17 | ±nd | ±nd | ±7 | ±nd | ±nd | ±nd | ±nd | ±nd |
| Analysed | 103 | 425 | 1216 | 63 | 169 | 506 | 37,339 | 56,410 | 9388 |
| [mg/kg] | ±4 | ±19 | ±100 | ±7 | ±4 | ±24 | ±3160 | ±3115 | ±331 |
| recovery [%] | 91 | 92 | 98 | 108 | 84 | 83 | 98 | 89 | 85 |
| GO mg/kg DM LOQ | 1 | 10 | 10 | 10 | 10 | 10 | 10 | 50 | 30 |
| GW mg/kg DM LOD | 0.3 | 3 | 3 | 3 | 3 | 3 | 3 | 17 | 10 |

The same CPM with the EDXRF apparatus (PX-375 Horiba analyser) was applied to obtain the results for PM10 mass concentration and the data of the elemental composition of PM10. Nine elements (Cu, Zn, Cr, Ni, Fe, Mn, K, Ca and Pb) were selected for analysis. Their concentrations were determined with the non-destructive energy-dispersive X-ray fluorescence spectroscopy (EDXRF). The EDXRF unit has a complementary metal-oxide semiconductor (CMOS) camera for sample images.

We used a standard reference material SRM 2738 (air particulate on filter media) certified by NIST for quality control and to assess the elemental quantification of X-ray spectra. The blank tape was checked three times to derive the average value. The calibration of the CPM was performed at the beginning and end of the experiment by the qualified Horiba workers. Additionally, we checked it during the sampling by DryCal Defender 530 to assure that the flow did not change. The lowest detection limits (LLD), expressed as double standard deviations of blank samples, were as follows: Cr (2.05 ng/m$^3$), Ca (1.1 ng/m$^3$), Cu (1.85 ng/m$^3$), Fe (7.00 ng/m$^3$), K (4.8 ng/m$^3$), Mn (1.45 ng/m$^3$), Ni (0.9 ng/m$^3$), Pb (1.05 ng/m$^3$) and Zn (1.25 ng/m$^3$). The repeatability of the results ranged within ±2% of the equivalent film value. Furthermore, according to manufacturer-provided information, a strong correlation was revealed among metal concentrations determined by CPM EDXRF (Horiba, PX-375) and conventional methods including ICP-MS.

### *2.3. Weather Conditions*

A Davis Vantage® portable automatic weather station (Davis Instruments, Hayward, CA, USA) equipped with a data logger was installed at the sampling point to record weather conditions. The following parameters that characterised the weather were recorded simultaneously with the PM10 measurements: temperature (T), wind speed (Ws), wind direction (Wd), atmospheric pressure (Ap) and precipitation (P). Portable stations are usually used in tests to register the weather conditions [19,52]. The weather station was installed 10 m

from the PM aspirators. The sensors, similar to the case of the PM10 aspiration headers, were installed 2.4 m above the ground. The standard measurement uncertainty was equal to RH 0.5%, T 0.5 °C, Ap 0.06 hPa, Ws 0.06 m/s and Wd 1°, respectively.

### 2.4. Statistics

TIBCO STATISTICA version 13.3 was used to prepare charts and perform statistical analyses. The result of the Shapiro-Wilk test indicated that none of the recorded cases were found to correspond to a normal distribution of data; therefore, non-parametric tests were used to assess differences between the concentrations as determined by two different methods (Wilcoxon). The winter-spring relation was checked by using the Mann-Whitney U test. For comparison of elements, EDXRF-AAS relation in the selected season, the Wilcoxon test was used. The relationships between variables were examined using Spearman's rank correlation coefficient. A significance level of 0.05 was adopted.

Factor analysis (FA) was applied to the data derived from field measurements to justify the sources of emission.

## 3. Results

### 3.1. Concentration of PM10

Figure 2 shows the distribution of PM10 mass concentrations determined using both methods. The average concentration of PM10 for the whole measurement period in January–February was 34 and 44.3 $\mu g/m^3$ for CPM and GM, respectively. It was below the daily PM10 limit value determined by the European Commission (50 $\mu g/m^3$) [53], which must not be exceeded for more than 35 days a year. Days which exceeded the daily limit value were also observed, that is, days 1–6, 9, 10, 12, 20, 21 and 1–6, 9–15 19–21 in the CPM and GM measurements, respectively. Despite the observed fluctuations, it can be concluded that the PM10 concentrations measured with CPM and GM were similar only during the winter period. The coefficient of variation was at a similar level, that is, 51% for CPM and 65% for GM.

The variability of PM10 concentration during the observation period in spring is presented in Figure 3. In contrast to the winter period and especially at the beginning of the observation period (early April), the concentrations determined by the two methods were clearly different. A significant difference was also observed in the average values for the whole period. The average concentration of PM10 for the whole measurement period was 29.8 and 49.5 $\mu g/m^3$ for CPM and GM, respectively. In addition, only two days with exceedances of CPM were recorded, while there were four such days in the case of GM. For both CPM and GM, the coefficient of variation was at almost the same level as it was during the winter period—52% and 67%, respectively. Furthermore, in the case of GM, the relation of PM10 concentration—values of meteorological parameters (Ws, T, P)—was identical to that observed for winter. Such a relationship did not occur for concentrations determined using CPM.

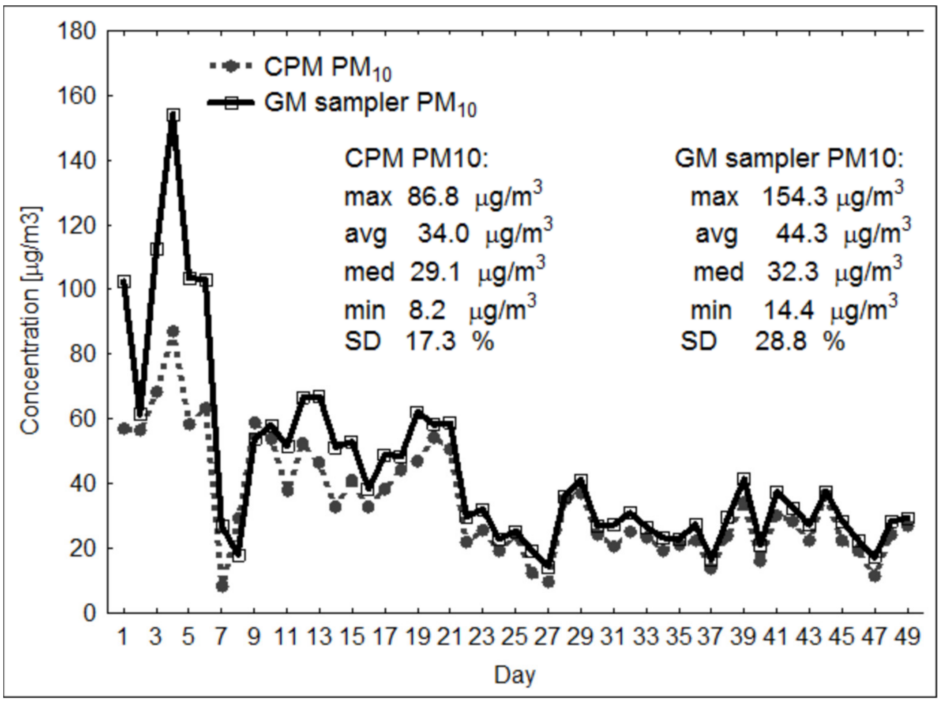


**Figure 2.** Average 24 h PM10 mass concentration obtained by two methods in winter campaign.

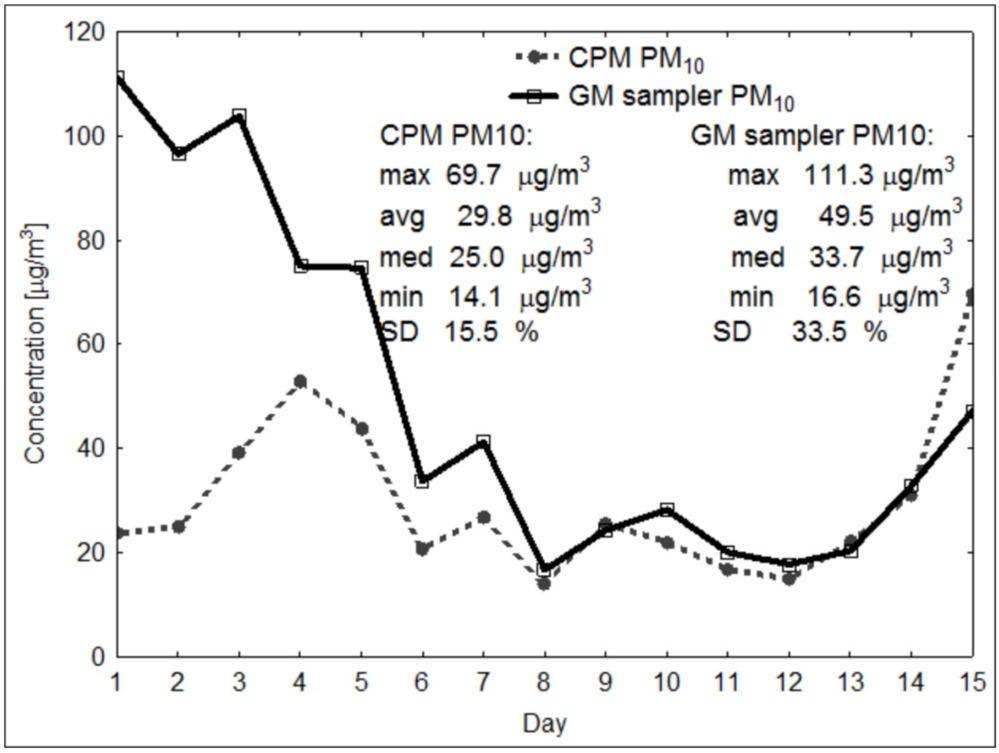


**Figure 3.** Average 24 h PM10 mass concentration obtained by two methods in spring campaign.

### *3.2. Concentration of Elements*

Figure 4 shows the full measurement data for PM10-bound elements for the winter period. The mean concentrations of selected elements associated with PM10 ranged widely, with values from 0.61 ng/m$^3$ (Ni) to 219 ng/m$^3$ (Ca) for EDXRF and 1.46 ng/m$^3$ (Ni) to 250 ng/m$^3$ (Ca) for AAS. The masses of the nine elements represented almost 1.6% of the total PM10 mass for EDXRF and 2.0% for AAS. For both techniques, Ca, K and Fe

were the most abundant among the determining elements. Toxic trace elements were present in very low concentrations (Ni, Cr, Mn) not exceeding 10 ng/m$^3$ (mean daily value) or low (Pb). The mean concentrations of Ni and Pb in Kotórz Mały did not exceed the permissible values of annual concentrations established by the European Commission (20 ng/m$^3$ and 0.5 µg/m$^3$, respectively; [53]). When considering the position of the median, it may appear that for both methods, the concentrations of Mn, Ni, Zn and Ca can be taken as equivalent. On average over the whole measurement period, the elements associated with the PM10 particulate matter under observation for EDXRF can be ranked as follows: Ca > K > Fe > Zn > Pb > Mn > Cu > Cr > Ni, while for AAS, the order was almost identical: K > Ca > Fe > Zn > Mn > Cu > Cr > Pb > Ni. In the case of EDXRF, two groups of elements can be distinguished because they were characterised by similar coefficients of variation (CV); CV ranging from 52% to 70% (Zn, Cr, Ca, Mn) and CV ranging from 70% to 88% (Pb, K, Fe). Two extreme CVs were also recorded: 39% and 115% for Ni and Cu, respectively. There was much more variability in the elements determined by the AAS method. With the exception of Cr in which the CV was 47%, the concentrations of the other elements showed a significant quartile range, with CVs for Ca, K, Pb, Zn, Cu, Mn, Fe and Ni ranging from 104% to 167%. Significant discrepancies were observed between the results of the two techniques, particularly in the mass concentration of Cr (more than 4 times the median value for AAS) and Cu (more than 3 times the median value for AAS).

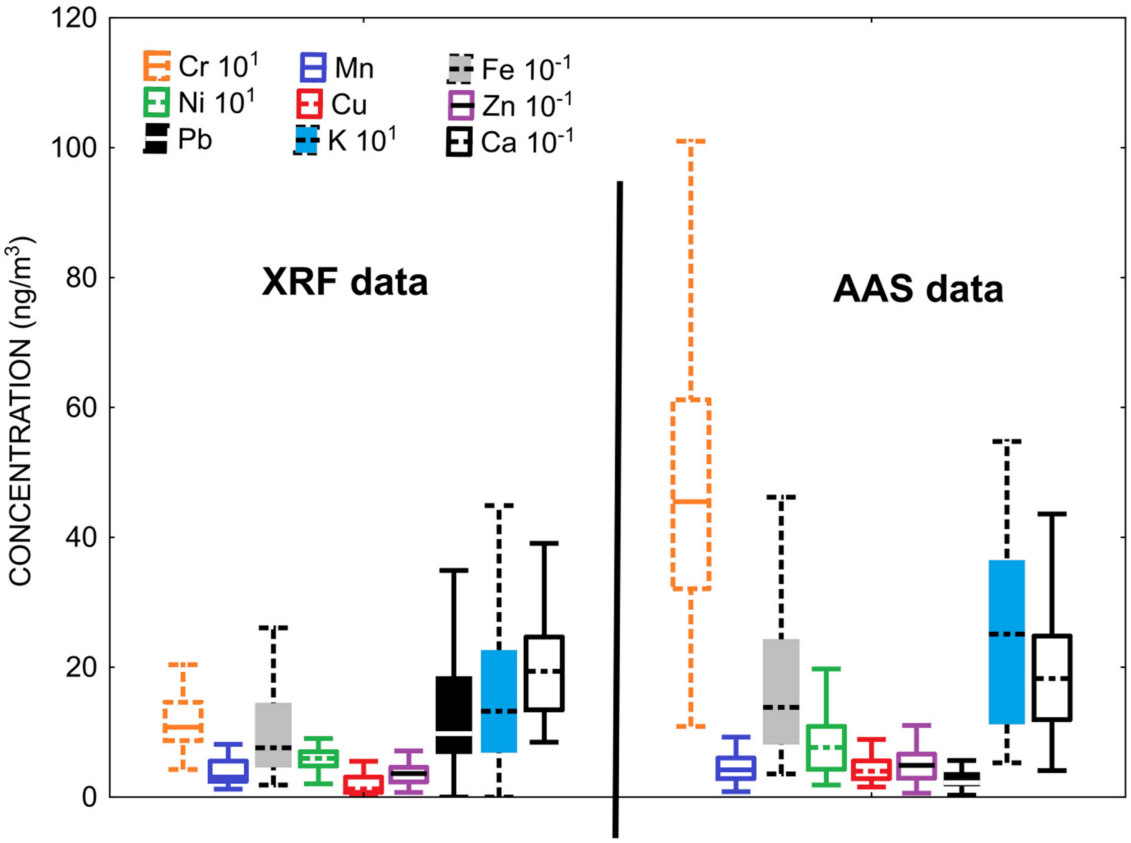


**Figure 4.** PM10-bound elements data for winter period. Boxes show the range between the 25th and 75th percentiles. The whiskers extend from the edge of the box to the 5th and 95th percentiles of data. The horizontal line inside indicates the median value.

The full measurement data of PM10-bound elements for the spring period is presented in Figure 5. The mean concentrations of selected elements associated with PM10 ranged widely, with values from 0.82 ng/m$^3$ (Ni) to 472 ng/m$^3$ (Ca) for EDXRF and 1.68 ng/m$^3$ (Pb) to 1718 ng/m$^3$ (Ca) for AAS. The masses of the nine elements represented almost 3.4% of the total PM10 mass for EDXRF and 5.2% for AAS. For both techniques, Ca, K and Fe

were the most abundant among the determining elements. From EDXRF data, the mean daily values of toxic trace elements were present in very low concentrations (Ni, Cr, Mn, Pb), not exceeding 10 ng/m$^3$. From AAS data, the mean daily values of toxic trace elements were present in very low concentrations (Ni, Pb), not exceeding 11 ng/m$^3$ or low (Cr, Mn). The mean concentrations of Ni and Pb in Kotórz Mały did not exceed the permissible values of annual concentrations established by the European Commission (20 ng/m$^3$ and 0.5 µg/m$^3$, respectively; European Parliament; European Council, 2008). The position of the median may suggest that for both methods, the Fe and Zn concentrations can be taken as equivalent. Based on an average over the entire measurement period, the PM10-bound elements for EDXRF are ranked as: Ca > Fe > K > Zn > Pb > Mn > Cu > Cr > Ni. In contrast, the order of the elements for AAS is ranked as: Ca > Fe > K > Cu > Zn > Mn > Cr > Ni > Pb. In the case of EDXRF, three groups of elements characterised by a similar coefficient of variation can be distinguished: CV 45% and 53% (Cr, Mn); CV between 62% and 70% (Cu, Zn, Fe); and CV between 79% and 92% (Pb, K, Ca). The maximum variation was in Ni concentration (112%). For the concentrations determined by AAS, in addition to Ca and K (CV 16% and 23%, respectively), more balanced values were observed for Mn, Cu, Ni, Cr and Fe; CV ranged from 51% (Mn) to 65% (Fe). Zn and Pb were in the last group, with CVs of 82% and 84%, respectively. Very significant discrepancies were observed between the results of the two techniques, especially in the mass concentrations of Cu (more than 20-fold higher median value for AAS), Ni (more than 13-fold higher median value for AAS), Cr (more than 8-fold higher median value for AAS), Ca (more than 5-fold higher median value for AAS) and Pb (more than 5-fold higher median value for EDXRF).

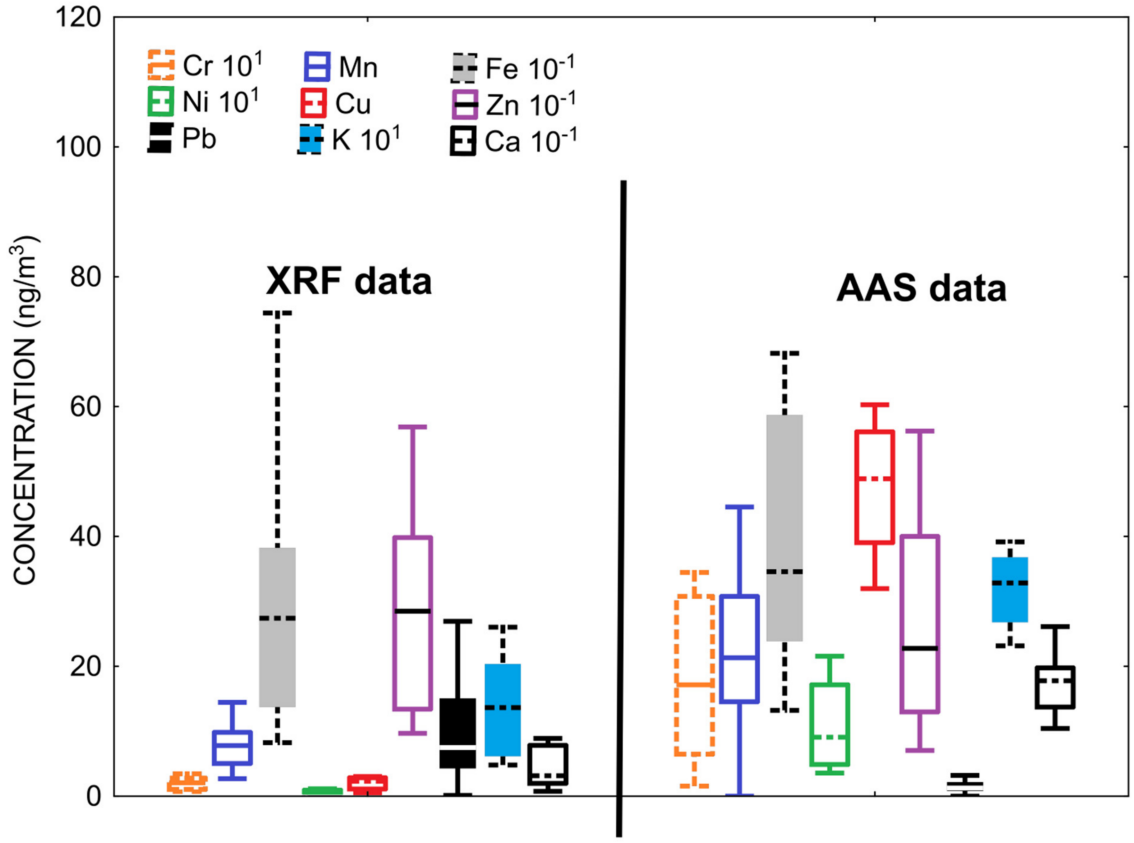


**Figure 5.** Data for PM10-bound elements for spring period. Boxes show the range between the 25th and 75th percentiles. The whiskers extend from the edge of the box to the 5th and 95th percentiles of data. The horizontal line inside indicates the median value.

### 3.3. Meteorological Data

Meteorological data were recorded simultaneously with PM10 and elemental measurements. During the winter campaign, the average temperature was 2 °C, reaching min and max values of −6.9 °C and 9.3 °C, respectively. With the exception of a few days associated with the impact of the cyclone, the pressure was stable and ranged between 996–1046 hPa (mean 1017.6 hPa). The measurement period was dominated by days with very low winds. The movement of air masses was mainly from the NW, S and W directions. The maximum wind velocity was 10.7 m/s, with an average of 4.4 m/s. The total precipitation of 38 mm was lower than the multi-year average. There was no precipitation for 71% of the measurement days. The maximum rainfall was 8.6 mm/h, but the daily average was only 0.8 mm. The average temperature was 6.5 °C during 15 days of measurements in April, reaching daily minimum and maximum values of 1.9 °C and 11.4 °C, respectively. Atmospheric pressure was stable and ranged between 995 and 1015 hPa (mean 1001.3 hPa). Days with very light winds dominated during the measurement period. Air masses moved mainly from the S, SE and NW directions. The maximum wind velocity was 7.4 m/s and the mean was 3.6 m/s. The total precipitation of 13.6 mm was lower than the multi-year average. No precipitation was recorded on 12 of the 15 measurement days. The maximum precipitation was 7.1 mm/h, but the daily average was only 0.9 mm.

## 4. Discussion

### 4.1. Comparison of GM and CPM—Concentration of PM10

PM10 concentration values in the vicinity of receptors are determined not only by emission sources but also by the impact of meteorological parameters. Differences in PM10 values may also result from changes in the boundary layer of the atmosphere, which are expressed in different values for temperature, wind speed or precipitation. The analysis of the basic meteorological parameters (Mann-Whitney U test, $\alpha = 0.05$) registered in the winter as well as spring indicated that there were considerable statistical differences between seasons with regard to the values of T, Ap and Wd ($p$-value: 0.00; 0.00 and 0.04, respectively) and no considerable statistical differences between seasons with regard to the values of Ws and P ($p$-value: 0.12; 0.00 and 0.54, respectively).

Table 4 shows the results of the Spearman correlation between PM10 concentration determined with CPM and GM and between PM10 concentration values and recorded meteorological parameters.

**Table 4.** Spearman correlation. Relationship between the PM10 concentration and meteorological parameters. Bold values are statistically significant with $p = 0.05$. Normal font relates to winter data and italic font to spring data.

| | CPM PM10 | GM PM10 | T | Ap | Ws | Wd | P |
|---|---|---|---|---|---|---|---|
| CPM PM10 | | **0.94** | **−0.61** | 0.21 | **−0.40** | 0.02 | **−0.40** |
| GM PM10 | *0.68* | | **−0.58** | 0.14 | −0.28 | 0.04 | **−0.45** |
| T | *0.32* | *−0.17* | | | | | |
| Ap | *−0.46* | *−0.38* | | | | | |
| Ws | *−0.28* | *−0.40* | | | | | |
| Wd | *−0.18* | *−0.30* | | | | | |
| P | ***−0.53*** | ***−0.48*** | | | | | |

For both winter and spring periods, a statistically significant, high (spring) and almost full (winter), correlation was obtained between PM10 concentrations determined by both methods. The result of the Wilcoxon test (for $p < 0.05$) confirmed the consistency of the results from both methods only for the winter period. The $p$-values of the Wilcoxon test for winter and spring sessions were 0.08 and 0.01, respectively. Thus, hypothesis #1 can only be considered true for the winter campaign period. In the season-to-season comparison (Mann-Whitney U test, $p < 0.05$), no statistically significant differences were found. In the

winter-spring relationship for PM10 concentrations determined by CPM, the test probability was 0.40 and by GM, 0.86.

For both methods, the highest daily PM10 concentration values were obtained in January, which corresponded to negative air temperature, very weak advection and lack of precipitation. Such meteorological conditions significantly did not favour dilution and deposition of pollutants. On the other hand, both in the winter and spring seasons, the lowest PM10 concentrations were observed during days characterised by opposite values of the above meteorological parameters. This may suggest that in the so-called 'heating season', local emissions are responsible for air quality in terms of dustiness [19,54].

During the second campaign, significant differences became evident in PM10 concentration values determined by the two methods. It is difficult to explain the reason for a significant disproportion during the first five days of spring measurements. Although there is no correlation between PM10 concentration and wind direction and velocity, the movement of air masses from the S direction (the least numerous buildings—Figure 1) was observed at this time. The CPM aspiration head was distant from the GM head by 18 m to the east. Perhaps this distance was sufficient for the two receptors to be in different air streams, the 'purer' (CPM) and more 'polluted' (GM). The following facts were also of importance: ideally to the south of the GM aspirator head, there was an outlet of a cyclone serving exhaust from a production hall in a nearby woodwork business; and the GM aspirator was located closer to buildings with active emitters and to home gardens where field work (digging and fertilising beds) was initiated at the end of March. These facts may also have influenced a slightly higher value of PM10 concentration determined by the gravimetric method in the spring campaign compared to the winter one.

For the January–February period, a significant statistical relationship was found in both cases between PM10 concentration and T and P. Similar results regarding the mutual relationship between aerosol concentration and temperature were found in a study in a Czech village [55]. The increase in PM10 concentration corresponded to the intensification of the use of domestic emission sources forced by a decrease in outdoor temperature. At the same time, the occurrence of precipitation (regardless of temperature) effectively reduced the mass of aerosol reaching the receptors. During the spring observations, a clear lack of correlation between PM10 and T is noticeable, which may be due to the fact that the variability of T values during the spring campaign was more than three times lower than in winter. For both full observations, no correlation was found between PM10 concentration and Ap and Wd and Ws. In the last case, there was an exception in winter for GM aspiration.

In comparison with the data received during winter and spring measurement campaigns in different places, results from Kotórz Mały were similar to other small villages, namely Przezchlebie, PL; 67 $\mu g/m^3$ (winter) and 24 $\mu g/m^3$ (spring) [45]; Zloukovice, CZ; 38 $\mu g/m^3$ (spring) [54]; and Brzezina, PL; 80 $\mu g/m^3$ (winter) [48].

### *4.2. Comparison of EDXRF and AAS—PM10-Bound Elements*

Figure 6 presents the results of the cluster analysis in the form of dendrograms. The clusters were separately created for winter and spring data. Dendrograms were constructed to assess the multidimensional structure of the elemental concentration [56]. The assembled Euclidean distances between the compositional points with clr-transformed coordinates were used to create a dissimilarity matrix. The dendrograms were constructed using Ward's clustering method. For the winter campaign, there were two clearly distinguished clusters in the dendrogram, with the structure predominantly defined by groups of metals, namely Ca, Fe and K in the first group and Zn, Pb, Cu, Mn, Cr and Ni in the second group. The elements in the first group mainly come from natural sources, including form surface erosion of soils and from plants [18,55,57–59]. Elements in the second group are associated with anthropogenic sources, mainly from coal and biomass burning [54,60–64] and from the exploitation of motor vehicles [65–69].

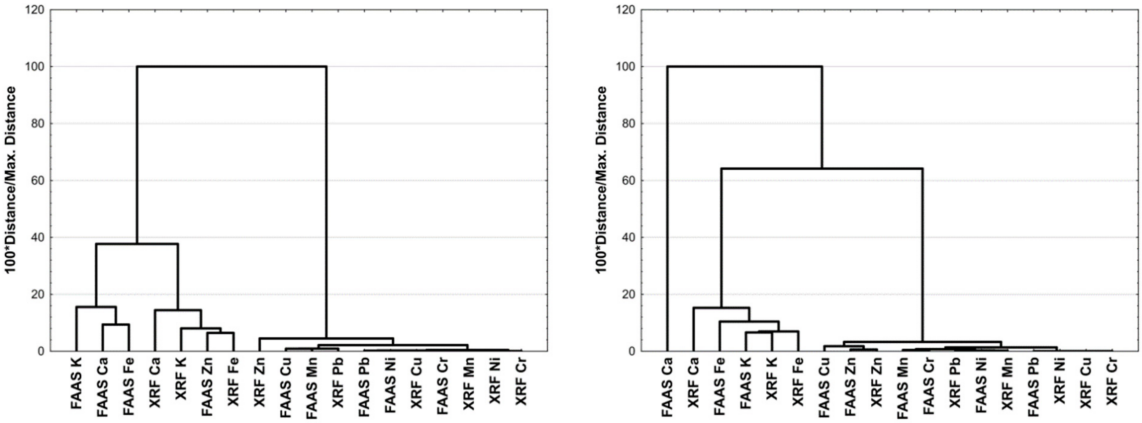


**Figure 6.** Dendrograms of the elemental composition of PM10 in relation to the analytical method EDXRF and AAS (winter on the left and spring on the right).

For spring observations, three main clusters were found. At first glance, two of them would be known as winter clusters, but the situation with AAS Ca is interesting and definitely stands out. This is most likely the result of human activity and represents an isolated incident related to local gardening. As mentioned earlier, the GM sampler was located close to domestic gardens where the inhabitants very often fertilised with ground eggshells to enrich the soil.

Table 5 presents a summary of the results of Spearman correlations between elements determined using EDXRF and AAS. Excluding correlations between PM10 concentrations and elements determined in PM10, the winter period data showed a higher number of statistically significant correlations between variables than did the spring data (143 vs. 40, respectively). For the winter period, a statistically significant high correlation (>0.7) was found for seven pairs of variables determined by the EDXRF technique and for 11 pairs of variables determined by the AAS technique. However, for the elements determined by EDXRF, Fe−Mn and Zn−Pb correlations can be described by a linear relationship. For the elements determined by AAS, a linear relationship was found for Zn−Mn and Ca−Mn pairs. In the remaining cases, there were no linear relationships or they were described by a non-monotonic function. For the spring period, statistically significant high correlation was found for 10 pairs of variables determined by the EDXRF technique and for only 1 pair of variables determined by the AAS technique. For the elements determined here by EDXRF, the correlations Fe−Mn, Cr−Ni, K−Mn, Fe−K, Ca−Fe and Ca−K can be described by a linear relationship. In the case of elements determined by the AAS technique, no linear relationships occurred. In other cases, there were no linear relationships or they were described by a non-monotonic function. Considering the correlations of the same elements that were determined by different methods, 6 pairs in the winter period (Cu−Ni, Cu−Cu, Fe−Zn, Zn−Zn, Ni−Pb and K−Ni) had statistically significant high correlations. For the spring period, no statistically significant high correlations were found. In other cases, for example, for statistically significant compounds with respect to elemental composition, some correlations may explain the origin of the aerosol, but it does not seem appropriate to draw specific conclusions from such an analysis.

In general, statistically significant correlations of individual element concentrations with PM10 concentrations became apparent in the studies conducted in the winter. High correlations (>0.7) for non-destructive techniques occurred for Fe, Zn, Pb and K. In the case of AAS, such correlations did not occur other than for Cu and Pb. In the spring campaign, for EDXRF, such situations were observed only for Fe, while for AAS, they were observed for Cr, Fe and Ni.

**Table 5.** Spearman correlation. Relationship between the PM10 concentration and meteorological parameters. Bold values are statistically significant with $p = 0.05$. Normal font relates to winter data and italic font to spring data.

| | CPM PM10 | XRF Cr | XRF Mn | XRF Fe | XRF Ni | XRF Cu | XRF Zn | XRF Pb | XRF K | XRF Ca | GM PM10 | AAS Cr | AAS Mn | AAS Fe | AAS Ni | AAS Cu | AAS Zn | AAS Pb | AAS K | AAS Ca |
|---|---|---|---|---|---|---|---|---|---|---|---|---|---|---|---|---|---|---|---|---|
| CPM PM10 | | 0.23 | **0.63** | **0.70** | **0.45** | **0.69** | **0.89** | **0.77** | **0.79** | **0.56** | | | | | | | | | | |
| XRF Cr | *0.32* | | **0.60** | **0.62** | **0.49** | **0.46** | **0.31** | 0.20 | 0.21 | **0.46** | | **0.43** | **0.31** | **0.29** | 0.27 | 0.20 | 0.28 | 0.17 | 0.23 | **0.31** |
| XRF Mn | ***0.58*** | ***0.72*** | | **0.89** | **0.54** | **0.63** | **0.54** | **0.36** | **0.43** | **0.74** | | **0.49** | **0.57** | **0.59** | **0.41** | **0.41** | **0.47** | **0.33** | **0.48** | **0.55** |
| XRF Fe | ***0.69*** | ***0.76*** | ***0.93*** | | **0.66** | **0.72** | **0.61** | **0.45** | **0.47** | **0.82** | | **0.60** | **0.59** | **0.67** | **0.52** | **0.58** | **0.50** | **0.35** | **0.54** | **0.61** |
| XRF Ni | *0.28* | ***0.84*** | ***0.65*** | ***0.69*** | | **0.64** | **0.38** | **0.39** | **0.37** | **0.58** | | **0.40** | **0.45** | **0.60** | **0.63** | **0.44** | **0.39** | **0.29** | **0.34** | **0.50** |
| XRF Cu | *0.19* | *0.18* | *0.28* | *0.25* | *0.35* | | **0.68** | **0.60** | **0.63** | **0.56** | | **0.65** | **0.60** | **0.68** | **0.70** | **0.75** | **0.54** | **0.42** | **0.53** | **0.63** |
| XRF Zn | *0.51* | *0.36* | ***0.57*** | ***0.56*** | *0.33* | *0.12* | | **0.81** | **0.79** | **0.42** | | **0.64** | **0.68** | **0.70** | **0.58** | **0.59** | **0.74** | **0.61** | **0.67** | **0.61** |
| XRF Pb | *0.25* | *−0.04* | *0.27* | *0.18* | *0.13* | *0.12* | ***0.72*** | | **0.90** | 0.19 | | **0.58** | **0.63** | **0.63** | **0.70** | **0.52** | **0.61** | **0.61** | **0.65** | **0.55** |
| XRF K | ***0.74*** | ***0.65*** | ***0.87*** | ***0.95*** | ***0.56*** | *0.16* | ***0.54*** | *0.19* | | 0.25 | | **0.61** | **0.67** | **0.60** | **0.70** | **0.50** | **0.66** | **0.63** | **0.68** | **0.58** |
| XRF Ca | ***0.59*** | ***0.71*** | ***0.88*** | ***0.97*** | ***0.67*** | *0.17* | *0.50* | *0.11* | ***0.94*** | | | **0.38** | **0.47** | **0.49** | **0.36** | **0.49** | **0.45** | 0.25 | **0.34** | **0.62** |
| GM PM10 | | | | | | | | | | | | **0.73** | **0.80** | **0.82** | **0.73** | **0.63** | **0.76** | **0.68** | **0.75** | **0.72** |
| AAS Cr | ***0.61*** | *0.23* | *0.36* | *0.46* | *0.28* | *0.16* | *0.29* | *0.24* | *0.47* | *0.43* | ***0.85*** | | **0.68** | **0.68** | **0.74** | **0.74** | **0.68** | **0.65** | **0.58** | **0.64** |
| AAS Mn | *0.23* | *−0.11* | *0.08* | *−0.08* | *−0.10* | *−0.05* | *0.06* | *0.14* | *−0.08* | *−0.16* | *0.42* | *0.35* | | **0.73** | **0.71** | **0.57** | **0.82** | **0.64** | **0.59** | **0.82** |
| AAS Fe | ***0.64*** | *0.36* | ***0.55*** | ***0.59*** | *0.36* | *0.35* | *0.45* | *0.13* | ***0.61*** | ***0.55*** | ***0.80*** | ***0.70*** | *0.26* | | **0.78** | **0.66** | **0.64** | **0.57** | **0.66** | **0.71** |
| AAS Ni | ***0.55*** | *0.16* | *0.36* | *0.38* | *−0.02* | *−0.31* | *0.15* | *−0.12* | *0.46* | *0.35* | ***0.77*** | ***0.56*** | *0.19* | ***0.55*** | | **0.69** | **0.66** | **0.69** | **0.59** | **0.71** |
| AAS Cu | *−0.29* | *0.06* | *−0.17* | *−0.20* | *0.07* | *−0.12* | *−0.16* | *−0.04* | *−0.40* | *−0.21* | *−0.27* | *−0.22* | *0.16* | *−0.29* | *−0.39* | | **0.55** | **0.52** | **0.50** | **0.65** |
| AAS Zn | *−0.17* | *0.36* | *0.29* | *0.22* | *0.43* | *0.18* | *0.38* | *0.18* | *0.11* | *0.28* | *0.29* | *0.30* | *−0.05* | *0.48* | *0.06* | *0.08* | | **0.75** | **0.58** | **0.74** |
| AAS Pb | *−0.21* | *0.32* | *0.01* | *0.02* | *0.44* | *0.22* | *−0.29* | *−0.29* | *−0.11* | *0.02* | *0.12* | *0.26* | *−0.08* | *0.28* | *0.17* | *0.07* | ***0.52*** | | **0.65** | **0.59** |
| AAS K | *0.34* | *0.14* | *0.28* | *0.24* | *0.03* | *0.09* | *0.06* | *−0.15* | *0.23* | *0.24* | *0.48* | *0.14* | *0.15* | 0.53 | *0.27* | *0.03* | *0.22* | *0.11* | | **0.48** |
| AAS Ca | *−0.28* | ***−0.55*** | *−0.50* | ***−0.52*** | *−0.23* | *0.05* | *−0.25* | *0.14* | ***−0.54*** | *−0.47* | *−0.44* | *−0.37* | *0.07* | *−0.43* | ***−0.66*** | *0.36* | *−0.23* | *−0.24* | *0.10* | |

For the purpose of comparison, Table 6 presents the average values of element concentrations in particulate matter determined at different locations. Due to differences in concentration values of particular elements determined by the two different methods, the analytical techniques used by the quoted authors are also given. Attention is drawn by significantly higher concentration values of most analytes compared to the results obtained in rural areas in the Czech Republic and France. The differences most probably result from lower ecological awareness of the Polish rural population and their use of much older and outdated heating systems.

**Table 6.** The mean concentration of PM10-bound elements at various sites in the rural area.

| Place; Country | Season | Technique | Cr ng/m$^3$ | Mn ng/m$^3$ | Fe ng/m$^3$ | Ni ng/m$^3$ | Cu ng/m$^3$ | Zn ng/m$^3$ | Pb ng/m$^3$ | K ng/m$^3$ | Ca ng/m$^3$ | References |
|---|---|---|---|---|---|---|---|---|---|---|---|---|
| Kotórz Mały, PL | winter | AAS | 4.84 | 9.07 | 222 | 1.46 | 6.49 | 68.6 | 3.36 | 306 | 251 | *this study* |
| Kotórz Mały, PL | spring | AAS | 18.0 | 22.9 | 421 | 11.0 | 53.3 | 29.3 | 1.68 | 318 | 1719 | *this study* |
| Kotórz Mały, PL | winter | EDXRF | 1.28 | 4.21 | 114 | 0.61 | 2.44 | 38.4 | 12.9 | 148 | 220 | *this study* |
| Kotórz Mały, PL | spring | EDXRF | 2.03 | 8.48 | 324 | 0.82 | 2.22 | 32.2 | 10.0 | 164 | 472 | *this study* |
| Grajów, PL | spring | SSMS | | 8.0 | 280 | 19.0 | 12.0 | 80.0 | | | | [46] |
| Przezchlebie, PL | winter | GFAAS | 23.9 | 16.8 | 443 | 4.95 | 11.1 | 135 | 53.4 | | | [45] |
| Przezchlebie, PL | spring | GFAAS | 239.4 | 12.3 | 217 | 6.20 | 2.60 | 72.7 | 20.4 | | | [45] |
| Montagney, FR | winter | ICPMS; INAA | 1.2 | 3.8 | 105 | 1.50 | 4.50 | 23.3 | 9.70 | 267 | 234 | [25] |
| Zloukovice, CZ | spring | ICP-MS | 0.5 | 0.5 | | | | 16.8 | 13.1 | | | [54] |
| Brzezina, PL | winter | EDXRF | 30 | 40 | 500 | | 32.0 | 188 | 85.0 | 648 | 376 | [48] |

Table 7 summarises the results of the Wilcoxon test, which aims to verify the hypotheses stating that: #2—the concentration levels of PM10-bound elements are identical regardless of the method of sampling and analysis; and #3—the concentration levels of PM10 and PM10-bound elements are identical regardless of the season (winter-spring relation). It was suggested in Section 3.2 that the position of the median in Figures 4 and 5 indicates equivalence in concentrations of Mn, Ni, Zn and Ca in winter and Fe and Zn in spring. The results of the Wilcoxon test clearly indicate that these suggestions were true for the observations from the second measurement campaign (in spring) and only for Ca in winter. For the winter campaign, only the contributions of Mn, Ni and Zn to PM10 are equivalent for both techniques. Thus, hypothesis #2 can be considered true only for a very limited range.

**Table 7.** EDXRF-AAS *p*-values of Wilcoxon test for winter and spring sessions. Bold values indicate that the results are significant with $p < 0.05$.

| Relation | Mass Concentration | Elements Share in PM10 |
|---|---|---|
| | Winter session | |
| EDXRF-AAS Cr | 0.000 | 0.000 |
| EDXRF-AAS Mn | 0.001 | **0.368** |
| EDXRF-AAS Fe | 0.000 | 0.000 |
| EDXRF-AAS Ni | 0.000 | 0.250 |
| EDXRF-AAS Cu | 0.000 | 0.000 |
| EDXRF-AAS Zn | 0.000 | **0.082** |
| EDXRF-AAS Pb | 0.000 | 0.000 |
| EDXRF-AAS K | 0.000 | 0.000 |
| EDXRF-AAS Ca | **0.238** | 0.001 |
| | Spring session | |
| EDXRF-AAS Cr | 0.000 | 0.001 |
| EDXRF-AAS Mn | 0.001 | 0.035 |
| EDXRF-AAS Fe | **0.099** | **0.609** |
| EDXRF-AAS Ni | 0.000 | 0.001 |
| EDXRF-AAS Cu | 0.000 | 0.001 |
| EDXRF-AAS Zn | **0.820** | 0.023 |
| EDXRF-AAS Pb | 0.001 | 0.001 |
| EDXRF-AAS K | 0.005 | 0.035 |
| EDXRF-AAS Ca | 0.000 | 0.003 |

Hypothesis #3 (Table 8) may be considered true for a much larger range. The levels of PM10 concentrations determined by the compared methods for the winter-spring relationship are very similar. As far as elements are concerned, the comparison of winter and spring results from the EDXRF technique did not provide different results with the exception of chromium and elements of mainly natural origin. In the case of AAS, the hypothesis is true only for potassium.

**Table 8.** EDXRF-AAS *p*-values of Mann-Whitney U test for season-to-season data. Bold values indicate that the results are significant with $p < 0.05$.

| | CPM PM10 | GM PM10 | Cr | Mn | Fe | Ni | Cu | Zn | Pb | K | Ca |
|---|---|---|---|---|---|---|---|---|---|---|---|
| CPM-EDXRF | **0.400** | | 0.002 | 0.000 | 0.000 | **0.824** | **0.267** | **0.178** | **0.281** | **0.787** | 0.006 |
| GM-AAS | | **0.862** | 0.000 | 0.000 | 0.000 | 0.000 | 0.000 | 0.005 | 0.000 | **0.055** | 0.000 |

### *4.3. Identification of Sources of PM10 and PM10-Bound Elements*

As previously mentioned, the order of elements during the winter measurement campaign as determined by EDXRF was as follows: Ca > K > Fe > Zn > Pb > Mn > Cu > Cr > Ni. The order was almost identical for AAS: K > Ca > Fe > Zn > Mn > Cu > Cr > Pb > Ni. In spring, the order for EDXRF was Ca > Fe > K > Zn > Pb > Mn > Cu > Cr > Ni; for AAS, it was Ca > Fe > K > Cu > Zn > Mn > Cr > Ni > Pb. Mach et al. [18] presented results from the same receptor and the same apparatus (EDXRF) but they were obtained during the summer campaign. During the summer season, the order of elements in Kotorz Maly was Ca > Fe > K > Zn > Cu > Mn > Cr > Pb > Ni. Comparing only the data from the device (PX-375 Horiba, Osaka, Japan) both in the summer and the spring, the order of the first four and the last place elements was identical (in the winter, the sequence differed slightly). Significant differences appeared in the order of Pb, Mn, Cr and Cu, which may indicate differences in the contribution of individual sources in relation to the warm and cold seasons. In Mach et al. [18], the authors identified five significant sources based on records with an interval of 1 h which determined aero-sanitary conditions in the village in the summer: mineral matter emission, traffic emission, remote low-stack emission, industrial (local and regional) sources and fossil fuel and/or biomass combustion in local households.

Factor analysis (FA) was used to determine the types of sources which were affecting air quality within the receptor. Factor analysis, such as PCA, is a frequently used statistical tool to determine the sources of PM [70,71].

Factor analysis was performed according to the method described by Pohlmann [72]. This was performed by utilising the orthogonal transformation method with Varimax rotation and retention of principal components for which the eigenvalues were close to the unit. The selection of factors was mainly based on Cattell's scree test [73], whereas the ultimate verification was undertaken by an analysis of residual correlations. Factor loadings indicate the correlation of each element with each component and are related to the source emission composition. In order to avoid the trap of too few variables in relation to the cases, only those elements that showed a high correlation for each method were selected for analysis, that is, Ca, Cu, Fe, Mn and Zn. Elements considered to be derived from both natural and anthropogenic emissions were represented in the tested group.

The eigenvalues of the correlation matrix (Table 9) reflect the significance of the principal components in explaining the information resources of the input variables (percentage share of variation in the dataset). The higher the correlation coefficient of a variable with a component, the more relevant this variable is to the component. In the analysed cases, the first two principal components were decisive for winter (both methods) and spring (EDXRF) and describe 88%, 93.5% and 88.2% of the variability of the original data, respectively. For the analysis of the spring data (AAS), three main factors were identified that explain almost 85% of the variability.

**Table 9.** Eigenvalues of the correlation matrix.

| | No. of Factor | Eigenvalues | % of Total Variance | Accumulated Eigenvalues | Cumulative % of Explained Variance |
|---|---|---|---|---|---|
| EDXRF winter | 1 | 3.58 | 71.68 | 3.58 | 71.7 |
| | 2 | 0.82 | 16.45 | 4.41 | **88.1** |
| AAS winter | 1 | 3.86 | 77.39 | 3.86 | 77.4 |
| | 2 | 0.8 | 16.07 | 4.67 | **93.5** |
| EDXRF spring | 1 | 3.38 | 67.53 | 3.38 | 67.5 |
| | 2 | 1.03 | 20.65 | 4.41 | **88.2** |
| AAS spring | 1 | 1.97 | 39.43 | 1.97 | 39.4 |
| | 2 | 1.38 | 27.54 | 3.35 | 67.0 |
| | 3 | 0.89 | 17.76 | 4.24 | **84.7** |

The principal components obtained are interpreted on the basis of the values of their coefficients, which are also the coefficients of the linear correlation between the input variables and the principal components. For winter (EDXRF), the first principal component carried almost 72% of the information contained primarily in variables representing elements from natural sources, while the second principal component explained more than 16% of the variation in the data through a variable identified with elements from anthropogenic sources (Table 10). During 49 days of observations, there was no snow cover in Kotórz Mały, indicating that the main source of Mn, Fe and Ca was resuspension from the surface of the fields surrounding the village. Local energy sources of conventional fuel combustion and transport were responsible for Cu and Zn emissions. As for data obtained from AAS analysis, the first principal component carried almost 78% and the second 16% of the information. Here, as in the case from EDXRF data, the same main emission sources can be distinguished, with additional emphasis on the impact of industrial influx emissions, most probably from the Opole cement plant (Cu) [74].

**Table 10.** Factor loadings matrix for the PM10 chemical composition obtained after applying the factor analysis.

| | **EDXRF Winter** | | **AAS Winter** | | **EDXRF Spring** | | **AAS Spring** | | |
|---|---|---|---|---|---|---|---|---|---|
| | F1 | F2 | F1 | F2 | F1 | F2 | F1 | F2 | F3 |
| Mn | **0.868** | 0.362 | **0.846** | 0.479 | 0.536 | **0.814** | 0.446 | −0.615 | 0.362 |
| Fe | **0.833** | 0.489 | **0.958** | 0.210 | 0.667 | **0.702** | **0.954** | 0.063 | −0.133 |
| Cu | 0.218 | **0.895** | 0.180 | **0.966** | **0.875** | −0.022 | −0.091 | −0.051 | **0.970** |
| Zn | 0.342 | **0.853** | **0.808** | 0.520 | −0.041 | **0.926** | **0.889** | 0.051 | 0.023 |
| Ca | **0.933** | 0.154 | **0.934** | 0.078 | **0.871** | 0.371 | −0.244 | **−0.890** | −0.041 |

For spring (EDXRF), the first principal component carried 67.5% and the second 20% of the information. The main sources of emission were transport, surface erosion and low-stack emission from rural household heating. In the case of data collected by AAS analysis, the cumulative explained variance reached almost 85%, with three factors contributing 39.4%, 27.5% and 17.8%, respectively. Here, the same sources as identified for the EDXRF results were responsible for the emissions, with the additional influence of an atypical anthropogenic source, namely fertilisation of soils with ground eggshells (Ca).

## 5. Conclusions

The results of monitoring PM10 concentrations in a typical rural area during the winter and spring season using two measurement methods (GM and CPM) indicate that:

- The concentrations of PM10 measured by both methods in the winter were equivalent. In the case of the spring season, only after the fifth day of measurements was it observed that the PM10 concentrations were comparable, with both methods indicating the same trend of increase and decrease in PM10 concentrations.
- The lack of significant seasonal differences in PM10 concentrations probably results from the fact that April in Poland is also included in the heating season. Significant changes in PM concentrations were noticeable with the beginning and end of the heating season, which is conventionally assumed to last from 15 October to 25 April.
- Atmospheric conditions had a significant impact on PM10 concentrations. The highest concentrations were recorded at weak advection, lack of precipitation and temperature drop.

Conclusions on the elemental composition analysis of PM10 using two methods (destructive AAS and non-destructive EDXRF) are as follows:

- Both methods showed that Ca, Fe and K had the highest mass shares in PM10 mass both in winter and spring.
- The indications of both methods slightly differed in the case of elements with the lowest share in PM10 mass. In winter, the order for AAS was Cr > Pb > Ni, while in spring, it was Cr > Ni > Pb. For EDXRF, the order was the same for the elements with the lowest concentrations: Cu > Cr > Ni.
- Clear discrepancies were observed in the concentrations of PM10-bound elements in individual seasons. Higher concentrations of PM-bound elements and, thus, higher shares in PM mass were observed in the spring (3.2% for EDXRF; 5.2% for AAS) compared to the winter (1.6% for EDXRF; 2.0% for AAS).

The assessment of the origin of PM10 through factor analysis and the analysis of the correlation between the examined factors showed:

- In winter, the concentration of PM10 and its elemental composition were determined by two components: natural sources (erosion from soil that was not covered with snow at the time of measurement, erosion from plants) and anthropogenic sources, that is, combustion of coal and biomass in home furnaces and combustion of fuel in car engines. In spring, the concentration and elemental composition of

PM10 was determined by the two sources indicated above as well as by the local horticultural activity.

- The amount of variance explained by factor analysis varies in both seasons, which suggests a variability in the impact of different emission sources. With the simultaneous influence of several sources or the presence of one dominant source, precise determination of the origin of PM is difficult and requires further analysis.

Comparing the results using different methods (GM vs. CPM and AAS vs. EDXRF) showed that:

- Hypothesis 1 is only true for the winter campaign period.
- Hypothesis 2 can be considered true only for the second measurement campaign in the case of spring measurements and only for Ca in the winter.
- Hypothesis 3 may be considered true for PM10 and PM10-bound elements with the exception of chromium and crustal elements for EDXRF. For AAS, the hypothesis is true only for potassium.

In order to compare the results obtained with different methods, it is necessary to ensure that both types of measuring and sampling equipment are located directly next to each other. The conducted research indicated that even a small distance (18 m in this study) may influence the variability of the results.

The conducted measurements and analysis of the results indicate a plan for further research, which should also include the fine PM fraction, for example, PM2.5. The fine particles are more enriched in trace elements (Cr, Ni, Pb, Cu) than in coarse. Analysis of fine PM could provide additional information on the origin of the PM at the receptor as well as the equivalence of the methods. The results obtained in this study do not exclude any of the proposed methods for the determination of concentrations and elemental composition, as both provided similar conclusions regarding the origin of PM10 in the receptor. Although the measurement method and its equivalence to the reference method prove the reliability of the results, an important source of information about the factors influencing these results requires a detailed correlation analysis, for example, between concentrations of elements and atmospheric conditions as well as the source apportionment using the methods of factor analysis (FA), principal components analysis (PCA) or positive matrix factorisation (PMF). A limitation for a complete analysis of the problem was the low number of records collected (for the spring season). The authors plan further research in this area, devoted to improving the accuracy of the quantitative analysis. A dedicated calibration procedure will be further developed to obtain accurate and more precise results.

**Author Contributions:** Conceptualization, T.M., T.O., W.R.-K., J.R., P.R.-K. and G.M.; Formal analysis, M.B. and A.K.; Investigation, T.M. and T.O.; Methodology, T.M., T.O., W.R.-K. and G.M.; Resources, T.M. and T.O.; Supervision, J.R.; Validation, J.R. and Z.Z.; Writing—Original draft, T.M., T.O. and K.B.; Writing—Review & editing, W.R.-K. and Z.Z. All authors have read and agreed to the published version of the manuscript.

**Funding:** The project was funded with private initiative.

**Informed Consent Statement:** Not applicable.

**Acknowledgments:** The authors wish to kindly thank Krystyna Wieczorek and Wacław Siudyła for their help in conducting surveys among the residents of Kotórz Mały. The authors also wish to kindly thank the authorities of the Mechanics Department of the Opole University of Technology for financial support, without which it would not have been possible to carry out this research project. The authors would like to give special thanks to Piotr Długosz for allowing the research apparatus to be located on his property and for providing a source of electricity.

**Conflicts of Interest:** The authors declare they have no conflict of interest and no financial interests.

**Statements & Declarations:** All authors declare that they have met all ethical criteria and have agreed to participate in the publication. All authors have read and agreed to the published version of the manuscript. The authors declare the availability of data and materials.

**Compliance with Ethical Standards:** The authors declare that no studies involving humans and/or animals were carried out.

## References


1. Wang, J.; Pan, Y.; Tian, S.; Chen, X.; Wang, L.; Wang, Y. Size distributions and health risks of particulate trace elements in rural areas in northeastern China. *Atmos. Res.* **2016**, *168*, 191–204. [CrossRef]
2. Roy, D.; Seo, Y.-C.; Kim, S.; Oh, J. Human health risk assessment for airborne PM10-bound metals in Seoul, Korea. *Env. Sci Pollut. Res.* **2019**, *26*, 24247–24261. [CrossRef]
3. Crilley, L.R.; Lucarelli, F.; Bloss, W.J.; Harrison, R.M.; Beddows, D.C.; Calzolai, G.; Nava, S.; Valli, G.; Bernardoni, V.; Vecchi, R. Source apportionment of fine and coarse particles at a roadside and urban background site in London during the 2012 summer ClearfLo campaign. *Environ. Pollut.* **2017**, *220*, 766–778. [CrossRef] [PubMed]
4. Santos, M.L.O.; Santos, K.M.B.; França, E.J. Comparison Between Edxrf and Faas for Zn Determination in Terrestrial Mollusks. In Proceedings of the 2015 International Nuclear Atlantic Conferen, São Paulo, Brazil, 4–9 October 2015; p. 7.
5. Visser, S.; Slowik, J.G.; Furger, M.; Zotter, P.; Bukowiecki, N.; Canonaco, F.; Flechsig, U.; Appel, K.; Green, D.C.; Tremper, A.H.; et al. Advanced source apportionment of size-resolved trace elements at multiple sites in London during winter. *Atmos. Chem. Phys.* **2015**, *15*, 11291–11309. [CrossRef]
6. Venter, A.D.; Van Zyl, P.G.; Beukes, J.P.; Josipovic, M.; Hendriks, J.; Vakkari, V.; Laakso, L. Atmospheric trace metals measured at a regional background site (Welgegund) in South Africa. *Atmos. Chem. Phys.* **2017**, *17*, 4251–4263. [CrossRef]
7. Tahri, M.; Benchrif, A.; Bounakhla, M.; Benyaich, F.; Noack, Y. Seasonal variation and risk assessment of PM2.5 and PM2.5-10 in the ambient air of Kenitra, Morocco. *Environ. Sci. Process. Impacts* **2017**, *19*, 1427–1436. [CrossRef]
8. Enamorado-Báez, S.M.; Gómez-Guzmán, J.M.; Chamizo, E.; Abril, J.M. Levels of 25 trace elements in high-volume air filter samples from seville (2001–2002): Sources, enrichment factors and temporal variations. *Atmos. Res.* **2015**, *155*, 118–129. [CrossRef]
9. Contini, D.; Cesari, D.; Donateo, A.; Chirizzi, D.; Belosi, F. Characterization of PM10 And PM2.5 and their metals content in different typologies of sites in South-Eastern Italy. *Atmosphere* **2014**, *5*, 435–453. [CrossRef]
10. Canepari, S.; Astolfi, M.L.; Farao, C.; Maretto, M.; Frasca, D.; Marcoccia, M.; Perrino, C. Seasonal variations in the chemical composition of particulate matter: A case study in the Po Valley. Part II: Concentration and solubility of micro- and trace-elements. *Environ. Sci. Pollut. Res.* **2014**, *21*, 4010–4022. [CrossRef]
11. Alleman, L.Y.; Lamaison, L.; Perdrix, E.; Robache, A.; Galloo, J.C. PM10 metal concentrations and source identification using positive matrix factorization and wind sectoring in a French industrial zone. *Atmos. Res.* **2010**, *96*, 612–625. [CrossRef]
12. Zunic, B.; Peter, S. *World's largest Science, Technology & Medicine Open Access Book Publisher*; INTECH: Houston, TX, USA, 2018; pp. 267–322.
13. Ukaogo, P.O.; Ewuzie, U.; Onwuka, C.V. Environmental pollution: Causes, effects, and the remedies. In *Microorganisms for Sustainable Environment and Health*; Elsevier: Amsterdam, The Netherlands, 2020; ISBN 9780128190012.
14. Yadav, I.C.; Devi, N.L. Biomass burning, regional air quality, and climate change. In *Encyclopedia of Environmental Health*; Elsevier: Amsterdam, The Netherlands, 2019; ISBN 9780444639523.
15. Coronas, M.V.; Bavaresco, J.; Rocha, J.A.V.; Geller, A.M.; Caramão, E.B.; Rodrigues, M.L.K.; Vargas, V.M.F. Attic dust assessment near a wood treatment plant: Past air pollution and potential exposure. *Ecotoxicol. Environ. Saf.* **2013**, *95*, 153–160. [CrossRef] [PubMed]
16. Majewski, G.; Rogula-Kozlowska, W.; Rozbicka, K.; Rogula-Kopiec, P.; Mathews, B.; Brandyk, A. Concentration, chemical composition and origin of PM1: Results from the first long-term measurement campaign in Warsaw (Poland). *Aerosol Air Qual. Res.* **2018**, *18*, 636–654. [CrossRef]
17. Rogula-Kozłowska, W.; Majewski, G.; Błaszczak, B.; Klejnowski, K.; Rogula-Kopiec, P. Origin-Oriented Elemental Profile of Fine Ambient Particulate Matter in Central European Suburban Conditions. *Int. J. Environ. Res. Public Health* **2016**, *13*, 715. [CrossRef] [PubMed]
18. Mach, T.; Rogula-Kozłowska, W.; Bralewska, K.; Majewski, G.; Rogula-Kopiec, P.; Rybak, J. Impact of municipal, road traffic and natural sources on PM10: The hourly variability at a rural site in Poland. *Energies* **2021**, *14*, 2654. [CrossRef]
19. Olszowski, T. Influence of individual household heating on PM2.5 concentration in a rural settlement. *Atmosphere* **2019**, *10*, 782. [CrossRef]
20. Błaszczyk, E.; Rogula-Kozłowska, W.; Klejnowski, K.; Fulara, I.; Mielżyńska-Švach, D. Polycyclic aromatic hydrocarbons bound to outdoor and indoor airborne particles (PM2.5) and their mutagenicity and carcinogenicity in Silesian kindergartens, Poland. *Air Qual. Atmos. Heal.* **2016**, *10*, 389–400. [CrossRef]
21. Khoshsima, M.; Ahmadi-Givi, F.; Bidokhti, A.A.; Sabetghadam, S. Impact of meteorological parameters on relation between aerosol optical indices and air pollution in a sub-urban area. *J. Aerosol Sci.* **2014**, *68*, 46–57. [CrossRef]
22. Massey, D.D.; Kulshrestha, A.; Taneja, A. Particulate matter concentrations and their related metal toxicity in rural residential environment of semi-arid region of India. *Atmos. Environ.* **2013**, *67*, 278–286. [CrossRef]
23. Grange, S.K.; Salmond, J.A.; Trompetter, W.J.; Davy, P.K.; Ancelet, T. Effect of atmospheric stability on the impact of domestic wood combustion to air quality of a small urban township in winter. *Atmos. Environ.* **2013**, *70*, 28–38. [CrossRef]
24. Maenhaut, W.; Vermeylen, R.; Claeys, M.; Vercauteren, J.; Matheeussen, C.; Roekens, E. Assessment of the contribution from wood burning to the PM10 aerosol in Flanders, Belgium. *Sci. Total Environ.* **2012**, *437*, 226–236. [CrossRef]

25. Gaudry, A.; Moskura, M.; Mariet, C.; Ayrault, S.; Denayer, F.; Bernard, N. Inorganic pollution in PM10 particles collected over three French sites under various influences: Rural conditions, traffic and industry. *Water Air Soil Pollut.* **2008**, *193*, 91–106. [CrossRef]
26. Khedairia, S.; Khadir, M.T. Impact of clustered meteorological parameters on air pollutants concentrations in the region of Annaba, Algeria. *Atmos. Res.* **2012**, *113*, 89–101. [CrossRef]
27. European Commission. *Ambient Air Pollution by AS, CD and NI Compounds*; European Commission: Luxembourg, 2000; ISBN 9289420545.
28. Bilo, F.; Borgese, L.; Wambui, A.; Assi, A.; Zacco, A.; Federici, S.; Eichert, D.M.; Tsuji, K.; Lucchini, R.G.; Placidi, D.; et al. Comparison of multiple X-ray fluorescence techniques for elemental analysis of particulate matter collected on air filters. *J. Aerosol Sci.* **2018**, *122*, 1–10. [CrossRef] [PubMed]
29. Diapouli, E.; Manousakas, M.; Vratolis, S.; Vasilatou, V.; Maggos, T.; Saraga, D.; Grigoratos, T.; Argyropoulos, G.; Voutsa, D.; Samara, C.; et al. Evolution of air pollution source contributions over one decade, derived by PM10 and PM2.5 source apportionment in two metropolitan urban areas in Greece. *Atmos. Environ.* **2017**, *164*, 416–430. [CrossRef]
30. Lomboy, M.F.T.C.; Quirit, L.L.; Molina, V.B.; Dalmacion, G.V.; Schwartz, J.D.; Suh, H.H.; Baja, E.S. Characterization of particulate matter 2.5 in an urban tertiary care hospital in the Philippines. *Build. Environ.* **2015**, *92*, 432–439. [CrossRef]
31. López-García, P.; Gelado-Caballero, M.D.; Collado-Sánchez, C.; Hernández-Brito, J.J. Solubility of aerosol trace elements: Sources and deposition fluxes in the Canary Region. *Atmos. Environ.* **2017**, *148*, 167–174. [CrossRef]
32. Nair, P.R.; George, S.K.; Sunilkumar, S.V.; Parameswaran, K.; Jacob, S.; Abraham, A. Chemical composition of aerosols over peninsular India during winter. *Atmos. Environ.* **2006**, *40*, 6477–6493. [CrossRef]
33. Galvão, E.S.; Santos, J.M.; Lima, A.T.; Reis, N.C.; Orlando, M.T.D.A.; Stuetz, R.M. Trends in analytical techniques applied to particulate matter characterization: A critical review of fundaments and applications. *Chemosphere* **2018**, *199*, 546–568. [CrossRef]
34. Bizo, M.L.; Roba, C.; Levei, E.A.; Hoaghia, M.A.; Modoi, C.O.; Ozunu, A. Comparison of FAAS and XRF performance for metal monitoring in brownfields. *Environ. Eng. Manag. J.* **2015**, *14*, 2515–2521. [CrossRef]
35. Custódio, P.J.; Pessanha, S.; Pereira, C.; Carvalho, M.L.; Nunes, M.L. Comparative study of elemental content in farmed and wild life Sea Bass and Gilthead Bream from four different sites by FAAS and EDXRF. *Food Chem.* **2011**, *124*, 367–372. [CrossRef]
36. Mäkinen, E.; Korhonen, M.; Viskari, E.L.; Haapamäki, S.; Järvinen, M.; Lu, L.I. Comparison of XRF and FAAS methods in analysing CCA contaminated soils. *Water Air Soil Pollut.* **2006**, *171*, 95–110. [CrossRef]
37. Morley, J.C.; Clark, C.S.; Deddens, J.A.; Ashley, K.; Roda, S. Evaluation of a portable X-ray fluorescence instrument for the determination of lead in workplace air samples. *Appl. Occup. Environ. Hyg.* **1999**, *14*, 306–316. [CrossRef] [PubMed]
38. Sterling, D.A.; Lewis, R.D.; Luke, D.A.; Shadel, B.N. A portable X-ray fluorescence instrument for analyzing dust wipe samples for lead: Evaluation with field samples. *Environ. Res.* **2000**, *83*, 174–179. [CrossRef]
39. Mohammed, H.; Sadeek, S.; Mahmoud, A.R.; Zaky, D. Comparison of AAS, EDXRF, ICP-MS and INAA performance for determination of selected heavy metals in HFO ashes. *Microchem. J.* **2016**, *128*, 1–6. [CrossRef]
40. Gerboles, M.; Buzica, D.; Alleman, L.; Pfeffer, U.; Gladtke, D.; Olschewski, A.; Leary, B.O.; Pockeviciute, D.; Tursic, J.; Yardley, R. *Intercomparison Exercise for Heavy Metals in PM 10*; European Commission: Luxembourg, 2008; ISBN 9789279082061.
41. Yatkin, S.; Belis, C.A.; Gerboles, M.; Calzolai, G.; Lucarelli, F.; Cavalli, F.; Trzepla, K. An interlaboratory comparison study on the measurement of elements in PM10. *Atmos. Environ.* **2016**, *125*, 61–68. [CrossRef]
42. Gupta, S.; Soni, P.; Gupta, A.K. Optimization of WD-XRF analytical technique to measure elemental abundance in PM2.5 dust collected on quartz-fibre filter. *Atmos. Pollut. Res.* **2021**, *12*, 345–351. [CrossRef]
43. Osán, J.; Börcsök, E.; Czömpöly, O.; Dian, C.; Groma, V.; Stabile, L.; Török, S. Experimental evaluation of the in-the-field capabilities of total-reflection X-ray fluorescence analysis to trace fine and ultrafine aerosol particles in populated areas. *Spectrochim. Acta Part B* **2020**, *167*, 105852. [CrossRef]
44. Bartley, D.L.; Slaven, J.E.; Rose, M.C.; Andrew, M.E.; Harper, M. Uncertainty determination for nondestructive chemical analytical methods using field data and application to XRF analysis for lead. *J. Occup. Environ. Hyg.* **2007**, *4*, 931–942. [CrossRef]
45. Mainka, A.; Zajusz-Zubek, E.; Kaczmarek, K. PM10 composition in urban & rural nursery schools in Upper Silesia, Poland: A trace elements analysis. *Int. J. Environ. Pollut.* **2017**, *61*, 98. [CrossRef]
46. Konarski, P.; Hałuszka, J.; Ćwil, M. Comparison of urban and rural particulate air pollution characteristics obtained by SIMS and SSMS. *Appl. Surf. Sci.* **2006**, *252*, 7010–7013. [CrossRef]
47. Olszowski, T.; Tomaszewska, B.; Góralna-Włodarczyk, K. Air quality in non-industrialised area in the typical Polish countryside based on measurements of selected pollutants in immission and deposition phase. *Atmos. Environ.* **2012**, *50*, 139–147. [CrossRef]
48. Samek, L.; Zwoździak, A.; Sówka, I. Chemical characterization and source identification of particulate matter pm 10 in a rural and urban site in poland. *Environ. Prot. Eng.* **2013**, *39*, 91–103. [CrossRef]
49. Austrian Standards Institute Ambient Air—Standard Gravimetric Measurement Method for Hte Determination of the PM10 or PM2. *5 Mass Concentration of Suspended Particulate Matter*; Austrian Standards Institute: Vienna, Austria, 2012.
50. Scheme, A.; Laboratories, F.O.R. SAC-SINGLAS A Guide on Measurement Uncertainty in Chemical & Microbiological Analysis. 2008. Available online: https://fdocuments.in/document/a-guide-on-measurement-uncertainty-in-chemical-guide-on-measurement-uncertainty.html?page=1 (accessed on 8 September 2021).
51. Liberti, A. Modern methods for air pollution monitoring. *Pure Appl. Chem.* **1975**, *44*, 519–534. [CrossRef]

52. Castro, A.; Alonso-Blanco, E.; González-Colino, M.; Calvo, A.I.; Fernández-Raga, M.; Fraile, R. Aerosol size distribution in precipitation events in León, Spain. *Atmos. Res.* **2010**, *96*, 421–435. [CrossRef]
53. European Parliament. European Council Directive 2008/50/EC on ambient air quality and cleaner air for Europe. *Off. J. Eur. Communities.* **2008**. Available online: https://ec.europa.eu/environment/archives/cafe/pdf/cafe_dir_en.pdf (accessed on 9 May 2021).
54. Braniš, M.; Domasová, M.; Řezáčová, P. Particulate air pollution in a small settlement: The effect of local heating. *Appl. Geochem.* **2007**, *22*, 1255–1264. [CrossRef]
55. Jandačka, D.; Ďurčanská, D. Air Pollution by Gases and PM in Rural Areas. *Trans. Transp. Sci.* **2014**, *7*, 143–152. [CrossRef]
56. Kaufman, L.; Rousseeuw, P. *Finding Groups in Data: An Introduction to Cluster Analysis*; John Wiley & Sons: Hoboken, NJ, USA, 2009.
57. Kim, M.K.; Jo, W.K. Elemental composition and source characterization of airborne PM10 at residences with relative proximities to metal-industrial complex. *Int. Arch. Occup. Environ. Health* **2006**, *80*, 40–50. [CrossRef]
58. Pan, Y.; Wang, Y.; Sun, Y.; Tian, S.; Cheng, M. Size-resolved aerosol trace elements at a rural mountainous site in Northern China: Importance of regional transport. *Sci. Total Environ.* **2013**, *461–462*, 761–771. [CrossRef]
59. Pant, P.; Harrison, R.M. Critical review of receptor modelling for particulate matter: A case study of India. *Atmos. Environ.* **2012**, *49*, 1–12. [CrossRef]
60. Jandacka, D.; Durcanska, D. Differentiation of particulate matter sources based on the chemical composition of PM10 in functional urban areas. *Atmosphere* **2019**, *10*, 583. [CrossRef]
61. Pant, P.; Harrison, R.M. Estimation of the contribution of road traffic emissions to particulate matter concentrations from field measurements: A review. *Atmos. Environ.* **2013**, *77*, 78–97. [CrossRef]
62. Samek, L. Source apportionment of the PM10 fraction of particulate matter collected in Kraków, Poland. *Nukleonika* **2012**, *57*, 601–606.
63. Khare, P.; Baruah, B.P. Elemental characterization and source identification of PM2.5 using multivariate analysis at the suburban site of North-East India. *Atmos. Res.* **2010**, *98*, 148–162. [CrossRef]
64. Rajšić, S.; Mijić, Z.; Tasić, M.; Radenković, M.; Joksić, J. Evaluation of the levels and sources of trace elements in urban particulate matter. *Environ. Chem. Lett.* **2008**, *6*, 95–100. [CrossRef]
65. Kuo, C.Y.; Wang, J.Y.; Liu, W.T.; Lin, P.Y.; Tsai, C.T.; Cheng, M.T. Evaluation of the vehicle contributions of metals to indoor environments. *J. Expo. Sci. Environ. Epidemiol.* **2012**, *22*, 489–495. [CrossRef]
66. Richter, P.; Griño, P.; Ahumada, I.; Giordano, A. Total element concentration and chemical fractionation in airborne particulate matter from Santiago, Chile. *Atmos. Environ.* **2007**, *41*, 6729–6738. [CrossRef]
67. Sternbeck, J.; Sjödin, Å.; Andréasson, K. Metal emissions from road traffic and the influence of resuspension—Results from two tunnel studies. *Atmos. Environ.* **2002**, *36*, 4735–4744. [CrossRef]
68. Toscano, G.; Moret, I.; Gambaro, A.; Barbante, C.; Capodaglio, G. Distribution and seasonal variability of trace elements in atmospheric particulate in the Venice Lagoon. *Chemosphere* **2011**, *85*, 1518–1524. [CrossRef]
69. Kulshrestha, A.; Satsangi, P.G.; Masih, J.; Taneja, A. Metal concentration of PM2.5 and PM10 particles and seasonal variations in urban and rural environment of Agra, India. *Sci. Total Environ.* **2009**, *407*, 6196–6204. [CrossRef]
70. Escrig Vidal, A.; Monfort, E.; Celades, I.; Querol, X.; Amato, F.; Minguillón, M.C.; Hopke, P.K. Application of optimally scaled target factor analysis for assessing source contribution of ambient PM10. *J. Air Waste Manag. Assoc.* **2009**, *59*, 1296–1307. [CrossRef]
71. Kavouras, I.G.; Koutrakis, P.; Cereceda-Balic, F.; Oyola, P. Source apportionment of PM10 and PM2.5 in five Chilean cities using factor analysis. *J. Air Waste Manag. Assoc.* **2001**, *51*, 451–464. [CrossRef] [PubMed]
72. Pohlmann, J.T. Use and Interpretation of Factor Analysis in 'The Journal of Educational Research': 1992–2002. *J. Educ. Res.* **2004**, *98*, 14–22. [CrossRef]
73. Cattell, R.B. The scree test for the number of factors. *Multivar. Behav. Res.* **1966**, *1*, 245–276. [CrossRef] [PubMed]
74. Fernández-Camacho, R.; Rodríguez, S.; de la Rosa, J.; Sánchez de la Campa, A.M.; Alastuey, A.; Querol, X.; González-Castanedo, Y.; Garcia-Orellana, I.; Nava, S. Ultrafine particle and fine trace metal (As, Cd, Cu, Pb and Zn) pollution episodes induced by industrial emissions in Huelva, SW Spain. *Atmos. Environ.* **2012**, *61*, 507–517. [CrossRef]

*materials*

MDPI

*Article*

# Characteristics of Particles Emitted from Waste Fires—A Construction Materials Case Study

**Jan Stefan Bihałowicz [1,*], Wioletta Rogula-Kozłowska [1], Adam Krasuski [1], Małgorzata Majder-Łopatka [1], Agata Walczak [2], Mateusz Fliszkiewicz [2], Patrycja Rogula-Kopiec [3] and Tomasz Mach [4]**

1 Institute of Safety Engineering, The Main School of Fire Service, 52/54 Słowackiego Street, 01-629 Warsaw, Poland; wrogula@sgsp.edu.pl (W.R.-K.); akrasuski@sgsp.edu.pl (A.K.); mmajder@sgsp.edu.pl (M.M.-Ł.)
2 Faculty of Safety Engineering and Civil Protection, The Main School of Fire Service, 52/54 Słowackiego Street, 01-629 Warsaw, Poland; awalczak@sgsp.edu.pl (A.W.); mfliszkiewicz@sgsp.edu.pl (M.F.)
3 Institute of Environmental Engineering, Polish Academy of Sciences, 34 M. Skłodowska-Curie St., 41-819 Zabrze, Poland; patrycja.rogula-kopiec@ipis.zabrze.pl
4 Faculty of Environmental Engineering, Wroclaw University of Science and Technology, Plac Grunwaldzki 13, 50-377 Wrocław, Poland; tomasz.mach@pwr.edu.pl
* Correspondence: jbihalowicz@sgsp.edu.pl

**Abstract:** This study aimed to determine the relative densities of populations of particles emitted in fire experiments of selected materials through direct measurement and parametrization of size distribution as number (NSD), volume (VSD), and mass (MSD). As objects of investigation, four typical materials used in construction and furniture were chosen: pinewood (PINE), laminated particle board (LPB), polyurethane (PUR), and poly(methyl methacrylate) (PMMA). The NSD and VSD were measured using an electric low-pressure impactor, while MSD was measured by weighing filters from the impactor using a microbalance. The parametrization of distributions was made assuming that each distribution can be expressed as the sum of an arbitrary number of log-normal distributions. In all materials, except PINE, the distributions of the particles emitted in fire experiments were the sum of two log-normal distributions; in PINE, the distribution was accounted for by only one log-normal distribution. The parametrization facilitated the determination of volume and mass abundances, and therefore, the relative density. The VSDs of particles generated in PINE, LPB, and PUR fires have similar location parameters, with a median volume diameter of 0.2–0.3 μm, whereas that of particles generated during PMMA burning is 0.7 μm. To validate the presented method, we burned samples made of the four materials in similar proportions and compared the measured VSD with the VSD predicted based on the weighted sum of VSD of raw materials. The measured VSD shifted toward smaller diameters than the predicted ones due to thermal decomposition at higher temperatures.

**Keywords:** volume size distribution; mass size distribution; density; pinewood; laminated particle board; polyurethane; poly(methyl methacrylate)



**Citation:** Bihałowicz, J.S.; Rogula-Kozłowska, W.; Krasuski, A.; Majder-Łopatka, M.; Walczak, A.; Fliszkiewicz, M.; Rogula-Kopiec, P.; Mach, T. Characteristics of Particles Emitted from Waste Fires—A Construction Materials Case Study. *Materials* **2022**, *15*, 152. https://doi.org/10.3390/ma15010152

Academic Editor: Valentina Gargiulo

Received: 5 November 2021
Accepted: 21 December 2021
Published: 26 December 2021



## 1. Introduction

Waste disposal is an emerging problem in developed [1] as well as developing [2] countries. Even though many efforts have been made to limit waste production, the effects remain limited [3] Although many types of waste can be recycled and successfully used in different applications [4], recycled materials are often more expensive and hence less attractive for the industry than raw materials [5,6]. However, one of the most popular methods of waste treatment is landfilling [7], which has a negative effect on the environment [8]. Incineration is another important method, but it has negative social effects because waste incineration induces a false social belief that any burning of waste material is allowed. Household waste, especially in non-urban areas, is burned in bonfires in the backyard [9–12] or in barrels [13], especially in North America. The burning of waste at

landfills or in stoves is also of significance [14] because the ion composition of the particulates indicates that solid waste is used as a fuel. Furthermore, the open burning of materials containing chlorine generates dioxins during incomplete burning [15]. Small-scale open burning waste incinerators emit more than 200 times the amount of dioxins than municipal waste incinerators [16], due to uncontrolled burning and lack of air pollution control [17]. Moreover, the open burning of waste generates greenhouse gases (GHGs) [18], which are not considered in global GHG inventories [19]. Furthermore, the open burning of waste produces volatile and semi-volatile organic compounds (VOCs and SVOCs), polycyclic aromatic hydrocarbons (PAHs), and polychlorinated dibenzofurans (PCDD/Fs). The emission factors of more than 160 pollutants and toxic substances generated during open burning were previously determined [20–25].

One of the most common sources of open waste burning is the burning of crop residues. Many recent studies have focused mostly on the number size distributions (NSDs) of particles emitted during the burning of crops. Investigations have been performed on chili and perilla crop residues [26], rice straw [27], and crop straw [28]. Nevertheless, waste burning in rural areas is not limited to these materials [29]. There is a saying in Poland that "waste in Poland can be divided into non-flammable and flammable waste and flammable waste can be further divided into waste that can be burned during the day and that during the night" [30,31]. This attitude signifies that almost everything can be burned in stoves or bonfires in backyards. Although recycling centers were introduced in every municipality (Local Administrative Unit level 2 [32]), the limited hours of operation of these centers and distance from the settlements have led to the inadequate disposal of furniture and construction materials.

Wood is the most commonly used material for the construction of single-family houses and is the main substance utilized for furniture [33]. The most popular tree used in the East European Plain, North European Plain, and Baltic Shield belongs to the *Pinus* spp. [34,35]. The mechanical properties and the heat properties of pinewood (PINE) have been well investigated [36–38]. Therefore, PINE is commonly used for construction purposes. Because of their popularity in furniture construction, PINE and chemically treated PINE have been the focus of indoor air quality studies [39]. PINE is also used as firewood.

The gaseous products emitted by the thermal decomposition of PINE are well known [40]. However, the NSD and mass size distribution (MSD) of the particles generated during PINE burning/combustion are known only with respect to furnace burning [41]. There remains a need to characterize the particle size distribution in the case of partial thermal decomposition such as in open burning, bonfires, or poorly ventilated heating stoves. In addition to plain wood, furniture can also be made from structural panels, such as laminated particle boards (LPBs) [42]. Regarding LPBs, the combustion properties LPB [43], heat release rates [44], and the yield of fire products [45] are well understood; however, particle emission remains to be investigated.

Polyurethane (PUR) is commonly used for the upholstery padding of furniture and its heat release rates [44] and fire toxicity [46] are well known. The NSD of particles generated by the thermal degradation of polyurethane has been investigated with respect to indoor air quality [47], but not with respect to burning.

Poly (methyl methacrylate) (PMMA) is used in households for decoration purposes (as a safe glass replacement) in picture frames, art objects, and aquarium walls. The burning of PMMA has been the object of many studies [48–51] since its use for the construction of objects contributed to the Summerland disaster [52].

In the present work, the size distributions of the particles generated by the burning of selected materials related to building fires and open burning were analyzed. The results provide information on the physical characteristics of populations of particles such as volume size distribution (VSD) and MSD and the possibilities of determining the relative densities of particles generated during PINE, LPB, PUR, and PMMA fires. The characterization of the size distributions of particles facilitates the identification of pollution sources [53,54]. The investigated materials can be burned either intentionally in waste fires

or accidentally during residential building fires. Therefore, the results of this study can be applied to identify the origin of particles from both waste and residential fires. Moreover, it is important to determine the size distribution of the particles from fires to assess the health impact related to the inhalation of those particles [55–57].

This work includes an original method for determining the relative densities of populations of particles generated during fire experiments. The NSD and VSD were determined using low-pressure electric impactor measurements, and the MSD was obtained using gravimetric measurements. The crucial point in determining the density is to fit the densities in such a way that the parametrized VSD multiplied by the density equals the MSD.

## 2. Materials and Methods

### *2.1. General Description*

Four different materials, that is, PINE, LPB, PUR, and PMMA, and a mixture of all materials (MIX), were used in our experiments. The experiments were conducted in a closed 75 $m^3$ chamber, which was designed to evaluate fire detection systems. The sample was ignited, burned for a given time, and extinguished. Subsequently, the chamber was ventilated. During this process, the particle number concentration was measured using an impactor, that is, Dekati® High-Temperature ELPI+® (HT-ELPI, Dekati, Kangasala, Finland). The components of the impactor and substrates were prepared for experiments in a laboratory dedicated to environmental monitoring measurements at the Institute of Safety Engineering. Substrates from the manufacturer of the impactor (aluminum foil ø25 mm, Dekati, Kangasala, Finland, product code CF-300) were used for the experiment. The substrates were covered with Apiezon-L grease (Dekati, Kangasala, Finland, product code DS-515). The mass of the particles generated during each stage of the impactor was determined by weighing the covered substrates before and after the fire experiment. The filters were weighed using an MYA 5.3Y.F microbalance (1 µg resolution, RADWAG, Radom, Poland). Prior to weighing, the substrates were conditioned for 48 h in a weighing room at a temperature of 20 ± 2 °C and relative air humidity of 50 ± 5%.

The impactor measurement was carried out to determine the NSD and thus the VSD of the particulates emitted during the fire experiments. The substrates attached to the impactor stage were used for the determination of the MSD, which was not recalculated from online impactor measurements but determined by gravimetric measurements. All size distributions were evaluated as cumulative distributions instead of d/dlogDp distributions. Based on this approach, exact values can be maintained while allowing for a better interpretation of diameters, eliminating problems related to the median diameter of the stage, and focusing only on the cutoff diameter. In addition, potential confusion with respect to the assignment of particles on stages can be avoided and the proportions of different populations of particles as well as their densities can be identified.

The analysis of size distributions depends on the choice of the particle diameter definition. In this work, we focused on determining the relative densities of particles emitted during fire experiments. Therefore, all size distributions are discussed as functions of the Stokes diameter [58]. All measured distributions were based on Stokes diameters calculated using the Dekati ELPI+XLS v2.01 software (Dekati, Kangasala, Finland) [58].

### *2.2. Experimental Setup of the Impactor*

The NSD and VSD measurements were performed using the HT-ELPI. The HT-ELPI is a 15-stage electrical, low-pressure impactor that is capable of the direct measurement of particles in hot gases without prior cooling, which makes it ideal for the analysis of particles generated during fires. The nominal particle sizes range from 6 nm to 10 µm. The data obtained from the impactor were analyzed using the ELPI+XLS 2.01 data processing spreadsheet [58]. The sampling time of the VSD obtained by using the ELPI is the same as that of the MSD collected on aluminum foils and determined using the microbalance. For each test fire, we obtained 14 data points representing the VSD $\{f_{V,i},\ i \in [1,14] \cap \mathbb{N}\}$, expressed in

$\frac{\mu m^3}{cm^3}$, using the ELPI+XLS and 14 data points representing the MSD $\{f_{m,i},\ i \in [1,14] \cap \mathbb{N}\}$ obtained with the microbalance.

### *2.3. Material Fire Experiments*

The fire experiments were conducted in the fire laboratory of The Main School of Fire Service in a chamber designed to evaluate the efficiency of fire detection systems, especially that of smoke detectors. The chamber was approximately 5 m × 5 m × 3 m in size. Five samples were burned during the experiment.

First, the sample was prepared and weighed, and then placed inside the test chamber. Subsequently, sampling using the HT-ELPI was started. To ignite the sample, 40 mL of denatured alcohol (>97% vol.) was poured onto it and ignited with a gas soldering lamp. After 5 min, the ELPI sampling was stopped and the fire was extinguished with approximately 350 mL of water. The filter stage block was disassembled and greased aluminum foils were replaced with new ones. The chamber was ventilated using a powered ventilation system. While the ELPI sampling was stopped, particle concentration in the chamber was monitored using DustTrak 8534 DRX Aerosol Monitor sampler (TSI, MN, USA), which was calibrated using a previously reported procedure [59]. The ventilation continued until the concentration of particles with diameters less than 10 µm, as measured using DustTrak 8534 DRX (TSI, MN, USA), was less than $10^4$ $m^{-3}$. The procedure was repeated for all five samples.

The first sample was PINE (50 square cuboids arranged in five layers). The scantlings are presented in Figure 1 (upper left). The scantlings were placed perpendicularly in the neighboring layers. The total mass was 397.7 ± 0.1 g. The second sample was LPB, which was cut into oblong prisms presented in Figure 1 (upper right). The pieces were spaced and layered, allowing for the free flow of air between them. The total mass was 203.7 ± 0.1 g. The third sample was a 50.0 ± 0.1 g PUR foam sheet; a small piece from this sample is presented in Figure 1 (lower left). The PUR foam had a low density and thus the mass of the sample was lower. The sheet was cut into pieces, one piece per layer. The height and perimeter of the sample were similar to those of PINE and LPB; however, there was no airflow between the pieces of the sheet. The fourth sample consisted of PMMA granules with a diameter of <3 mm (Figure 1, lower right), which were arranged in a pile (heap) according to the angle of repose. The total weight was 200.2 ± 0.1 g. The fifth sample consisted of all materials used before, but four times smaller amounts of these materials were used to maintain the order of the number concentration of the particles. The weights of the PINE, LPB, PUR, and PMMA were 102.5 ± 0.1, 49.5 ± 0.1, 12.5 ± 0.1, and 50.1 ± 0.1 g, respectively, leading to a total weight of 214.6 ± 0.4 g. This sample was denoted as MIX. The PUR foam was placed on the bottom of the sample and the PMMA was placed in four low piles. Pieces of the LPB were partially supported on PMMA piles and partially supported on PUR foam; however, they were separated from each other, allowing for airflow. The top of the LPB layer was set roughly horizontally; PINE scantlings were placed on the LPB layer while maintaining the spacing between them.

**Figure 1.** Four materials used in the experiment. The pinewood scantlings (PINE, **upper left**), laminated particleboard (LPB, **upper right**), fragment of PUR foam sheet (**lower left**), granules of PMMA (**lower right**).

### *2.4. Size Distribution of Particulates Emitted from Fires*

#### 2.4.1. Volume Size Distribution

The data were analyzed using ELPI+VI 2.1 software and ELPI+XLS 2.01 provided by the manufacturer, Dekati (Kangasala, Finland), as well as Python 3 [60]. The ELPI+XLS software was used to read data collected by the HT-ELPI, and it transformed the NSDs into 14-point data sets $\{f_{V,i}\}$ representing the VSD at each stage of the impactor. The remaining part of the analysis was conducted using Python.

Based on the literature [61,62], the particle sizes can be described using a log-normal distribution; however, in our experiment, we assumed the presence of more than one population of particles. Therefore, our VSD $f_{VSD}(x)$ is a sum of arbitrary numbers $n \geq 1$ of log-normal distributions. The probability density function (PDF) $f_{VSD}(x)$ (1) and cumulative distribution function $CDF_{VSD}(x)$ (2) are presented below.

$$f_{VSD}(x) = \sum_{j=1}^{n} f_{VSD}^{j}(x) = \sum_{j=1}^{n} \frac{A_j}{\sigma_j x} \exp\left(-\frac{\left(\ln x - \mu_j\right)^2}{2\sigma_j}\right) \tag{1}$$

$$CDF_{VSD}(x) = \sum_{j=1}^{n} CDF_{VSD}^{j}(x) = \int_0^x f_{VSD}(y)dy = \sum_{j=1}^{n} \int_0^x \frac{A_j}{\sigma_j y} \exp\left(-\frac{\left(\ln y - \mu_j\right)^2}{2\sigma_j}\right) dy = \sum_{j=1}^{n} \frac{a_j}{2}\left(1 + \operatorname{erf}\left(\frac{\ln x - \mu_j}{\sigma_j\sqrt{2}}\right)\right), \tag{2}$$

where $x$ is the diameter, $A$ is a proportionality constant, $\mu$ is the natural logarithm of the mean diameter, $\sigma$ is the shape parameter, $y$ is the integration variable, $a_j$ is the abundance, and erf is the error function. Each summand in Equation (2) adds three fitting parameters. Hence, the fitting procedure depends on the measured VSD $\{f_{V,i}\}$ (support of the PDF, number of modes) and measured volume CDF $\left\{CDF_{V,i} = \frac{\sum_{k=1}^{i} f_{V,i}}{\sum_{k=1}^{14} f_{V,i}}\right\}$. When the number of degrees of freedom did not permit the fitting of coefficients and their uncertainties, the fitted function was limited to a smaller number of summands. The $CDF_{VSD}$ was fitted to the measured set $\{CDF_{V,i}\}$ in Python using the least squares method [63] from lmfit package [64] and erf function from scipy.special [65].

2.4.2. Mass Size Distribution and Density

The MSD of the particles emitted from each test fire was obtained by measuring the increase in the mass of aluminum filters $\{f_{m,i}\}$ and mass CDF $\left\{CDF_{m,i} = \frac{\sum_{k=1}^{i} f_{m,i}}{\sum_{k=1}^{14} f_{m,i}}\right\}$. The MSD can be derived from the VSD using the density of the substance $\rho$, as shown in Equation (3). In general, each type of particle (each distribution) has a different density, $\rho_j$. The cumulative MSD $CDF_{MSD}(x)$ can be calculated from the $\rho_j$ and cumulative VSD, as shown in Equation (4) ($\rho_0$ is a normalization constant).

$$f_{MSD}(x) = \sum_{j=1}^{n} \frac{\rho_j}{\rho_0} \frac{A_j}{\sigma_j x} \exp\left(-\frac{\left(\ln x - \mu_j\right)^2}{2\sigma_j}\right) = \sum_{j=1}^{n} \frac{\rho_j}{\rho_0} f_{VSD}^{j}(x) \tag{3}$$

$$\begin{aligned} CDF_{MSD}(x) &= \sum_{j=1}^{n} CDF_{MSD}^{j}(x) = \int_0^x f_{MSD}(y)dy = \int_0^x \sum_{j=1}^{n} \frac{\rho_j}{\rho_0} f_{VSD}^{j}(x)dy = \sum_{j=1}^{n} \frac{\rho_j}{\rho_0} \int_0^x f_{VSD}^{j}(y)dy = \sum_{j=1}^{n} \frac{\rho_j}{\rho_0} CDF_{VSD}^{j}(x) \\ &= \sum_{j=1}^{n} \frac{b_j}{2}\left(1 + \operatorname{erf}\left(\frac{\ln x - \mu_j}{\sigma_j\sqrt{2}}\right)\right), \end{aligned} \tag{4}$$

where $b_j$ is the mass abundance. The parameterized MSD $CDF_{MSD}^{j}(x)$ and parametrized VSD $CDF_{VSD}(x)$ share shape $\sigma_j$ and location parameters $\mu_j$. The sum of Equation (4) can be expressed in terms of Equation (2). The $CDF_{MSD}(x)$ can be fitted to a set of $\{CDF_{m,i}\}$ using the $b_j$ values, as shown in Equation (5). Since $\sum_{j=1}^{n} a_j = 1$ and $\sum_{j=1}^{n} b_j = 1$, $b_l$ can be expanded, as shown in Equation (6).

$$CDF_{MSD}^{j}(x) = \frac{\rho_j}{\rho_0} CDF_{VSD}^{j}(x) \Longrightarrow \frac{b_j}{2}\left(1 + \operatorname{erf}\left(\frac{\ln x - \mu_j}{\sigma_j\sqrt{2}}\right)\right) = \frac{\rho_j}{\rho_0}\frac{a_j}{2}\left(1 + \operatorname{erf}\left(\frac{\ln x - \mu_j}{\sigma_j\sqrt{2}}\right)\right) \Longrightarrow b_j = \frac{\rho_j}{\rho_0} a_j \tag{5}$$

$$b_l = \frac{b_l}{\sum_{j=1}^{n} b_j} = \frac{\frac{\rho_l}{\rho_0} a_l}{\sum_{j=1}^{n} \frac{\rho_j}{\rho_0} a_j} = \frac{\rho_l a_l}{\sum_{j=1}^{n} \rho_j a_j} \tag{6}$$

Equation (5) can be rewritten as a system of equations $\rho_l a_l = \sum_{j=1}^{n} \rho_j a_j b_l$ in the form of a matrix with unknown densities $\rho$.

$$\begin{bmatrix} a_1 b_1 - a_1 & a_2 b_1 & \cdots & a_n b_1 \\ a_1 b_2 & a_2 b_2 - a_2 & \cdots & a_n b_2 \\ \vdots & \vdots & \ddots & \vdots \\ a_1 b_n & a_2 b_n & \cdots & a_n b_n - b_n \end{bmatrix} \begin{bmatrix} \rho_1 \\ \rho_2 \\ \vdots \\ \rho_n \end{bmatrix} = 0 \tag{7}$$

Based on $\sum_{j=1}^{n} a_j = 1$ and $\sum_{j=1}^{n} b_j$, the rank of the left matrix in Equation (7) is equal to $n - 1$; according to the Rouché–Capelli theorem (Kronecker–Capelli theorem), we can express $\{\rho_2, \ldots, \rho_n\}$ as a function of $\rho_1$.

The results for each family $j$ of particles include four parameters: volume abundance $a_j$, mean diameter $D_m^j = \exp(\mu_j)$, geometric standard deviation $GSD_j = \exp(\sigma_j)$, and mass abundance $b_j$. If the fitting procedure included $n \geq 2$ log-normal distributions, the additional parameter–density $\rho_j$, as a function of $\rho_1$, was obtained for $2 \leq j \leq n$.

2.4.3. Goodness of Fit and Uncertainties

Each fit was evaluated using the reduced chi-square $\chi_\nu^2 = \frac{\chi^2}{\nu}$. The fitting procedure minimizes $\chi^2$. The number of degrees of freedom $\nu$ is the difference between the number of data points (14) and the number of fitted parameters, that is, $3n$, based on Equations (2) or (4). For each fit, we provide both $\chi_\nu^2$, $\nu$ and the right-hand side probability $p$ of this value according to the $\chi^2$ distribution. In general, very low $p$ values (and $\chi_\nu^2 \gg 1$) represent "underfitted" data, whereas very high $p$ values ($\chi_\nu^2 \ll 1$) represent "overfitted" data. A detailed discussion is provided for each fit.

The fitting procedure in the lmfit package provides uncertainties for the parameters ($a_j$, $\mu_j$, $\sigma_j$) fitted during VSD fitting and $b_j$ fitted during MSD fitting. The uncertainties of $D_m^j$, $GSD_j$, and $\rho_j$ must be determined according to [66]. In the case of $D_m^j$ and $GSD_j$, which are one-variable functions of the fitted parameters, the uncertainties can be described by Equations (8) and (9). The uncertainty of the density $\rho_j(a_1, \ldots, a_n, b_1, \ldots, b_n)$ for $j \neq 1$ is provided in Equation (10). Depending on $n$, the solution of Equation (7) has more or fewer summands in the numerator and denominator and thus Equation (10) becomes more or less complex.

$$\Delta D_m^j = \left| \frac{\partial D_m^j}{\partial \mu_j} \right| \Delta \mu_j \tag{8}$$

$$\Delta GSD_j = \left| \frac{\partial GSD_j}{\partial \sigma_j} \right| \Delta \sigma_j \tag{9}$$

$$\Delta \rho_j = \sqrt{\sum_{l=1}^{n} \left( \left| \frac{\partial \rho_j}{\partial a_l} \right|^2 \Delta a_l^2 + \left| \frac{\partial \rho_j}{\partial b_l} \right|^2 \Delta b_l^2 \right)} \tag{10}$$

## 3. Results and Discussion

### *3.1. Raw ELPI Result*

The first analysis of the data collected by the HT-ELPI was performed using the ELPI+XLS sheet provided by Dekati (Kangasala, Finland). The number concentrations, number median diameters (NMDs), and volume median diameters (VMDs) obtained with this software are presented in Table 1. The total number concentration ranges from 2 to 7 million particles per cubic centimeter. Values of this order (millions of particles per cubic centimeter) were obtained for smoke from cotton smoldering and wood smoke. The NMDs were comparable for all materials (within a factor of two). The highest concentration was obtained for MIX. In this case, the NMD is the highest among the samples, whereas the VMD is lower than that of PMMA. Half of the number of particles emitted from the MIX fire had a diameter less than 115 nm and the total volume was much smaller than half of the total volume of all particles, because half of the volume consists of particles with diameters below 426 nm. The smallest particles represent the largest proportion, whereas their total volume is low; it is likely that their weight is also small. Similar conclusions can be drawn for all other burned materials, that is, the NMD is generally 4–6 times smaller than the VMD. The number concentration, NMD, and VMD of LPB were the smallest among the investigated samples. The NMD ranged from 50 to 100 nm, corresponding to the Aitken nuclei range based on Whitby [67], that is, every second particle emitted during the fire test is a fine particle in the Aitken nuclei range. Furthermore, more than half of the volume of all particles consisted of fine particles because all VMDs are smaller than 2 µm.

**Table 1.** The number concentration of particles (*C*), number median diameter (NMD), and volume median diameter (VMD) obtained using HT-ELPI for pinewood (PINE), laminated particle board (LPB), polyurethane (PUR), poly(methyl methacrylate) (PMMA), and the sample containing all materials (MIX).

| Parameter | Pinewood | LPB | PUR | PMMA | MIX |
|---|---|---|---|---|---|
| $C$ (cm$^{-3}$) | $3.53 \times 10^6$ | $2.03 \times 10^6$ | $4.25 \times 10^6$ | $5.97 \times 10^6$ | $6.54 \times 10^6$ |
| NMD (µm) | 0.058 | 0.045 | 0.077 | 0.109 | 0.115 |
| VMD (µm) | 0.359 | 0.277 | 0.365 | 0.666 | 0.426 |

### *3.2. Parametrization of the Particulates from Fire Experiments*

The cumulative VSD obtained using the HT-ELPI impactor was fitted with the procedure presented in Section 2.4. The fitted sums of the log-normal distributions for PINE (Figure 2a), LPB (Figure 2b), PUR (Figure 2c), and PMMA (Figure 2d) are presented below

(denoted as Fit). The fitted sums could be split into separate summands if $n \geq 2$. Fit 1 in Figure 2 corresponds to the first summand in Equation (2), that is, the summand with index $j = 1$. Fit 2 corresponds to the second summand in Equation (2), with index $j = 2$. The measurements for the PINE sample did not allow the fit of more than an $n = 1$ distribution using Equation (2). In Figure 2b–d, $n = 2$. Hence, the relative density of the particles according to Equation (7) was not determined for PINE, whereas it was used for the other three materials. The fitted numeric abundance ($a$), mean Stokes diameter ($D_m$) and geometric standard deviation ($GSD$) values are presented in Table 2.

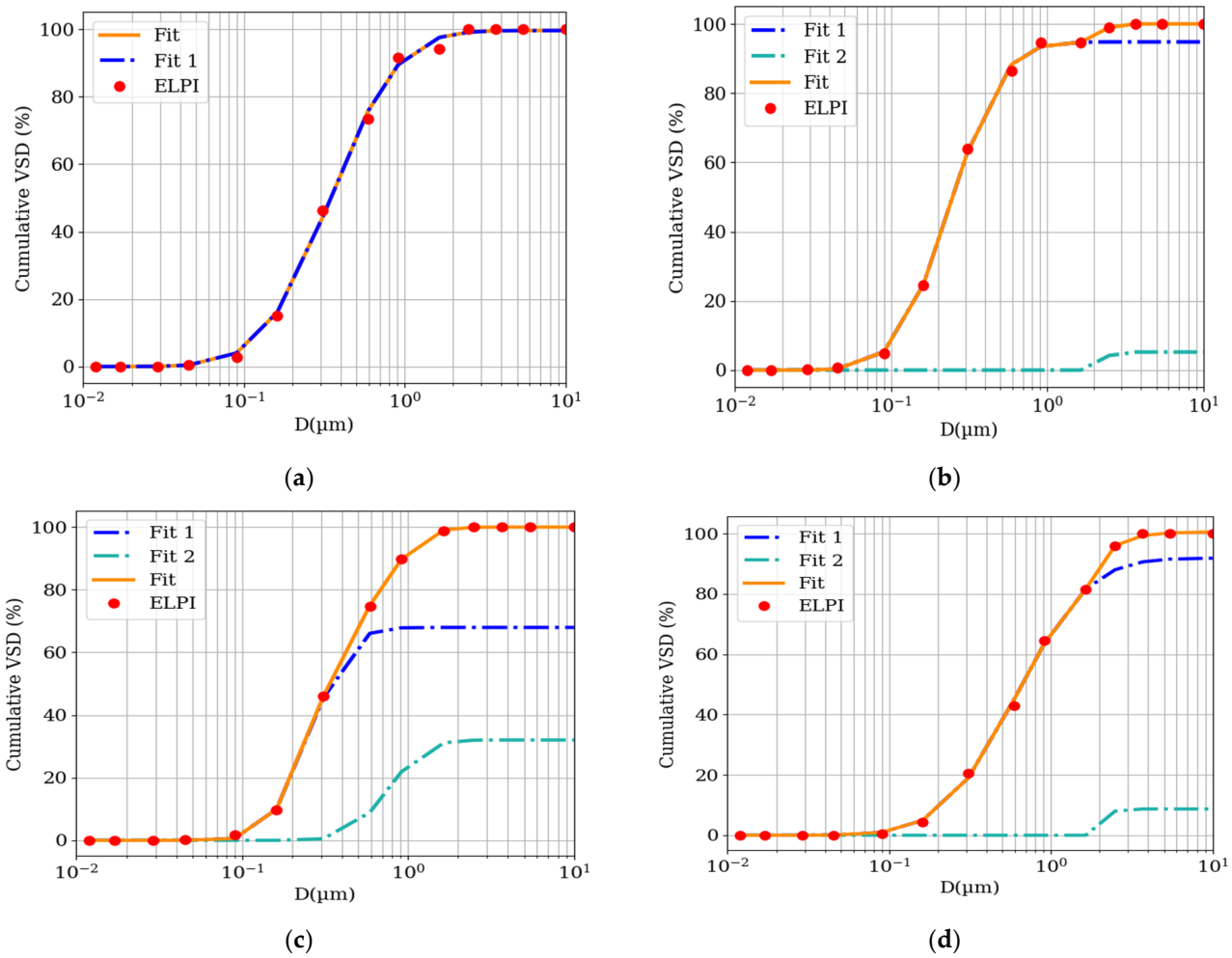


**Figure 2.** Cumulative volume size distributions of particles emitted during (**a**) pinewood (PINE), (**b**) laminated particle board (LPB), (**c**) PUR foam, and (**d**) PMMA fires. The red dots represent the results obtained with ELPI. The orange line is the best-fit line parametrization of the distribution based on two summands (blue: Fit 1, sea green: Fit 2). In the case of pinewood, it was impossible to fit the sum of two distributions; therefore, the orange line overlaps the blue one.

In the case of the PINE sample, the fitted abundance $a$ is within uncertainty equal to 100%, and the relative uncertainty of $a$ is below 1%. The fit statistics are as follows: $\chi^2_\nu = 2.431$ and $\nu = 14 - 3 = 11$. The corresponding $p = 0.12$ is neither low nor high, representing a reliable fit, which can also be confirmed by Figure 2a. The fitted volume abundance value $a_j$ also proves that the size distribution can be described well using a single (unimodal) log-normal distribution. These results must be considered together with the resolution of the impactor. If the impactor used in the experiment had more than 15 stages covering a range of 0.01–10 µm, especially in the range 0.1–1 µm, the characteristics of the particles generated during PINE fires can be investigated further. Potentially, the single mode can be split into a few modes that are close to each other if the resolving power of the

device (i.e., the stage density) allows it. However, the results show that during the burning of PINE, no particles with diameters in the range of 2.5 to 10 µm were emitted, and more than 90% of the volume of all measured particles was between 100 nm and 1 µm.

**Table 2.** Fitted volume abundance $a$, mean diameter $D_m$, geometric standard deviation $GSD$, and mass abundance $b$ of the particles emitted during pinewood (PINE), laminated particle board (LPB), polyurethane (PUR), and poly(methyl methacrylate) (PMMA) fires.

| Material | Parameter | Fit 1 | Fit 2 |
|---|---|---|---|
| PINE | $a$ (%) | 99.6 ± 0.7 | – |
| | $D_m$ (µm) | 0.344 ± 0.008 | – |
| | $GSD$ | 2.15 ± 0.06 | – |
| LPB | $a$ (%) | 94.8 ± 0.6 | 5.2 ± 0.8 |
| | $D_m$ (µm) | 0.238 ± 0.003 | 2.38 [1] |
| | $GSD$ | 1.81 ± 0.03 | 1.05 [1] |
| | $b$ (%) | 73.6 ± 3.4 | 27.0 ± 4.0 |
| PUR | $a$ (%) | 68 ± 13 | 32 ± 13 |
| | $D_m$ (µm) | 0.26 ± 0.03 | 0.75 ± 0.15 |
| | $GSD$ | 1.55 ± 0.08 | 1.5 ± 0.2 |
| | $b$ (%) | 68.9 ± 9.5 | 30 ± 10 |
| PMMA | $a$ (%) | 91.8 ± 2.6 | 8.6 ± 2.5 |
| | $D_m$ (µm) | 0.60 ± 0.03 | 2.45 [1] |
| | $GSD$ | 2.27 ± 0.09 | 1.05 [1] |
| | $b$ (%) | 88.8 ± 1.6 | 9.5 ± 2.1 |

[1] This value is for location purposes only and should be treated as approximate. It is caused by the characteristics of the impactor.

The results from the studies in which the Dekati low-pressure impactor (DLPI) was used to determine the MSD of particles emitted during the pyrolysis of PINE in a furnace at 1300 °C [41] showed that the majority of the mass consisted of particles with diameters between 20 nm and 500 nm. The difference between the results obtained in the present study and the previous work [41] shows that two modes exist. That is, the particles were in the nucleation mode in the furnace studies [67], whereas with respect to open burning, as could be expected, the burning was incomplete, the emitted particles were not products of complete thermal decomposition, and the products were mainly in the accumulation mode [67].

In the case of the PINE sample, it was impossible to evaluate the size distribution as the sum of more than one log-normal distribution, whereas the data for all remaining samples were analyzed as the sum of two log-normal distributions.

Figure 2b presents the VSD for the fire experiment using the LPB sample. The fit of the sum of two log-normal distributions to the data from the ELPI yielded the following values: $\chi^2_\nu = 0.6847$, $\nu = 14 - 6 = 8$, and $p = 0.9996$. As indicated in Section 2.4.3, this $p$-value is high. Although one can use the one log-normal distribution for the fit, which has a value of $\chi^2_\nu$ closer to 1 than that presented in the fit in Figure 2b, the increase in the diameters (1.6 and 2.5 µm) shows that fitting Equation (2) with $n = 1$ is not suitable. The fit parameters are presented in Table 2. The log-normal distributions, Fits 1 and 2, have abundances of 94.8 ± 0.6% and 5.2 ± 0.8%, respectively, leading to a sum of 100.0 ± 1.4%. Although the sum is correct, with a small uncertainty, there are problems with respect to the shape and location parameters of Fit 2. Based on the resolution of the impactor, $D^2_m \in [1.6, 3.6]$ µm, that is, between Stokes cut-off diameters of stage 11 and stage 13 of the impactor. Therefore, we cannot provide the $D^2_m$ and its uncertainty as well as $GSD_2$ and its uncertainty. The value of 2.48 in Table 2 is only included for location purposes because it was used in the equation for Fit 2 and thus for the best-fit line in Figure 2b. In the case of LPB, around 95% of the volume of particles is from particles with a diameter less than 1 µm.

However, uncertainties in $D_m$ and $GSD$ are not required to determine the relative densities based on Equation (7) and their uncertainties based on Equation (10). The mass abundances $b_j$ are obtained by fitting the cumulative MSD using Equation (4) with the

$\mu_j$ and $\sigma_j$ values obtained from the fit of the cumulative VSD using Equation (2), that is, during the fit of the cumulative MSD, only the $b_j$ values are obtained. The results of the LPB fit are presented in Table 2. Although Fit 2 constitutes a small proportion of the volume of the particulates ($5.2 \pm 0.8\%$), its proportion in the mass of the particles is approximately five times higher. Hence, the calculated density of the particles described by Fit 2 is $\rho_2 = (6.74 \pm 1.04) \cdot \rho_1$. The $\rho_2$ value is high because if we assume that $\rho_1 = 1 \frac{\mathrm{g}}{\mathrm{cm}^3}$, $\rho_2 = 6.74 \pm 1.04 \frac{\mathrm{g}}{\mathrm{cm}^3}$. This value can be explained by the high abundance of metal particles. This is questionable because there are few substances, such as metals, that have a density of this order. The generation of pure metal particles in LPB fires can rather be excluded. Further experiments covering the region between 1.6 and 3.6 µm could reveal the true shape and location of Fit 2; without this the $\rho_2$ value cannot be determined more accurately.

The third sample burned in our experiment was PUR foam. The visible discrepancies between the data and fitted one log-normal distribution suggest that the VSD is a result of the sum of more distributions. The $\{f_{V,i}\}$ values measured using the ELPI allow for the fit of the CDF with $n = 2$ (Figure 2c); however, uncertainties were determined for all fit parameters. The volume abundances of Fits 1 and 2 have a 2:1 ratio (Table 2) and significantly higher uncertainties; however, the sum equals $100 \pm 26\%$. The reduced chi-square of the fit is $\chi^2_\nu = 0.2364$, $\nu = 14 - 6 = 8$, and $p = 0.999993$, representing an overpredictive model. However, these values were accepted as the best-fit data because the data fit well and the uncertainties of all parameters are determined. The fit of the cumulative MSD shows that the mass proportions of Fits 1 and 2 are very similar to the volume proportions. However, the sum equals $98.9 \pm 19.5\%$, which is correct within uncertainty. Because the mass proportions are equal to the abundances of Fits 1 and 2, the densities of both types of particles are, within uncertainty, equal, that is, $\rho_2 = (0.91 \pm 0.42) \cdot \rho_1$. The high relative uncertainty of $\rho_2$ (46%) is due to the high relative uncertainties of the fitted volume and mass abundances $a_j$ and $b_j$, which exceed 30% of the fitted value for Fit 2. This might be due to the resolution of the impactor. An increase in the number of stages will lead to intermediate points and thus a higher fit quality. The majority of particles emitted from burning PUR are in the range of 100 nm to 2 µm, and the proportion of particles measured by the impactor to be bigger than 2 µm or smaller than 100 nm is insignificant.

The PUR is widely used for padding upholstered furniture; therefore, the products of its thermal decomposition have been widely investigated. This was discussed in the context of room fire experiments and smoke detector performance [68]. The particles emitted from these experiments were analyzed using the ELPI (non-HT version). It is difficult to compare this experiment to ours because the methodology used for the mass determination was poorly described and no distributions were presented therein.

The fourth investigated material was PMMA. The cumulative VSD is significantly shifted toward higher diameters compared with all other samples. The data collected by the ELPI permitted fitting the sum of two log-normal distributions, Equation (2). In this case, $\chi^2_\nu$ is almost equal to 1, representing a perfect fit ($\chi^2_\nu = 0.9866$, $\nu = 14 - 6 = 8$, $p = 0.998$, Figure 2d). Unfortunately, similar to the LPB sample, the location and shape parameters of Fit 2 could not be precisely determined, and thus the diameter $D_m$ and $GSD$ were roughly estimated (Table 2). In this case, $D_m$ ranges between stages 11 and 13 of the impactor, that is, between 1.6 and 3.6 µm, respectively. In contrast to previous sums of distributions, the sum of the volume abundances exceeds 100%, that is, $100.4 \pm 5.1\%$, which is still correct within uncertainty. The fit of the cumulative MSD resulted in values of mass abundances $b_j$ which summed within uncertainty to 100% (i.e., $98.3 \pm 3.7\%$). Similarly, as in the case of PUR, the mass abundances $b_j$ are similar to the volume abundances $a_j$. The particle densities obtained by Fits 1 and Fit 2 can be assumed to be equal within the uncertainty $\rho_2 = (1.12 \pm 0.33) \cdot \rho_1$.

The MSD of the particles emitted from burning PMMA was previously discussed [69]. The distributions presented in this study show that two types of particles are emitted from the PMMA fire: (1) particles with a mean diameter of 0.1–0.3 µm; and (2) particles with a mean diameter of 1–3 µm. These values were obtained for ventilated combustion using

a cone calorimeter. The location of the second type of particles is in agreement with our study; the coarse particles [67] emitted during the burning of PMMA are similar regardless of the burning condition. The location of the first type of particles differs in our experiment, which might be due to partial thermal decomposition and the observation of accumulation particles [67], whereas particles in [69] shifted toward nucleation particles [67].

Predicting VSD of Particles

To evaluate the results of the fire experiments on four raw material samples, we prepared and burned a sample containing all raw materials (MIX). The masses of the ingredients were four times smaller than those used for the burning of pure materials. The cumulative VSD of the particles emitted during the burning of MIX should be a weighted sum of the parametrized distributions for the separate materials. As the weight, we used the concentration ($C$) of the given material divided by the sum of the concentrations of all materials (presented in Table 1), as described in Equation (11). This normalization of the CDF of MIX should result in a good CDF estimate based on the CDFs of the pure materials. The cumulative VSD obtained from ELPI measurements is presented in Figure 3, together with the volume CDF estimated from Equation (11), which can be decomposed into separate summands corresponding to the pure materials.

$$CDF_{VSD}^{MIX}(x) = \frac{C^{PINE} \cdot CDF_{VSD}^{PINE}(x) + C^{PB} \cdot CDF_{VSD}^{PB}(x) + C^{PUR} \cdot CDF_{VSD}^{PUR}(x) + C^{PMMA} \cdot CDF_{VSD}^{PMMA}(x)}{C^{PINE} + C^{PB} + C^{PUR} + C^{PMMA}} \quad (11)$$

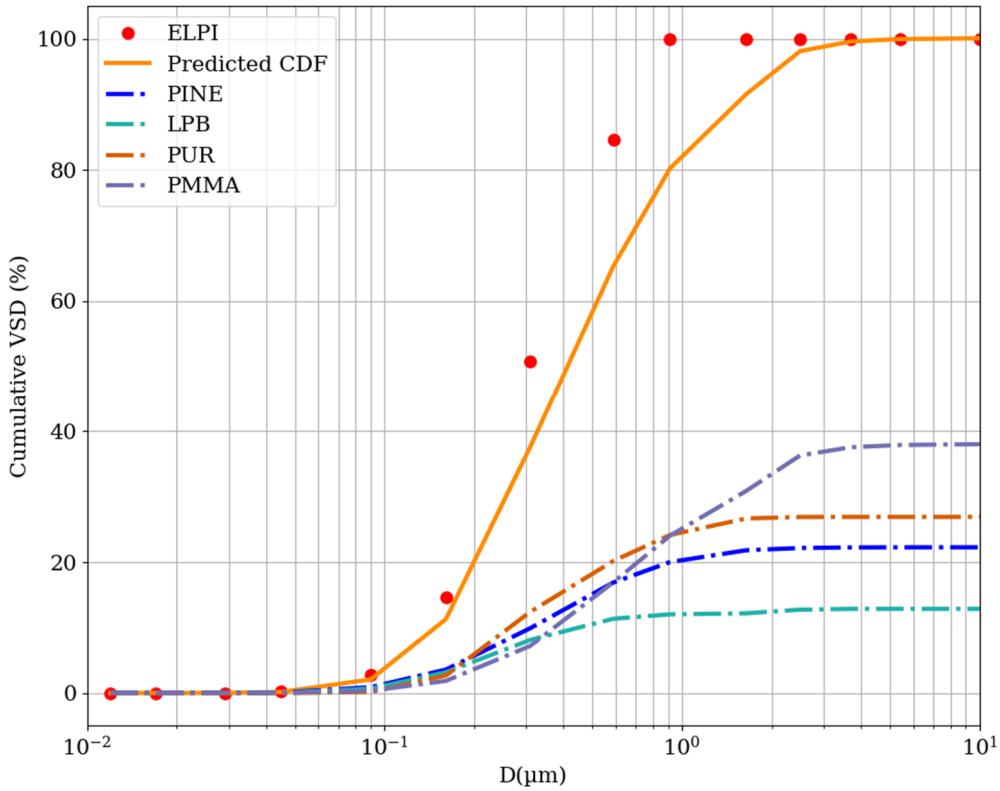


**Figure 3.** Cumulative volume size distribution of particles emitted during the MIX fire. The red dots represent values measured with the ELPI. The orange line is the predicted CDF line, which is the normalized sum of the four CDFs of the raw materials (dash-dotted lines; blue—pinewood, sea green—particle board, dark orange—PUR foam, and medium purple—PMMA).

There is a systematic discrepancy between the predicted and measured ELPI values. The CDF of MIX is shifted toward smaller diameters compared with the predicted CDF, which might have many reasons. One possible reason for this is the decomposition temperature. Based on the differential scanning calorimetry results, the thermal decomposition of

PINE starts at 150 °C [37], whereas LPB burns at temperatures higher than raw wood [42], and PUR foam and PMMA are burned at temperatures higher than 300 °C [70,71]. Therefore, the thermal decomposition of PINE in MIX will occur at a higher temperature than in the PINE fire, the decomposition will be less partial, and the distribution of particles emitted in such a fire will be shifted to smaller diameters. We cannot evaluate the exact shifts of the CDFs toward lower diameters; however, the measured and predicted CDFs fall into the Aitken particle range [67]. The difference observed for higher diameters and the lack of coarse particles (diameter higher than 1 μm) show that particles emitted from the MIX fire are the result of a more complete decomposition of materials.

## 4. Conclusions

The results of our experiments depend on our specific experimental setup. Although our chamber was relatively small, spatial nonuniformities might have affected the derived number concentrations. In addition, the arrangement of the sample before burning might affect the way it burns and thus the particle emission. Nevertheless, the research allowed us to draw following conclusions:

1. The mathematical limitations do not allow for the determination of the absolute density of particles based on comparing VSD and MSD. However, it has been proven that the densities of the particles can be expressed as a function of the density of the first type of particles if at least two types of particles can be distinguished (i.e., the fit contains at least two summands). The use of VSD and MSD in this work shows that it is possible to provide more precise results by violating the approach in which a constant density is assumed for all particulates.
2. The relative density obtained for one population of particles, from the fire of LPB, is questionable, which is mainly due to the resolving power of the distribution measured by the impactor.
3. The results show that the use of the cascade impactor with only 15 stages is adequate, even for the determination of six parameter distributions; however, it should be treated as the edge of applicability if more than 90% of the volume of particles is in the range of 100 nm to 1 μm.
4. The prediction of the VSD from the burning of the mixture of materials based on the VSD of the raw material led to a distribution shift toward larger Stokes diameters than that measured with the impactor, which indicates a more complete thermal decomposition during the MIX fire because LPB decomposes at higher temperatures than raw wood. Another possible cause is the interference between the decomposition products of different materials.

The results of our research open two further directions of study. Firstly, the aerosols from construction waste fires can be investigated in the range of 0.01–10 μm, providing more precise values of the parameters determined in this study; secondly, the cross-interactions of products emitted from different materials can be investigated using differential scanning calorimetry (DSC) and thermogravimetry (TG) analyses.

**Author Contributions:** Conceptualization, W.R.-K. and J.S.B.; methodology, J.S.B.; software, J.S.B.; validation, W.R.-K., A.K. and A.W.; formal analysis, M.M.-Ł. and M.F.; investigation, T.M., P.R.-K., A.W., M.F. and M.M.-Ł.; resources, T.M.; data curation, J.S.B., T.M. and A.K.; writing—original draft preparation, J.S.B.; writing—review and editing, A.K., M.F., W.R.-K. and P.R.-K.; visualization, J.S.B.; supervision, W.R.-K. All authors have read and agreed to the published version of the manuscript.

**Funding:** This research was supported within PRELUDIUM 19 funding scheme: The impact of landfill fires on atmospheric air quality—methodology and estimation of emissions (National Science Centre, Poland, 2020/37/N/ST10/02997). This research was also a part of the project "Implementation doctorate–edition II Faculty W-7 (03DW/0001/18)", financed by the National Centre for Research and Development, Warsaw, Poland. The research methodology was a result of the OPUS 12 funding scheme: Transitions of some chemical elements (metals and metalloids) during migration on the way emitter–atmosphere–soil (National Science Centre, Poland, 2016/23/B/ST10/02789). Publication of

the article was supported by a subsidy of the Ministry of the Interior and Administration, Poland, to The Main School of Fire Service, Warsaw, Poland. The funders played no role in the design of the study, collection, analyses, or interpretation of data, writing of the manuscript or decision to publish the results.

**Data Availability Statement:** The data presented in this study are available on request from the corresponding author.

**Acknowledgments:** The authors would like to thank BioWell s.r.o. and Dekati for providing the measurement equipment (Dekati® High-Temperature ELPI+®). The authors would like to thank Andrzej Gancarczyk from The Main School of Fire Service for his technical help during the experiment.

**Conflicts of Interest:** The authors declare no conflict of interest.

## References

1. Jaligot, R.; Chenal, J. Decoupling municipal solid waste generation and economic growth in the canton of Vaud, Switzerland. *Resour. Conserv. Recycl.* **2018**, *130*, 260–266. [CrossRef]
2. Jambeck, J.; Hardesty, B.D.; Brooks, A.L.; Friend, T.; Teleki, K.; Fabres, J.; Beaudoin, Y.; Bamba, A.; Francis, J.; Ribbink, A.J.; et al. Challenges and emerging solutions to the land-based plastic waste issue in Africa. *Mar. Policy* **2018**, *96*, 256–263. [CrossRef]
3. Borrelle, S.B.; Ringma, J.; Law, K.L.; Monnahan, C.C.; Lebreton, L.; McGivern, A.; Murphy, E.; Jambeck, J.; Leonard, G.H.; Hilleary, M.A.; et al. Predicted growth in plastic waste exceeds efforts to mitigate plastic pollution. *Science* **2020**, *369*, 1515–1518. [CrossRef]
4. Powęzka, A.; Szulej, J.; Ogrodnik, P. Reuse of Heat Resistant Glass Cullet in Cement Composites Subjected to Thermal Load. *Materials* **2020**, *13*, 4434. [CrossRef] [PubMed]
5. Lee, J. Recycled plastic is now more expensive than PET. That's not just an economic problem. *The Print*, 7 October 2019, p. 5.
6. Ambrose, J. War on plastic waste faces setback as cost of recycled material soars. *Guardian*, 13 October 2019, p. 2.
7. EUROSTAT. Municipal Waste Statistics. Available online: https://ec.europa.eu/eurostat/statistics-explained/index.php?title=Municipal_waste_statistics#Municipal_waste_treatment (accessed on 21 August 2021).
8. Agbeshie, A.A.; Adjei, R.; Anokye, J.; Banunle, A. Municipal waste dumpsite: Impact on soil properties and heavy metal concentrations, Sunyani, Ghana. *Sci. Afr.* **2020**, *8*, e00390. [CrossRef]
9. Das, B.; Bhave, P.V.; Sapkota, A.; Byanju, R.M. Estimating emissions from open burning of municipal solid waste in municipalities of Nepal. *Waste Manag.* **2018**, *79*, 481–490. [CrossRef]
10. Wang, Y.; Cheng, K.; Wu, W.; Tian, H.; Yi, P.; Zhi, G.; Fan, J.; Liu, S. Atmospheric emissions of typical toxic heavy metals from open burning of municipal solid waste in China. *Atmos. Environ.* **2017**, *152*, 6–15. [CrossRef]
11. Cheng, K.; Hao, W.; Wang, Y.; Yi, P.; Zhang, J.; Ji, W. Understanding the emission pattern and source contribution of hazardous air pollutants from open burning of municipal solid waste in China. *Environ. Pollut.* **2020**, *263*, 114417. [CrossRef]
12. Chaudhary, P.; Garg, S.; George, T.; Shabin, M.; Saha, S.; Subodh, S.; Sinha, B. Underreporting and open burning—The two largest challenges for sustainable waste management in India. *Resour. Conserv. Recycl.* **2021**, *175*, 105865. [CrossRef]
13. Blakeman, J.S. A Retrospective Analysis of Open Burning Activity in Kentucky. Master's Thesis, University of Kentucky, Lexington, KY, USA, 2017.
14. Badyda, A.; Krawczyk, P.; Bihałowicz, J.S.; Bralewska, K.; Rogula-Kozłowska, W.; Majewski, G.; Oberbek, P.; Marciniak, A.; Rogulski, M. Are BBQs Significantly Polluting Air in Poland? A Simple Comparison of Barbecues vs. Domestic Stoves and Boilers Emissions. *Energies* **2020**, *13*, 6245. [CrossRef]
15. Zhang, M.; Buekens, A.; Li, X. Open burning as a source of dioxins. *Crit. Rev. Environ. Sci. Technol.* **2017**, *47*, 543–620. [CrossRef]
16. Chen, C.-M. The emission inventory of PCDD/PCDF in Taiwan. *Chemosphere* **2004**, *54*, 1413–1420. [CrossRef]
17. Zhang, G.; Huang, X.; Liao, W.; Kang, S.; Ren, M.; Hai, J. Measurement of Dioxin Emissions from a Small-Scale Waste Incinerator in the Absence of Air Pollution Controls. *Int. J. Environ. Res. Public Health* **2019**, *16*, 1267. [CrossRef]
18. Balthi, M.R. Evaluation of greenhouse gas emissions from solid waste management practices in state capitals of North Eastern Nigeria. *J. Eng. Stud. Res.* **2021**, *26*, 40–46. [CrossRef]
19. Balcom, P.; Cabrera, J.M.; Carey, V.P. Extended exergy sustainability analysis comparing environmental impacts of disposal methods for waste plastic roof tiles in Uganda. *Dev. Eng.* **2021**, *6*, 100068. [CrossRef]
20. Pansuk, J.; Junpen, A.; Garivait, S. Assessment of Air Pollution from Household Solid Waste Open Burning in Thailand. *Sustainability* **2018**, *10*, 2553. [CrossRef]
21. US EPA. *AP-42: Compilation of Air Pollutant Emission Factors*; United States Enviromental Protection Agency: Washington, DC, USA, 1995.
22. EEA. *EMEP/EEA Air Pollutant Emission Inventory Guidebook 2016*; European Environment Agency: Copenhagen, Denmark, 2016.
23. Akagi, S.K.; Yokelson, R.J.; Wiedinmyer, C.; Alvarado, M.J.; Reid, J.S.; Karl, T.; Crounse, J.D.; Wennberg, P.O. Emission factors for open and domestic biomass burning for use in atmospheric models. *Atmos. Chem. Phys.* **2011**, *11*, 4039–4072. [CrossRef]
24. Lemieux, P.M.; Lutes, C.C.; Santoianni, D.A. Emissions of organic air toxics from open burning: A comprehensive review. *Prog. Energy Combust. Sci.* **2004**, *30*, 1–32. [CrossRef]

25. Wu, D.; Li, Q.; Shang, X.; Liang, Y.; Ding, X.; Sun, H.; Li, S.; Wang, S.; Chen, Y.; Chen, J. Commodity plastic burning as a source of inhaled toxic aerosols. *J. Hazard. Mater.* **2021**, *416*, 125820. [CrossRef] [PubMed]
26. Kim, M.; Jo, S.; Woo, J.; Jeon, E.-C. Studies on characteristics of fine particulate matter emissions from agricultural residue combustion. *Energy Environ.* **2021**, *32*, 1361–1377. [CrossRef]
27. Kim Oanh, N.T.; Ly, B.T.; Tipayarom, D.; Manandhar, B.R.; Prapat, P.; Simpson, C.D.; Sally Liu, L.-J. Characterization of particulate matter emission from open burning of rice straw. *Atmos. Environ.* **2011**, *45*, 493–502. [CrossRef] [PubMed]
28. Li, T.; Dai, Q.; Bi, X.; Wu, J.; Zhang, Y.; Feng, Y. Size distribution and chemical characteristics of particles from crop residue open burning in North China. *J. Environ. Sci.* **2021**, *109*, 66–76. [CrossRef] [PubMed]
29. Oleniacz, R. Świadomość społeczna z zakresu niekontrolowanego spalania odpadów i problemu dioksyn. In *Dioksyny w Przemyśle i Środowisku, Proceedings of the X Konferencja Naukowa, Kraków, Poland, 12–13 June 2008*; Politechnika Krakowska, Laboratorium Analiz Śladowych/EmiPro/Hamilton Poland Ltd.: Kraków, Poland, 2008.
30. Urząd Gminy w Choceniu Urząd Gminy w Choceniu Problem Spalania Śmieci w Paleniskach Domowych. Available online: https://chocen.pl/8-aktualnosci/4601-problem-spalania-smieci-w-paleniskach-domowych.html (accessed on 22 August 2021).
31. Toborek, P. W Polsce odpady dzielą się na palne i niepalne. Gospodarka o obiegu zamkniętym? Nie za naszego życia. *Portal Samorządowy*, 22 May 2017, p. 2.
32. Local Administrative Units (LAU)—NUTS—Nomenclature of Territorial Units for Statistics—Eurostat. Available online: https://ec.europa.eu/eurostat/web/nuts/local-administrative-units (accessed on 24 May 2021).
33. Eriksson, L.; Gustavsson, L.; Hänninen, R.; Kallio, A.; Hurttala, H.; Pingoud, K.; Pohjola, J.; Sathre, R.; Svanaes, J.; Valsta, L. Climate Implications of Increased Wood Use in the Construction Sector—Towards an Integrated Modeling Framework. *Eur. J. For. Res.* **2009**, *131*, 131–144. [CrossRef]
34. Brus, D.J.; Hengeveld, G.M.; Walvoort, D.J.J.; Goedhart, P.W.; Heidema, A.H.; Nabuurs, G.J.; Gunia, K. Statistical mapping of tree species over Europe. *Eur. J. For. Res.* **2012**, *131*, 145–157. [CrossRef]
35. Dudek, T. Influence of selected features of forests on forest landscape aesthetic value—Example of se Poland. *J. Environ. Eng. Landsc. Manag.* **2018**, *26*, 275–284. [CrossRef]
36. Krzosek, S.; Burawska-Kupniewska, I.; Mańkowski, P. The Influence of Scots Pine Log Type (*Pinus sylvestris* L.) on the Mechanical Properties of Lumber. *Forests* **2020**, *11*, 1257. [CrossRef]
37. Fernandes, C.; Gaspar, M.J.; Pires, J.; Alves, A.; Simões, R.; Rodrigues, J.C.; Silva, M.E.; Carvalho, A.; Brito, J.E.; Lousada, J.L. Physical, chemical and mechanical properties of *Pinus sylvestris* wood at five sites in Portugal. *IForest* **2017**, *10*, 669–679. [CrossRef]
38. Kodur, V.K.R.; Harmathy, T.Z. Properties of Building Materials. In *SFPE Handbook of Fire Protection Engineering*; Springer: New York, NY, USA, 2016; pp. 277–324.
39. Alapieti, T.; Castagnoli, E.; Salo, L.; Mikkola, R.; Pasanen, P.; Salonen, H. The effects of paints and moisture content on the indoor air emissions from pinewood (*Pinus sylvestris*) boards. *Indoor Air* **2021**, *31*, 1563–1576. [CrossRef] [PubMed]
40. Gottuk, D.T.; Lattimer, B.Y. Effect of Combustion Conditions on Species Production. In *SFPE Handbook of Fire Protection Engineering*; Springer: New York, NY, USA, 2016; pp. 486–528.
41. Deng, C.; Liaw, S.B.; Wu, H. Characterization of Size-Segregated Soot from Pine Wood Pyrolysis in a Drop Tube Furnace at 1300 °C. *Energy Fuels* **2019**, *33*, 2293–2300. [CrossRef]
42. Food and Agriculture Organization of the United Nations. *Forest Products Annual Market Review 2019–2020*; Food and Agriculture Organization: Rome, Italy, 2020.
43. Moreno, A.I.; Font, R.; Conesa, J.A. Combustion of furniture wood waste and solid wood: Kinetic study and evolution of pollutants. *Fuel* **2017**, *192*, 169–177. [CrossRef]
44. Babrauskas, V. Heat Release Rates. In *SFPE Handbook of Fire Protection Engineering*; Springer: New York, NY, USA, 2016; pp. 799–904.
45. Hurley, M.J.; Gottuk, D.; Hall, J.R.; Harada, K.; Kuligowski, E.; Puchovsky, M.; Torero, J.; Watts, J.M.; Wieczorek, C. (Eds.) *SFPE Handbook of Fire Protection Engineering*; Springer: New York, NY, USA, 2016; ISBN 978-1-4939-2564-3.
46. McKenna, S.T.; Hull, T.R. The fire toxicity of polyurethane foams. *Fire Sci. Rev.* **2016**, *5*, 3. [CrossRef]
47. Dahlin, J.; Spanne, M.; Dalene, M.; Karlsson, D.; Skarping, G. Size-separated sampling and analysis of isocyanates in workplace aerosols—Part II: Aging of aerosols from thermal degradation of polyurethane. *Ann. Occup. Hyg.* **2008**, *52*, 375–383. [CrossRef] [PubMed]
48. Tang, R.; Zeng, F.; Chen, Z.; Wang, J.-S.; Huang, C.-M.; Wu, Z. The Comparison of Predicting Storm-Time Ionospheric TEC by Three Methods: ARIMA, LSTM, and Seq2Seq. *Atmosphere* **2020**, *11*, 316. [CrossRef]
49. Zeng, W.R.; Li, S.F.; Chow, W.K. Preliminary Studies on Burning Behavior of Polymethylmethacrylate (PMMA). *J. Fire Sci.* **2002**, *20*, 297–317. [CrossRef]
50. Zeng, W.R.; Li, S.F.; Chow, W.K. Review on Chemical Reactions of Burning Poly (methyl methacrylate) PMMA. *J. Fire Sci.* **2002**, *20*, 401–433. [CrossRef]
51. An, W.; Hu, K.; Wang, T.; Peng, L.; Li, S.; Hu, X. Effects of Overlap Length on Flammability and Fire Hazard of Vertical Polymethyl Methacrylate (PMMA) Plate Array. *Polymers* **2020**, *12*, 2826. [CrossRef]
52. Khoo, B.; Skitt, J. The 1973 Summerland disaster-lessons to the building industry from the process industry. *Loss Prev. Bull.* **2019**, *269*, 3.

53. Rogula-Kozłowska, W.; Majewski, G.; Czechowski, P.O. The size distribution and origin of elements bound to ambient particles: A case study of a Polish urban area. *Environ. Monit. Assess.* **2015**, *187*, 240. [CrossRef]
54. Rivas, I.; Beddows, D.C.S.; Amato, F.; Green, D.C.; Järvi, L.; Hueglin, C.; Reche, C.; Timonen, H.; Fuller, G.W.; Niemi, J.V.; et al. Source apportionment of particle number size distribution in urban background and traffic stations in four European cities. *Environ. Int.* **2020**, *135*, 105345. [CrossRef]
55. Ramachandran, G.; Werner, M.A.; Vincent, J.H. Assessment of particle size distributions in workers' aerosol exposures. *Analyst* **1996**, *121*, 1225. [CrossRef]
56. Bralewska, K.; Rogula-Kozłowska, W.; Bralewski, A. Size-Segregated Particulate Matter in a Selected Sports Facility in Poland. *Sustainability* **2019**, *11*, 6911. [CrossRef]
57. Nielsen, E.; Dybdahl, M.; Larsen, P.B. Health effects assessment of exposure to particles from wood smoke. *Toxicol. Lett.* **2007**, *172*, S120. [CrossRef]
58. Dekati Ltd. *Dekati ELPI+ User Manual Ver. 1.55*; Dekati Ltd.: Kangasala, Finland, 2018.
59. Kuskowska, K.; Rogula-Kozłowska, W.; Widziewicz, K. A preliminary study of the concentrations and mass size distributions of particulate matter in indoor sports facilities before and during athlete training. *Environ. Prot. Eng.* **2019**, *45*, 103–112. [CrossRef]
60. van Rossum, G.; Drake, F.L. *Python 3 Reference Manual*; CreateSpace: Scotts Valley, CA, USA, 2009; ISBN 1441412697.
61. Kolmogorov, A.N. Uber das logarithmisch normale Verteilungsgesetz der Teilchen bei Zerstuckelung. *Dokl. Akad. Nauk SSSR-C. R. Acad. Sci. URSS Seriya A* **1941**, *31*, 99–101.
62. Hinds, W.C. *Aerosol Technology: Properties, Behaviour, and Measurement of Airborne Particles*; John Wiley & Sons: Hoboken, NJ, USA, 1982.
63. Björck, Å. Least squares methods. In *Handbook of Numerical Analysis*; North-Holland Publishing Company: Amsterdam, The Netherlands, 1990; pp. 465–652.
64. Newville, M.; Otten, R.; Nelson, A.; Ingargiola, A.; Stensitzki, T.; Allan, D.; Fox, A.; Carter, F.; Michał; Pustakhod, D.; et al. *Lmfit/lmfit-py*, version 1.0.2; CERN: Geneva, Switzerland, 2021.
65. Virtanen, P.; Gommers, R.; Oliphant, T.E.; Haberland, M.; Reddy, T.; Cournapeau, D.; Burovski, E.; Peterson, P.; Weckesser, W.; Bright, J.; et al. SciPy 1.0: Fundamental algorithms for scientific computing in Python. *Nat. Methods* **2020**, *17*, 261–272. [CrossRef]
66. Hase, T.; Hughes, I. *Measurements and Their Uncertainties*; Oxford University Press: Oxford, UK, 2010.
67. Whitby, K.T. The Physical Characteristics of Sulfur Aerosols. In *Sulfur in the Atmosphere*; Elsevier: Amsterdam, The Netherlands, 1978; pp. 135–159.
68. Cleary, T. Particle Size Distributions from Smokes and Cooking Aerosols Sampled from Room Fire Experiments. In Proceedings of the Suppression, Detection, and Signaling Research and Aplication Conference (SUPDET 2017)/16th International Conference on Fire Detection (AUBE 2017), College Park, MD, USA, 12–14 September 2017; National Fire Protection Association: Quincy, MA, USA, 2017.
69. Motzkus, C.; Chivas-Joly, C.; Guillaume, E.; Ducourtieux, S.; Saragoza, L.; Lesenechal, D.; Macé, T.; Lopez-Cuesta, J.-M.; Longuet, C. Aerosols emitted by the combustion of polymers containing nanoparticles. *J. Nanoparticle Res.* **2012**, *14*, 687. [CrossRef]
70. Kumar, M.; Chung, J.S.; Hur, S.H. Controlled atom transfer radical polymerization of MMA onto the surface of high-density functionalized graphene oxide. *Nanoscale Res. Lett.* **2014**, *9*, 345. [CrossRef] [PubMed]
71. Yao, X.; Tan, S.; Zhang, X.; Huang, Z.; Jiang, D. Low-temperature sintering of SiC reticulated porous ceramics with $MgO–Al_2O_3–SiO_2$ additives as sintering aids. *J. Mater. Sci.* **2007**, *42*, 4960–4966. [CrossRef]

# 11th International Aerosol Conference

#IAC2022_Athens

HYBRID

IAC 2022

4-9 September 2022

Megaron Athens International Conference Centre (M.A.I.C.C.)

ATHENS
Greece

www.iac2022.gr

Organized by:

HAAQR

AIRA

Under the auspices of

HELLENIC REPUBLIC
REGION OF ATTICA

CITY OF ATHENS

## Abstract Book

# High time-resolution measurements of particulate size distribution in controlled fires of construction materials

W. Rogula-Kozłowska[1], J.S. Bihałowicz[1], A. Krasuski[1], M. Majder-Łopatka[1], A. Walczak[1] and T. Mach[2]

[1]The Main School of Fire Service, 01-629 Warsaw, Juliusza Słowackiego 52/54, Poland
[2]Wroclaw University of Science and Technology, 50-377 Wrocław, Plac Grunwaldzki 13, Poland
Keywords: number size distribution, ELPI, construction materials, indoor fires, MMAD.
Presenting author email: wrogula@sgsp.edu.pl

The average number of daily interventions of Fire Service in Poland due to the fire is 321. Within this set 20% are compartment fires (KG PSP 2020 (www.kgpsp.gov.pl/panstwowa_straz_pozarna/interwencje_psp). Every fire contributes to air pollution, providing particles significant also from global emissions point of view - particulate matter (PM) (Xu et al. 2020; Bihałowicz et al. 2021). Depending on the way the rescue and firefighting operation is carried out, and the extinguishing agents used, compartment fires can also be a serious source of water and soil pollution (Fernandez-Marcos 2022). So far, the scale of this phenomenon is little recognized and it seems that fires, especially compartment fires, are very poorly characterized as sources of emissions, especially PM emissions. Our experiment is probably one of the first study that describes the physical characteristics and variability of particles emitted during simulated fires of interiors (Table 1). Moreover, we compared the obtained results against data of typical waste materials fires. In this paper we present the results obtained during the test fires of the mixture of the typical materials used in the manufacturing of household equipment (construction and upholsters elements) – pine wood, laminated particle boards, polyvinyl chloride PVC and poly(methyl methacrylate) PMMA. The summary for individual materials is presented in (Bihałowicz et al. 2022).

Table 1. Mass median aerodynamic diameter (MMAD) and mass geometric standard deviation (MGSD) in three phases of experiment.

| Phase | MMAD | MGSD |
|---|---|---|
| | µm | |
| Burn | 6.14-6.98 | 1.76-2.08 |
| Extinguishing | 3.71-5.06 | 2.05-2.63 |
| After | 5.99-6.18 | 2.16-2.21 |

To determine number (NSD) mass (MSD) and volume (VSD) size distribution (Figure 1; Table 1) we used 14-stage low pressure electrical impactor designed to analyze hot aerosols Dekati® High Temperature ELPI®+. The measurements were performed in the fire laboratory of The Main School of Fire Service, in the chamber designed to evaluate efficiency of fire detection systems.

MMAD for PM emitted during the combustion of the mixture of the tested material was at the value of 6-7 µm (Table 1). However, the median diameter for the number size distribution during experiment did not exceed 120 nm (Fig. 1). In the initial phase of the experiment, both NSD and MSD were highly variable. After some stabilization of the environmental conditions in the chamber in which the experiment was conducted and during the extinguishing phase, the material, size distributions of PM, regardless of whether numerical or mass, did not varied in time. Therefore, typical for the PM emitted from the combustion of material of given type. During the extinguishing phase and a few minutes after the combustion process was completed, the media diameter for NSD did not exceed 80 nm.

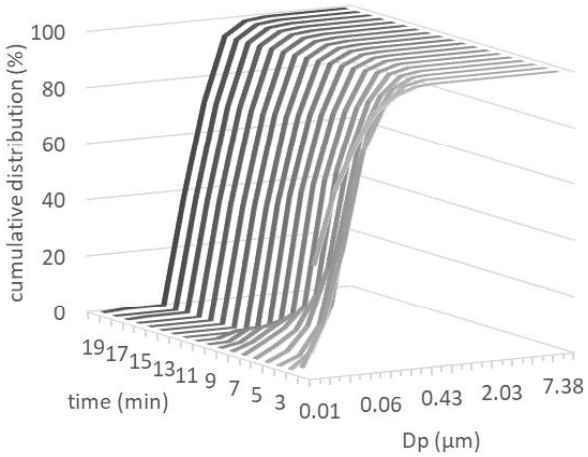


Figure 1. Temporal variability of cumulative number size distributions of PM emitted during combustion of mix of construction materials.

This work was supported by the National Science Centre, Poland (PRELUDIUM 19; 2020/37/N/ST10/02997)

Xu, R. et al. (2020) *N. Engl. J Med.* 383, 2173–2181. (2020).
Bihałowicz, J S, Rogula-Kozłowska, W and Krasuski, A (2021) *Waste Manage*. 125 182–9.
Fernandez-Marcos, M.L. (2022) *Toxics* 10, 31.
Bihałowicz, J.S. et al. (2022) *Materials* 15, 152.

HYBRID

# 11th International Aerosol Conference

ATHENS Greece

www.iac2022.gr

# IAC 2022

4-9 September 2022 Megaron Athens International Conference Centre (M.A.I.C.C.)

PCO professional congress organizer

convin

www.convin.gr

# Energetyka i ochrona środowiska – współczesne rozwiązania i perspektywy na przyszłość

Redakcja:
Alicja Danielewska
Kinga Kalbarczyk

Lublin 2021

**Wydawnictwo Naukowe TYGIEL składa serdecznie podziękowania dla zespołu Recenzentów za zaangażowanie w dokonane recenzje oraz merytoryczne wskazówki dla Autorów.**

**Recenzentami niniejszej monografii byli:**

- prof. dr hab. inż. Eugeniusz Mokrzycki
- prof. dr hab. Małgorzata Krystyna Pawłowska
- dr hab. inż. Tomasz Cholewa, prof. PL
- dr hab. inż. Urszula Kaźmierczak
- dr hab. inż. Alina Kowalczyk-Juśko
- dr hab. inż. Tomasz Kujawa
- dr hab. Monika Naumowicz, prof. UwB
- dr hab. inż. Sylwia Polesek-Karczewska
- dr Weronika Goraj
- dr Sławomir Gułkowski
- dr Agnieszka Kuźniar
- dr inż. Łukasz Szałata
- dr inż. Mateusz Wnukowski

Wszystkie opublikowane rozdziały otrzymały pozytywne recenzje.

Skład i łamanie:
Monika Maciąg

Projekt okładki:
Marcin Szklarczyk

Korekta:
Jagoda Biszkont



ISBN 978-83-66489-83-7

Wydawca:
Wydawnictwo Naukowe TYGIEL sp. z o.o.
ul. Głowackiego 35/341, 20-060 Lublin
www.wydawnictwo-tygiel.pl

Tomasz Mach[1], Joanna Bihałowicz[2], Jan Stefan Bihałowicz[3]

# Dobowa i godzinowa zmienność stężeń Pb, Ni, Zn, Mn i V w powietrzu atmosferycznym: badania pilotażowe w wybranym receptorze centralnej Polski

## 1. Wstęp

Obecnie zanieczyszczenie powietrza jest jednym z najczęściej podnoszonych tematów na świecie, a pył zawieszony (*Particulate Matter*, PM) jest najpoważniejszym i najczęściej badanym zanieczyszczeniem powietrza w niemal wszystkich zurbanizowanych krajach świata [1, 2]. Pomimo iż stan jakości powietrza w Polsce w ostatnich latach się poprawia, wciąż znajduje się wśród najbardziej zanieczyszczonych państw Europy [3, 4]. Pył zawieszony to drobne cząsteczki stanowiące część aerozolu atmosferycznego. Problem pyłu zawieszonego w powietrzu dotyczy niemal wszystkich większych miast w Polsce, jak również rejonów podmiejskich, w których sposób ogrzewania, jak również emisja z transportu drogowego stanowią podstawowe źródła zanieczyszczenia powietrza [5, 6].

Wiele instytucji i ośrodków naukowych, również w Polsce, bada jakość powietrza pod kątem stężenia pyłu i jego składników [7, 8]. Niemniej brakuje wciąż informacji na ten temat w wielu miejscach i rejonach. Są dwa tego główne powody:

- monitorowanie ilości i jakości pyłu zawieszonego odbywa się wciąż w zbyt rzadkiej siatce pomiarowej (w Polsce dotąd stały monitoring jakości powietrza pod względem stężenia PM prowadzony jest w ponad 500 punktach pomiarowych, rzadziej niż 1 punkt na 650 $km^2$);
- monitorowanie pyłu zarówno ilościowe, jak i jakościowe ma zbyt małą rozdzielczość czasową (zwłaszcza w przypadku monitorowania jakości – składu chemicznego pyłu stosuje się w najlepszym przypadku dobowe, a często średniotygodniowe próbki), co powoduje konieczność prowadzenia badań ukierunkowanych na ocenę pochodzenia pyłu, w jednym punkcie pomiarowym, przez wiele miesięcy [9].

Obecnie najczęściej stosowanym podziałem pyłu ze względu na rozmiar jego cząstek jest podział na:

- pył $PM_{10}$ – frakcja pyłu zawieszonego o średnicach zastępczych cząstek poniżej 10 μm;
- pył $PM_{2,5}$ – frakcja pyłu zawieszonego o średnicach zastępczych cząstek poniżej 2,5 μm, zwana także pyłem drobnym.

W literaturze spotykane jest określanie cząstek o średnicach mniejszych od 2,5 μm pyłem drobnym (ang. fine), a cząstek o wymiarach pomiędzy 2,5 μm i 10 μm pyłami

[1] tomasz.mach@pwr.edu.pl, Wydział Inżynierii Środowiska, Politechnika Wrocławska, https://wis.pwr.edu.pl/.
[2] joanna_bihalowicz@sggw.edu.pl, Katedra Sztuki Krajobrazu, Instytut Inżynierii Środowiska, Szkoła Główna Gospodarstwa Wiejskiego, https://iis.sggw.edu.pl/instytut-inzynierii-srodowiska/o-instytucie/katedry/katedra-sztuki-krajobrazu/.
[3] jbihalowicz@sgsp.edu.pl, Instytut Inżynierii Bezpieczeństwa, Szkoła Główna Służby Pożarniczej, https://www.sgsp.edu.pl/.

grubymi (ang. *coarse*). Te dwa rodzaje pyłu – pył drobny oraz był gruby ze względu na swoje powiązania z różnymi zjawiskami środowiskowych i oddziaływaniem na elementy środowiska są dwiema najczęściej badanymi frakcjami [10]. Początkowo wydawało się, iż ustalenie dopuszczalnych wartości dla frakcji $PM_{10}$ będzie wystarczające na cele ochrony środowiska, jednak wraz z rozszerzeniem zakresu badań nad pyłem, zaczęto dowodzić silniejszych korelacji między zachorowalnością na choroby górnych dróg oddechowych, a stężeniami $PM_{2,5}$. W jego skład wchodzi przede wszystkim sadza oraz inne produkty powstałe w procesach spalania, a ze względu na niewielkie rozmiary cząstek może przenikać do najgłębszych części układu oddechowego, do pęcherzyków płucnych i dalej do krwiobiegu – cząsteczki są bardziej respirabilne [11-13].

W powietrzu atmosferycznym, a konkretnie w pyle zawieszonym może występować około 40 pierwiastków śladowych. Osiem z nich, tj. arsen As, kadm Cd, chrom Cr, rtęć Hg, mangan Mn, nikiel Ni, ołów Pb i wanad V – Światowa Organizacja Zdrowia (WHO) umieściła na liście 35 substancji szczególnie niebezpiecznych dla zdrowia człowieka [14], natomiast według klasyfikacji Międzynarodowej Agencji Badań nad Nowotworami (IARC) pierwiastki As, Cd, Cr(VI) i Ni należą do grupy związków o potwierdzonym działaniu kancerogennym na organizm człowieka [15].

Pierwiastki śladowe w pyle mogą pochodzić ze źródeł naturalnych, np. pył z wybuchów wulkanów czy aerozol morski oraz antropogenicznych, czyli ze spalania paliw, odpadów, a także wszelkiego rodzaju przeróbki, wytapiania i produkcji metali, stopów metali, itp. [16-18]. W zurbanizowanych obszarach Polski najpoważniejszymi źródłami pierwiastków śladowych, w tym zwłaszcza toksycznych i kancerogennych, są spalanie paliw stałych i płynnych. Szeroko rozumiana emisja komunikacyjna stanowi w wielu polskich miastach podstawowy problem zanieczyszczenia powietrza większością metali [9].

Powoduje to tym samym, że zwłaszcza ze względu na sposób emisji (kondensacja i zestalanie par metali) największy masowy udział wielu metali, w tym metali toksycznych obserwuje się w pyle drobnym $PM_{2,5}$. We frakcji grubego pyłu udział różnych pierwiastków kształtują zazwyczaj źródła naturalne i szereg różnego rodzaju procesów mechanicznych [19].

Celem głównym pracy było przeprowadzenie wstępnych badań dobowej i godzinowej zmienności stężeń pięciu wybranych pierwiastków (Pb, Ni, Zn, Mn i V) związanych z drobnym pyłem zawieszonym $PM_{2,5}$ w typowym ośrodku miejskim pod Warszawą. Wybrano pierwiastki, które zazwyczaj wskazuje się jako markery oddziaływania emisji komunikacyjnej na powietrze atmosferyczne i punkt pomiarowy, który narażony był na oddziaływanie takiej emisji [5, 19-21].

Celem dodatkowym pracy była próba wskazania możliwości wykorzystania wyników godzinowej zmienności stężenia pyłu i związanych z nim pierwiastków jako bardzo prostej i szybkiej metody wskazania wpływu konkretnego źródła emisji zanieczyszczeń oraz oceny jakościowej tego wpływu na ich stężenie w powietrzu.

## 2. Metodyka

### 2.1. Miejsce prowadzenia badań

Badanie wykonywane było przez 7 dni, w sierpniu, poza sezonem grzewczym, żeby wyeliminować wpływ emisji związanej z indywidualnym ogrzewaniem gospodarstw domowych. Punkt pomiarowy zlokalizowany był w podwarszawskiej miejscowości przy skrzyżowaniu drogi wojewódzkiej 634 i dróg lokalnych (rys. 1), z których jedna prowadzi do stacji kolejowej i okolicznych wsi. Na skrzyżowaniu znajduje się sklep spożywczy, do którego licznie przyjeżdżają klienci z okolicy. Skrzyżowanie jest dość ruchliwe i dochodzi na nim do częstych zatrzymań ruchu w związku z dużym natężeniem skrętów w lewo na skrzyżowaniu (do stacji) i brakiem sygnalizacji świetlnej. W godzinach szczytu komunikacyjnego korki do tego skrzyżowania mają około 1 km długości. Urządzenie usytuowane było w odległości 9 m od osi drogi, a pomiędzy nim a drogą nie było przeszkód.

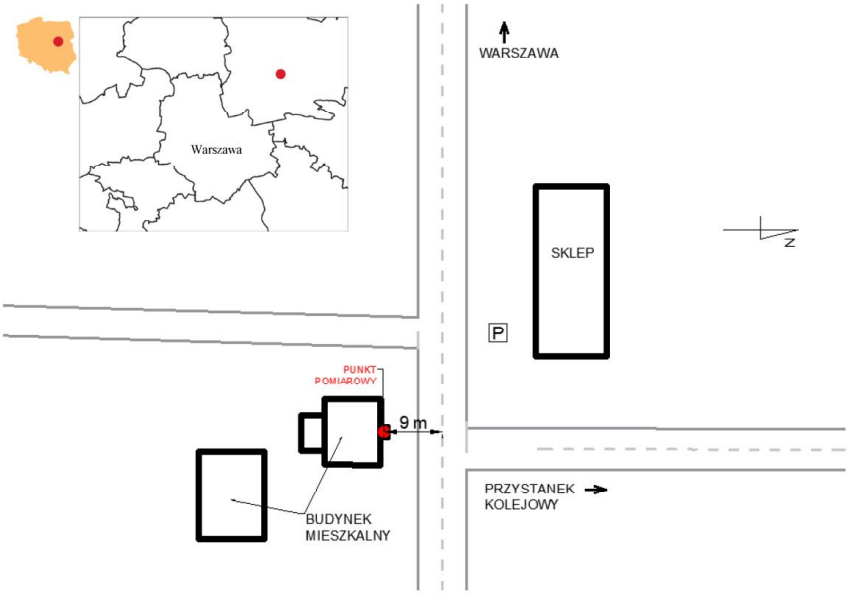


Rysunek 1. Schemat lokalizacji punktu pomiarowego, który przedstawia miejsce przeprowadzonych badań względem granic Warszawy, jak i usytuowanie aparatury pomiarowej przy skrzyżowaniu [opracowanie własne]

### 2.2. Aparatura pomiarowa

Masa pyłu $PM_{2,5}$ oraz stężenia pierwiastków V, Mn, Ni, Zn i Pb były mierzone na miejscu z częstotliwością godzinową za pomocą urządzenia Horiba PX-375 (HORIBA ltd., Kyoto, Japonia). Urządzenie to pobiera próbkę na taśmę pomiarową, a następnie przy pomocy czujnika wykorzystującego metodę tłumienia promieniowania beta, określa całkowitą masę pyłu $PM_{2,5}$. W kolejnym etapie za pomocą nieniszczącej próbki analizy spektroskopowej EDXRF (*energy-dispersive X-ray fluorescence*) oceniane jest stężenie wybranych pierwiastków. Moduł EDXRF wyposażony jest dodatkowo w kamerę CMOS do obrazowania mierzonych próbek.

Jako taśmę pomiarową do zbierania pyłu zastosowano dwuwarstwową taśmę z włókniny PTFE o bardzo dużej czystości pierwiastkowej (pozbawionej śladów metali). Przepływ powietrza do analizatora był stabilizowany regulatorem masowym i wynosił 16,7 L/min (1 $m^3$/h), średnica zebranych próbek na taśmie wynosiła ok. 11 mm każda.

Po pobraniu pojedynczych próbek co godzinę przeprowadzono badanie masy zebranego pyłu metodą osłabiania promieniowania beta, a następnie wykonywano analizę EDXRF przez 500 s (15 kV lub 50 kV w zależności od ilości pierwiastka w próbce godzinowej). Dodatkowo sprawdzano barwę badanych próbek, co pozwoliło uzyskać bardziej wiarygodne wyniki.

Do określenia składu pierwiastkowego widm rentgenowskich i kontroli jakości wyników zastosowano materiał wzorcowy certyfikowany przez National Institute of Standards and Technology NIST (SRM 2783) w postaci pyłu osadzonego na podłożu filtracyjnym. Dolne granice wykrywalności (LDL jako podwójne odchylenie standardowe analizowanej czystej taśmy pomiarowej) dla poszczególnych pierwiastków wynosiły: V (1,7 ng/$m^3$), Mn (1,45 ng/$m^3$), Ni (0,9 ng/$m^3$), Zn (1,25 ng/$m^3$) i Pb (1,05 ng/$m^3$).

## 3. Analiza wyników

### 3.1. Średnie dobowe stężenia $PM_{2,5}$ oraz analizowanych pierwiastków

W przebiegu średnich stężeń dobowych nie odnotowano znaczących różnic w odczytach w ciągu siedmiu dni pomiarów co pokazano na wykresie 1. Stężenie $PM_{2,5}$ wynosiło w zasadzie przez cały okres pomiarowy ok. 12 µg/$m^3$. Jedynie we wtorek i czwartek zauważono lekkie odchylenie w górę tej wartości co może mieć związek z wynikami obserwacji aktywności i zwyczajów lokalnej ludności. Przykładowo, we wtorek najwięcej osób robi zakupy spożywcze po weekendzie [22]. W czwartek natomiast na lokalnym targowisku zlokalizowanym w pobliżu punktu pomiarowego jest dzień handlowy [23].

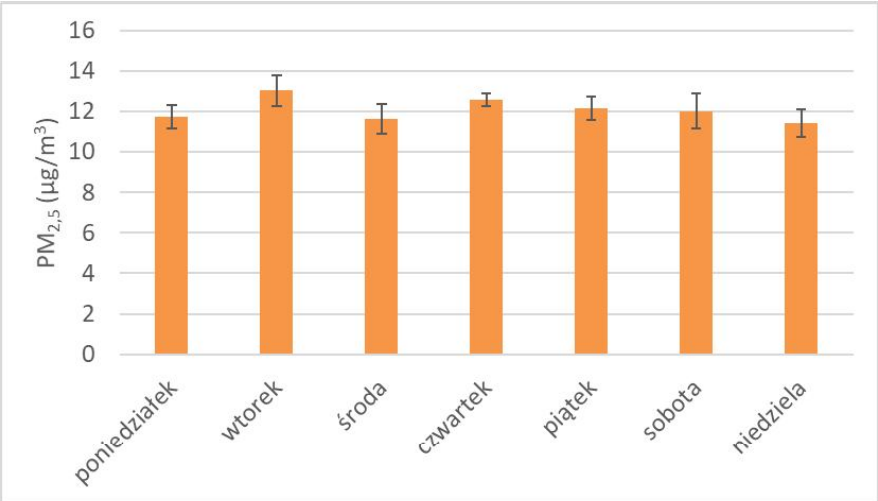


Wykres 1. Średnie dobowe stężenia pyłu $PM_{2,5}$ [opracowanie własne]

Średnie dobowe stężenie wanadu związanego z pyłem drobnym w powietrzu w badanym punkcie pomiarowym wahało się od 0,12 do 0,18 ng/m$^3$. Najwyższe dobowe stężenia tego pierwiastka zanotowano we wtorek i w sobotę (wyk. 2).

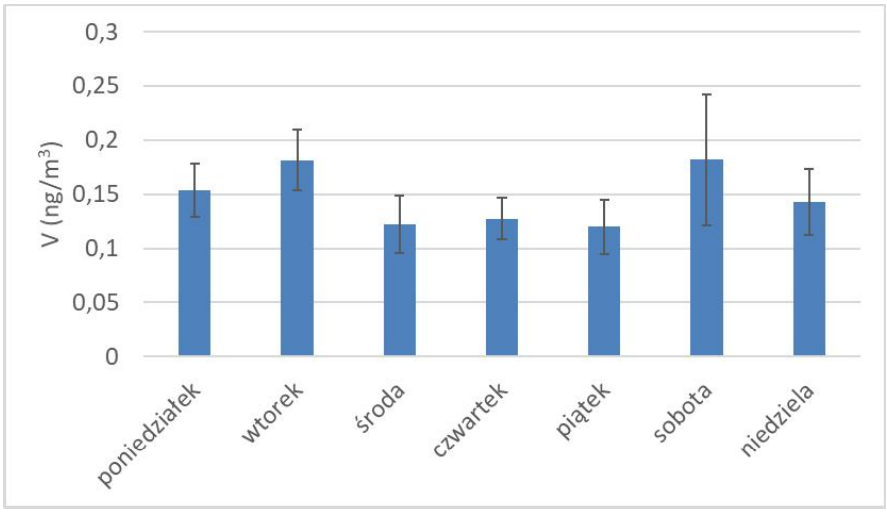


Wykres 2. Średnie dobowe stężenia wanadu [opracowanie własne]

Średnie dobowe stężenia manganu utrzymywały się na poziomie – 2-2,5 ng/m$^3$. Wyraźnie niższe stężenie (1,55 ng/m$^3$) zanotowano jedynie w niedzielę (wyk. 3).

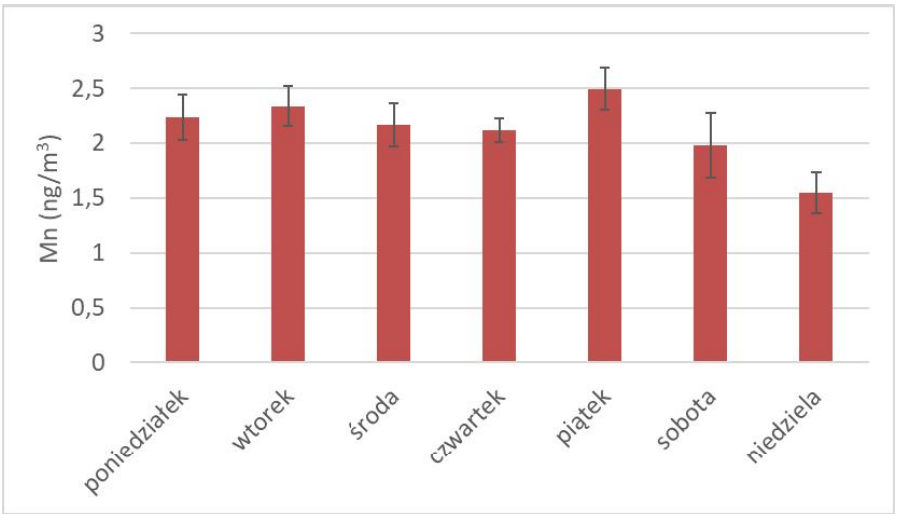


Wykres 3. Średnie dobowe stężenia manganu [opracowanie własne]

W przypadku dobowych stężeń niklu najwyższe wartości odnotowano w poniedziałek, wtorek i czwartek, kiedy oscylowały one pomiędzy 0,09 a 0,12 ng/m$^3$. Są to znacznie wyższe wartości niż w pozostałe dni tygodnia, kiedy stężenia dobowe niklu znajdowały się w przedziale od 0,02 do 0,06 ng/m$^3$ (wyk. 4).

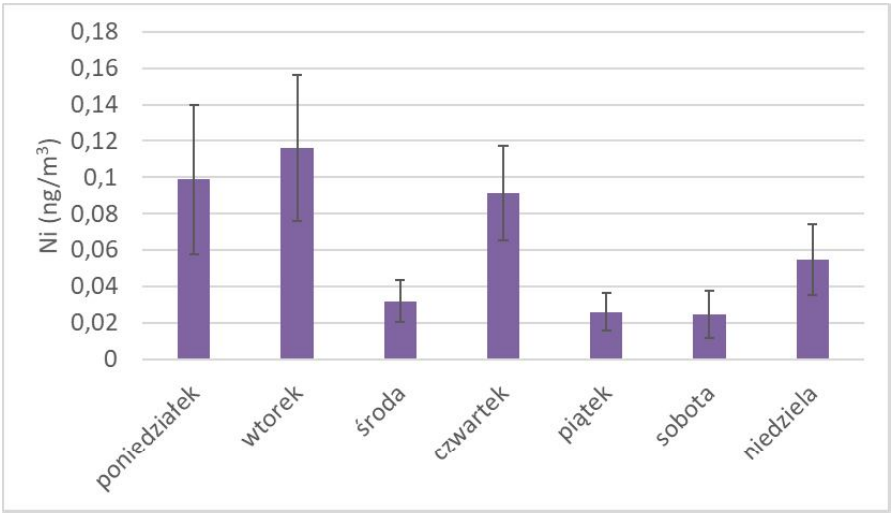


Wykres 4. Średnie dobowe stężenia niklu średnie [opracowanie własne]

Dla cynku związanego z drobnym pyłem zawieszonym w badanym punkcie pomiarowym najwyższe dobowe stężenie, wynoszące 22 i 23 ng/m$^3$, odnotowano w poniedziałek i piątek. W pozostałe dni tygodnia stężenia dobowe oscylowały w granicach od 11 do 15 ng/m$^3$ (wyk. 5).

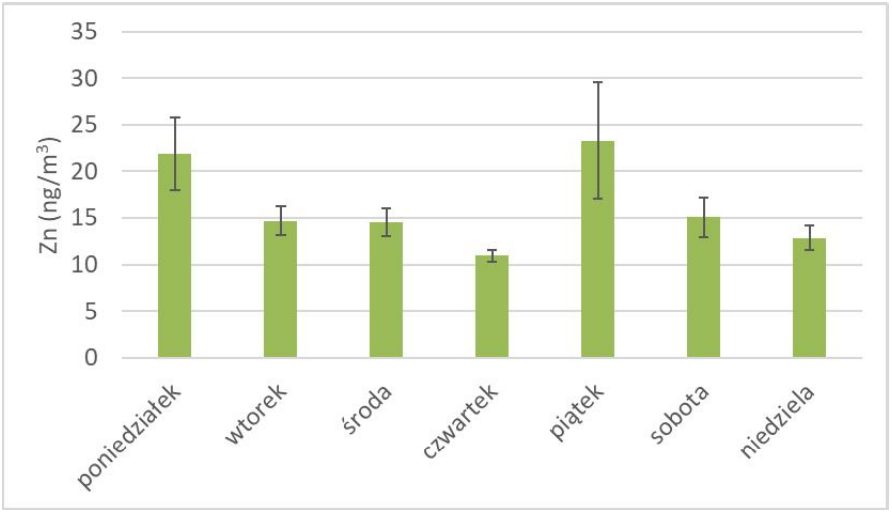


Wykres 5. Średnie dobowe stężenia cynku średnie [opracowanie własne]

Wykres 6 przedstawia średnie dobowe stężenie ołowiu w każdym dniu pomiarów. Najwyższe wartości, powyżej 2 ng/m$^3$, wystąpiły w poniedziałek i piątek. Najniższe stężenie odnotowano we czwartek i wynosiło ono 1,15 ng/m$^3$.

Generalnie można uznać, że stężenia dobowe wszystkich badanych pierwiastków były niższe w weekendy niż w pozostałe dni tygodnia.

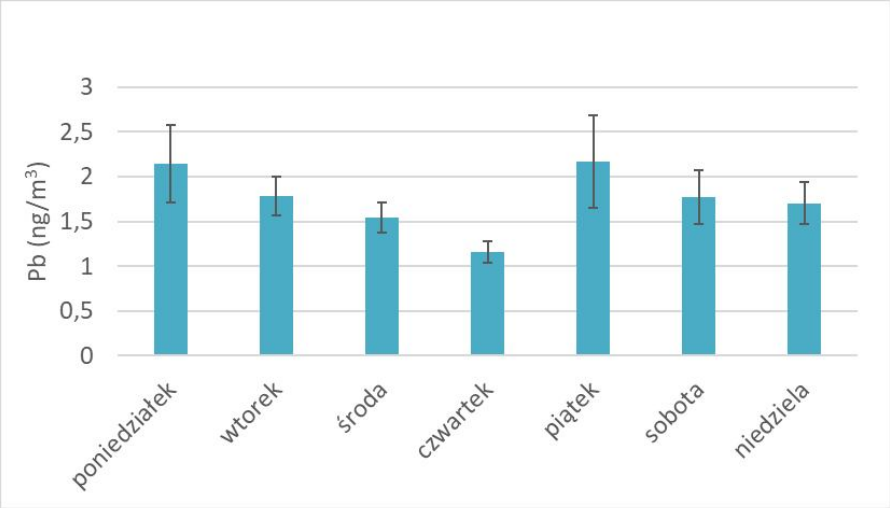


Wykres 6. Średnie dobowe stężenia ołowiu [opracowanie własne]

## 3.2. Średnie godzinowe stężenia $PM_{2,5}$ oraz analizowanych pierwiastków

Stężenia godzinowe $PM_{2,5}$ wahają się w ciągu doby ,co przedstawiono na wykresie 7. Wyniki te uzyskano poprzez uśrednienie każdorazowo wyników 7 pomiarów stężeń godzinowych (jeden pomiar dla jednej godziny każdego dnia). Słupki błędów przedstawione na wykresach są odchyleniem standardowym średniej 7 pomiarów przemnożonym przez współczynnik t-Studenta [24]. Najniższe stężenie występowało o godzinie 16:00 i wynosiło 8 $\mu g/m^3$, a najwyższe (13-17 $\mu g/m^3$) zanotowano w godzinach pomiędzy 19:00, a 1:00.

Mimo tego, że spodziewaliśmy się wyższych stężeń godzinowych w trakcie szczytu ruchu drogowego po południu (15:00-18:00) zaobserwowaliśmy, że najwyższe stężenia notowane są w późniejszych godzinach dnia – wieczornych i późnowieczornych. Może być to spowodowane faktem, iż w zasadzie o godzinie 16:00 na skrzyżowaniu występuje zator drogowy, a w godzinach wieczornych ruch dalej jest wzmożony, ale prędkość poruszania się samochodów istotnie wzrasta. To z kolei wynika z faktu, że dopiero w godzinach wieczornych (po 18:00) rozpoczyna się powrót mieszkańców okolic z pracy w centrum Warszawy. Ten efekt może powodować pewna bezwładność stężeń drobnego pyłu, a rozkład sugeruje, że stężenie związane jest z unosem wtórnym.

Poza tym zauważyć należy wyraźny skok stężeń $PM_{2,5}$ w godzinach pomiędzy 6:00 a 7:00, kiedy to rozpoczyna się wyjazd mieszkańców podwarszawskich miejscowości do miejsc pracy zlokalizowanych w Warszawie (wyk. 7).

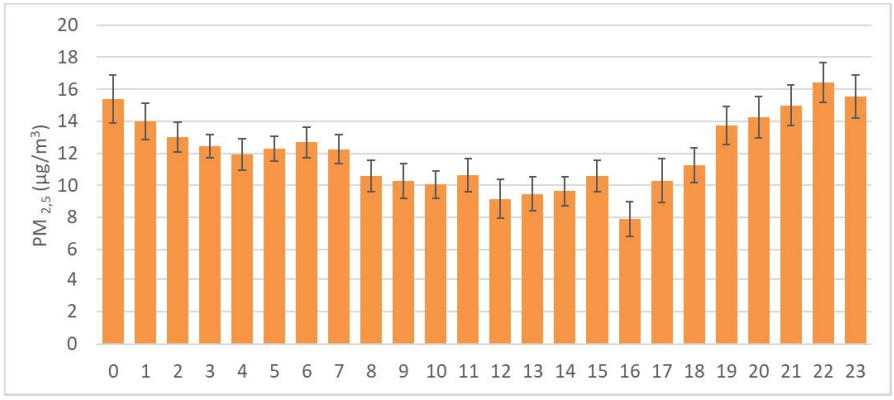


Wykres 7. Średnie godzinowe stężenia pyłu $PM_{2,5}$ (średnia dwutygodniowa) [opracowanie własne]

Analogicznie, jak w przypadku pyłu, zbadano także przebieg średnich godzinowych stężeń wybranych metali. W przypadku wanadu zauważono wyraźny wzrost stężeń godzinowych w dwóch okresach doby – porannym i wieczornym – co obrazuje wykres 8. Najwyższą wartość średnie stężenie godzinowe wanadu osiągało o 23:00 i wynosiło ponad 0,3 ng/m$^3$. Najniższe wartości wynoszące około 0,05 ng/m$^3$ zanotowano o godzinie 3:00 i 15:00.

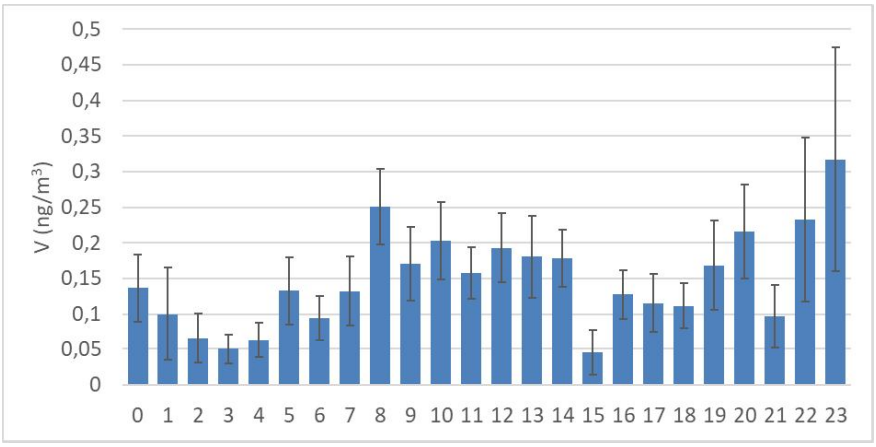


Wykres 8. Średnie godzinowe stężenie wanadu (średnia dwutygodniowa) [opracowanie własne]

Średnie stężenia manganu, przedstawione na wykresie 9, w każdej godzinie pomiarów, podobnie jak w przypadku wanadu, wzrastają w godzinach porannych i wieczornych. Poranny wzrost występuje w godzinach od 6:00 do 10:00, a wartości stężeń wahają się od 2,2 do 2,8 ng/m$^3$. Popołudniowy skok wartości stężeń przypada na godziny od 19:00 do 00:00; stężenia w tych godzinach średnio wynoszą od 2,2 do 3 ng/m$^3$. Najniższe średnie stężenia godzinowe (ok. 0,25 ng/m$^3$) zanotowano w godzinach od 2:00 do 5:00 (wyk. 9).

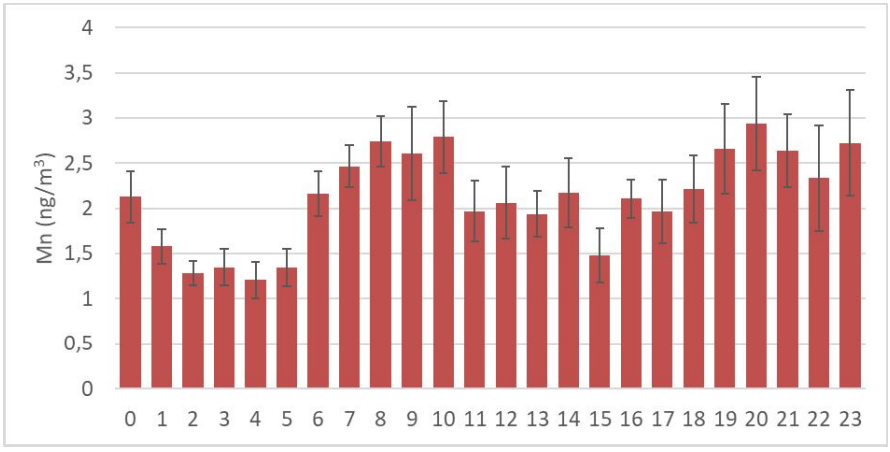


Wykres 9. Średnie godzinowe stężenie manganu (średnia dwutygodniowa) [opracowanie własne]

W przebiegu dobowym uśrednionych dla okresu pomiarowego stężeń godzinowych cynku, niklu i ołowiu (wyk. 10-12) widać komunikacyjny szczyt poranny, który trwa krócej niż szczyt popołudniowy rozkładający się na więcej godzin. Najwyższe stężenia godzinowe tych trzech pierwiastków przypadają na godziny od 8:00 do 10:00. Najwyższe stężenie niklu odnotowano dla godziny 10:00 i wynosi ono 0,3 ng/m$^3$; jest to wartość ponad dwa razy większa niż w pozostałych godzinach (wyk. 10).

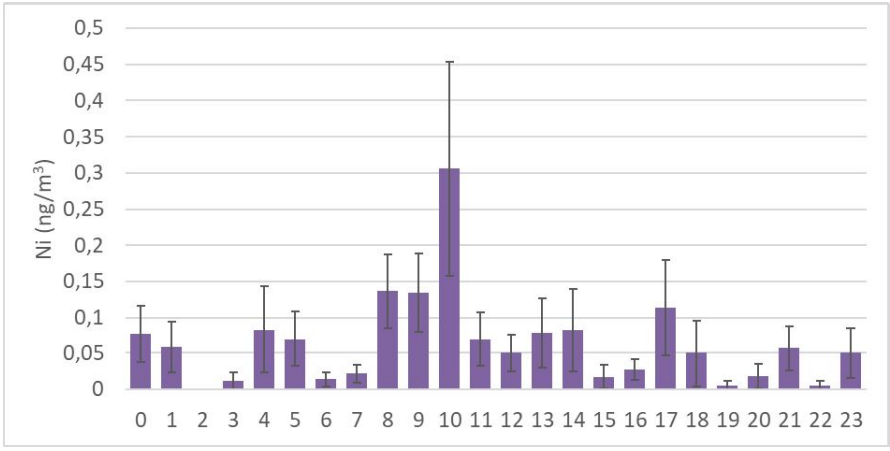


Wykres 10. Średnie godzinowe stężenie niklu (średnia dwutygodniowa) [opracowanie własne]

Średnie godzinowe stężenie cynku w okresie doby waha się od 10 do 20 ng/m$^3$. Wyjątkiem jest wyraźny skok stężenia w godzinach porannych, między 8:00 a 10:00, kiedy wartości godzinowych stężeń cynku wahają się między 28 a 45 ng/m$^3$ (wyk. 11).

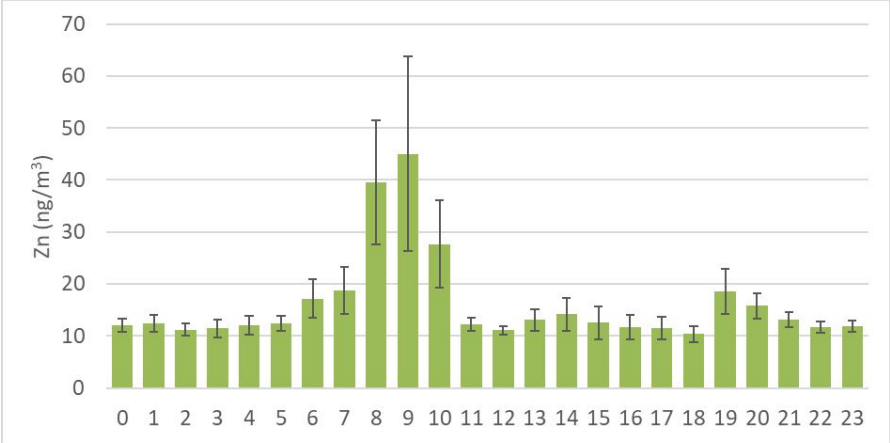


Wykres 11. Średnie godzinowe stężenie cynku (średnia dwutygodniowa) [opracowanie własne]

Średnie godzinowe stężenia ołowiu, tak jak w przypadku dwóch wcześniej omawianych pierwiastków, przez większość okresu doby są stałe i oscylują w granicach między 1 a 2 ng/m$^3$. Skok tej wartości (aż do 4 ng/m$^3$) ma miejsce w godzinach między 8:00 a 10:00 (wyk. 12).

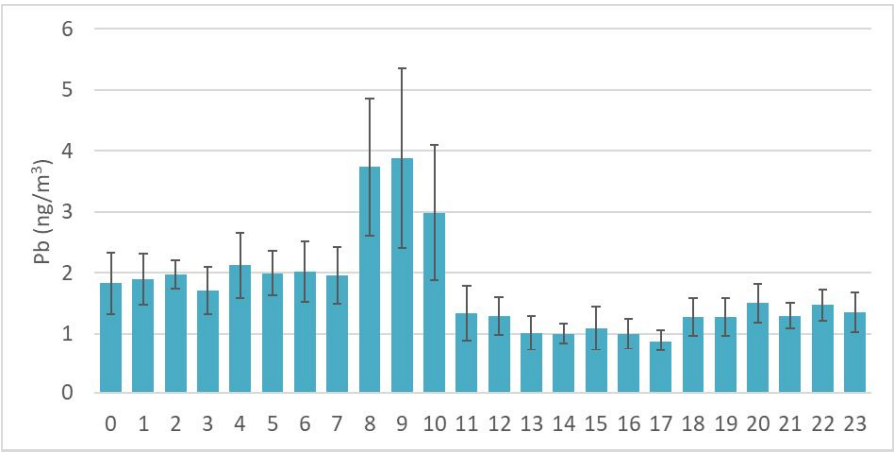


Wykres 12. Średnie godzinowe stężenie ołowiu (średnia dwutygodniowa) [opracowanie własne]

Generalnie udowodniono, że zarówno cynk, jak i nikiel są wskaźnikami oddziaływania emisji pierwiastków z ruchu drogowego na skład pyłu zawieszonego [25-28]. Wiadomo też, że dotyczy to zarówno pyłu drobnego, jak i grubego. W przypadku pyłu drobnego wpływ oddziaływania ruchu drogowego na skład pyłu zawieszonego polega na emisji bardzo drobnych cząstek pyłu (kondensujących par) w trakcie spalania paliwa w silniku – paliwa zanieczyszczonego śladami tych metali. Również oleje i smary zawierają ślady tych metali. W przypadku pyłu grubego wpływ emisji z transportu drogowego polega na wzbogacaniu cząstek metalami ze ścierania opon, okładzin hamulcowych, karoserii i innych elementów samochodu [29-31].

Ołów do lat 90. był typowym markerem emisji pierwiastków do powietrza atmosferycznego ze spalania benzyny [21, 26, 32]. Od czasu wprowadzenia zakazu dodawania ołowiu do benzyny nie jest już typowym markerem. Niemniej nadal w wielu rejonach miejskich, w okolicach dróg i skrzyżowań, obserwuje się podwyższone stężenia ołowiu [33]. Podobnie jak w przypadku pozostałych metali, tak i w przypadku ołowiu obserwowano jego podwyższone stężenia w godzinach porannego szczytu natężenia ruchu pojazdów.

## 3.3. Porównanie godzinowych stężeń pomiędzy wtorkiem a sobotą

Porównując szeregi czasowe godzinowego rozkładu stężeń pyłu $PM_{2,5}$ w jeden wybrany dzień roboczy – wtorek i jeden wybrany dzień wolny od pracy – sobota widać wyraźne różnice w stężeniach godzinowych (wyk. 13). Dotyczą one zwłaszcza godzin porannych i popołudniowych, a więc tych w których natężenie ruchu pojazdów na drogach jest największe.

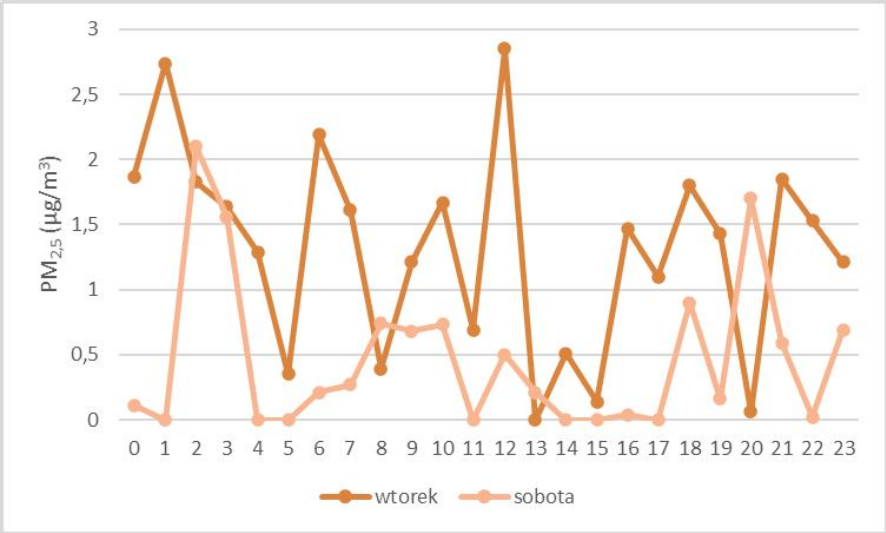


Wykres 13. Przebieg godzinowych stężeń pyłu $PM_{2,5}$ we wtorek i sobotę [opracowanie własne]

Podobnie jak w przypadku pyłu $PM_{2,5}$ dokładniejszy obraz zmienności godzinowych stężeń badanych pierwiastków śladowych pod wpływem emisji komunikacyjnej można zauważyć, porównując przebiegi dobowe godzinowych stężeń tych pierwiastków w dwa wybrane dni tygodnia (sobota i wtorek). Wyraźnie widać, że godzinowe stężenia wanadu we wtorek przez większą część doby były wyższe niż w sobotę i oscylowały pomiędzy 0 a 1 ng/m$^3$, podczas gdy w sobotę były w granicach od 0 do 0,5 ng/m$^3$ (wyk. 14). Jedynie od godziny 21:00 w sobotę widoczny jest gwałtowny wzrost stężenia wanadu do ok. 2,3 ng/m$^3$.

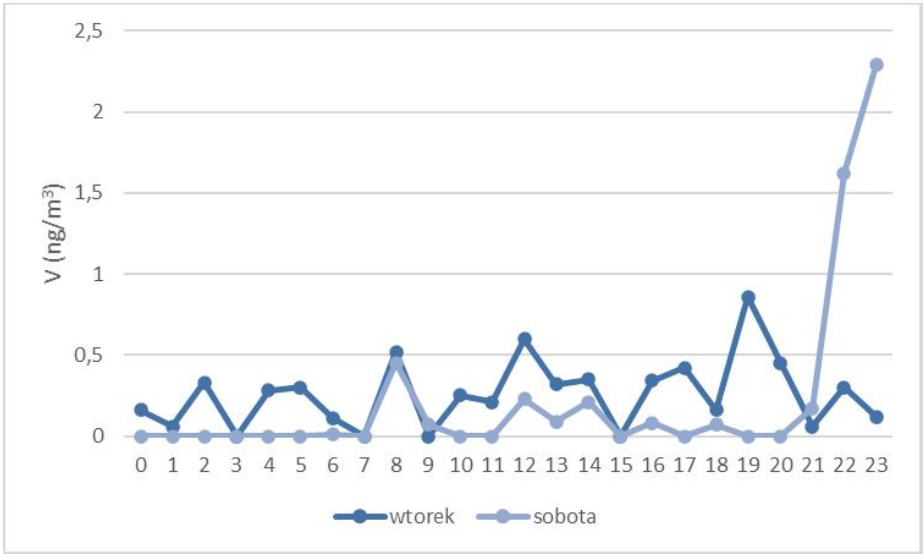


Wykres 14. Przebieg godzinowych stężeń wanadu we wtorek i sobotę [opracowanie własne]

Podobnie w przypadku manganu obserwowane są wyższe stężenia godzinowe przez większą część doby we wtorek niż w sobotę, poza wyraźnym wzrostem w godzinach wieczornych w sobotę. W dzień powszedni godzinowe stężenia manganu utrzymywały się w granicach od 1 do 6 ng/m$^3$. Natomiast w weekend do godziny 19:00 stężenie godzinowe manganu nie przekraczał 4 ng/m$^3$ powietrza i wzrasta do 10 ng/m$^3$ o godzinie 23:00 (wyk. 15).

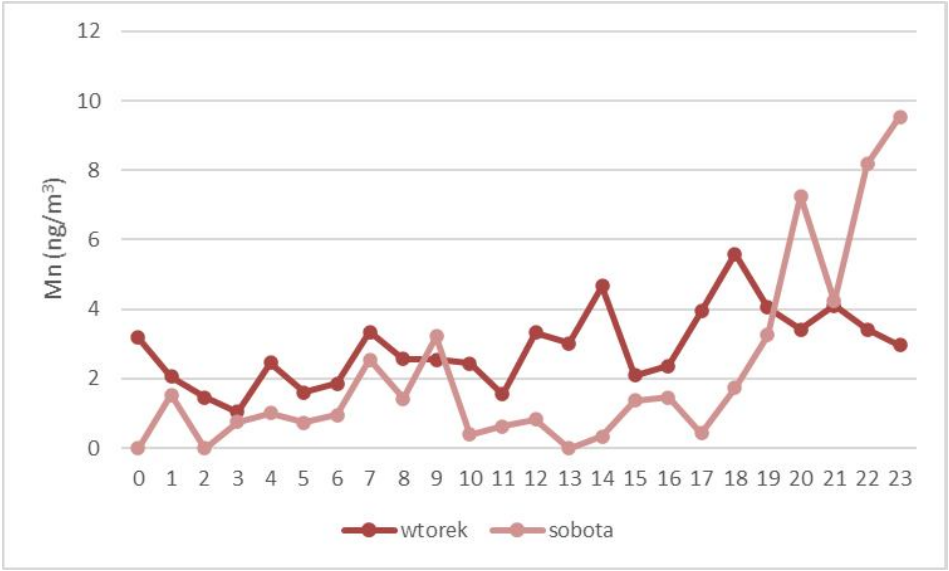


Wykres 15. Przebieg godzinowych stężeń manganu we wtorek i sobotę [opracowanie własne]

Wyższe wartości godzinowych stężeń w dzień roboczy niż w weekend dotyczą także stężeń niklu i cynku, co przedstawiono na wykresie 16 i 17, choć w przypadku tego drugiego różnice nie są tak wyraźne. Zaobserwowano również wysokie stężenia cynku w sobotę w godzinach 7:00-9:00.

Wartości stężeń niklu w sobotę oscylowały w okolicach 0 poza skokiem pomiędzy 6:00 a 10:00 kiedy osiągają nawet 0,4 ng/m$^3$. Najwyższą wartość godzinowego stężenia niklu – 0,8 ng/m$^3$ zaobserwowano we wtorek o godzinie 17:00 (wyk. 16).

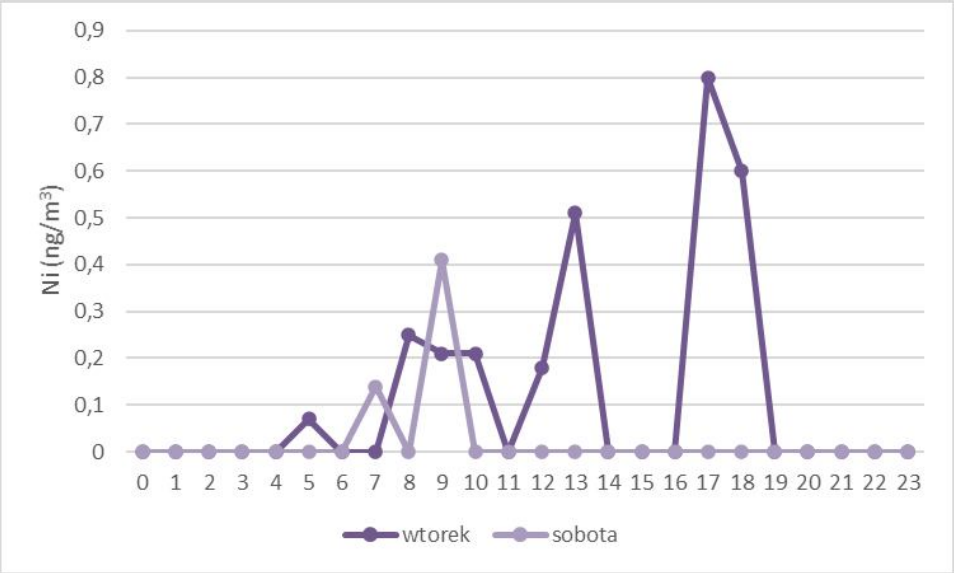


Wykres 16. Przebieg godzinowych stężeń niklu we wtorek i sobotę [opracowanie własne]

Wartości godzinowych stężeń cynku we wtorek rosły niewielkimi skokami przez całą dobę. Początkowo jest to około 9 ng/m$^3$ w godzinach 0:00-4:00 do około 17 ng/m$^3$ w godzinach 18:00-22:00. W sobotę można wyróżnić dwa skoki godzinowych stężeń cynku – jeden w godzinach 7:00-8:00 (stężenia dochodziły do 17 ng/m$^3$), drugi w godzinach 20:00-23:00 (godzinowe stężenia osiągnęły 15 ng/m$^3$).

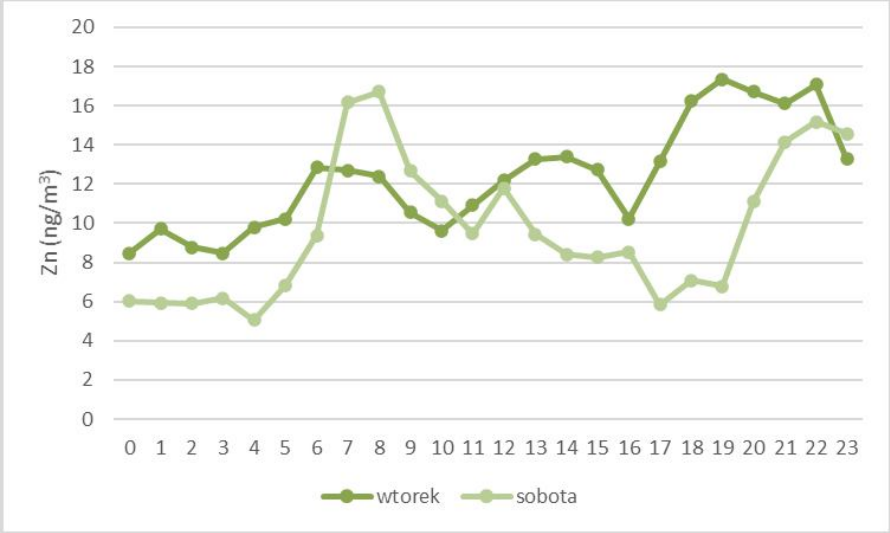


Wykres 17. Przebieg godzinowych stężeń cynku we wtorek i sobotę [opracowanie własne]

Notowane stężenia ołowiu zazwyczaj były wyższe we wtorek niż w sobotę, co zobrazowano na wykresie 18. W dzień roboczy wartości stężeń godzinowych wahały się od 0 do prawie 3 ng/m$^3$. W weekend przez większość doby stężenia godzinowe nie przekraczały 1 ng/m$^3$, poza dwoma pikami. Pierwszy z wartościami między 1,5 a 2,2 ng/m$^3$ wystąpił w godzinach 1:00-2:00, a drugi o godzinie 20:00 (stężenie ołowiu osiągnęło 1,7 ng/m$^3$).

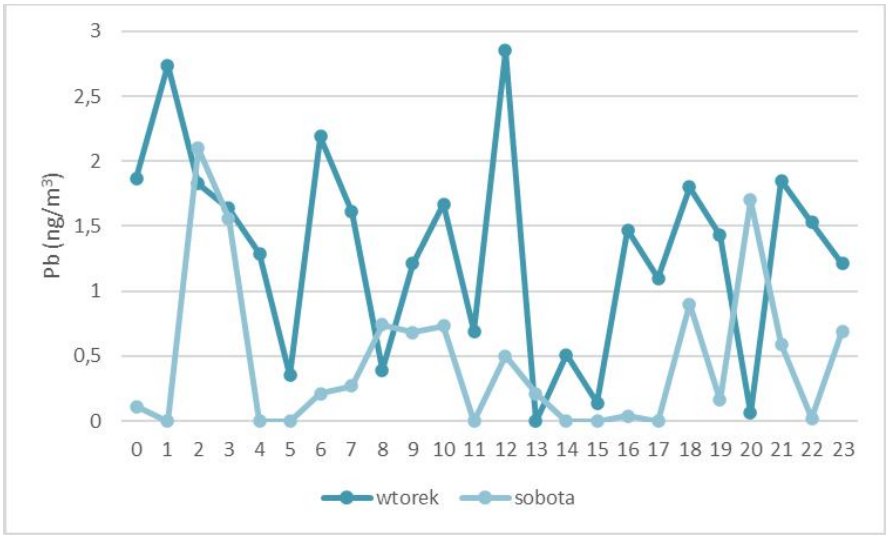


Wykres 18. Przebieg godzinowych stężeń ołowiu we wtorek i sobotę [opracowanie własne]

Warto podkreślić, że generalnie stężenia badanych pierwiastków, w tym ołowiu, w badanym obszarze są bardzo niskie – znacznie niższe niż notowane w innych częściach Polski, np. na Górnym lub Dolnym Śląsku albo w Warszawie zimą [34-38].

Niemniej należy mieć na uwadze, że analiza dotyczy jednego, wybranego dnia. Takie wyniki mogą być przypadkowe i aby ocenić w pełni skalę i przyczyny zjawiska należy w przyszłości przeanalizować dane z dłuższego okresu, a co najmniej porównać kilka dni roboczych i weekendowych. Jednak mimo to, stosując nowoczesne urządzenie pomiarowe, jakim jest PM-375, można przy tak nawet niskich wartościach wychwycić różnice w godzinowych stężeniach pierwiastków śladowych skumulowanych w drobnym pyle. Biorąc pod uwagę, że naważka dobowa nie przekracza w analizowanych przypadkach 300 $\mu g/m^3$, a godzinowa nie przekracza kilkunastu $\mu g/m^3$ można uzmysłowić sobie jak trudne, a wręcz niemożliwe byłoby wykonanie takich analiz metodami manualnymi, a więc w sposób tradycyjny – pobierając próbkę pyłu i analizując w laboratorium.

## 4. Podsumowanie

Zmienność zarówno dobowa jak i godzinowa stężeń $PM_{2,5}$ i związanych z nim 5 badanych pierwiastków nie była duża, co wynikało z faktu, że notowane w okresie pomiarowym stężenia były nieduże, a jakość powietrza była bardzo dobra [10]. Czynnikiem warunkującym wartości stężeń badanych substancji i ich zmienność w sezonie letnim była praktycznie wyłącznie intensywność emisji związanej z ruchem drogowym, a więc:

- całkowite stężenie pyłu było najmniejsze w godzinach zatorów drogowych, co może wskazywać na unos wtórny jako źródło pyłu;
- wartości stężeń metali były związane z natężeniem ruchu drogowego;
- we wtorek wartości stężeń były większe niż w sobotę, ale porównanie trendów stężeń metali zaobserwowanych w trakcie tych dni (położenie maksimów, minimów) wskazuje na inną aktywność komunikacyjną mieszkańców w poszczególnych godzinach.

W pracy wykazano, że nawet w bardzo krótkim okresie pomiarowym wykorzystanie analizatora HORIBA PX-375 pozwala na jakościowe powiązanie niektórych pierwiastków śladowych w powietrzu ze źródłami emisji. Najlepsze rezultaty w tym zakresie daje analiza zmienności godzinowej stężeń tych pierwiastków w ciągu doby. Uśrednianie stężeń pierwiastków w kolejnych dobach powoduje zbyt duże wyrównanie stężeń w tak krótkich okresach pomiarowych. Nie ma wątpliwości, że zastosowanie urządzenia HORIBA PX-375 w systemie monitoringu jakości powietrza w Polsce pozwoliłoby prowadzić ten monitoring znacznie wydajniej. Zamiast wieloletnich pomiarów w pojedynczych/stałych punktach można by było w krótkich okresach pomiarowych (np. miesiąc w lecie i miesiąc w zimie) z dobrą dokładnością ocenić pochodzenie pyłu i związanych z nim priorytetowych metali w wielu obszarach/punktach pomiarowych [39-41]. Takie podejście pozwoliłoby w dalszej kolejności wyznaczyć dużo lepiej, niż ma to miejsce obecnie, przestrzenne zmiany stężeń pierwiastków w powietrzu atmosferycznym w Polsce, a na tej podstawie ocenić narażenie mieszkańców wielu rejonów na zanieczyszczenie powietrza atmosferycznego.

## Finansowanie

Badania zostały wykonane jako część Doktoratu wdrożeniowego II edycja II, W-7 (03DW/0001/18) finansowanego przez Narodowe Centrum Badań i Rozwoju, Polska.

## Podziękowania

Autorzy pragną podziękować firmom HORIBA oraz MLU-recordum Environmental Monitoring Solutions GmbH za użyczenie aparatury pomiarowej (PX-375 Horiba, Japan).

Dziękujemy również dr hab. inż. Wiolecie Roguli-Kozłowskiej, prof. uczelni za pomoc w interpretacji uzyskanych wyników i konsultacje.

## Literatura

1. Viana M., Kuhlbusch T.A.J., Querol X., Alastuey A., Harrison R.M., Hopke P.K., Winiwarter W., Vallius M., Szidat S., Prévôt A.S.H., *Source Apportionment of Particulate Matter in Europe: A Review of Methods and Results*, J. Aerosol Sci., 39, 2008, s. 827-849, doi:https://doi.org/10.1016/j.jaerosci.2008.05.007.
2. Belis C.A., Karagulian F., Larsen B.R., Hopke P.K., *Critical Review and Meta-Analysis of Ambient Particulate Matter Source Apportionment Using Receptor Models in Europe*, Atmos. Environ., 69, 2013, s. 94-108, doi:https://doi.org/10.1016/j.atmosenv.2012.11.009.
3. European Environment Agency, *Air Quality in Europe*, Luxembourg 2015.
4. European Environment Agency, *Air Quality in Europe*, Luxembourg 2020.
5. Lough G.C., Schauer J.J., Park J.-S., Shafer M.M., DeMinter J.T., Weinstein J.P., *Emissions of Metals Associated with Motor Vehicle Roadways*, Environ. Sci. Technol., 39, 2005, s. 826-836, doi:10.1021/es048715f.
6. Majewski G., Rogula-Kozłowska W., *The Elemental Composition and Origin of Fine Ambient Particles in the Largest Polish Conurbation: First Results from the Short-Term Winter Campaign*, Theor. Appl. Climatol., 125, 2016, s. 79-92, doi:10.1007/s00704-015-1494-y.
7. Rogula-Kozłowska W., Majewski G., Błaszczak B., Klejnowski K., Rogula-Kopiec P., *Origin-Oriented Elemental Profile of Fine Ambient Particulate Matter in Central European Suburban Conditions*, Int. J. Environ. Res., Public Health, 13, 2016, s. 715, doi:10.3390/ijerph13070715.
8. Rogula-Kozłowska W., Majewski G., Czechowski P.O., *The Size Distribution and Origin of Elements Bound to Ambient Particles: A Case Study of a Polish Urban Area*, Environ. Monit. Assess., 187, 2015, s. 240, doi:10.1007/s10661-015-4450-5.
9. Mach T., Rogula-Kozłowska W., Bralewska K., Majewski G., Rogula-Kopiec P., Rybak J., *Impact of Municipal, Road Traffic, and Natural Sources on PM10: The Hourly Variability at a Rural Site in Poland*, Energies, 2021, s. 14.
10. Majewski G., Rogula-Kozłowska W., Rozbicka K., Rogula-Kopiec P., Mathews B., Brandyk A., *Concentration, Chemical Composition and Origin of PM1: Results from the First Long-Term Measurement Campaign in Warsaw (Poland)*, Aerosol Air Qual. Res., 18, 2018, s. 636-654, doi:10.4209/aaqr.2017.06.0221.
11. Trojanowska M., Świetlik R., *Investigations of the Chemical Distribution of Heavy Metals in Street Dust and Its Impact on Risk Assessment for Human Health, Case Study of Radom (Poland)*, Hum. Ecol. Risk Assess. An Int. J., 26, 2020, s. 1907-1926, doi:10.1080/10807039.2019.1619070.
12. Rogula-Kozłowska W., *Environmental Characteristics of Gaseous Pollutants and Related Adverse Health Effects*, In *Synergic Influence of Gaseous, Particulate, and Biological Pollutants on Human Health*, CRC Press, 2015, s. 13-48.
13. Samek L., *Overall Human Mortality and Morbidity Due to Exposure to Air Pollution*, Int. J. Occup. Med. Environ. Health, 29, 2016, s. 417-426, doi:10.13075/ijomeh.1896.00560.

14. World Health Organization, Regional Office for EuropeCopenhagen, *Air Quality Guidelines for Europe Second Edition*, WHO Regional Publications, European Series, No. 91, 2000; ISBN 92 890 1358 3.
15. International Agency for Research on Cancer IARC Monographs on the Identification of Carcinogenic Hazards to Humans, https://monographs.iarc.who.int/agents-classified-by-the-iarc/.
16. Shuhaimi-Othman M., Yakub N., Ramle N.-A., Abas A., *Toxicity of Metals to a Freshwater Ostracod: Stenocypris Major*, J. Toxicol., 2011, 2011, s. 1-8, doi:10.1155/2011/136104.
17. Chakraborty A., Gupta T., *Chemical Characterization and Source Apportionment of Submicron (PM1) Aerosol in Kanpur Region, India*, Aerosol Air Qual. Res., 10, 2010, s. 433-445, doi:10.4209/aaqr.2009.11.0071.
18. Rogula-Kozłowska W., Rybak J., Wróbel M., Bihałowicz J.S., Krasuski A., Majder-Łopatka M., *Site Environment Type – The Main Factor of Urban Road Dust Toxicity?*, Ecotoxicol. Environ. Saf., 218, 2021, s. 112290, doi:https://doi.org/10.1016/j.ecoenv.2021.112290.
19. Hwang H.-M., Fiala M.J., Park D., Wade T.L., *Review of Pollutants in Urban Road Dust and Stormwater Runoff: Part 1. Heavy Metals Released from Vehicles*, Int. J. Urban Sci., 20, 2016, s. 334-360, doi:10.1080/12265934.2016.1193041.
20. Cui W., Meng Q., Feng Q., Zhou L., Cui Y., Li W., *Occurrence and Release of Cadmium, Chromium, and Lead from Stone Coal Combustion*, Int. J. Coal Sci. Technol., 6, 2019, s. 586-594, doi:10.1007/s40789-019-00281-4.
21. Deng S., Shi Y., Liu Y, Zhang C., Wang X., Cao Q., Li S., Zhang F., *Emission Characteristics of Cd, Pb and Mn from Coal Combustion: Field Study at Coal-Fired Power Plants in China*, Fuel Process. Technol., 126, 2014, s. 469-475, doi:10.1016/j.fuproc.2014.06.009.
22. *W jaki dzień Polacy najchętniej robią zakupy w sklepach? Koronawirus sporo zmienił w zachowaniach konsumentów,* Wydawnictwo Gospodarcze, https://www.wiadomoscihandlowe.pl/artykul/polacy-wciaz-najchetniej-robia-zakupy-w-sobote-ale-goni-ja-wtorek.
23. Rada Miejska w Wołominie XXXVIII-58/2014 w Sprawie Uchwalenia Regulaminu Targowiska Miejskiego Nr 1 Przy Ul. 1-Go Maja w Wołominie, https://wolomin.bip.net.pl/?a=8715.
24. Szydłowski H., *Pracownia Fizyczna*, Państwowe Wydawnictwo Naukowe, 1980; ISBN 8301024879.
25. Naderizadeh Z., Khademi H., Ayoubi S., *Biomonitoring of Atmospheric Heavy Metals Pollution Using Dust Deposited on Date Palm Leaves in Southwestern Iran*, Atmósfera, 29, 2016, s. 141, doi:10.20937/ATM.2016.29.02.04.
26. Pant P., Harrison R.M., *Estimation of the Contribution of Road Traffic Emissions to Particulate Matter Concentrations from Field Measurements: A Review*, Atmos. Environ., 77, 2013, s. 78-97, doi:https://doi.org/10.1016/j.atmosenv.2013.04.028.
27. Sternbeck J., Sjödin Å., Andréasson K., *Metal Emissions from Road Traffic and the Influence of Resuspension – Results from Two Tunnel Studies*, Atmos. Environ., 36, 2002, s. 4735-4744, doi:https://doi.org/10.1016/S1352-2310(02)00561-7.
28. Kuo C.-Y., Wang J.-Y., Liu W.-T., Lin P.-Y., Tsai C.-T., Cheng M.-T., *Evaluation of the Vehicle Contributions of Metals to Indoor Environments*, J. Expo. Sci. Environ. Epidemiol., 22, 2012, s. 489-495, doi:10.1038/jes.2012,55.
29. Adamiec E., Jarosz-Krzemińska E., Wieszała R., *Heavy Metals from Non-Exhaust Vehicle Emissions in Urban and Motorway Road Dusts*, Environ. Monit. Assess., 188, 2016, s. 369, doi:10.1007/s10661-016-5377-1.

30. Duong T.T.T., Lee B.-K., *Determining Contamination Level of Heavy Metals in Road Dust from Busy Traffic Areas with Different Characteristics*, J. Environ. Manage., 92, 2011, s. 554-562, doi:10.1016/j.jenvman.2010.09.010.
31. Lee P.-K., Touray J.-C., Baillif P., Ildefonse J.-P., *Heavy Metal Contamination of Settling Particles in a Retention Pond along the A-71 Motorway in Sologne, France*, Sci. Total Environ., 201, 1997, s. 1-15, doi:10.1016/S0048-9697(97)84048-X.
32. Goix S., Resongles E., Point D., Oliva P., Duprey J.L., de la Galvez E., Ugarte L., Huayta C., Prunier J., Zouiten C., *Transplantation of Epiphytic Bioaccumulators (Tillandsia Capillaris) for High Spatial Resolution Biomonitoring of Trace Elements and Point Sources Deconvolution in a Complex Mining/Smelting Urban Context*, Atmos. Environ., 80, 2013, s. 330-341, doi:10.1016/j.atmosenv.2013.08.011.
33. Rybak J., *Accumulation of Major and Trace Elements in Spider Webs*, Water, Air, Soil Pollut., 226, 2015, s. 105, doi:10.1007/s11270-015-2369-7.
34. Widziewicz K., Rogula-Kozlowska W., Loska K., Kociszewska K., Majewski G., *Health Risk Impacts of Exposure to Airborne Metals and Benzo(a)Pyrene during Episodes of High PM10 Concentrations in Poland,* Biomed. Environ. Sci., 31, 2018, s. 23-36, doi:10.3967/bes2018.003.
35. Rogula-Kozłowska W., Błaszczak B., Szopa S., Klejnowski K., Sówka I., Zwoździak A., Jabłońska M., Mathews B., *PM2,5 in the Central Part of Upper Silesia, Poland: Concentrations, Elemental Composition, and Mobility of Components*, Environ. Monit. Assess., 185, 2013, s. 581-601, doi:10.1007/s10661-012-2577-1.
36. Rogula-Kozłowska W., Klejnowski K., Rogula-Kopiec P., Ośródka L., Krajny E., Błaszczak B., Mathews B., *Spatial and Seasonal Variability of the Mass Concentration and Chemical Composition of PM2,5 in Poland*, Air Qual. Atmos. Heal., 7, 2014, s. 41-58, doi:10.1007/s11869-013-0222-y.
37. Jabłońska M., Janeczek J., *Identification of Industrial Point Sources of Airborne Dust Particles in an Urban Environment by a Combined Mineralogical and Meteorological Analyses: A Case Study from the Upper Silesian Conurbation, Poland*, Atmos. Pollut. Res., 10, 2019, s. 980-988, doi:https://doi.org/10.1016/j.apr.2019.01.006.
38. Sówka I., Chlebowska-Styś A., Pachurka Ł., Rogula-Kozłowska W., Mathews B., *Analysis of Particulate Matter Concentration Variability and Origin in Selected Urban Areas in Poland*, Sustain, 2019, s. 11.
39. Harrison R.M., Jones A.M., Gietl J., Yin J., Green D.C., *Estimation of the Contributions of Brake Dust, Tire Wear, and Resuspension to Nonexhaust Traffic Particles Derived from Atmospheric Measurements*, Environ. Sci. Technol., 46, 2012, s. 6523-6529, doi:10.1021/es300894r.
40. Pant P., Shi Z., Pope F.D., Harrison R.M., *Characterization of Traffic-Related Particulate Matter Emissions in a Road Tunnel in Birmingham, UK: Trace Metals and Organic Molecular Markers*, Aerosol Air Qual. Res., 17, 2017, s. 117-130, doi:10.4209/aaqr.2016.01.0040.
41. Thorpe A., Harrison R.M., *Sources and Properties of Non-Exhaust Particulate Matter from Road Traffic: A Review*, Sci. Total Environ., 400, 2008, s. 270-282, doi:10.1016/j.scitotenv.2008.06.007.

## Dobowa i godzinowa zmienność stężeń Pb, Ni, Zn, Mn i V: badania pilotażowe w wybranym receptorze centralnej Polski

Streszczenie

W powietrzu atmosferycznym występuje około 40 pierwiastków śladowych. Osiem z nich, tj.: As, Cd, Cr, Hg, Mn, Ni, Pb i V Światowa Organizacja Zdrowia (WHO) umieściła na liście 35 substancji szczególnie niebezpiecznych dla zdrowia człowieka, natomiast według klasyfikacji Międzynarodowej Agencji Badań nad Nowotworami (IARC) pierwiastki As, Cd, Cr (VI) i Ni należą do grupy związków o potwierdzonym działaniu kancerogennym na organizm człowieka. Pierwiastki śladowe mogą pochodzić ze źródeł naturalnych, np. wybuchów wulkanów i erozji gleb oraz antropogenicznych, czyli ze spalania paliw, odpadów, a także wszelkiego rodzaju przeróbki, wytapiania i produkcji metali, stopów metali, itp. W zurbanizowanych obszarach Polski najpoważniejszymi źródłami pierwiastków śladowych, w tym zwłaszcza toksycznych i kancerogennych, jest spalanie paliw stałych i płynnych. Szeroko rozumiana emisja komunikacyjna stanowi w wielu polskich miastach podstawowy problem zanieczyszczenia powietrza większością metali. W pracy przeprowadzono pilotażowe badania dobowej i godzinowej zmienności stężeń Pb, Ni, Zn, Mn i V związanych z drobnym pyłem zawieszonym $PM_{2,5}$ w typowym ośrodku miejskim pod Warszawą. Wykorzystano ciągły analizator pierwiastków PX-375 firmy Horiba, którego zasada działania oparta jest o spektrometrię fluorescencji rentgenowskiej. Stężenia $PM_{2,5}$ i związanych z nim Pb, Ni, Zn, Mn i V mierzono przez tydzień z rozdzielczością czasową (1 godzina) w lokalizacji narażonej na silne oddziaływanie emisji komunikacyjnej. Wykazano, że w zasadzie wszystkie analizowane pierwiastki, w badanym obszarze, związane są z transportem drogowym. Ponadto pokazano, że zastosowana unikatowa w światowej skali aparatura umożliwia powiązanie konkretnego źródła emisji z wybranymi pierwiastkami śladowymi nawet wówczas, gdy bazować można na wynikach względnie krótkich serii pomiarowych.

Słowa kluczowe: $PM_{2,5}$, spektrometr, zmienność stężeń, EDXRF

## Hourly and daily variation of concentrations of Pb, Ni, Zn, Mn and V: a pilot study in the chosen receptor central Polish

Abstract

In the atmospheric air, the circulating movements of 40 trace elements. Eight of them, i.e. As, Cd, Cr, Hg, Mn, Ni, Pb and V – the World Health Organization (WHO) placed 35 specialist work for health in forestry, while according to the classification of the international cancer research agency (IARC), the elements As , Cd, Cr (VI) and Ni rough to a group with a confirmed carcinogenic effect on the human body. Trace elements may come from natural sources, e.g. volcanic eruptions and soil erosion as well as anthropogenic ones, i.e. from the sale of fuels, waste, as well as the share of processing, metal smelting and the production of metals, alloys, etc. this toxic and carcinogenic issue are the combustion of fuels and liquids. Broadly understood traffic emission is a diagnostic problem in many Polish studies. In the pilot work, the daily and hourly variability of the study of Pb, Ni, Zn, Mn and V concentrations of lamps with $PM_{2,5}$ fine suspended dust in a typical urban center near Warsaw. The PX-375 continuous element analyzer by Horiba was used, which is based on the principle of X-ray fluorescence spectrometry. Concentrations of $PM_{2,5}$ and its release of Pb, Ni, Zn, Mn and V measured for a week with a time experience of 1 hour in damage exposed to heavy transport impact. It has been shown that in the samples all the examined elements in the studied area are transported by road. Moreover, the applied apparatus, which is unique in the scale, makes it possible to link the purchase with selected trace elements, even when the results of relatively short measurement series can be based on.

Keywords: $PM_{2,5}$, spectrometer, variability concentrations, EDXRF

JEE Journal of Ecological Engineering

Journal of Ecological Engineering 2022, 23(10), 89–97
https://doi.org/10.12911/22998993/152282
ISSN 2299–8993, License CC-BY 4.0

Received: 2022.07.08
Accepted: 2022.08.12
Published: 2022.09.01

# Quasi Real-Time X-Ray Fluorescence Spectrometer in Source Apportionment of Particulate Matter in a Typical Suburban Area

Tomasz Mach[1], Justyna Rybak[1], Jan Bihałowicz[2*], Wioletta Rogula-Kozłowska[2]

[1] Faculty of Environmental Engineering, Wroclaw University of Science and Technology, Wybrzeże Wyspiańskiego 27, 50-370 Wrocław, Poland

[2] The Main School of Fire Service, ul. Słowackiego 52/54, 01-629 Warsaw, Poland

[*] Corresponding author's e-mail: jbihalowicz@sgsp.edu.pl

**ABSTRACT**

The article studies the data from a weekly campaign devoted to the study of the elemental composition of $PM_{10}$ in a selected receptor, in a suburban area (Mazowieckie Voivodeship). The sampling point was located at the intersection of main roads and in the vicinity of a typical single-family housing, not far from the electrified Warsaw-Białystok railway line and a small heating plant. The research was carried out in the summer season, in order to minimize the impact of municipal emissions on the concentrations and elemental composition of $PM_{10}$. A Horiba PX-375 X-ray fluorescence spectrometer was used to measure the one-hour concentrations of elements related to $PM_{10}$. On the basis of the obtained results, the enrichment factors for $PM_{10}$ in the analyzed elements (EF) were calculated and the principal components analysis (PCA) was performed. It was found that although the elemental composition of $PM_{10}$ in all tested time intervals was noticeably influenced by the emissions from transport, the municipal emissions had a significant impact on the elemental composition, especially those related to coal combustion, and thus the concentration of $PM_{10}$ during the study period. It seems that the possibility of observing the influence of all relevant sources on the composition and concentration of $PM_{10}$ was possible owing to the use of hourly-averaged measurements of the elemental composition of $PM_{10}$. In the case of daily averaged measurements, in a receptor with such $PM_{10}$ elemental profile, it would be impossible to determine the periods, in which specific – qualitatively completely different – emission sources dominate.

**Keywords:** atmospheric aerosol; traffic emissions; enrichment factor; 24-h concentrations; diurnal variability; PX-375; XRF analysis.

## INTRODUCTION

The elemental composition of particulate matter (PM) is one of its most important environmental and health characteristics, and also allows defining the origin of PM at a specific receptor. Knowing that the elemental composition of the PM that comes from a given emission source is more or less defined; this can be used to determine the origin of the PM in a given area. For this purpose, mathematical models are used (Hopke 2016). The data on the concentrations of elements in PM are used to assess its origin for two main reasons. Most of the elements that are part of PM are found in chemically stable compounds. These compounds, together with the particulate matter, are transported from the emitters to the receptor in a similar chemical form and in amounts depending on the number of PM particles, emitted by the sources containing these elements (Pernigotti, Belis, and Spanó 2016; Zhu et al. 2018). The situation is different in the case of carbon, sulfur and nitrogen compounds, the presence of which in PM depends not only on the number of stable compounds emitted in PM, but also on the presence of gaseous organic and inorganic substances – secondary aerosol precursors in the atmosphere, as well as on meteorological factors determining the changes in volatile and semi-volatile compounds in the atmosphere (Hallquist et al. 2009). The second reason is that some elements can be effective markers of a specific

PM source. These are the elements characteristic of only one source or group of PM sources, which makes it possible to distinguish a given source from others, e.g., the presence of silicon or aluminum is characteristic of PM from soil or sand erosion, and also from biomass combustion (Liang et al. 2019). Sometimes, the mass ratios of the trace elements it contains are also used to assess the origin of PM (Pervez et al. 2018). In conclusion, the comprehensive assessment of the origin of PM, based on the concentrations of the elements identified in it, and using various approaches and modeling, is particularly effective in the areas where elemental profiles from various sources are highly diversified and repeatable over a long period of time (Pokorná, Hovorka, and Hopke 2016). In order to use these models correctly and to obtain the right conclusions, it is necessary to collect a large amount of data. This, in turn, depends on many factors: the meteorological and emission characteristics of the area or the model used. In the area where PM emissions from different sources overlap or where one source is clearly dominant, the correct determination of the origin of PM may be very difficult or even impossible (Rogula-Kozłowska et al. 2013, 2016). In such regions, the data on element concentrations from averaged measurements, at intervals shorter than 24 hours, may be more useful in assessing the origin of PM than the typically collected daily data. It is clear that the concentration, chemical composition and elemental profiles of PM can change dynamically throughout the day, which is related to, i.a. variable impact of road and municipal emissions. Conventional methods of testing the elemental composition of PM usually make it impossible to analyze the concentrations at shorter intervals than a day or even week. The possibility of correct application of conventional methods is determined by the amount of collected and analyzed material, which in this case is the mass of PM. Nevertheless, there are highly sensitive analytical techniques that allow reaching sampling resolution higher than daily, including energy dispersive X-ray spectroscopy (EDXRF). Due to the possibility of testing advanced and relatively recently existing on the market measuring equipment – the EDXRF spectrometer, working in short averaging periods (e.g. 30-min, 1-hour), in this study, it was planned to conduct a measurement campaign in a selected receptor, averaging over time 1-hr concentrations using EDXRF. The measurement point was located where emissions are defined by traffic, at a road junction where congestion is formed. A detailed hourly analysis of the content of elements in PM allowed for the examination of the impact of road traffic on the composition of PM. The variability was determined and the origin of the PM was assessed through the determination of the enrichment factors of the elements in PM, as well as the principal component analysis.

## METHODS AND MATERIALS

### Location and time of measurements

Measurements were carried out for 7 days, in August 2020, in the Mazowieckie Voivodeship, Wołomin poviat (Wołomin County), in the Wołomin commune, at the intersection of provincial road 634 and poviat roads. One of the largest shops – within 2 km – was located 40 m from the measuring point. The lack of a well-developed public transport network means that with a large number of customers, temporary traffic stops often occur, related to entering a car park, joining traffic and stopping at pedestrian crossings, through which store customers pass. Traffic jams form at the intersection where the measuring equipment was standing, reaching about 500–1000 m in length during rush hours. Despite the fact that the measurements were performed in the administrative area of the village, the buildings there showed a typical suburban character – loose single-family housing. There are water, sewage and gas installations in the village. In addition, at a distance of 500 m from the sampling point, there is the electrified Warsaw-Białystok railway line, and at a distance of 1250 m in a straight line, there is a heating plant smokestack, 120 m above ground level, discharging fumes from the complex with a rated power of 64.57 MW (ZEC Wołomin 2022). During the measurement period, the plant was involved in the supply of hot water to recipients in the Wołomin commune. In addition, many residents in the vicinity of the measuring point have individual natural gas-powered hot water systems. The minimum temperature during the measurements exceeded 14°C; therefore, the influence of individual heating on the air quality was negligible (IMGW-PIB 2021).

Due to the fact that the place selected for the study is exposed to high emissions from communication sources, and the study time was selected

so that the impact of individual heating was negligible, the day was divided into four equal intervals corresponding to the different types of traffic and lifestyle of residents. The starting hours of the intervals have been adopted, i.a. on the basis of (Mach, Bihałowicz, and Bihałowicz 2021). The first period (I) – night – covered the hours 22:01 to 4:00. During this time period, both the traffic and the need for domestic hot water are minimal. The second period (II) – morning – began at 4:01 am and ended at 10:00. Road traffic at the measurement site begins early in the morning, as the road by the sampling point is one of the main access roads for residents of the Wołomin County to work and study places in the Warsaw agglomeration. The third period (III) – afternoon hours – covered the hours 10:01–16:00, in which road traffic remains at a constant, quite intense level, but there are no road jams, and the emission related to the demand for hot water is low, because only a few residents stay at home during the day. The fourth period (IV) – evening – covered the hours 16:01–22:00.

## Measurement method

During the measurements, the concentration of $PM_{10}$ (μg/m$^3$) and the concentration of selected elements in $PM_{10}$, also expressed in mass units per unit volume, were tested. The measurements were performed in a continuous way using a Horiba PX-375 XRF analyzer (HORIBA ltd, Kyoto, Japan). During the measurements, the concentrations of Ti, V, Cr, Mn, Fe, Ni, Cu, Zn, Pb, Al, Si, S, K and Ca were analyzed. PX-375 allows collecting an atmospheric PM sample on the surface of a non-woven, elementally pure Teflon fiber (PTFE) tape. The mass of PM collected in the sample was determined by beta ray attenuation. After the mass of PM was determined, the tape was moved under EDXRF spectrometer equipped with a palladium lamp, so that the element concentrations were determined. The samples were taken for 60 minutes at a flow of 16.7 l/min. Then, after collection, they were induced and analyzed by EDXRF for 2000 s. The EDXRF system was additionally equipped with a camera that allows controlling the position of the sample in relation to the spectrometer. In order to control the quality of the collected spectra, the NIST SRM 2783 calibration material was used.

The sensitivity of the spectrometer – the lower detection limit – was dependent on the tested element, and with the parameters used in the experiment it was: for Al (56.7 ng/m$^3$), As (3.7 ng/m$^3$), Ca (1.1 ng/m$^3$), Cr (2.05 ng/m$^3$), Cu (1.85 ng/m$^3$), Fe (7.00 ng/m$^3$), K (4.8 ng/m$^3$), Mn (1.45 ng/m$^3$), Ni (0.9 ng/m$^3$), Pb (1.05 ng/m$^3$), S (1.55 ng/m$^3$), Si (8.85 ng/m$^3$), Ti (0.25 ng/m$^3$), V (1.7 ng/m$^3$), and for Zn (1.25 ng/m$^3$). The data were collected for 7 full days, yielding 168 measurement points.

## Analysis of the obtained results

In order to determine the influence of anthropogenic sources on the elemental composition of $PM_{10}$, the enrichment factors *EF* (Barbieri 2016) were used. *EF* (Formula 1) is defined as the ratio of the anthropogenic impact factor $CF_n$ for the element $n$ divided by the same factor for the reference element $CF_{ref}$. The *CF* factor is the ratio of the concentration of an element in $PM_{10}$ $C_n$ divided by the concentration in the environment (background) $C_{n,b}$, as shown in Eq (1).

$$EF_n = \frac{CF_n}{CF_{ref}} = \frac{\frac{C_n}{C_{n,b}}}{\frac{C_{ref}}{C_{ref,b}}} \quad (1)$$

The concentrations of elements in the upper Earth's crust (Hans Wedepohl 1995) were adopted as the values representing the concentration in the environment. Aluminum is often used as the reference element (Reimann and Caritat 2000; Rybak et al. 2020; Stojanowska et al. 2021). The obtained values of the *EF* coefficients were divided into five classes, according to (YONGMING et al. 2006), where the enrichment of PM with a specific element is:

- for EF ≤ 2 minimal enrichment,
- for 2 ≤ 5< EF moderate enrichment,
- for 5 < EF ≤ 20 significant enrichment,
- for 20 < EF 40 very high enrichment,
- for EF > 40 extremely high enrichment.

The *EF* analysis was performed separately for each time interval, providing the view into the temporal variability of the PM enrichment in individual elements. The next method used in the analysis was the principal components analysis of PCA. The successive principal components *PC* are the variables that account for less and less variability in the data set. PCA is a frequently used technique to reduce the dimensionality of the problems related to the elemental profile

(Bokwa 2008; Idriss et al. 2021; Kormoker et al. 2021; Li et al. 2020; Qu et al. 2018; Rybak et al. 2020). In this study, the content of 14 elements was analyzed and the dimensionality was reduced to 4, i.e., four main components were determined. Similarly, as in case of *EF*, it was done for each time interval separately. Data standardization was performed prior to *PC* designation.

Subsequently, the similarity of individual main components, i.e., *PC1* with *PC1* and *PC2* with *PC2* etc., between the time intervals was compared using the cosine similarity $r_c$ (Jones and Furnas 1987), which for the *PC* is described by the Eq. (2), where $PCn$ is the vector of the $n\text{-}th$ principal component, $t1$, $t2$ are two different time intervals. In Eq. (2), a modulus was introduced, in order to not distinguish the parallel and antiparallel principal components. The reason for choosing cosine similarity was that each *PC* is a vector; therefore the cosine of the angle between these vectors is a good measure of similarity, and in addition, this approach has already been used in previous works (Stojanowska et al. 2020).

$$r_C(PCn_{t1}, PCn_{t2}) = |PCn_{t1} \cdot PCn_{t2}| \qquad (2)$$

## RESULTS AND DISCUSSION

### Enrichment factors EFs

In order to determine the impact of selected emission sources on the elemental composition of $PM_{10}$ and its concentration in the study area (road intersection in a suburban area), among others, enrichment factors EF were calculated. The results are shown in Table 1. $PM_{10}$ does not indicate enrichment with respect to the composition of the upper Earth's crust, UCC, (Hans Wedepohl 1995) in potassium, silicon, titanium and vanadium. The EF values for these elements, which, regardless of the time of day, did not exceed 2 (Table 1), indicate that they are typical elements of the Earth's crust. It can therefore be assumed that they come from natural sources (Majewski and Rogula-Kozłowska 2016; Rogula-Kozłowska et al. 2016). It cannot be ruled out that these elements come from the resuspension of sand, soil and dust deposited on the crossroads and shoulders, instigated by intensive car traffic. On the basis of the determined values of the enrichment factors, $PM_{10}$ was the most highly enriched in Zn and S; this is true for each averaging period and therefore it occurs irrespective of the time of day. This clearly shows that regardless of the averaging period of the results during the day, the emission related to coal combustion has a strong influence on the elemental composition of $PM_{10}$, and thus the concentration of $PM_{10}$.

This, in turn, suggests the influence of emissions from nearby buildings and heating plant on the composition and concentration of $PM_{10}$ in the research area. Although the research was carried out in the warm period, when the impact of these sources should not be dominant (no emissions related to the heating of flats and houses, and municipal emissions determined mainly by processes related to water heating, cooking, etc.), they can be clearly observed. It is rather clear that when averaging the daily data on the elemental composition of $PM_{10}$, this impact could be masked by the traffic emission dominating in this area and in this period.

Regardless of the time of day, $PM_{10}$ was significantly enriched in chromium and strongly enriched in copper. This, in turn, demonstrates the existing and clear influence of communication emissions on the composition of $PM_{10}$. In the morning and afternoon periods, this thesis is reinforced by the enrichment of $PM_{10}$ with manganese and nickel. The traffic emission shown here is not

**Table 1.** Values of the enrichment coefficient for the tested elements, associated with $PM_{10}$ mean values were calculated, for each hour during the day over the study period. Time periods: I – night, II – morning, III – noon, IV – evening

| Period | Ti | V | Cr | Mn | Fe | Ni | Cu | Zn | Pb | Si | S | K | Ca |
|---|---|---|---|---|---|---|---|---|---|---|---|---|---|
| I | ○ 1 | ○ 2 | ◑ 8 | ○ 2 | ○ 1 | ○ 1 | ● 45 | ● 90 | ◕ 30 | ○ 1 | ● 381 | ○ 1 | ◔ 3 |
| II | ○ 0 | ○ 2 | ◑ 8 | ◔ 2 | ◔ 2 | ◔ 3 | ● 49 | ● 142 | ◕ 34 | ○ 1 | ● 475 | ○ 1 | ◔ 4 |
| III | ○ 0 | ○ 2 | ◑ 9 | ◔ 3 | ◔ 2 | ○ 1 | ◑ 11 | ● 123 | ◑ 19 | ○ 1 | ● 574 | ○ 1 | ◔ 4 |
| IV | ○ 0 | ○ 1 | ◑ 7 | ◔ 3 | ○ 2 | ○ 1 | ◕ 22 | ● 101 | ◕ 22 | ○ 1 | ● 402 | ○ 1 | ◔ 4 |

**Note:** The ○ symbol represents minimal enrichment, ◔ represents moderate enrichment, ◑–significant enrichment, ◕ – very high enrichment, ● – extremely high enrichment

only fuel combustion in engines, but most of all abrasion of vehicle components (wheels, brakes) and road surfaces. For example, while chromium is used in vehicle steel, also automotive cylinders are usually coated with a chrome layer (Moore, Polidori, and Sioutas 2011). The remaining elements are characterized by enrichment depending on the averaging time of the tests performed. It was found, i.a. that there is no manganese enrichment in $PM_{10}$ at night, iron enrichment only in the morning and early afternoon hours, nickel – only in the morning, copper and lead – less enrichment during the day and evening. The presence of manganese and nickel is related to the combustion of gasoline (Moore et al. 2011). In turn, brake wear in road vehicles is an important source of copper concentration in the atmosphere (Hulskotte et al. 2007). Iron is the most abundant metal in nature. Low cost and high strength make it an essential element in many engineering structures, and is widely used in the construction of machines and vehicles. Although the consumption of unleaded gasoline has decreased, the presence of lead in the air is still high and is associated with heavy vehicle traffic (Moore et al. 2011). The relationship between the lead concentration in the air and the emissions from coal combustion is also known (Rogula-Kozłowska et al. 2012, 2013; Rogula-Kozłowska, Majewski, and Czechowski 2015).

In summary, the observed hourly variability may result from the congestion and traffic peaks that could be observed in the study area (morning peak, more intense traffic in the afternoon and more extended afternoon peak).

## Share of $PM_{10}$ emission sources

In order to identify the main sources of $PM_{10}$ in the investigated suburban area, the main component analysis (PCA; Table 2) was used. Principal components for 14 elements were analyzed and four main components (PC1–PC4) were identified. The components were determined, as in the case of EF, separately for each time interval. The similarity of each component for the four time zones was compared using cosine similarity (Table 3).

In the case of the main component of PC1, the highest similarity was obtained for the time intervals III (noon) and IV (evening) (above 0.9; Table 3). The cosine similarity of PC1 for the remaining ranges was above 0.8, which suggests that PC1 represents a constant and intense source of emissions, independent of the period of the day. The general analysis of PCA shows that there were no strongly correlated elements in any time interval with PC1. Almost all elements determined are correlated with PC1 at the level of 0.1–0.4 (Table 2). These higher correlation values, regardless of the time of day, were recorded for Si, Al, Cr, V, Mn, Fe and Ca. It seems that PC1 may indicate a source of the road dust mixture enriched with elements typical for transport emissions (Majewski and Rogula-Kozłowska 2016; Penkała, Ogrodnik, and Rogula-Kozłowska 2018). PC1 contributes to the variance from 0.32 (morning (II)) to 0.5 (night (I)).

In the case of PC2, the greatest similarity was noted for the periods: night (I) and morning (II) – see Table 3; all the observed cosine similarities did not exceed the value of 0.63. For these periods, the share of PC2 in the variance is 0.16 (Table 2). Judging by the fact that V, Cr, S and K were the most strongly correlated with this component during the night and morning, it can be suspected that PC2 in these two periods represents the effect of heating, namely carbon combustion, on the elemental composition and $PM_{10}$ concentration in the research area. In particular, this is evidenced by the correlations of PC2 with S and K (Li et al. 2010), which in the case of the conducted research may indicate that an important source of $PM_{10}$ and the elements related to it, is a heating plant or residential buildings located in a short distance (water heating, cooking). Sulfur and potassium (especially potassium) may also be released during the combustion of biomass, waste and garbage in small-sized installations, i.e. home furnaces and local boiler houses (Samek et al. 2016). These sources cannot be excluded in the case of the conducted research, because there are single-family houses in the area that may be a source of this type of pollution. Moreover, the source of sulfur in $PM_{10}$ may be secondary inorganic aerosols (sulphates), also released from the above-mentioned sources (Cesari et al. 2016).

There was no similarity between PC2 determined for noon (III) and evening (IV) (Table 3), which may indicate the presence of other, dominant emission sources in periods I and II, than those in periods III and IV. Specifically, it seems that these sources also differ in periods III and IV. In the afternoon (III) period, Ti, Fe and Ca were the most strongly correlated with PC2, and in the evening (IV) period, Ti, V and Cr were the most

strongly correlated with PC2 (Table 2). Both in the first and the second period of the day, it seems that PC2 can be characterized by a communication source. In the afternoon, it is more focused on the erosion of various elements of vehicles and surfaces, and in the evening, on the emissions related to fuel combustion in car engines (Pant and Harrison 2013; Rodriguez et al. 2004; Sternbeck, Sjödin, and Andréasson 2002). The share of this component in the variance in periods III and IV ranges from 0.13–0.15 (Table 2).

The main component of PC3 was characterized by the greatest cosine similarity in the morning (II) and noon (III) periods, which indicates PC3 as a common source of emissions for these periods. However, in each of these periods, different elements were correlated with PC3 (Table 2). In period II (morning), Ni, S and K were correlated with PC3, and in period III (noon) – V and Cr. It seems obvious that PC3 in the morning can be identified with municipal emission (similarly to PC2 during the night (I) and in the morning (II)), and in the afternoon (III) PC3 may indicate communication emission (analogous to PC2 in the evening (IV). No significant similarities were found with PC3 at other times of the day (Table 3). During the night (I), PC3 was most strongly correlated with Cu, Zn and Pb, and in the evening period with V, Cr and Ni (Table 2). Thus, in the evening period, analogically to the previous considerations, the traffic emissions related to fuel combustion in engines were identified, and during the night also traffic emissions, but related more to the typical erosion of brake pads (Pant and Harrison 2013; Rodriguez et al. 2004; Sternbeck et al. 2002).

The main component of PC4 with the lowest share of cumulative variance (Table 2) was characterized by the greatest cosine similarity in the periods: night (I) and noon (III), and morning (II) and noon (III) (Table 3). In the period I and III, PC4 was most strongly correlated with Ni and Zn. In period II (morning), the correlation of PC4 with Zn and Pb is observed. At night (period (IV)), the only notable correlations with PC4 are for Zn, Pb and Mn (Table 2). Taking into account completely different dependencies in the previous components, where the impact of communication and municipal emissions was identified, it is clear that a different source of emissions was qualitatively identified in PC4.

Probably with varying strength depending on the time of day, the elemental composition and $PM_{10}$ concentration in this area are influenced by the nearby small, local non-ferrous metals processing point (70 m from the measurement point to the north), the paint shop located about 300 m to the south-west east as well as a tire repair and car repair shops (from 200 to 500 m to the west)

**Table 2.** Summary of the results of the principal component analysis (PCA) performed on the time intervals related to the elemental composition of $PM_{10}$. Time periods: I – night, II – morning, III – noon, IV – evening

| Time interval | Component | Ti | V | Cr | Mn | Fe | Ni | Cu | Zn | Pb | Al | Si | S | K | Ca | PC VAR |
|---|---|---|---|---|---|---|---|---|---|---|---|---|---|---|---|---|
| I | PC1 | 0.31 | 0.34 | 0.34 | 0.34 | 0.26 | 0.06 | 0.10 | 0.19 | -0.06 | 0.36 | 0.31 | -0.02 | 0.34 | 0.30 | 0.50 |
| | PC2 | 0.32 | 0.21 | 0.22 | 0.07 | -0.41 | -0.24 | 0.16 | -0.21 | -0.06 | 0.04 | -0.35 | 0.42 | 0.25 | -0.38 | 0.16 |
| | PC3 | -0.02 | -0.08 | -0.09 | -0.03 | 0.04 | -0.21 | 0.56 | 0.47 | 0.63 | -0.05 | -0.05 | 0.06 | 0.04 | -0.03 | 0.13 |
| | PC4 | -0.07 | 0.16 | 0.13 | -0.17 | -0.12 | 0.85 | 0.15 | 0.31 | -0.07 | -0.04 | -0.14 | 0.12 | -0.02 | -0.18 | 0.07 |
| II | PC1 | 0.00 | 0.16 | 0.18 | 0.33 | 0.44 | -0.06 | -0.04 | 0.09 | 0.18 | 0.44 | 0.45 | 0.04 | 0.14 | 0.43 | 0.32 |
| | PC2 | 0.00 | 0.59 | 0.58 | -0.09 | -0.10 | 0.02 | 0.28 | -0.05 | -0.18 | 0.04 | -0.14 | 0.25 | 0.28 | -0.17 | 0.16 |
| | PC3 | 0.00 | -0.23 | -0.20 | 0.24 | -0.03 | 0.32 | -0.33 | -0.17 | -0.10 | 0.20 | -0.12 | 0.54 | 0.48 | -0.17 | 0.13 |
| | PC4 | 0.00 | -0.05 | -0.06 | -0.15 | -0.01 | -0.02 | 0.14 | 0.68 | 0.61 | 0.02 | -0.14 | 0.17 | 0.19 | -0.18 | 0.12 |
| III | PC1 | 0.08 | 0.22 | 0.23 | 0.35 | 0.36 | 0.15 | 0.18 | 0.20 | 0.10 | 0.39 | 0.37 | 0.27 | 0.26 | 0.32 | 0.39 |
| | PC2 | 0.32 | -0.31 | -0.28 | 0.06 | 0.31 | -0.31 | -0.01 | -0.07 | -0.32 | -0.01 | 0.29 | -0.39 | -0.20 | 0.38 | 0.15 |
| | PC3 | 0.01 | 0.57 | 0.58 | -0.13 | 0.06 | -0.20 | -0.24 | -0.21 | -0.15 | -0.08 | 0.02 | -0.24 | -0.26 | 0.15 | 0.11 |
| | PC4 | 0.41 | 0.08 | 0.01 | -0.09 | 0.04 | 0.48 | 0.17 | 0.33 | 0.33 | -0.19 | -0.11 | -0.11 | -0.52 | 0.13 | 0.09 |
| IV | PC1 | 0.18 | 0.25 | 0.26 | 0.30 | 0.35 | 0.07 | 0.28 | 0.27 | 0.23 | 0.34 | 0.35 | 0.14 | 0.26 | 0.32 | 0.48 |
| | PC2 | 0.41 | 0.42 | 0.41 | -0.16 | -0.09 | -0.23 | 0.12 | -0.33 | -0.39 | -0.03 | -0.04 | -0.32 | 0.14 | -0.02 | 0.13 |
| | PC3 | -0.28 | 0.39 | 0.37 | -0.02 | 0.15 | 0.40 | 0.29 | 0.08 | 0.08 | -0.32 | -0.30 | 0.18 | -0.29 | -0.22 | 0.09 |
| | PC4 | 0.01 | 0.09 | 0.13 | 0.27 | 0.12 | -0.35 | -0.25 | 0.34 | 0.27 | -0.25 | -0.05 | -0.55 | -0.37 | 0.12 | 0.09 |

**Note:** PC VAR – variance described by a component.

**Table 3.** Cosine similarity of principal components between time intervals

| PC1 | | | | | PC2 | | | | |
|---|---|---|---|---|---|---|---|---|---|
| | I | II | III | IV | | I | II | III | IV |
| I | 1.000 | 0.808 | 0.889 | 0.900 | I | 1.000 | 0.635 | 0.500 | 0.420 |
| II | | 1.000 | 0.887 | 0.866 | II | | 1.000 | 0.592 | 0.588 |
| III | | | 1.000 | 0.964 | III | | | 1.000 | 0.138 |
| IV | | | | 1.000 | IV | | | | 1.000 |
| PC3 | | | | | PC4 | | | | |
| | I | II | III | IV | | I | II | III | IV |
| I | 1.000 | 0.314 | 0.400 | 0.145 | I | 1.000 | 0.251 | 0.504 | 0.345 |
| II | | 1.000 | 0.508 | 0.187 | II | | 1.000 | 0.314 | 0.126 |
| III | | | 1.000 | 0.283 | III | | | 1.000 | 0.292 |
| IV | | | | 1.000 | IV | | | | 1.000 |

(Kaivosoja et al. 2013; Yang et al. 2019). The share of PC4 in the variance, depending on the time of day, is from 0.07 to 0.12.

## CONCLUSIONS

In the research, the data from the period of a seven-day measurement campaign conducted in the suburban area was used. It was shown that in a typical suburban area, in the central part of Poland, the impact of emissions from transport on the elemental composition of $PM_{10}$ can be observed in practically all tested time intervals, which is directly related to the nature of the examined place (location near a large intersection). Most car drivers who pass there are probably professionally or otherwise connected with Warsaw, e.g., they commute to work or for other purposes to the capital every day, which has a significant impact on the pollution of the studied area. Additionally, the emissions related to the proximity of ZEC Wołomin are a significant source (about 1.4 km in a straight line there is the ZEC Wołomin smokestack) and they have a significant impact on the elemental composition of $PM_{10}$ during the study period. There was also a clear influence of small, local production and service facilities. It is highly likely that if a similar analysis of the origin of $PM_{10}$ in the same measurement period were performed on the basis of daily averaged data, on the elemental composition of $PM_{10}$, the impact of non-communication emission sources in this research area would not be noticed. This shows that sampling with high temporal resolution constitutes a much better, cheaper and more efficient (short 7-day campaign) method of collecting data to assess the origin of PM in an urban or suburban area.

### Acknowledgments

This research was carried out as a part of the "Implementation doctorate-edition II Faculty W-7 (03DW/0001/18)" project, financed by the National Centre for Research and Development.

The research results were connected with the project OPUS 12 "Transitions of some chemical elements (metals and metalloids) during migration on the way emitter–atmosphere–soil", financed by National Science Centre, Poland, 2016/23/B/ST10/02789.

The authors acknowledge the companies HORIBA and MLU-recordum Environmental Monitoring Solutions GmbH for supplying the measurement equipment (PX-375 Horiba, Japan).

## REFERENCES

1. Barbieri, M. 2016. The Importance of Enrichment Factor (EF) and Geoaccumulation Index (Igeo) to Evaluate the Soil Contamination. Journal of Geology & Geophysics, 5.
2. Bokwa, A. 2008. Environmental Impacts of Long-Term Air Pollution Changes in Kraków, Poland. Polish Journal of Environmental Studies, 17.
3. Cesari, D., Amato, F., Pandolfi, M., Alastuey, A., Querol, X., Contini, D. 2016. An inter-comparison of PM10 source apportionment using PCA and PMF receptor models in three European sites. Environmental Science and Pollution Research, 23, 15133–15148.
4. Hallquist, M., Wenger, J.C., Baltensperger, U., Rudich, Y., Simpson, D., Claeys, M., Dommen, J., Donahue, N.M., George, C., Goldstein, A.H., Hamilton,

J.F., Herrmann, H., Hoffmann, T., Iinuma, Y., Jang, M., Jenkin, M.E., Jimenez, J.L., Kiendler-Scharr, A., Maenhaut, W., McFiggans, G., Mentel, T.F., Monod, A., Prévôt, A.S.H., Seinfeld, J.H., Surratt, J.D., Szmigielski, R., Wildt, J. 2009. The formation, properties and impact of secondary organic aerosol: current and emerging issues. Atmospheric Chemistry and Physics, 9, 5155–5236.

5. Hans Wedepohl, K. 1995. The composition of the continental crust. Geochimica et Cosmochimica Acta.
6. Hopke, P.K. 2016. Review of receptor modeling methods for source apportionment. Journal of the Air and Waste Management Association.
7. Hulskotte, J.H.J., van der Gon, H.A.C.D., Visschedijk, A.J.H., Schaap, M. 2007. Brake wear from vehicles as an important source of diffuse copper pollution. In: Water Science and Technology.
8. Idriss, I.E.A., Abdel-Azim, M., Karar, K.I., Osman, S., Idris, A.M. 2021. Isotopic and chemical facies for assessing the shallow water table aquifer quality in Goly Region, White Nile State, Sudan: focusing on nitrate source apportionment and human health risk. Toxin Reviews, 40, 764–776.
9. IMGW-PIB. 2021. Dane publiczne IMGW-PIB.
10. Jones, W.P., Furnas, G.W. 1987. Pictures of relevance: A geometric analysis of similarity measures. Journal of the American Society for Information Science, 38, 420–442.
11. Kaivosoja, T., Jalava, P.I., Lamberg, H., Virén, A., Tapanainen, M., Torvela, T., Tapper, U., Sippula, O., Tissari, J., Hillamo, R., Hirvonen, M.R., Jokiniemi, J. 2013. Comparison of emissions and toxicological properties of fine particles from wood and oil boilers in small (20–25 kW) and medium (5–10 MW) scale. Atmospheric Environment, 77, 193–201.
12. Kormoker, T., Proshad, R., Islam, M.S., Shamsuzzoha, M., Akter, A., Tusher, T.R. 2021. Concentrations, source apportionment and potential health risk of toxic metals in foodstuffs of Bangladesh. Toxin Reviews, 40, 1447–1460.
13. Li, J., Deng, Q., Lu, C., Huang, B. 2010. Chemical compositions and source apportionment of atmospheric PM10 in suburban area of Changsha, China. Journal of Central South University of Technology, 17, 509–515.
14. Li, Q., Zhang, H., Guo, S., Fu, K., Liao, L., Xu, Y., Cheng, S. 2020. Groundwater pollution source apportionment using principal component analysis in a multiple land-use area in southwestern China. Environmental Science and Pollution Research, 27, 9000–9011.
15. Liang, S.Y., Cui, J.L., Bi, X.Y., Luo, X.S., Li, X.D. 2019. Deciphering source contributions of trace metal contamination in urban soil, road dust, and foliar dust of Guangzhou, southern China. Science of the Total Environment.
16. Mach, T., Bihałowicz, J., Bihałowicz, J.S. 2021. Dobowa i godzinowa zmienność stężeń Pb, Ni, Zn, Mn i V w powietrzu atmosferycznym: badania pilotażowe w wybranym receptorze centralnej Polski. In: Energetyka i ochrona środowiska – współczesne rozwiązania i perspektywy na przyszłość. Wydawnictwo Naukowe TYGIEL, 145–163.
17. Majewski, G., Rogula-Kozłowska, W. 2016. The elemental composition and origin of fine ambient particles in the largest Polish conurbation: first results from the short-term winter campaign. Theoretical and Applied Climatology, 125, 79–92.
18. Moore, K., Polidori, A., Sioutas, C. 2011. Toxicological Assessment of Particulate Emissions from the Exhaust of Old and New Model Heavy- and Light-Duty Vehicles. This research was sponsored by the U.S. Department of Transportation.
19. Pant, P., Harrison, R.M. 2013. Estimation of the contribution of road traffic emissions to particulate matter concentrations from field measurements: A review. Atmospheric Environment.
20. Penkała, M., Ogrodnik, P., Rogula-Kozłowska, W. 2018. Particulate Matter from the Road Surface Abrasion as a Problem of Non-Exhaust Emission Control. Environments, 5, 9.
21. Pernigotti, D., Belis, C.A., Spanó, L. 2016. SPECIEUROPE: The European data base for PM source profiles. Atmospheric Pollution Research.
22. Pervez, S., Bano, S., Watson, J.G., Chow, J.C., Matawle, J.L., Shrivastava, A., Tiwari, S., Pervez, Y.F. 2018. Source Profiles for PM10–2.5 Resuspended Dust and Vehicle Exhaust Emissions in Central India. Aerosol and Air Quality Research, 18, 1660–1672.
23. Pokorná, P., Hovorka, J., Hopke, P.K. 2016. Elemental composition and source identification of very fine aerosol particles in a European air pollution hot-spot. Atmospheric Pollution Research.
24. Qu, M., Wang, Y., Huang, B., Zhao, Y. 2018. Source apportionment of soil heavy metals using robust absolute principal component scores-robust geographically weighted regression (RAPCS-RGWR) receptor model. Science of The Total Environment, 626, 203–210.
25. Reimann, C., Caritat, P. de. 2000. Intrinsic Flaws of Element Enrichment Factors (EFs) in Environmental Geochemistry. Environmental Science & Technology, 34, 5084–5091.
26. Rodriguez, S., Querol, X., Alastuey, A., Viana, M., Alarcon, M., Mantilla, E., Ruiz, C. 2004. Comparative PM10–PM2.5 source contribution study at rural, urban and industrial sites during PM episodes in Eastern Spain. Science of The Total Environment, 328, 95–113.

27. Rogula-Kozłowska, W., Błaszczak, B., Szopa, S., Klejnowski, K., Sówka, I., Zwoździak, A., Jabłońska, M., Mathews, B. 2013. PM2.5 in the central part of Upper Silesia, Poland: Concentrations, elemental composition, and mobility of components. Environmental Monitoring and Assessment.
28. Rogula-Kozłowska, W., Klejnowski, K., Rogula-Kopiec, P., Mathews, B., Szopa, S. 2012. A Study on the Seasonal Mass Closure of Ambient Fine and Coarse Dusts in Zabrze, Poland. Bulletin of Environmental Contamination and Toxicology, 88, 722–729.
29. Rogula-Kozłowska, W., Majewski, G., Błaszczak, B., Klejnowski, K., Rogula-Kopiec, P. 2016. Origin-oriented elemental profile of fine ambient particulate matter in central European suburban conditions. International Journal of Environmental Research and Public Health, 13.
30. Rogula-Kozłowska, W., Majewski, G., Czechowski, P.O. 2015. The size distribution and origin of elements bound to ambient particles: a case study of a Polish urban area. Environmental Monitoring and Assessment.
31. Rybak, J., Wróbel, M., Bihalowicz, J.S., Rogula-Kozlowska, W. 2020. Selected metals in Urban road dust: Upper and lower silesia case study. Atmosphere, 11, 290.
32. Samek, L., Gdowik, A., Ogarek, J., Furman, L. 2016. Elemental composition and rough source apportionment of fine particulate matter in air in Cracow, Poland. Environment Protection Engineering.
33. Sternbeck, J., Sjödin, Å., Andréasson, K. 2002. Metal emissions from road traffic and the influence of resuspension – Results from two tunnel studies. Atmospheric Environment.
34. Stojanowska, A., Mach, T., Olszowski, T., Bihałowicz, J.S., Górka, M., Rybak, J., Rajfur, M., Świsłowski, P. 2021. Air Pollution Research Based on Spider Web and Parallel Continuous Particulate Monitoring–A Comparison Study Coupled with Identification of Sources. Minerals, 11, 812.
35. Stojanowska, A., Rybak, J., Bożym, M., Olszowski, T., Bihałowicz, J.S. 2020. Spider Webs and Lichens as Bioindicators of Heavy Metals: A Comparison Study in the Vicinity of a Copper Smelter (Poland). Sustainability, 12, 8066.
36. Yang, H.-H., Gupta, S. K., Dhital, N. B., Lee, K.-T., Hsieh, Y.-S., Huang, S.-C. 2019. Establishment of Indicatory Metals for Filterable and Condensable PM2.5 Emitted from Important Stationary Emission Sources. Energy & Fuels, 33, 10878–10887.
37. Yongming, H., Peixuan, D., Junji, C., Posmentier, E. 2006. Multivariate analysis of heavy metal contamination in urban dusts of Xi'an, Central China. Science of The Total Environment, 355, 176–186.
38. ZEC Wołomin. 2022. System ciepłowniczy – ZEC Wołomin.
39. Zhu, Y., Huang, L., Li, J., Ying, Q., Zhang, H., Liu, X., Liao, H., Li, N., Liu, Z., Mao, Y., Fang, H., & Hu, J. 2018. Sources of particulate matter in China: Insights from source apportionment studies published in 1987–2017. Environment International. Elsevier Ltd.

Environment Protection Engineering

Vol. 45 2019 No. 1

DOI: 10.5277/epe190113

WIOLETTA ROGULA-KOZŁOWSKA[1, 2], TOMASZ MACH[3],
PATRYCJA ROGULA-KOPIEC[2], JUSTYNA RYBAK[3], KATARZYNA NOCOŃ[2]

# CONCENTRATION AND ELEMENTAL COMPOSITION OF QUASI-ULTRAFINE PARTICLES IN UPPER SILESIA

The ambient concentrations and elemental composition of particles with aerodynamic diameters between 30 and 108 nm (quasi-ultrafine particles, q-UFP) were studied. The data came from 6 sites in Katowice and Zabrze, big cities in Upper Silesia, where particulate matter was sampled at urban background site and crossroads in Katowice and Zabrze, at highway in Katowice, and at urban road in Zabrze. The ambient concentrations of q-UFP and of 24 q-UFP-bound elements at these six sampling sites have been discussed in the paper. The q-UFP mass concentrations in Upper Silesia did not appear high, they were not higher than in other areas. The percentages of the total mass of the examined elements in the q-UFP mass suggest that in Upper Silesia, within a typical residential area, q-UFP consist mainly of primary matter. At the sites under strong influence of road traffic emissions, where the contributions of the examined elements to the q-UFP mass were small, most probably, carbonaceous matter and elemental carbon build the core q-UFP mass. The majority of the elements in q-UFP are anthropogenic. Clear effects of local PM sources can be seen on the ambient concentrations of q-UFP-bound Al, Si, S, Cl, K, Sc, Ti, V, Cd, Cr, Mn, Co, and Sb.

## 1. INTRODUCTION

Although ultrafine particles (UFP), i.e., particles with the aerodynamic diameter not greater than 0.1 μm (PM0.1)), make only a small part of the total mass of atmospheric particulate matter (PM) [1–3], they significantly outnumber other airborne particles in urban areas [4–7]. Because of their great number concentrations and tiny sizes their

[1]The Main School of Fire Service, Faculty of Fire Safety Engineering, ul. Słowackiego 52/54, 01-629 Warsaw, Poland.

[2]Institute of Environmental Engineering, Polish Academy of Sciences, ul. Skłodowskiej-Curie 34, 41-819 Zabrze, Poland.

[3]Wrocław University of Science and Technology, Faculty of Environmental Engineering, Wybrzeże Wyspiańskiego 27, 50-370 Wrocław, Poland, corresponding author J. Rybak, e-mail address: justyna.rybak@pwr.edu.pl

correlation with the adverse health effects in humans are stronger than those of coarser PM fractions. The great pulmonary deposition efficiency of UFP, their toxicity due to their large surface area and the amounts of transition metals they adsorb can cause serious cardiopulmonary issues [8, 9]. Their presence in the air is linked with exacerbation and promotion of asthma, chronic obstructive pulmonary disease, atherosclerosis and hypertension [10, 11]. There is general agreement among the scientists about the importance of investigating the UFP for their properties and the relations of their presence in the air with health effects [4–6]. The monitoring of (most often number) UFP concentrations has become routine in some European regions [4–7].

UFP are either emitted directly from high-temperature processes or they are formed in the air as secondary particles. They come mainly from road traffic (those with the median diameters between 20 and 100 nm), from combustion of coal, fuel oil (35–100 nm), and natural gas (15–30 nm) for residential heating, and from nucleation (1 nm, the smallest measurable particles) [4].

Health effects of PM in humans are due to the combination of its ambient concentrations and chemical composition [12–16]. In Poland, the chemical composition of PM1, PM2.5, and PM10 is recognized quite well, e.g., [1–3, 16–18]. PM contains trace elements (metals), including those toxic, in PM2.5, organic and elemental carbon and secondary inorganic compounds (ammonium sulfate and nitrate) prevail [17, 18]. In Polish urban areas, not only the concentrations but also some toxic element content of PM2.5 are alarmingly high compared to other urban areas worldwide. The issue is especially severe in the southern part of the country, where not only emissions from traffic and coal combustion are high, but also very high industrial emissions contribute to PM--bound elements [1, 17, 18].

The mass contribution of UFP to total PM is very small, they are mainly secondary and they dynamically change in the air, therefore, in general, they are investigated using automatic samplers [5, 6]. However, although the UFP mass possible to receive from direct sampling is extremely small, besides mere forecasting and modeling of UFP composition and origin [19], some attempts have been made recently to use the classical sampling of UPF directly from the air and then determining their chemical composition in laboratory [12].

Two papers discussing the chemical composition of UFP in Poland, both presenting classical approach [2, 3] have been published so far. The results were used in the discussion concerning some human health issues due to the mass size distributions of PM and its components [20]. The present work presents the data that they contain on the particles having aerodynamic diameters between 30 and 60 nm and between 60 and 108 nm, directly sampled in the southern part of Poland, to present the properties of the particles having aerodynamic diameters between 60 and 108 nm (called quasi-ultrafine particles, q-UFP). Our technical possibilities did not allow to sample smaller particles, however, the particles we sampled contain a greater part of the UFP mass and their diameters

cover about 2/3 of the diameter interval of UFP. Besides, the q-UFP are of special importance in the area of sampling because very intense emissions of UFP from industry and combustion of coal, gasoline, and diesel oil present within this area.

## 2. MATERIALS AND METHODS

The q-UFP samples were collected in southern Poland, in two Upper Silesian cities, Zabrze and Katowice, at three sites in each (Fig. 1). In each city, one measuring site was situated within the area representing urban background air pollution [21]. The urban background sites were located in the central parts of the cities, close to residential and commercial buildings, both surrounded by lawns.

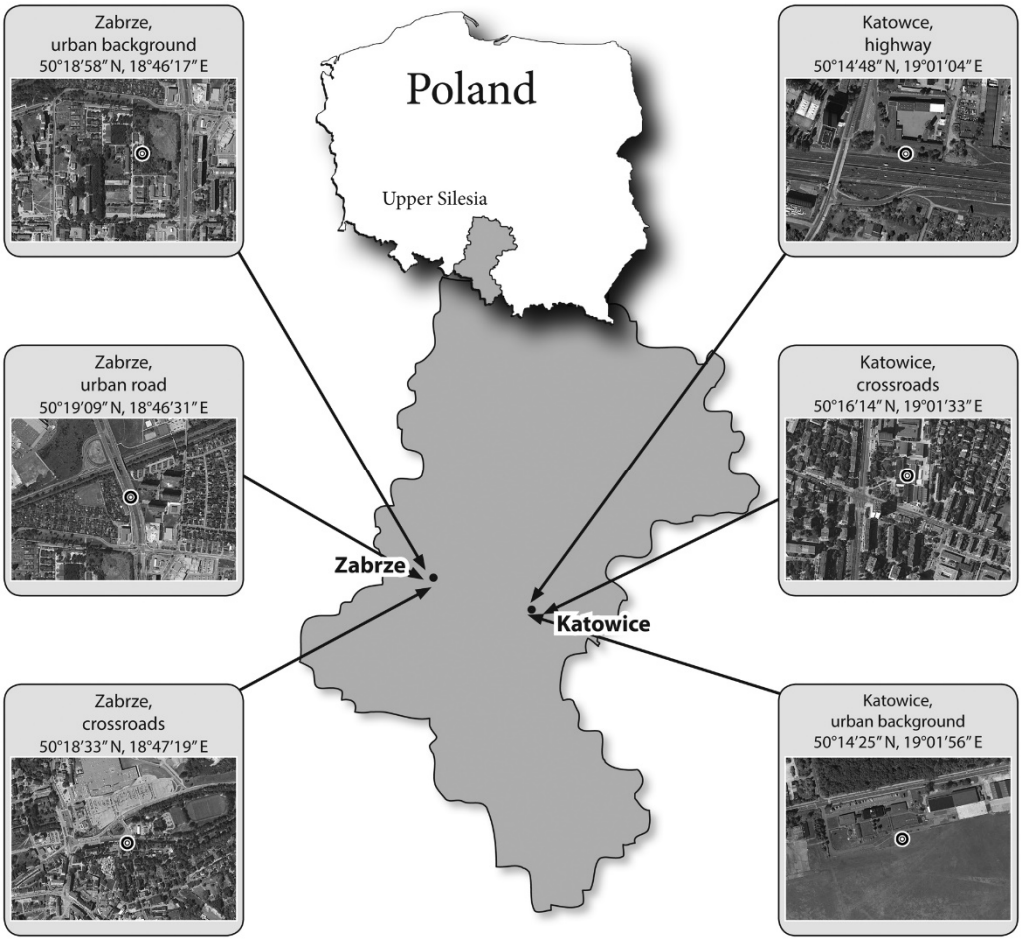


Fig. 1. Sampling sites (map source: Google Earth)

One measuring site in each city was situated at a crossroads in the city center. The direct neighborhood of the sites were the crossing roads. The traffic intensities on the crossroads were about 40 000 vehicles per day in Zabrze and 28 000 vehicles per day in Katowice.

In Zabrze, the third measuring site was located at a grassy side of a busy six-lane urban road, about 800 m away from the city center and 350 m from the urban background site. The traffic intensity on the road was about 30,000 vehicles per day. The third sampling site in Katowice was located on the shoulder of the highway A4, about 1500 m south of the city center and 1200 m northwest of the urban background site. Average traffic density through the highway was 30 000 cars per day. The meteorological conditions at the measuring sites were typical of the region during all the measuring period.

The samples of q-UFPs were taken using two thirteen-stage low pressure impactors from DEKATI (DLPI, Dekati low pressure impactor) and Nylon substrates (Whatman, nylon membrane filters 0,2 μm, ∅25 mm, Cat. No. 7402-002). They were collected in the period from the middle of March to the end of August in Katowice (16 sample--takings, 4 at the highway, 4 at the crossroads, and 8 at the urban background site), and from the beginning of May to the middle of October in Zabrze (21 sample-takings, 6 at the urban road, 6 at the crossroads, and 9 at the urban background site). The particular sample-takings lasted from about 3 to 5 days (the shortest lasted 62 hs, the longest – 128 h). The impactors and gravimetric analyses applied to the sample development have been described elsewhere [1–3].

The elemental composition of q-UFPs was determined by means of energy dispersive X-ray fluorescence (EDXRF). An Epsilon 5 (PANalytical B.V.), calibrated with the use of the thin-layer single-element standards (Micromatter) was used to measure the total concentrations of the elements. The NIST SRM2873 samples were measured to control the performance of the analytical procedure [1–3, 18]. To control the performance of the analytical procedure, the NIST SRM2873 samples were measured weekly (except 52% and 39% recoveries of V and Co, the recoveries were between 85 and 120% of the certified values) and the X-ray tube and detector drift were monitored monthly. The detection limits (from the statistical development of the blank results) were from 0.15 ng/cm$^2$ (Ti, Pb) to 16.8 ng/cm$^2$ (Si).

The results were analyzed for statistical significance of the differences of the concentration of q-UFP and of q-UFP-bound elements among the sampling sites using Statistica 8 (Stat Soft) (one-way ANOVA with post hoc Tukey HSD test, $p < 0.05$).

## 3. RESULTS AND DISSCISSION

On average, the q-UFP mass concentration slightly exceeded 800 ng/m$^3$ at the highway in Katowice. It was the greatest q-UFP concentration among all the sampling

sites. In Zabrze, at crossroads, it was 620 ng/m$^3$, and at the rest of the sites the q-UFP mass concentrations were in the range of 290–370 ng/m$^3$, being close to one another, (Fig. 2). These concentrations are relatively low. In small Alpine town of Morbengo (Sondrio), northern Italy, average UFP concentrations were 2 and 2.23 μg/m$^3$ [12], and at ten sites in the USA they were between 200 and 1000 ng/m$^3$ [20]. Yu et al. [22] showed that traffic emissions (diesel and gasoline) contribute relatively little to UFP mass concentrations at the sites or time periods of enhanced natural gas and wood combustion. In summer, when the emissions from residential heating ceases, traffic contributes to the UFP mass concentrations more. They also showed that at all the sites very few UFP came from nucleation [22].

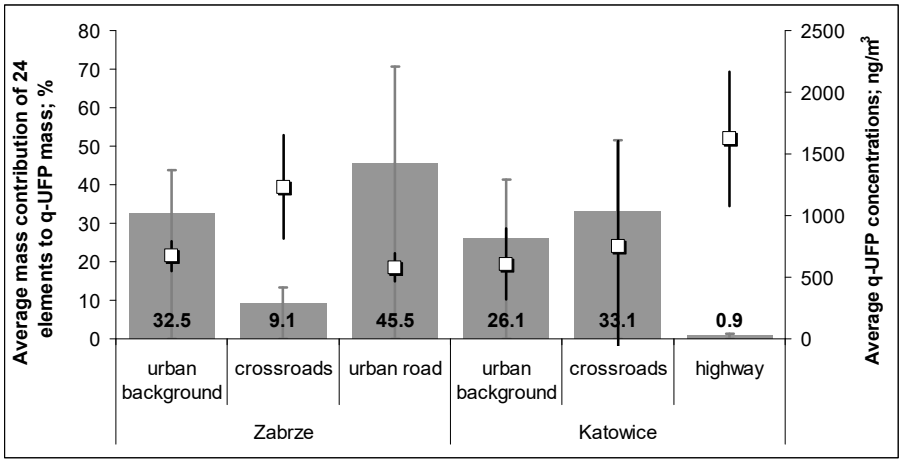


Fig. 2. Average q-UFP concentrations (the squares, black vertical line represents standard deviation from mean) and average mass contribution of 24 elements to q-UFP mass (grey bars, grey vertical line represents standard deviation from mean) at six sites in Upper Silesia

Here, the periods for the PM sampling were selected so that the emissions from combustion for residential heating (low-quality coal, wood, wastes) could be avoided. These emissions, very intense in heating periods in Upper Silesia, efficiently suppress emissions of PM from other sources [1, 18]. Nonetheless, in the heating season, the low concentration of q-UFP (around 500 ng/m$^3$) was also observed at the urban background in Zabrze. Therefore, according to results received by Yu et al. [22], the differences in q-UFP concentrations among the six sites investigated here seem to depend on the differences in road traffic intensities at these sites.

The highest q-UFP concentrations were observed in the sites under influence of heavy road traffic, i.e. at the highway in Katowice and the very busy crossroads in Zabrze (Fig. 2). In Katowice, the q-UFP concentrations at the crossroads were higher than at the urban background site not being effected directly by road traffic (Fig. 2). Statisti-

cally significant differences in the q-UFP concentrations were noted between the highway in Katowice and each of the urban background site in Katowice, urban road in Zabrze, urban background site in Zabrze, and between the crossroads and urban background in Zabrze (Fig. 2). Also, the average total element contents of q-UFP make q-UFP at the highway in Katowice and at the urban background site in Zabrze essentially different from q-UFP at the remaining sites. The average mass contribution of the investigated elements to the q-UFP mass at the highway in Katowice does not exceed 1%, and at the crossroads in Zabrze it is about 9%. At the remaining sites it is much higher, the highest being at the urban road in Zabrze (more than 40%). At the urban background sites, the examined elements are no more than 30% of q-UFPs mass (Fig. 2). Therefore, these two sampling sites, the highway in Katowice and background site in Zabrze, are specific among all the six sampling sites.

According to the earlier investigations of the effects of road traffic emissions on 13 PM fractions at the highway in Katowice [2], at this site, the carbonaceous matter, including hydrocarbons and elemental carbon, contributes more to the finest PM fraction than other components together do, and this contribution is greater than it is to PM sampled at the urban background site in Katowice at the same time. The small contribution of the investigated elements (among which there are not carbon, oxygen, or hydrogen) to q-UFP proves that at heavily affected by road traffic both the highway in Katowice and crossroads in Zabrze the chemical composition of q-UFP is shaped by road traffic emissions. It is highly probable that q-UFP at these sites are composed primarily of elemental carbon and organic compounds comprising, besides carbon, also oxygen and hydrogen.

Instead, at the two other traffic sites, the urban road in Zabrze and crossroads in Katowice, the mass q-UFP concentrations and the contribution of the element sum to the q-UFP mass were close to those at the urban background sites in these cities (Fig. 2). Although affected by road traffic, the urban road in Zabrze and crossroads in Katowice are surrounded by residential and commercial housing that affects these sites by releasing emissions from combustion of natural gas and wood, and periodically of oil or coal, for heating and cooking. Most probably these municipal sources affect stronger q-UFP than road traffic. The phenomenon of concealing road traffic effect on PM concentrations by municipal emissions was already observed in Upper Silesia earlier [1–3]. Besides, the traffic of heavy lorries, which probably are the most efficient sources of q-UFP, especially of those carbonaceous, e.g., [23], is practically banned from the road in Zabrze and crossroads in Katowice, while the traffic of heavy vehicles on the highway in Katowice and the crossroads in Zabrze is very intense.

Among 24 examined q-UFP-bound elements, Al, Si, S, Cl, K, Ca, Ti, Mn, Fe, and Sb had the greatest ambient concentrations at each site (Table 1). In a small Alpine town of Morbegno (Sondrio, Northern Italy), almost all these element concentrations were also highest, but the concentrations of Co, As, Cd, V, and Sr were visibly lower [12]. The latter can originate from industry [24, 25] or energy production from coal [26–28],

and in Poland, almost the whole of electric power and heat are produced from combustion of coal.

Table 1

Mean ambient mass concentrations [pg/m$^3$]
of q-UFP-bound elements at six sites in Upper Silesia

| Zabrze | | | | | | | | | | | | |
|---|---|---|---|---|---|---|---|---|---|---|---|---|
| Site | Element | | | | | | | | | | | |
| | Al | Si | S | Cl | K | Ca | Sc | Ti | V | Cr | Mn | Fe |
| Urban background | 8324 | 10014 | 23510 | 22736 | 3314 | 11000 | 2592 | 58334 | 8844 | 266 | 16034 | 6934 |
| Crossroads | 14490 | 15572 | 18794 | 6402 | 7464 | 7064 | 778 | 128 | 66 | 952 | 428 | 5834 |
| Urban road | 11362 | 11908 | 21598 | 21704 | 3632 | 11630 | 2988 | 68302 | 10070 | 298 | 19182 | 7788 |
| | Co | Ni | Cu | Zn | As | Rb | Sr | Cd | Sn | Sb | Ba | Pb |
| Urban background | 1244 | 116 | 1062 | 480 | 336 | 104 | 1024 | 1104 | 932 | 29808 | 5504 | 900 |
| Crossroads | 62 | 786 | 770 | 12858 | 2648 | 92 | 950 | 712 | 392 | 358 | 1648 | 3272 |
| Urban road | 1306 | 176 | 1440 | 424 | 378 | 164 | 1336 | 1570 | 944 | 36756 | 6856 | 1032 |
| Katowice | | | | | | | | | | | | |
| Site | Element | | | | | | | | | | | |
| | Al | Si | S | Cl | K | Ca | Sc | Ti | V | Cr | Mn | Fe |
| Urban background | 3842 | 3898 | 22416 | 19610 | 3144 | 3060 | 958 | 27778 | 3494 | 1234 | 7644 | 3144 |
| Crossroads | 3796 | 4152 | 25902 | 15662 | 3198 | 3198 | 1096 | 31310 | 3924 | 1530 | 8444 | 4536 |
| Urban road | 318 | 348 | 2746 | 2168 | 456 | 372 | 92 | 2668 | 336 | 122 | 736 | 490 |
| | Co | Ni | Cu | Zn | As | Rb | Sr | Cd | Sn | Sb | Ba | Pb |
| Urban background | 564 | 60 | 900 | 596 | 674 | 88 | 578 | 764 | 674 | 14346 | 3416 | 1900 |
| Crossroads | 458 | 60 | 1270 | 700 | 314 | 54 | 480 | 878 | 596 | 15726 | 3764 | 754 |
| Urban road | 56 | 6 | 94 | 160 | 48 | 4 | 46 | 64 | 48 | 1402 | 336 | 126 |

The element concentrations differed significantly between some sites. For Sc, Ti, V, Cr, Mn, Co, and Sb, the pairs of the sites between which the difference was statistically significant outnumbered a half of all the 15 pairs of sites. For Al, Si, S, Cl, K, Rb, Cd, and Ba, there were from 4 to 6 such pairs, and for Ni, Zn, As, and Pb there was none. The rest of the elements had only from 1 to 3 such pairs (Table 2).

Therefore, Zn, As, Pb, Cu, and Sr, whose presence in the atmosphere can be linked with coal combustion, e.g., because of the seasonal variability of their ambient concentrations [1, 18], have quite uniform ambient concentrations over Upper Silesia, what means that their main sources cannot be local. The concentrations of other elements, as well the PM microcomponents Al, Si, S, Cl, and K as the trace elements Sc, Ti, V, Cd, Cr, Mn, Co, and Sb, are explicitly affected by sources local to the considered sites.

The mass contributions of particular q-UFP-bound elements to the mass of all the 24 elements determined in q-UFP are very similar among five sites (Fig. 3), where the contributions (%) of Al, Si, S, Cl, K, Ca, Sc, Ti, V, Mn, Fe, Sb and Ba are greatest.

Despite the pointed out earlier differences, the site at the highway in Katowice is among these five sites (Fig. 3).

Table 2

q-UFP-bound elements and the pairs of sites between which their ambient concentrations statistically significantly differ (one-way ANOVA with post hoc HSD Tukey test, $p < 0.05$)

| | Pairs of sites with statistically significant difference between the element concentration |
|---|---|
| Al | CZ-CK,CZ-HK, CZ-UBK, HK-URZ |
| Si | UBZ-HK, URZ-HK, URZ-UBK, CZ-CK, CZ-HK, CZ-UBK |
| S | UBZ-HK, URZ-HK, CZ-HK, CK-HK, HK-UBK |
| Cl | UBZ-CZ, UBZ-HK, URZ-CZ, URZ-HK, CZ-UBK, HK-UBK |
| K | UBZ-CZ, URZ-CZ, CZ-CK, CZ-HK, CZ-UBK |
| Ca | UBZ-CK, UBZ-HK, UBZ-UBK, URZ-CK, URZ-HK, URZ-UBK, CZ-HK |
| Sc | UBZ-CZ, UBZ-CK, UBZ-HK, UBZ-UBK, URZ-CZ, URZ-CK, URZ-HK, URZ-UBK |
| Ti | UBZ-CZ, UBZ-CK, UBZ-HK, UBZ-UBK, URZ-CZ, URZ-CK, URZ-HK, URZ-UBK, CZ-CK, CK-CZ, CK-HK, HK-UBK |
| V | UBZ-CZ, UBZ-CK, UBZ-HK, UBZ-UBK, URZ-CZ, URZ-CK, URZ-HK, URZ-UBK, CZ-CK, CZ-UBK |
| Cr | UBZ-CZ, UBZ-CK, UBZ-UBK, URZ-CZ, URZ-CK, URZ-UBK, CZ-CK, CZ-HK, CZ-UBK, CK-HK, HK-UBK |
| Mn | UBZ-CZ, UBZ-HK, UBZ-UBK, URZ-CZ, URZ-CK, URZ-HK, URZ-UBK, CZ-CK, CZ-UBK |
| Fe | UBZ-HK, URZ-HK, CZ-HK |
| Co | UBZ-CZ, UBZ-CK, UBZ-HK, UBZ-UBK, URZ-CZ, URZ-CK, URZ-HK, URZ-UBK |
| Ni | – |
| Cu | URZ-HK, CK-HK |
| Zn | – |
| As | – |
| Rb | UBZ-HK, URZ-CK, URZ-HK, URZ-UBZ, CZ-HK |
| Sr | URZ-HK |
| Cd | UBZ-HK, URZ-CZ, URZ-HK, URZ-UBK |
| Sn | UBZ-HK, URZ-HK |
| Sb | UBZ-CZ, UBZ-HK, UBZ-UBK, URZ-CZ, URZ-CK, URZ-HK, URZ-UBK, CZ-UBK |
| Ba | UBZ-CZ, UBZ-HK, URZ-CZ, URZ-HK |
| Pb | – |

UBZ – urban background in Zabrze, UBK – urban background in Katowice, CZ – crossroads in Zabrze, CK – crossroads in Katowice, URZ – urban road in Zabrze, HK – highway in Katowice.

The crossroads in Zabrze differs explicitly from the other five sites with the high contributions of Zn and As (very low everywhere else except the highway in Katowice), contributions of Al and Si higher than at other sites, and almost lacking contributions of Ti and Sb that are relatively high at other sites. Because Zn share is considerably high also at the highway in Katowice (Fig. 3) and it is known that Zn occurs in cars (e.g., lubricating oil or tires), the Zn high contribution to the mass of the 24

q-UFP-bound elements at the crossroads in Zabrze can be attributed to road traffic [29, 30]. On the other hand, all the differences in the concentrations of q-UFP-bound Zn and As among the sites are not statistically significant (Table 2). The high average ambient concentrations and contributions to the total element mass of q-UFP-bound Zn and As derive from one (for Zn) and two (for As) very high measured values of their concentrations. Therefore, it is rather hard to decide what is the origin of Zn and As at the crossroads in Zabrze.

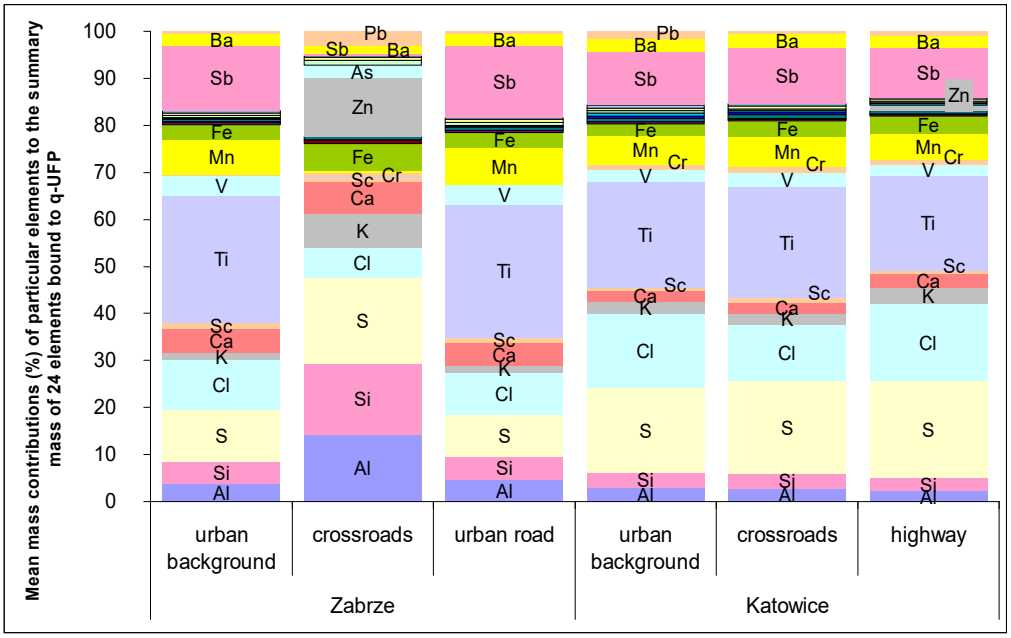


Fig. 3. Mean mass contributions of particular elements to the summary mass of all 24 determined in q-UFP elements at six sites in Upper Silesia (only symbols of the elements with contributions greater than 1% are given)

The high contribution of Si and Al to the mass of the 24 q-UFP-bound elements at the crossroads in Zabrze is probably due to re-suspension of road dust and soil caused by heavy road traffic. This crossroads is a very busy one, much busier than the crossroads in Katowice. Besides, the streets in Katowice, the capital and biggest city of Upper Silesia, are more often cleaned and sprinkled with water than in Zabrze. At all the sites, the effects of road traffic emissions were reflected in the contribution of q-UFP-bound Sb to the mass of the 24 q-UFP-bound elements [30]. However, the differences in ambient concentrations of q-UFP-bound Sb among the six sites are statistically significant.

At five sites, urban background and road in Zabrze and everywhere in Katowice, the Ti contribution to the 24 q-UFP-bound element mass and ambient concentrations

are high (Fig. 3, Table 1). The Ti concentrations differ significantly among the sites. This unusual Ti abundance can be due to the multiplicity of industrial Ti sources dispersed over Upper Silesia. Ti can be emitted in $TiO_2$ from various high-temperature processes. Ti is used as a component of alloys with other metals for stainless steel production [31]. $TiO_2$ is used as a pigment in paints (nearly 70% of all its production), it is also used as a pigment in glazes, enamels, plastics, paper, fibers, foods, pharmaceuticals, cosmetics, and toothpastes. Other $TiO_2$ uses include antimicrobial applications, catalysts for air and water purification, medical applications, and energy storage [32]. The global production of $TiO_2$ for all uses is in millions of tons per year.

Table 3

24 q-UFP-bound elements ordered by their enrichment factors increasing from the top to the bottom in columns at six sites in Upper Silesia

| Zabrze | | | Katowice | | |
|---|---|---|---|---|---|
| Urban background | Crossroads | Urban road | Urban background | Crossroad | Highway |
| Si | Ti | Si | Si | Si | Si |
| Al | Si | K | Al | Al | Al |
| K | Al | Al | Fe | Ca | Ca |
| Fe | Fe | Fe | Ca | K | Fe |
| Ca | Ca | Ca | K | Fe | K |
| Rb | K | Rb | Rb | Rb | Rb |
| Sr | Mn | Sr | Sr | Sr | Sr |
| Ni | Rb | Zn | Ni | Ni | Ni |
| Cr | V | Cr | Ba | Ba | Ba |
| Ba | Ba | Ni | Ti | Ti | Ti |
| Zn | Sr | Ba | Zn | Zn | Sn |
| Ti | Co | Ti | Mn | Sn | Mn |
| Sn | Sn | S | Sn | Mn | S |
| S | Cl | Sn | S | Cl | Zn |
| Mn | S | Cl | Cl | S | Cl |
| Cl | Cr | Mn | Cr | Co | Cr |
| Pb | Ni | Pb | Co | Cr | **Co** |
| Cu | Cu | Cu | **Cu** | Pb | V |
| Co | Sc | Co | V | V | Cu |
| **V** | Pb | As | Pb | Cu | Pb |
| **As** | Zn | V | Sc | Sc | Sc |
| **Sc** | Sb | Sc | As | As | As |
| **Cd** | **As** | **Cd** | **Cd** | **Cd** | **Cd** |
| **Sb** | **Cd** | **Sb** | **Sb** | **Sb** | **Sb** |

The background: white $EF \leq 10$, light gray $10 < EF \leq 100$, dark gray $100 < EF \leq 1000$, black $1000 < EF \leq 10\,000$, bold symbols $EF > 10\,000$.

To distinguish between anthropogenic or natural origin of the elements, their enrichment factors (*EF*) were computed for all the sites [1–3] (Table 3). The enrichment factor $EF_x$ for the element $x$ is defined as:

$$EF_x = \frac{\left(\frac{C_x}{C_{\text{ref}}}\right)_{\text{PM}}}{\left(\frac{C_x}{C_{\text{ref}}}\right)_{\text{crust}}} \tag{1}$$

where $C_x$ and $C_{\text{ref}}$ are the concentrations of the element $x$ and the reference element, and $(C_x/C_{\text{ref}})_{\text{PM}}$ and $(C_x/C_{\text{ref}})_{\text{crust}}$ are the proportions of these concentrations in PM and in the Earth crust, respectively. Here, Al is selected as the reference element, i.e., $EF_{\text{Al}} = 1$. The chemical composition of the upper continental crust was taken from [33].

The closer *EF* of an element to 1, the weaker the anthropogenic effect on the element ambient concentrations is. In Table 3, for each site, the symbols of elements are ordered by the element *EF* increasing from the top to the bottom in the columns. In general, q-UFP-bound Si, Al, K, Fe, Ca, and Rb, having EFs not greater than 10, are of natural origin, their presence can be linked with the presence of soil, sand, etc., at all the sites. At all the sites, excluding the crossroads in Zabrze, Sr and Ni had *EF* greater than 10, but much lower than other elements had. The majority of the q-UFP-bound elements should be considered anthropogenic because of their high EF. As, Cd, and Sb had the greatest EFs at all the sites (Table 3).

## 4. CONCLUSIONS

The paper presents the analysis of the elemental composition of ambient ultrafine particles in urban environment which was done in Poland for the first time. The data from PM measurements, earlier used by the authors to determine the mass size distributions of PM-bound elements, are here applied to characterize ambient mass concentrations and elemental composition of ultrafine particles with aerodynamic diameters between 30 and 108 nm (q-UFP) which are the least recognized subfraction of the fine PM fraction.

The average ambient concentrations of q-UFPs vary within Upper Silesia depending on the site. They depend on local sources of primary q-UFP such as road traffic and municipal sources, their values vary widely at a big crossroads or highway. They are quite uniform within area of residential and commercial housing. High contribution of the investigated elements to the mass of q-UFP proves the prevalence of primary matter content in q-UFP at four sites, the urban background site and road in Zabrze and the urban background site and crossroads in Katowice. At the big crossroads in Zabrze and

the highway Katowice, the prevalence of carbon, oxygen, and hydrogen, not investigated here, is expected. Most probably, also secondary matter contributes significantly to ultrafine particles at these two sites.

The chemical composition of q-UFP in Upper Silesia is quite uniform over its area. The ambient concentrations of Zn, As, Pb, Cu, Sr and their contributions to the mass of the 24 q-UFP-bound elements are comparable among sites, probably because they are influenced mainly by the same global factors such as coal combustion for energy and power production. The ambient concentrations of such q-UFP-bound elements as Al, Si, S, Cl, K, Sc, Ti, V, Cd, Cr, Mn, Co, and Sb are affected by local sources. Majority of elements bound to q-UFP are anthropogenic.

## REFERENCES

[1] ROGULA-KOZŁOWSKA W., MAJEWSKI G., CZECHOWSKI P.O., *The size distribution and origin of elements bound to ambient particles: A case study of a Polish urban area*, Environ. Monit. Asses., 2015, 187 (5), 240.

[2] ROGULA-KOZŁOWSKA W., *Traffic-generated changes in the chemical characteristics of size-segregated urban aerosols*, B Environ. Contam. Tox., 2014, 93 (4), 493.

[3] ROGULA-KOZŁOWSKA W., Size-segregated urban particulate matter: mass closure, chemical composition, and primary and secondary matter content, Air Qual. Atmos. Health, 2016, 9 (5), 533.

[4] SALMA I., BORSOS T., WEIDINGER T., ALTO P., HUSSEIN T., DAL MASO M., KULMALA M., *Production, growth and properties of ultrafine atmospheric aerosol particles in an urban environment*, Atmos. Chem. Phys., 2011, 11, 1339.

[5] KUMAR P., MORAWSKA L., BIRMILI W., PAASONEN P., HUG M., KULMALAE M., HARRISON R.M., NORFORD L., BRITTERK R., *Ultrafine particles in cities*, Environ. Int., 2014, 66, 1.

[6] MA N., BIRMILI W., *Estimating the contribution of photochemical particle formation to ultrafine particle number averages in an urban atmosphere*, Sci. Tot. Environ., 2015, 512, 154.

[7] DAMETO DE ESPANA C., WONASCHÜTZ A., STEINER G., ROSATI A., DEMATTIOA A., SCHUHA H., HITZENBERGER R., *Long-term quantitative field study of New Particle Formation (NPF) events as a source of Cloud Condensation Nuclei (CCN) in the urban background of Vienna*, Atmos. Environ., 2017, 164, 289.

[8] OBERDORSTER G., SHARP Z., ATUDOREI V., ELDER A., GELEIN R., LUNTS A., KREYLING W., COX C., *Extrapulmonary translocation of ultrafine carbon particles following whole-body inhalation 700 exposure of rats*, J. Toxicol. Environ. Health A, 2002, 65, 1531.

[9] WILSON M.R., LIGHTBODY J.H., DONALDSON K., SALES J., STONE V., *Interactions between ultrafine particles and transition metals in vivo and in vitro*, Tox. Appl. Pharmacol., 2002, 184, 172.

[10] GWINN M.R., VALLYATHAN V., *Nanoparticles. Health effects – pros and cons.*, Environ Health Perspect., 2006, 114 (12), 1818.

[11] LU S., ZHANG W., ZHANG R., LIU P. WANG Q., SHANG Y., WU M., DONALDSON K., WANG Q., *Comparison of cellular toxicity caused by ambient ultrafine particles and engineered metal oxide nanoparticles*, Part. Fibre Tox., 2015, 12 (5).

[12] CORSINI E., VECCHI R., MARABINI L., FERMO P., BECAGLI S., BERNARDONI V., CARUSO D., CORBELLA L., DELL'ACQUA M., GALLI C.L., LONATI G., OZGEN S., PAPALE A., SIGNORINI S., TARDIVO R., VALLI G., MARINOVICH M., *The chemical composition of ultrafine particles and associated biological effects at an alpine town impacted by wood burning*, Sci. Tot. Environ. 2017, 587, 223.

[13] VINZENTS P.S., LOLLER P., SORENSEN M., KNUDSENL., HERTEL O., JENSEN FP., SCHIBYE B., STEFFEN--LOFT S., *Personal exposure to ultrafine particles and oxidative DNA damage*, Environ. Health Perspect., 2005, 113, 1485.

[14] CORLIN L., WOODIN M., HART J.E., SIMON M.C., GUTE D.M., JOANNA STOWELL J.,TUCKER K.L., DURANT J.L., BRUGGE D., *Longitudinal associations of long-term exposure to ultrafine particles with blood pressure and systemic inflammation in Puerto Rican adults*, Environ. Health, 2018, 17 (1), 33.

[15] BADYDA A., GAYER A., CZECHOWSKI P. O., MAJEWSKI G., DĄBROWIECKI P., *Pulmonary function and incidence of selected respiratory diseases depending on the exposure to ambient PM10*, Int. J. Mol. Sci., 2016, 17 (11), 1954.

[16] SÓWKA I., CHLEBOWSKA-STYŚ A., PACHURKA Ł., ROGULA-KOZŁOWSKA W., *Seasonal variations of PM2.5 and PM10 concentrations and inhalation exposure from PM-bound metals (As, Cd, Ni). First studies in Poznań (Poland)*, Arch. Environ. Prot. 2018, 44 (4), 86.

[17] ROGULA-KOZŁOWSKA W., KLEJNOWSKI K., ROGULA-KOPIEC P., LESZEK OŚRÓDKA L., EWA KRAJNY E., BŁASZCZAK B., MATHEWS B., *Spatial and seasonal variability of the mass concentration and chemical composition of PM2.5 in Poland*, Air Qual. Atmos. Health, 2014, 7 (1), 41.

[18] ROGULA-KOZŁOWSKA W., MAJEWSKI G., BŁASZCZAK B. KLEJNOWSKI K., ROGULA-KOPIEC P., *Origin--oriented elemental profile of fine ambient particulate matter in central European suburban conditions*, Int. J. Environ. Res. Publ. Health, 2016, 13 (7), 715.

[19] POSNER L.N., PANDIS S.N., *Sources of ultrafine particles in the Eastern United States*, Atmos. Environ., 2015, 111, 103.

[20] WIDZIEWICZ K., ROGULA-KOZŁOWSKA W., *Urban environment as a factor modulating metals deposition in the respiratory track and associated cancer risk*, Atmos. Pollut. Res., 2018, 9 (3), 399.

[21] EC Directive 2008/50/EC of the European Parliament and of the Council of 21 May 2008 on ambient air quality and cleaner air for Europe, 2008.

[22] YU X., VENECEK M., HU J., TANRIKULU S., SOON S.-T., TRAN C., FAIRLEY D., KLEEMAN M., *Sources of airborne ultrafine particle number and mass concentrations in California*, Atmos. Chem. Phys. Discuss., 2018.

[23] CHINA S., SALVADORI N., MAZZOLENI C., *Effect of traffic and driving characteristics on morphology of atmospheric soot particles at freeway on-ramps*, Environ. Sci. Technol., 2014, 48 (6), 3128.

[24] TIAN H., LIU K., ZHOU J., LU L., HAO J., QIU P., GAO J., ZHU C., WANG K., HUA S., *Atmospheric emission inventory of hazardous trace elements from China's coal-fired power plants. Temporal trends and spatial variation characteristics*, Environ. Sci. Technol. 2014, 48 (6), 3575.

[25] ZHANG K., CHAI F., ZHENG Z., YANG Q., ZHONG X., FOMBA KW., ZHOU G., *Size distribution and source of heavy metals in particulate matter on the lead and zinc smelting affected area*, J. Environ. Sci., 2018, 71, 188.

[26] KOLKER A., *Minor element distribution in iron disulfides in coal. A geochemical review*, Int. J. Coal Geol., 2012, 94, 32.

[27] IZQUIERDO M., QUEROL X., *Leaching behavior of elements from coal combustion fly ash. An overview*, Int. J. Coal Geol., 2012, 94, 54.

[28] VEJAHATI F., XU Z., GUPTA R., *Trace elements in coal. Associations with coal and minerals and their behavior during coal utilization. A review*, Fuel, 2010, 89 (4), 904.

[29] PENKAŁA M., OGRODNIK P., ROGULA-KOZŁOWSKA W., *Particulate matter from the road surface abrasion as a problem of non-exhaust emission control*, Environ., 2018, 5 (1), 9.

[30] JOHANSSON C., NORMAN M., BURMAN L., *Road traffic emission factors for heavy metals*, Atmos. Environ., 2009, 43 (31), 4681.

[31] ELREFAEY A., TILLMANN W., *Brazing of titanium to steel with different filler metals. Analysis and comparison*, J. Mat. Sci., 2010, 45 (16), 4332.

[32] WEIR A., WESTERHOFF1 P., FABRICIUS L., GOETZ N., *Titanium dioxide nanoparticles in food and personal care products*, Environ. Sci. Technol., 2012, 46 (4), 2242.
[33] WEDEPOHL K.H., *The composition of the continental crust*, Geochim. Cosmochim. Acta, 1995, 59, 1217.

# Elemental composition and origin of PM10 in fire station in Poland: real time results from XRF analysis

Mach Tomasz, Department of Environmental Protection, Wroclaw University of Science and Technology, ORCID: 0000-0001-7371-3499, tomasz.mach@pwr.edu.pl
Rogula-Kozłowska Wioletta, The Main School of Fire Service, ORCID: 0000-0002-4339-0657,
Bihałowicz Jan Stefan The Main School of Fire Service ORCID: 0000-0003-3465-5315,
Rybak Justyna, Department of Environmental Protection, Wroclaw University of Science and Technology, ORCID: 0000-0002-3606-4220

## 1. Abstract

This work presents first results of the metal in particulate matter PM10 analysis and source apportionment in one of fire stations garage in Poland. The novelty of the study includes high temporal resolution of elemental composition of PM bound metals since in the study the gamma ray fluorescence spectrometer with the high temporal resolution was used. The concentrations of PM10 were measured in the same time using method of beta-ray attenuation. The concertation of PM10 and PM bound metals were analyzed with temporal resolution of 4h. To identify source apportionment of metals three models, that are commonly used for the source apportionment were applied: PCA (principal component analysis), EPA UNMIX, and EPA PMF (positive matrix factorization).
The concentrations of the investigated metals have high temporal variations while the concentrations of PM10 were low in the garage. The enrichment of PM10 was very high or high, especially in sulfur, zinc, arsenic, nickel, cadmium, and lead. PCA analysis as well as UNMIX and PMF showed high impact of factor related to sulfur on the variability. It showed the impact of combustion, including combustion of liquid fuels, in fire engines may have crucial impact on the air pollution in fire station. The PMF analysis allowed also to identify factor responsible from external anthropogenic emission on concentrations inside the garage. Another identified sources of PM10 and PM10-bound elements are mineral dust, and road dust related to non-exhaust emission, originating inside the firehouse (resuspension and abrasion) as well as from outside.

## 2. Introduction

It was found that some cancers and other health conditions such as cardiac events are very common among firefighters as they are exposed to combustion products i.e. different chemicals in the vapor state and particulate phase, mainly through inhalation, although ingestion and dermal way are also possible [1]. Air pollutants are the main cause of health issues and numerous studies have proved a strong association between high concentrations of ambient particulate and mortality rates. The smoke deriving from fires can be a reason for the sudden death of both: firefighters and victims due to inhalation of toxic gases [2].
Fire smoke contains particulate matter (PM) of different particle sizes, various substances in a gaseous phase, PM-bound compounds such as toxic and carcinogenic polycyclic aromatic hydrocarbons (PAHs), volatile organic compounds (VOCs), and metals [3].
Toxic compounds are also found on the personal protective equipment (PPE) and clothing of firefighters [1]. What is more, the storage location of PPE and clothing in the fire station can be a key issue as well as the effectiveness of post-fire decontamination or laundering which can highly

contribute to the contamination of fire stations [1]. Some studies suggest that the contamination of clothing and equipment of firefighters on the scene of a fire can also contribute to the contamination of fire stations [4]. Moreover, diesel engine exhaust from fire appliances may play a significant role in a potential health risk for firefighters [5].
Therefore, models that can predict the variability of elemental composition and origin of PM concentrations in fire stations would be a very important and crucial tool for protecting human life. What is more, designing a warning system could greatly facilitate achieving this goal.
Receptor models, which attribute concentrations to sources on the basis of statists and meteorological data, give a piece of clear information on the sources of aerosols [6]. Several receptor models i.e. principal component analysis (PCA) [7], UNMIX [8] are very useful in providing an easy and reliable tool for classifying sources [9], and positive matrix factorization (PMF) [10]. PCA, UNMIX and PMF analysis depend on the covariance matrix. All three models are good at identifying the dominant source categories of aerosols [11]. There are also other receptor models in use, although in models applied in this study the data concerning the elemental composition of PM are sufficient for the reliable prediction of the variability of elemental composition and origin of PM. However, in other models, different parameters are also required such as carbon contribution, etc.
For this purpose, fast and comprehensive assessment of the origin of PM based on the concentration of elements obtained from the measurements averaged in intervals of less than 24 hours would be the most effective tool. It can be achieved with automatic measurements based on the X-Ray fluorescence technique. The data obtained with this tool could provide a piece of reliable information that will allow for future actions to be taken against possible health risks among firefighters.
The aim of our study was to assess the elemental composition and origin of PM10 in selected fire station in Poland with the application of three different receptor models for source apportionment and with the use of XRF Horiba PX-375 (HORIBA ltd, Kyoto, Japan). Such studies have never been conducted before in Poland and can serve as inputs in the proposal of the warning system of ambient PM10 concentrations in fire stations.

## 3. Methods

### *3.1. Measurements*

During the measurements, the concentration of PM10 (μg/m$^3$) and the mass concentrations of some elements in PM10 have been studied in a selected fire station's garage in Poland. The fire station was located in Warsaw, in a typical residential district with single-family as well as multiple-family housing, where air quality is dependent mainly on emissions related to energy production and transport emissions. The measurements were carried out in the period from 24.06 to 08.07, i.e., full 336 hours.
Measurements were performed using the Horiba PX-375 XRF analyzer (HORIBA ltd, Kyoto, Japan). During the measurements, the concentrations of Ti, V, Cr, Mn, Fe, Ni, Cu, Zn, Pb, Al, Si, S, K, and Ca were measured. PX-375 collects PM on non-woven, elementally clean surface Teflon fiber tapes (PTFE). The mass of PM collected in the sample was determined with beta radiation attenuation. After determining the weight, the tape was moved so that using an X-ray fluorescence energy dispersion spectrometer (EDXRF) equipped with a palladium lamp to determine the concentration of elements. Samples were taken for 60 minutes and a flow of 16.7 l/min. Then, after collection, they were excited and analyzed by EDXRF for 2000 s. System EDXRF is additionally equipped with a camera that allows you to control the position of the sample relative to the spectrometer. In order to control the quality of the collected spectra, the National Institute of Technology (NIST) Standard Reference Material (SRM) 2783 was used. The sensitivity of the spectrometer - the lower detection limit - was dependent on the examined element, and parameters used in the experiment were for Al (56.7 ng/m$^3$), As (3.7 ng/m$^3$), Ca (1.1 ng/m$^3$), Cr (2.05 ng/m$^3$), Cu (1.85 ng/m$^3$), Fe (7.00 ng/m$^3$), K (4.8 ng/m$^3$), Mn (1.45 ng/m$^3$), Ni (0.9 ng/m$^3$), Pb (1.05 ng/m$^3$), S (1.55 ng/m $^3$), Si (8.85 ng/m$^3$), Ti (0.25 ng/m$^3$), V (1.7 ng/m$^3$), and for Zn (1.25 ng/m$^3$).

### *3.2. Source apportionment*

The data collected by the Horiba PX-375 were analyzed employing statistical models.

The correlations between the observed concentrations of elements were examined using Pearson's coefficient of correlation $r$ available through package Seaborn package [12]. The significance of the correlations was also evaluated using this package. We evaluated significance at three levels - $\alpha = 0.1$, $\alpha = 0.05$, and $\alpha = 0.01$.

The enrichment of the elements in the PM10 was assessed using Enrichment Factor (EF), used according to [13] with the conservative reference element – aluminum. The classes of enrichment are presented in Table 1. The interpretation of the EF value was based on previous work and experience. The enrichment factor of element $i$ is given by the formula (1):

$$EF_i = \frac{\frac{C_i}{C_{\mathrm{Al}}}}{\frac{B_i}{B_{\mathrm{Al}}}} \tag{1}$$

Where $C_i$ is concentration of element $i$ in the sample, $C_{\mathrm{Al}}$ is a concentration of aluminum in the sample, $B_i$ and $B_{\mathrm{Al}}$ are concentrations of elements in the upper crust according to Wedepohl [14]. Although $B$ and $C$ are expressed in different units the ratios in such formulation of $EF_i$ allows to reduce units without losing generality of formulation.

Table 1. The classes of the enrichment factor of PM10-bound elements.

| Value | Class |
|---|---|
| $EF \leq 2$ | Natural origin (soil, sand, etc.) |
| $2 < EF \leq 5$ | Deficiency to minimal enrichment |
| $5 < EF \leq 20$ | Moderate enrichment |
| $20 < EF \leq 40$ | Significant enrichment |
| $40 < EF \leq 100$ | Very high enrichment |
| $EF > 100$ | Extremely high enrichment |

The classical principal component analysis, PCA, was performed to identify the directions, along which the variance of data points is minimized to reduce the dimensionality of data points that were originally from $\mathbb{R}_+^{15}$ space. The number of principal components (PC) in PCA can be between 1 and 15, however, 15 is useless since it does not reduce the dimensionality. As the criterion for the choice of the number of PC, we used the explained variance in a dataset with an arbitrarily chosen level minimum of 99%. The PCA analysis was performed using the KNIME Analytics Platform [15].

Since PCA is limited we used EPA UNMIX 6.0 model 6 [16]. EPA Unmix decomposes the matrix $X_{m\times n}$ of $m$ samples of $n$ elements as a product of two matrices $G_{m\times p}$ representing fractions of each of $p$ sources in $m$ samples and matrix $F_{p\times n}$ which consists of $n$ elements emission profiles of each of $p$ sources. The fundamental difference from PCA is that these two matrices are non-negative since the contributions as well as emission profiles have to have physical meaning. The objective of the procedure is to minimize the difference $E$ between $X$ and $FG$ (Equation 2).

$$X = FG + E \tag{2}$$

The next model used in the work is EPA PMF 5.0 [17]. It is a common practice, observed in many works [18] that UNMIX and PMF are used in parallel for source apportionment. EPA PMF also solves the

equation; however, the main difference is the presence of measurement uncertainties for individual samples and elements. The model objective is to minimize the sum over all samples and elements $Q$ defined by the equation (3) where $i$ is numbering samples, $j$ is numbering elements and $k$ is numbering source profiles.

$$Q = \sum_i \sum_j \left( \frac{x_j^i - \sum_k g_k^i f_j^k}{u_j^i} \right)^2 \quad (3)$$

## 4. Results and discussion

### *4.1. Characteristics of the data*

Table 2. Presents statistical characteristics for the measured parameters, i.e., the concentrations of PM10 and elements related to PM10.

| | min | 25th percentile | Median | 75th percentile | Maximum | Mean | St. Deviation |
|---|---|---|---|---|---|---|---|
| PM10 (µg/m³) | 4.83 | 7.64 | 10.64 | 12.66 | 19.35 | 10.66 | 3.53 |
| Ti (ng/m³) | 0* | 0 | 0.07 | 1.77 | 20.21 | 1.92 | 4.26 |
| V (ng/m³) | 0 | 0.03 | 0.15 | 0.29 | 1.6 | 0.2 | 0.26 |
| Cr (ng/m³) | 0 | 0.05 | 0.41 | 0.84 | 4.52 | 0.59 | 0.74 |
| Mn (ng/m³) | 0 | 1.01 | 1.68 | 2.18 | 7.55 | 2.1 | 1.8 |
| Fe (ng/m³) | 0 | 54.04 | 77.31 | 96.5 | 263.71 | 84.96 | 47.62 |
| Ni (ng/m³) | 0 | 0 | 0.11 | 0.34 | 0.83 | 0.19 | 0.23 |
| Cu (ng/m³) | 0 | 0.87 | 1.77 | 4.26 | 7.15 | 2.44 | 1.89 |
| Zn (ng/m³) | 0.11 | 5.26 | 6.83 | 13.3 | 461.21 | 47.29 | 107.41 |
| As (ng/m³) | 0 | 0 | 0 | 0.07 | 9.47 | 0.71 | 1.86 |
| Pb (ng/m³) | 0 | 1.14 | 2.09 | 3.63 | 37.25 | 4.93 | 8.17 |
| Al (ng/m³) | 0 | 62.69 | 83.62 | 103.14 | 195.02 | 82.48 | 39.04 |
| Si (ng/m³) | 10.72 | 77.89 | 90.82 | 111.07 | 232.58 | 96.89 | 39.21 |
| S (ng/m³) | 29.21 | 602.84 | 933.78 | 1219.07 | 3077.42 | 992.62 | 541.19 |
| K (ng/m³) | 0 | 8.42 | 15.84 | 20.38 | 51.62 | 16.25 | 11.17 |
| Ca (ng/m³) | 9.83 | 36.76 | 43.4 | 59.02 | 303.45 | 60.4 | 55.66 |

* 0 concentration was assumed for every result at a level lower than the limit of quantification for a given element - data on detection limits are provided in the "methods" section.

During the study period, PM10 concentrations inside the rescue and firefighting firehouse were relatively low. On average, one-hour PM10 concentrations did not exceed 11 µg/m$^3$ and ranged from about 5 µg/m$^3$ to 19 µg/m$^3$. In general, sulfur, calcium, silicon, aluminum, zinc, and iron dominated the dust. It should be underlined that the elemental composition of PM10 inside the room is different from the elemental composition of PM10 in the atmosphere; this applies to both PM10 previously studied in different parts of Warsaw [19] and in other parts of Poland and the world [20]. Throughout the measurement period, a strong hourly variability of concentrations was observed for PM10 and for almost all elements associated with it. The most strongly it was observed in the case of elements with relatively high concentrations, such as sulfur, potassium, silicon or zinc. The concentrations of these elements were definitely higher in those periods when cleaning of fire trucks and personal protective equipment was carried out, and in the hours when cars and rescue teams left or returned to/from field operations. Figure 1 presents histograms of the elemental concentrations to show in which concentration ranges PM10-bound elements occur most often. This information is crucial in creating scenarios of users exposure – firefighters- to the impact of toxic and potentially toxic elements in studied fire station [21].

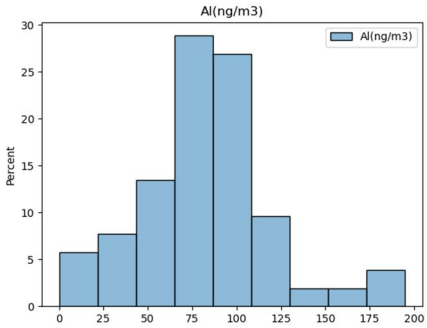
Al(ng/m3)
Al(ng/m3)
Percent
0
5
10
15
20
25
30
0
25
50
75
100
125
150
175
200

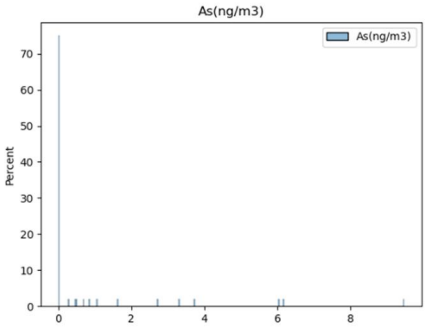
As(ng/m3)
As(ng/m3)
Percent
0
10
20
30
40
50
60
70
0
2
4
6
8

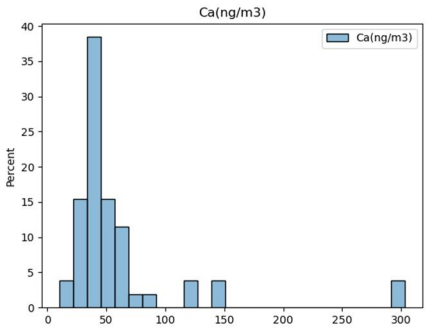
Ca(ng/m3)
Ca(ng/m3)
Percent
0
5
10
15
20
25
30
35
40
0
50
100
150
200
250
300

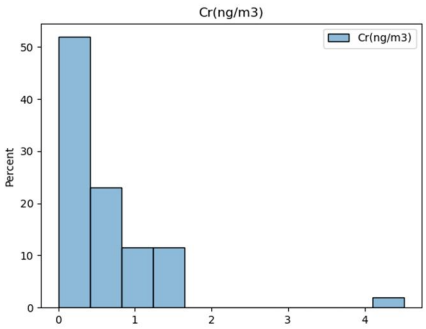
Cr(ng/m3)
Cr(ng/m3)
Percent
0
10
20
30
40
50
0
1
2
3
4

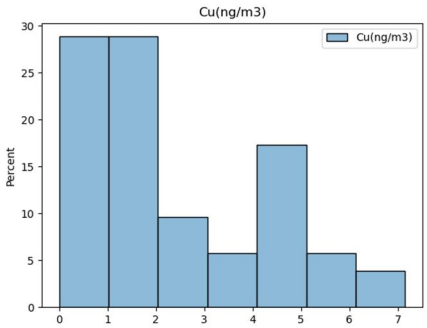
Cu(ng/m3)
Cu(ng/m3)
Percent
0
5
10
15
20
25
30
0
1
2
3
4
5
6
7

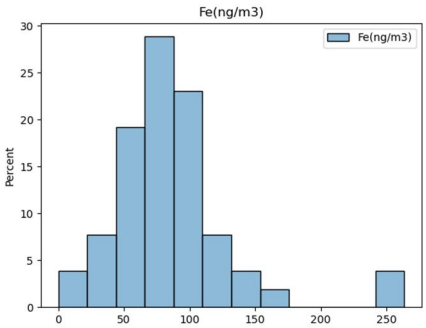
Fe(ng/m3)
Fe(ng/m3)
Percent
0
5
10
15
20
25
30
0
50
100
150
200
250

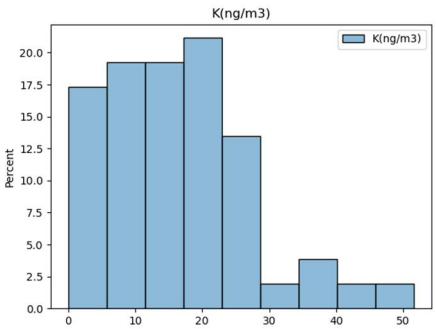
K(ng/m3)
K(ng/m3)
Percent
0.0
2.5
5.0
7.5
10.0
12.5
15.0
17.5
20.0
0
10
20
30
40
50

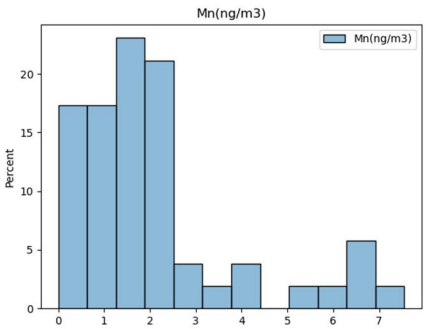
Mn(ng/m3)
Mn(ng/m3)
Percent
0
5
10
15
20
0
1
2
3
4
5
6
7

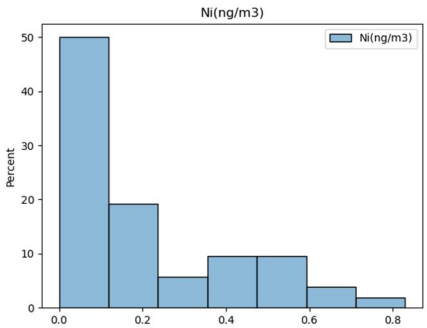
Ni(ng/m3)
Ni(ng/m3)
Percent
0
10
20
30
40
50
0.0
0.2
0.4
0.6
0.8

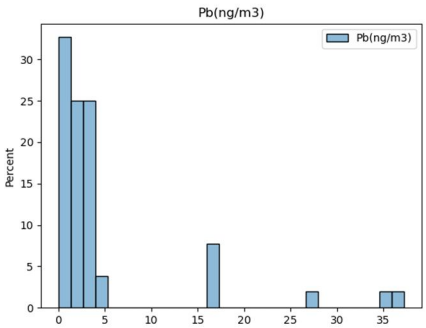
Pb(ng/m3)
Pb(ng/m3)
Percent
0
5
10
15
20
25
30
0
5
10
15
20
25
30
35

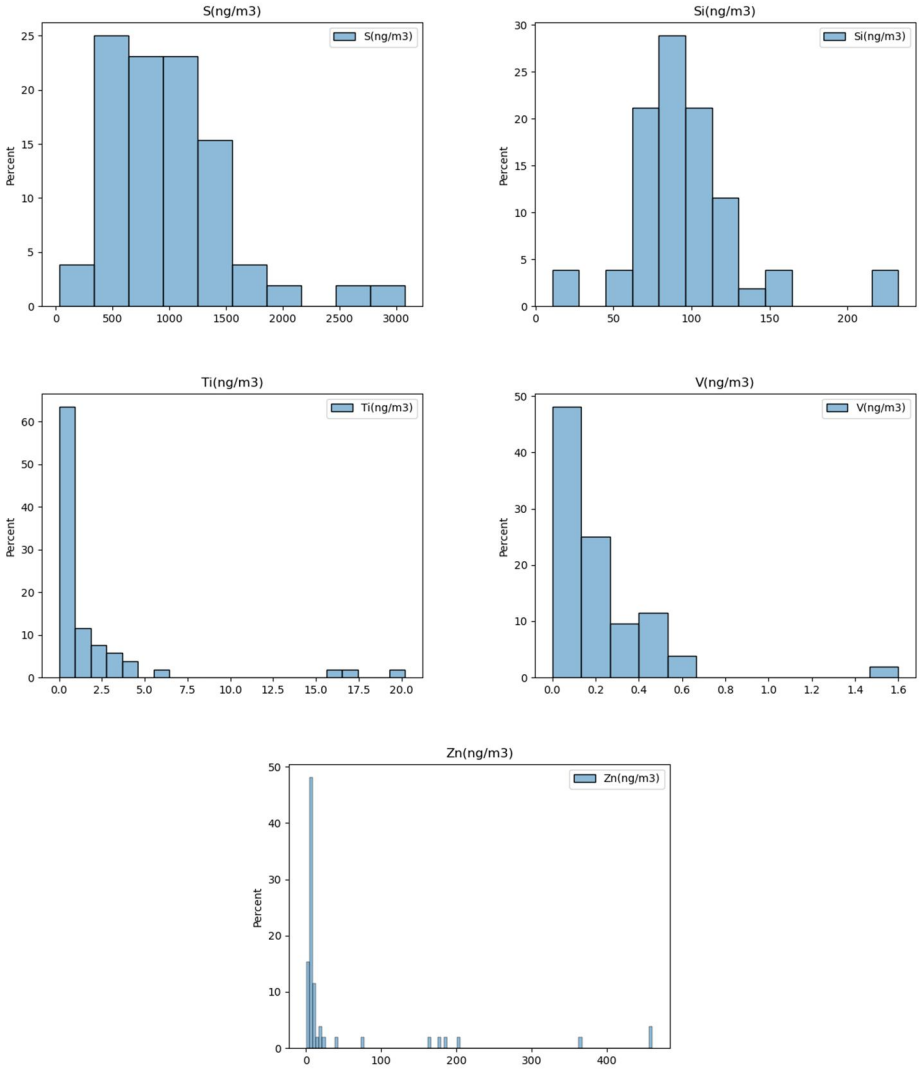


Fig. 1. Histograms of PM10-bound elements concentrations in the fire station in Warsaw.

The statistically significant correlations were observed between the elements with the highest concentrations (Table 3). Very high correlation among dataset has been recorded. There are 84 statistically significant (70% of all possible) correlations at $p<0.1$. Out of these 84 the biggest group are correlations significant at $p<0.01$ – 50 correlations while 24 correlations are significant at $\alpha=0.05$. The strongest correlations relate to sulfur, aluminum, zinc and iron. Sulfur concentrations are also correlated with concentrations of arsenic, lead, copper and manganese. This indicates a strong diversification of sulfur sources and other elements in the studied firehouse.

Table 3. Pearson's correlation matrix ($p<0.05$) among hourly concentrations of the analyzed elements in the selected rescue and firefighting firehouse in the central part of Poland.

| | *Ti* | *V* | *Cr* | *Mn* | *Fe* | *Ni* | *Cu* | *Zn* | *As* | *Pb* | *Al* | *Si* | *S* | *K* |
|---|---|---|---|---|---|---|---|---|---|---|---|---|---|---|
| V | 0.07 | | | | | | | | | | | | | |
| Cr | 0.07 | **0.99** | | | | | | | | | | | | |
| Mn | 0.02 | **0.56** | **0.59** | | | | | | | | | | | |
| Fe | **0.44** | **0.32** | **0.38** | **0.42** | | | | | | | | | | |

| | | | | | | | | | | | | | | |
|---|---|---|---|---|---|---|---|---|---|---|---|---|---|---|
| Ni | -0.04 | -0.03 | 0.00 | **0.23** | **0.26** | | | | | | | | | |
| Cu | 0.10 | **0.25** | **0.30** | **0.54** | **0.62** | **0.29** | | | | | | | | |
| Zn | -0.10 | **0.28** | **0.30** | **0.81** | **0.23** | **0.27** | **0.56** | | | | | | | |
| As | -0.11 | **0.23** | **0.25** | **0.70** | **0.23** | **0.28** | **0.49** | **0.91** | | | | | | |
| Pb | -0.06 | **0.26** | **0.28** | **0.82** | **0.28** | **0.30** | **0.58** | **0.97** | **0.92** | | | | | |
| Al. | **0.25** | 0.10 | 0.12 | **0.41** | **0.59** | **0.31** | **0.48** | **0.44** | **0.48** | **0.54** | | | | |
| Si | **0.31** | **0.58** | **0.61** | **0.31** | **0.67** | 0.07 | **0.28** | -0.06 | 0.02 | 0.00 | **0.37** | | | |
| S | 0.16 | **0.28** | **0.29** | **0.50** | **0.43** | **0.24** | **0.41** | **0.49** | **0.56** | **0.60** | **0.84** | **0.41** | | |
| K | **0.30** | 0.02 | 0.02 | **0.42** | **0.27** | **0.22** | **0.39** | **0.49** | **0.48** | **0.56** | **0.56** | 0.12 | **0.50** | |
| Cd | **0.87** | 0.19 | 0.17 | 0.11 | **0.29** | -0.07 | 0.03 | -0.09 | -0.11 | -0.07 | 0.14 | **0.38** | 0.14 | **0.30** |

means statistical significance at $p<0.05$ are in bold

It should be underlined that the enrichment of PM10 in sulfur, arsenic, copper and zinc is extremely high (Fig. 2). Therefore, it is clear that these elements are of anthropogenic origin. Probably they come from the same source. To assess this the PCA results were analyzed (Fig. 3).

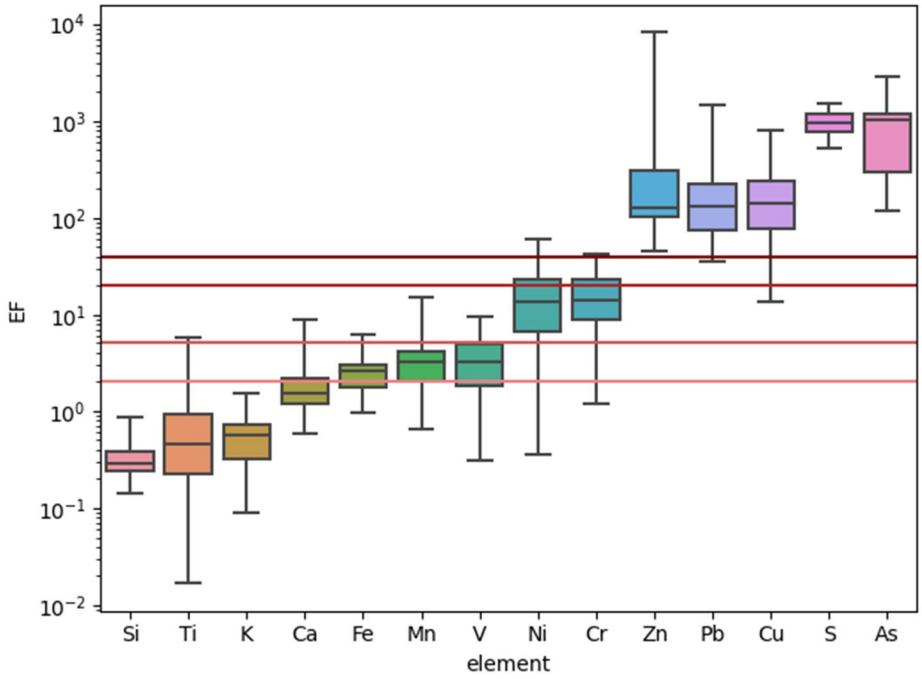


Fig. 2. Enrichment factor (EF) for PM10-bound elements in the indoor air of selected firehouse in central part of Poland (boxplots do not include points for which concertation of $i$th element was zero, the vertical scale is logarithmic and whiskers are from minimum value to maximum value).

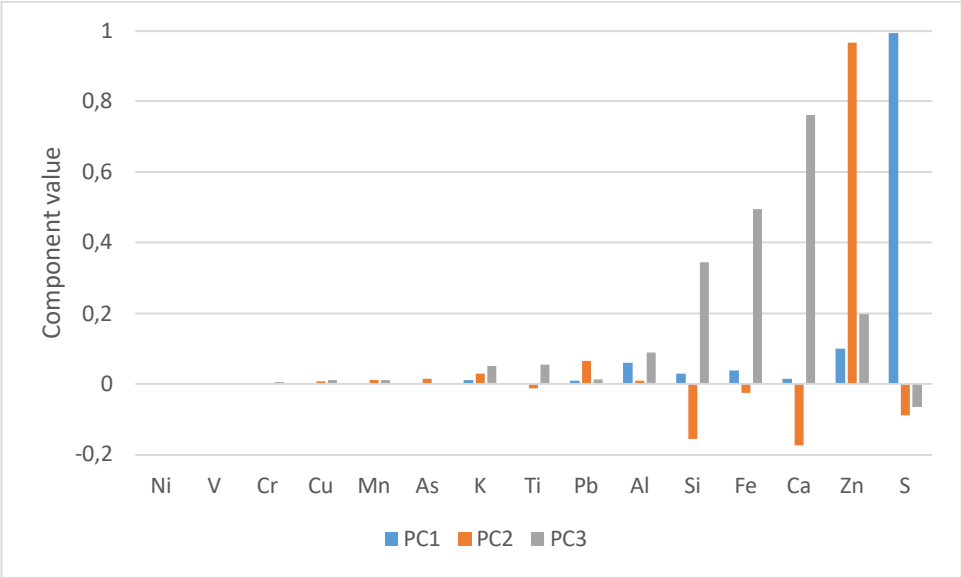


Fig. 3. Results of PCA analysis for PM10-bound elements in the indoor air of selected firehouse in central part of Poland.

Sulfur is correlated the most with PC1. Zinc is strongly correlated with PC2 component. The third component of PC3 is strongly related with calcium, silicon and iron. Taking into account the previous considerations regarding the enrichment of PM10 in the analyzed elements, this may indicate the existence of three basic sources of PM10 in the air of studied firehouse. The first may be combustion processes, including oil [22] and other materials. What is more, personal protective equipment, including special clothing could be a source of secondary emission of certain compounds and dust, which is unusual for other rooms [3]. Our studies were carried out in the area of the firehouse where, on the one hand, processes and emissions in the garage had an impact on air quality, and on the other hand, the measurement point was located close to the storage area for rescue and fire-fighting equipment, personal protective equipment and special clothes. In this area, firefighters change clothes before and after the rescue operation. During these activities periodic increases in sulfur concentrations were observed, which may confirm that part of this element is carried in the firemen's equipment from the outside to the inside on special clothes and other equipment. The second main component may be related to the movement of vehicles inside the garage of the firehouse and the related other type emissions (dust from the abrasion of brakes, tires, body parts, etc. [23]. This can be proven by the fact that the zinc enrichment of PM10 was very high at the study site (Fig. 2) and therefore the zinc was not of natural origin. In the case of elements related to the third component - iron, silicon and calcium PM10 did not show a strong enrichment with these elements, and therefore this component can be considered as natural origin. These can be soil and sand particles, carried from the outside to the inside as well as particles subjected to resuspension inside the studied firehouse. It is obvious that all particles and elements are strongly mixed and the division described above for interpretation needs. Nevertheless, thanks to a simple analysis of the PM10 elemental composition from a very short series of measurements, conclusions can be drawn about the origin of the dust inside the studied firehouse. This is also confirmed by the fact that three main components attributed to 99% of the variance. It is also clear that the correlations among principal components are completely different in the case of the analyzed room than those observed in indoor air studies [24]. This is in line with expectations and thus confirms that in the case of a specific firehouse and with the use of measuring equipment that allows to obtain measurements from short time intervals, a very short measurement period is sufficient to collect data suitable for conducting source apportionment. Such approach seems right taking into account that the contribution of various sources in such rooms in

shaping the PM concentration is variable in short periods of time (it changes during the day depending on the activity inside) and it is not the same as is the case with atmospheric air when we need longer periods - a month, a season (as it is shaped by changes in ambient temperature and thus the intensity of energy production or changes in transport emissions due to the holiday season, etc.).

### *4.2. UNMIX*

The UNMIX model is similar to PCA, with the constrains on positive values of coefficients. The source profiles of four components are presented in Figure 4. The constrain of positive coefficients significantly changed the source profiles. The variability explained by principal components (PCs) is now divided in few sources. The source #1 is main source of titanium, but also is responsible for almost half of calcium, and some of iron emission. According to the SPECIEUROPE, source profiles for Europe database [25] the important sources of titanium are combustion and dusts. The source #2 is mainly responsible for zinc, arsenic and lead emission which are also from the combustion of fuels. The source #3 is responsible mainly for chromium, vanadium, and manganese, that can be identified as elements from the abrasion of automotive elements and other non-combustion transport sources while source #4 is responsible for iron, coper, aluminum and sulfur. The source #4 is responsible for contribution of crustal elements as well as anthropogenic enriched elements. The analysis with the UNMIX allowed to differentiate the sources.

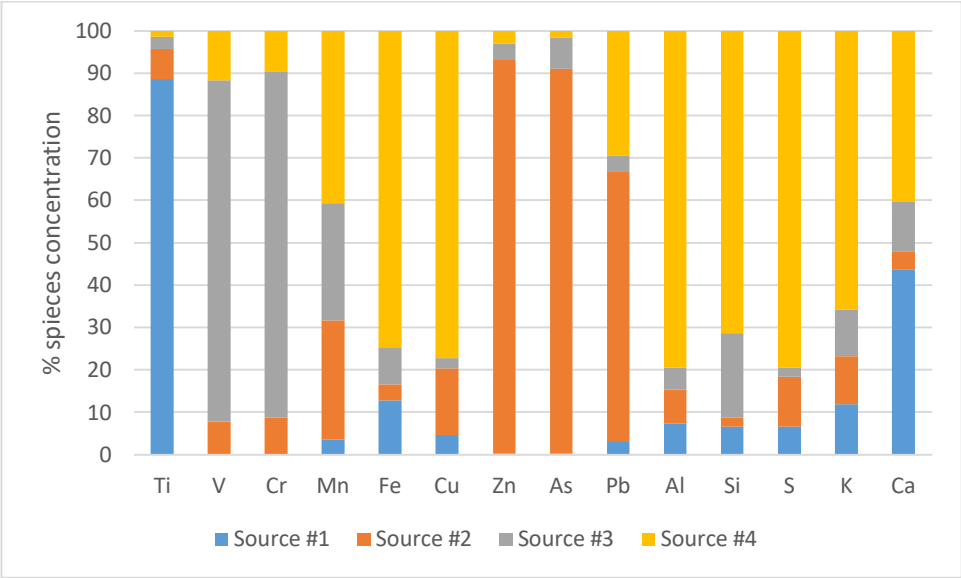


Fig. 4. Source profiles obtained in EPA UNMIX.

### *4.3. PMF*

Similar conclusions can be drawn by studding PMF results (Fig. 5).

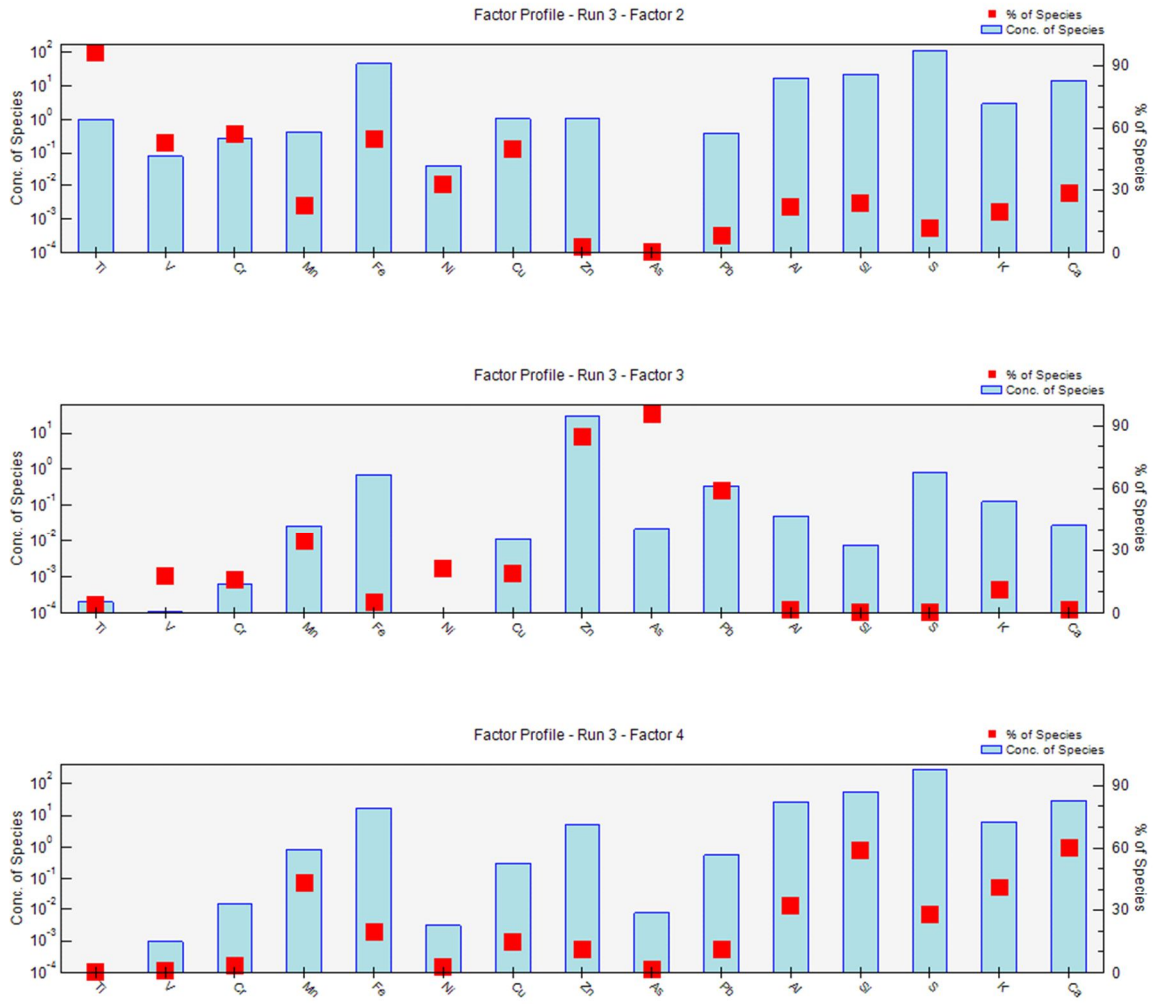


Fig. 5. Results of PMF analysis for PM10-bound elements in the indoor air of selected firehouse in central part of Poland (concentration of species in arbitrary units).

PMF analysis allowed to select four factors. Each represents a different, not necessarily independent, source of PM10 and PM10-bound elements. In the first factor, sulphur, nickel and aluminium have the highest share. Therefore, previous conclusion about the predominant share of combustion processes and about carrying sulphur compounds on firemen's equipment and clothes in shaping the concentrations of these elements and dust inside the firehouse is correct. In the case of the combustion of fuel oil and petroleum - we are dealing with characteristic elements - sulphur and nickel [26]. The first factor in the case of the three mentioned elements reflects from about 60% (sulphur) to 45% (Ni) of their concentration (Fig. 6). However, the share of this factor is smaller in the case of vanadium, chromium, iron or lead concentrations. This confirms that this factor can be identified with the combustion of fuels and other materials. This factor is similar to the source #4 in UNMIX, however, the introduction of the uncertainties related to the X-ray analysis done by the Horiba PX-375 changes the contribution of this factor to the given elements – the Mn from the source #4 is not present in factor 1 while species concentration of iron, copper, and aluminum are significantly lower in this factor. The second factor uses from over 90% (titanium), through 50-60% (vanadium, chromium, iron, copper) to 20-30% (nickel, aluminum, silicon, potassium, calcium) concentrations of the studied elements. Their common source may be a mixture of road dust related to the traffic emissions not deriving from exhaust emissions. Factor 2 is similar to source #3 which includes more elements from non-exhaust

emission than source #3. Combustion may also involve a third factor that uses over 90% concentrations of arsenic and zinc as well as 60% lead concentrations. It is difficult to define what type of combustion is and what is the specific source, but based on the specific elements, we can suggest that it is most likely a factor characterizing the impact of external anthropogenic emission of PM10 and PM10-bound elements from the combustion of fossil fuels, especially coal from energy production. This is important conclusion indicating the impact of atmospheric air on the quality of indoor air not only in typical rooms such as schools, flats or kindergartens [27], but also in the specific rooms such as rescue and firefighting firehouses with many internal sources of pollutant emissions.

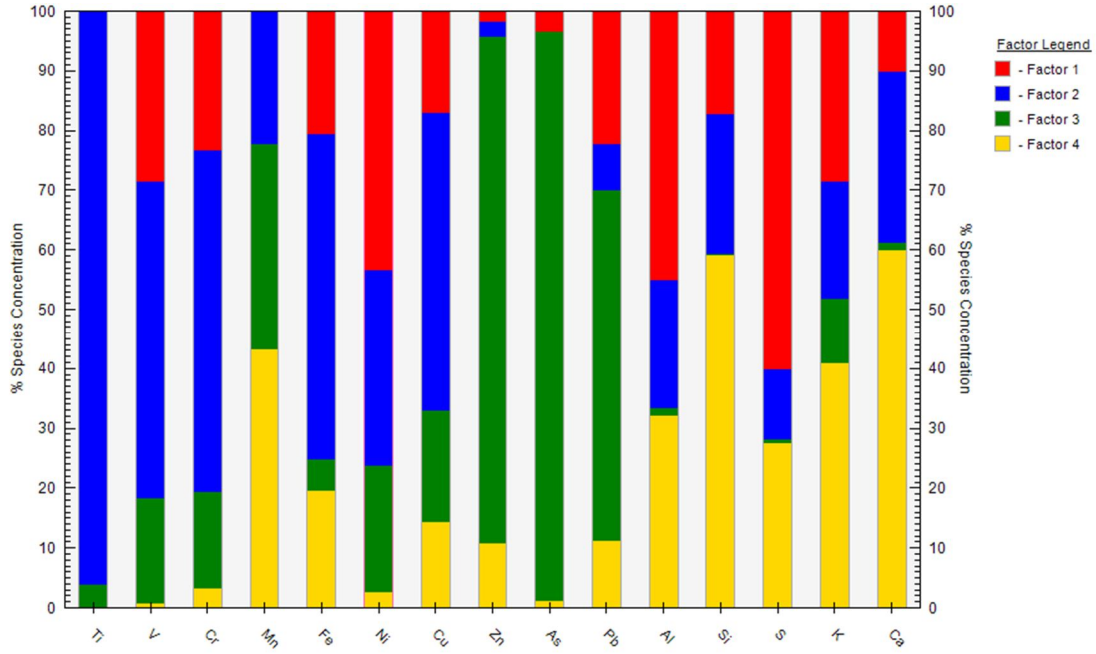


Fig. 6. The share of factors in PMF analysis in the concentrations of the studied elements.

It should be underlined that the separation of this specific third factor allows to show exactly how effective tool in the analysis of PM origin can be UNMIX and PMF than simple PCA. The negative coefficients in the PCA, especially for PC2, for calcium and silicon biased the decomposition. The UNMIX source #2 and PMF factor 3, which are similar, were only identifiable with these techniques. It is a reason for the limited applicability of PCA in source apportionment.

The fourth factor identified in PMF analysis is a factor that mainly uses the concentrations of typical crustal elements, which may partly be derived from natural sources, such as aluminium, silicon, calcium and potassium. Factor four also uses sulphur and manganese concentrations partly which indicate the possibility of transferring anthropogenic compounds of sulphur, manganese or other elements on mineral aluminosilicate particles coming from natural sources. The comparison of Sources identified in UNMIX and factors identified in PMF shows no 1-1 correspondence. This factor is similar to source #4 but in different proportions.

## 5. Conclusions

The paper presents the results of the first measurement campaign of PM10 bound elements which was carried out in a selected rescue and firefighting firehouse it in Poland. A typical firehouse located in the central part of Poland was selected for the study. A set of data on hourly concentrations of elements related to PM10 and PM10 concentrations from a two-week measurement campaign was

collected. The data was analyzed using PCA, PMF and UNMIX to demonstrate the origin of PM and PM-bound elements in the firehouse.

It was found that the concentrations of PM10 and most of the 14 studied elements in PM10 (Ti, V, Cr, Mn, Fe, Ni, Cu, Zn, As, Pb, Al., Si, S, K) are not high. Despite this, differences and strong variability of hourly concentrations were noticed. Although the data came from a short measurement series, their high time resolution, and thus a large number of individual data, allowed to use them in the assessment of the PM10 origin and PM10-bound elements in indoor air of the firehouse. The analysis of the results obtained by applying three different models to the collected data set gave similar results. First of all, it was found that the main source of PM10 and PM10 bound elements is anthropogenic emission. Most of the elements in PM10 were characterized by high and very high enrichment factors. Sulfur had the highest concentrations of all determined elements. Sulfur concentrations also determined the variability in all three models. This is probably the result of a strong enrichment of PM10 with sulfur which come from the fuel combustion in fire engine engines as well as from fuel oil emission. PMF model also allowed to find specific relationships of sulfur and several trace elements indicating the influence of external emissions from fuel combustion on internal concentrations of PM10 and PM10-bound elements. Identified dependences indicate the presence of mineral dust and dust from non-exhaust communication emissions in the firehouse. It is also possible that some of the elements and dust derive from the outside, and they were carried on vehicles or on firemen's equipment and clothes. However, in order to confirm this, further studies should be carried out at different points of firehouses and in different averaging periods.

It was shown undoubtedly, that in case of the high correlations among the dataset, that are statistically significant, the PCA analysis cannot be applied in source apportionment. The correlations in dataset cause that almost whole variability can be explained by first principal component. The additional problem that causes problem with interpretation of PCs are the possible negative values of coefficients in PCs. The step forward the better source apportionment is the application of UNMIX model that constrains the non-negativity of coefficients. It led to the essential change in the decomposition and resulted in sources that can be physically interpreted. The application of PMF model for source apportionment allowed to include the uncertainties related with the X-ray analysis precision. The results of the PMF analysis were slightly different from the results of UNMIX but they were comparable – the difference was not as big as in case between PCA and UNMIX or PCA and PMF.

Moreover, it is clear that, independently of the model used to assess origin based on modeling results, i.a. presented in this paper, it is necessary to know PM elemental profiles from various sources. So far, they are well recognized for certain sources of atmospheric dust, such as combustion of liquid and solid fuels (both in car engines and for municipal and living purposes), industrial emissions, emissions from mechanical processes, including those related to car traffic and many other. On the other hand, elemental profiles of PM indoors are poorly recognized. Few studies have been done on indoor dust so far. However, data on the physical and chemical properties of dust generated from specific sources, including those found in rescue and firefighting firehouses are lacking. Regardless of the object that is analyzed in terms of the origin of indoor air pollution, the important starting point is to determine these sources and examine the properties of dust generated from it.

## 6. References

1. Fent, K. W., Evans, D. E., Babik, K., Striley, C., Bertke, S., Kerber, S., et al. Airborne contaminants during controlled residential fires. J. Occup. Environ. Hyg., 2018, 15(5), 399–412. DOI: 10.1080/15459624.2018.1445260

2. Alharbi, B. H., Pasha, M. J., Al-Shamsi, M. A. S. Firefighter exposures to organic and inorganic gas emissions in emergency residential and industrial fires. Sci. Total Environ., 2021, 770, 1–9. DOI: 10.1016/j.scitotenv.2021.145332
3. Rogula-Kozłowska, W., Bralewska, K., Rogula-Kopiec, P., Makowski, R., Majder-Łopatka, M., Łukawski, A., et al. Respirable particles and polycyclic aromatic hydrocarbons at two Polish fire stations. Build. Environ., 2020, 184, 107255–107255. DOI: 10.1016/j.buildenv.2020.107255
4. Brown, F. R., Whitehead, T. P., Park, J. S., Metayer, C., Petreas, M. X. Levels of non-polybrominated diphenyl ether brominated flame retardants in residential house dust samples and fire station dust samples in California. Environ. Res., 2014, 135, 9–14. DOI: 10.1016/j.envres.2014.08.022
5. Bott, R. C., Kirk, K. M., Logan, M. B., Reid, D. A. Diesel particulate matter and polycyclic aromatic hydrocarbons in fire stations. Environ. Sci. Process. Impacts, 2017, 19 10, 1320–1326.
6. Lee, S., Liu, W., Wang, Y., Russell, A. G., Edgerton, E. S. Source apportionment of PM2.5: Comparing PMF and CMB results for four ambient monitoring sites in the southeastern United States. Atmos. Environ., 2008, 42(18), 4126–4137. DOI: 10.1016/j.atmosenv.2008.01.025
7. Larsen, R. K., Baker, J. E. Source Apportionment of Polycyclic Aromatic Hydrocarbons in the Urban Atmosphere: A Comparison of Three Methods. Environ. Sci. Technol., 2003, 37(9), 1873–1881. DOI: 10.1021/es0206184
8. Henry, R. C. UNMIX Version 2 Manual. Prep. US Environ. Prot. Agency, 2000, 536.
9. Lee, J.-H., Lim, J.-M., Kim, K.-H., Chung, Y. S., Lee, K.-Y. Trace element levels of aerosols at an urban area of Korea by instrumental neutron activation analysis. J. Radioanal. Nucl. Chem., 2003, 256(3), 553–560. DOI: 10.1023/A:1024520320578
10. Paatero, P., Tapper, U. Positive matrix factorization: A non-negative factor model with optimal utilization of error estimates of data values. Environmetrics, 1994. DOI: 10.1002/env.3170050203
11. Hu, S., McDonald, R., Martuzevicius, D., Biswas, P., Grinshpun, S. A., Kelley, A., et al. UNMIX modeling of ambient PM(2.5) near an interstate highway in Cincinnati, OH, USA. Atmospheric Environ. Oxf. Engl. 1994, 2006, 40(S2), 378–395. DOI: 10.1016/j.atmosenv.2006.02.038
12. Waskom, M. Seaborn: Statistical Data Visualization. J. Open Source Softw., 2021, 6(60), 3021. DOI: 10.21105/joss.03021
13. Barbieri, M. The Importance of Enrichment Factor (EF) and Geoaccumulation Index (Igeo) to Evaluate the Soil Contamination. J. Geol. Geophys., 2016. DOI: 10.4172/2381-8719.1000237
14. Hans Wedepohl, K. The composition of the continental crust. Geochim. Cosmochim. Acta, 1995. DOI: 10.1016/0016-7037(95)00038-2
15. Berthold, M. R., Cebron, N., Dill, F., Gabriel, T. R., Kötter, T., Meinl, T., et al. KNIME: The Konstanz Information Miner BT - Data Analysis, Machine Learning and Applications. (Preisach, C., Burkhardt, H., Schmidt-Thieme, L. and Decker, R., eds). Springer Berlin Heidelberg, Berlin, Heidelberg, 2008, 319–326.
16. USEPA. Unmix 6 . 0 Fundamentals & User Guide. 2007.
17. Norris, G., Duvall, R., Brown, S. and Bai, S. EPA Positive M atrix Factorization ( PMF ) 5 . 0 Fundamentals and User Guide, EPA/600/R-14/108. Environ. Prot. Agency Off. Researc Dev. Publushing House Whashington DC 20460, 2014.
18. Pekney, N. J., Davidson, C. I., Robinson, A., Zhou, L., Hopke, P., Eatough, D., et al. Major Source Categories for PM2.5 in Pittsburgh using PMF and UNMIX. Aerosol Sci. Technol., 2006, 40(10), 910–924. DOI: 10.1080/02786820500380271
19. Majewski, G., Rogula-Kozłowska, W., Czechowski, P., Badyda, A., Brandyk, A. The Impact of Selected Parameters on Visibility: First Results from a Long-Term Campaign in Warsaw, Poland. Atmosphere, 2015, 6(8), 1154–1174. DOI: 10.3390/atmos6081154
20. Faridi, S., Yousefian, F., Roostaei, V., Harrison, R. M., Azimi, F., Niazi, S., et al. Source apportionment, identification and characterization, and emission inventory of ambient particulate matter in 22 Eastern Mediterranean Region countries: A systematic review and

recommendations for good practice. Environ. Pollut. Barking Essex 1987, 2022, 310, 119889. DOI: 10.1016/j.envpol.2022.119889
21. Wang, Y.-X., Feng, W., Zeng, Q., Sun, Y., Wang, P., You, L., et al. Variability of Metal Levels in Spot, First Morning, and 24-Hour Urine Samples over a 3-Month Period in Healthy Adult Chinese Men. Environ. Health Perspect., 2016, 124(4), 468–476. DOI: 10.1289/ehp.1409551
22. Demirbas, A., Alidrisi, H., Balubaid, M. A. API Gravity, Sulfur Content, and Desulfurization of Crude Oil. Pet. Sci. Technol., 2015, 33(1), 93–101. DOI: 10.1080/10916466.2014.950383
23. Fussell, J. C., Franklin, M., Green, D. C., Gustafsson, M., Harrison, R. M., Hicks, W., et al. A Review of Road Traffic-Derived Non-Exhaust Particles: Emissions, Physicochemical Characteristics, Health Risks, and Mitigation Measures. Environ. Sci. Technol., 2022, 56(11), 6813–6835. DOI: 10.1021/acs.est.2c01072
24. Almeida-Silva, M., Faria, T., Saraga, D., Maggos, T., Wolterbeek, H. T., Almeida, S. M. Source apportionment of indoor PM10 in Elderly Care Centre. Environ. Sci. Pollut. Res. Int., 2016, 23(8), 7814–7827. DOI: 10.1007/s11356-015-5937-x
25. Pernigotti, D., Belis, C. A., Spanó, L. SPECIEUROPE: The European data base for PM source profiles. Atmospheric Pollut. Res., 2016. DOI: 10.1016/j.apr.2015.10.007
26. Querol, X., Fernández-Turiel, J., López-Soler, A. Trace elements in coal and their behaviour during combustion in a large power station. Fuel, 1995, 74(3), 331–343. DOI: 10.1016/0016-2361(95)93464-O
27. Diapouli, E., Chaloulakou, A., Koutrakis, P. Estimating the concentration of indoor particles of outdoor origin: A review. J. Air Waste Manag. Assoc., 2013, 63(10), 1113–1129. DOI: 10.1080/10962247.2013.791649